Functional analysis of a homeobox-containing gene expressed during early *Xenopus laevis* development

Margarida Trindade

Thesis submitted to the University College London for the degree of Doctor of Philosophy

October 1999

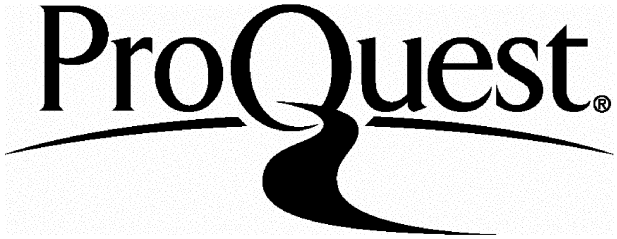

Abstract

Xom is a homeobox-containing gene expressed during early stages of *Xenopus laevis* development which is involved in the specification of ventral tissues. Expression of *Xom* is induced as an immediate-early response to Bone Morphogenetic Protein-4, a member of the Transforming Growth Factor-β family. Moreover, Xom contains a novel homeodomain, which might affect its DNA binding specificity.

This thesis describes a functional analysis of Xom. First, a preferred Xom DNA binding site was determined and the ability of Xom to bind potential binding sequences was tested in a series of *in vitro* assays. Together, these results showed that the sequence CTAATT(A/G) is critical for Xom to bind DNA, but that binding is greatly enhanced by the presence of an ATTA motif 6 or 7 nucleotides downstream of the core TAAT. A cell culture assay further demonstrated that Xom interacts with the selected sequence *in vivo*.

Second, the ability of Xom to regulate transcription was analysed. Xom was shown to behave as a transcriptional repressor in *Xenopus* embryos and its repressing activity was mapped to N-terminal and C-terminal regions flanking the homeodomain. Xom's transcriptional repressing activity, together with its ventral expression pattern and ventralising activity in the early *Xenopus* embryo, suggested that Xom could function by down-regulating the expression of genes that are required for dorsal development in *Xenopus*. Consistent with this suggestion, over-expression of *Xom* RNA, or of a dominant-negative version, indicated that Xom regulates the expression of *goosecoid*, a homeobox-containing gene expressed in the organizer capable of partially mimicking the activity of the organizer.

Finally, to test whether Xom acts by repressing *goosecoid* transcription directly, reporter constructs containing a *goosecoid* promoter fragment containing or lacking point mutations in potential Xom binding sites were co-injected with different effector RNAs into *Xenopus* embryos. These experiments suggested that at least part of the ability of Xom to repress *goosecoid* is direct, and identified a possible site to which Xom binds.

Acknowledgements

Time has come to write what is the trickiest, and surely the most requested, part of my thesis. Time to thank those who really did it.

I am grateful to António Coutinho and Alexandre Quintanilha for the creation of the Programa Gulbenkian de Doutoramento em Biologia e Medicina (PGDBM), which has financed me throughout the PhD and allowed me to spend an exciting year of tutorial courses based at the Gulbenkian Institute in Lisbon. I am also grateful to Eduardo Crespo, Professor at the Faculdade de Ciências in Lisbon, for his continuous interest in my work, to my PGDBM colleagues for the wonderful year we spent together and to Greta and Maria José Marinho for being there for us.

I am very grateful to my supervisor Jim Smith for the opportunity given to work in such a stimulating and culturally diverse environment as the NIMR at Mill Hill. Thanks for guidance and support throughout these years and for giving me some freedom to learn from my mistakes. I truly appreciate it. Thanks also for the ultra-fast reading of my thesis!

When I first arrived at Mill Hill, not yet sure in which country I was, Raj Ladher was the person who guided me both in the intricate secrets of Mill Hill and in the discovery of the city of London. Thank you for all the fun. I won't forget The Beauty of the whole mounts! Masa Tada (or shall I say Master Masa?) taught me most of what I know about Developmental Biology. Thanks for the infinite patience and friendship. Thanks to you I now know that there is always a better experiment to do! A big thanks goes to Joshua Brickman who contributed enormously to the final part of my thesis, by introducing me to the ways of transcription and lecturing me endlessly on how to present my work. And to think that everything started with salsa... Thanks Niall Armes for making me think in molecules (lots of them, all together, making complexes, shaking in the air, separating, fusing, spinning, getting obscene conformations!!...Uff, I am tired. Are you sure they all obey quantum mechanics?). Let's try seriously now: thanks! With Mike Jones I had the opportunity to go to the *Xenopus* course at the Gulbenkian Institute (and even try some serious frog transplant stuff!). I enjoyed it a lot! Thanks for helpful

advice, and this also applies to Frank Colon and Yasu Saka, but in particular to Branko Latinkic who encouraged me not to let the *goosecoid* promoter escape! I am grateful to Lynne Fairclough for all the technical support and four almost four years of sharing a laboratory bay without friction (I am sure it was Walter who took that!). Thanks to Surrendra Kotecha and to Tim Mohun for the help with the binding site selection. Thank you to all the Photographics staff, which made the figures of my thesis. My sincere admiration goes to Jacky Smith who provides the unnoticeable everything to keep the lab going and is always willing to help. A big thanks also goes to Leonor Saúde for keeping me in touch with life in the Institute during the writing up period and for top quality occasional post(wo)man services! Finally, many thanks to all other past and present members of the laboratory (and adjacent laboratories) with whom I had exciting discussions, exchanged ideas, reagents, or many times, purely entertaining gossip.

My thoughts also go to all my friends in London who transformed my life out of the lab in a very pleasant time. Perhaps without noticing, they greatly contributed to my mental sanity. To list them all would be too long and surely incomplete. However, a few lines are needed just to acknowlege my fantastic Medresco House ex-neighbours (Ana, Pedro, Josh, Leonor, Jacinto, Maria, Sérgio), Sofia, Rui (by the way, I won!), Ana Paula, Pedro, Andreas, Miguel, Kathy, Raj, Salvatore, CP, etc., etc., etc.

Thanks to my all my friends which came from far to enjoy the comfort of my B&B (I am sorry, Julia, I thought you should know), but only to those that did not forget the chouriços and the bacalhau! Thanks also to those that never came, but who I am sure will regret it for the rest of their lives.

My family has been exceptional during this period of my life, as in all others. Their support, encouragement and optimism are infinite. Obrigada mãe, pai, avós, Ana, Zé e André. A special thanks goes to Lounès for making the best of our life together. Sans toi je ne sais pas si je l'aurais fait. Merci.

Aos meus avós, Maria de Lourdes e Ruy

Table of contents

List of Figures

Fig. 5.1 Over-expression of *Xom* and *PV.1* causes ventralisation of *Xenopus* embryos and affects expression of dorsal early genes.

Fig. 5.2 Over-expression of *Xom* causes down-regulation of *goosecoid* expression in *Xenopus* embryos and in activin-induced animal caps.

Fig. 5.3 Xom^{L213P} over-expression causes partial secondary axis formation and ectopic muscle formation.

Fig. 5.4 Over-expression of *XomVP16* causes ectopic activation of *goosecoid.*

Fig 6.1 Time course of Xom repressing effect on activin-induced activation of the *goosecoid* promoter.

Fig. 6.2 Xom represses activin-induced activation of the *goosecoid* promoter.

Fig. 6.3 Point mutations increase the basal activity of a *goosecoid* promoter reporter construct in *Xenopus* embryos.

List of Tables

CHAPTER 1

INTRODUCTION

The general body plan of all vertebrate embryos becomes established during gastrulation, a stage in development during which extensive morphogenetic movements lead to the correct positioning of three distinct cell layers – the germ layers, from which all tissues of the adult will originate. Amongst different vertebrate species, the earliest phases of development occur by different processes. However, for a period starting during gastrulation and preceding the acquisition of species-specific morphological traits, the embryos present high morphological resemblance. This period, called the phylotypic stage (Slack et al., 1993), highlights the phylogenetic invariability of vertebrate development, in particular of the mechanisms that lead to and control gastrulation.

The amphibian *Xenopus laevis* has been used extensively as a model to study early vertebrate development. It lays large eggs and the embryos are easily accessible since amphibian development occurs outside the mother. In addition, *Xenopus* embryos are easy to culture and dissect and its development has been very well characterised from early to later stages of differentiation. Although it is unsuitable for genetic analysis because of its long generation time (18 months) and pseudo tetraploidy (Kobel and Du Pasquier, 1986), many of these disadvantages can be partially overcome by techniques involving expression of gain-of-function or dominant-negative constructs in the embryo.

In this thesis the *Xenopus* embryo was used as a biological model to assess the role of a homeobox-containing gene, *Xom,* which is involved in the early patterning of the *Xenopus* embryo. This introduction reviews classical and recent embryological experiments in *Xenopus*, together with a vast amount of molecular data generated only in the last two decades, that represent the basis for current models of early patterning in the vertebrate embryo. Xom is expressed ventrally in the gastrula embryo and acts as a potential Bmp response (Ladher et al., 1996). Emphasis will therefore be given to signals involved in establishing ventral phenotypes in the *Xenopus* embryo, in particular the Bone morphogenetic protein (Bmp) signalling pathway.

Early *Xenopus* development

Xenopus development starts with fertilisation of the mature egg (Fig. 1.1). Fertilisation is immediately followed by a period of rapid and synchronous cell divisions. At this stage, cell division is uncoupled from cell growth and within several hours a compact cluster of cells known as the morula is formed, with approximately the same volume as the uncleaved egg. By this time a cavity begins to form in the centre of the embryo - the blastocoel – which separate the large vegetal blastomeres from the smaller animal blastomeres and the embryo is called a blastula (Gilbert, 1994). Until this stage, development has occurred at the expense of maternal gene products. However, by blastula stage (stage 8, Fig.1.1), a coordinated group of changes occurs, including the onset of zygotic expression and the breakdown of cleavage synchrony, which are collectively called the mid-blastula transition (Yasuda and Schubiger, 1992). They prepare the embryo for gastrulation, which will result in the correct positioning of the three primary germ layers, ectoderm, mesoderm and endoderm. Briefly, the ectoderm will generate the epidermis and neural tissue of the embryo, the mesoderm will originate the notochord, somites, muscle and lateral plate mesodermal derivatives (blood, pronephros) and the endoderm will originate the embryo gut and parts of the head (Dale and Slack, 1987).

The first indication of gastrulation is the local invagination of a particular set of presumptive endodermal cells, the bottle cells, at a precise place in the marginal zone of the embryo (Fig. 1.2). This can be visualised from the exterior by the appearance of the dorsal blastopore lip in the marginal zone, on the future dorsal side of the embryo. Marginal cells then involute through this blastopore lip: the most dorsal cells involute first at the most dorsal position and the most ventral cells involute last at progressively more lateral and ventral positions, eventually leading to the formation of a circular blastopore in the vegetal pole of the embryo (Gilbert, 1994). This involution movement of the marginal cells displaces and reduces the blastocoel and begins the formation of another cavity, the archenteron (Fig. 1.2). The migration of mesodermal precursors inside the embryo involves a narrowing (convergence) and a lengthening (extension) of the involuting marginal zone just below the blastopore lip, which leads to the formation

of dorsal mesodermal structures such as notochord and muscle. There is also a temporal correlation between involution time and the position of the tissue along the anterior-posterior axis. The first cells to move as a result of involution movements (the anterior endoderm and the prechordal mesoderm) will originate anterior structures, and, conversely, the later cells to involute will contribute to more posterior structures. During involution of marginal zone cells, ectodermal tissue expands to take its place through movements known as epiboly, involving cell division and the integration of previously independent cell layers (Gilbert, 1994).

The formation of neural tissue also starts during gastrulation, when the midline ectodermal cells become elongated to form the neural plate and then invaginate and fuse at their edges to form a hollow tube beneath the ectoderm, the neural tube (Gilbert, 1994). The induction and patterning of the neural tissue continues throughout neurula stages. Neural induction occurs by signalling events between the dorsal ectoderm and the involuting dorsal mesoderm (reviewed by Kessler and Melton, 1994). Two modes of signalling have been suggested to operate: a vertical signal from involuting chordamesoderm (presumptive notochord) to the overlying ectoderm, and a planar signal spreading horizontally within the same plane from the mesoderm to the ectoderm. The type of neural tissue induced reflects the antero-posterior character of the inducing mesoderm, as was proposed initially by Otto Mangold in 1933 (reviewed in Kessler and Melton, 1994). At the end of gastrulation the embryo is a polarised structure, with defined antero-posterior and dorso-ventral axes and many precursors of adult tissues already specified (Gilbert, 1994).

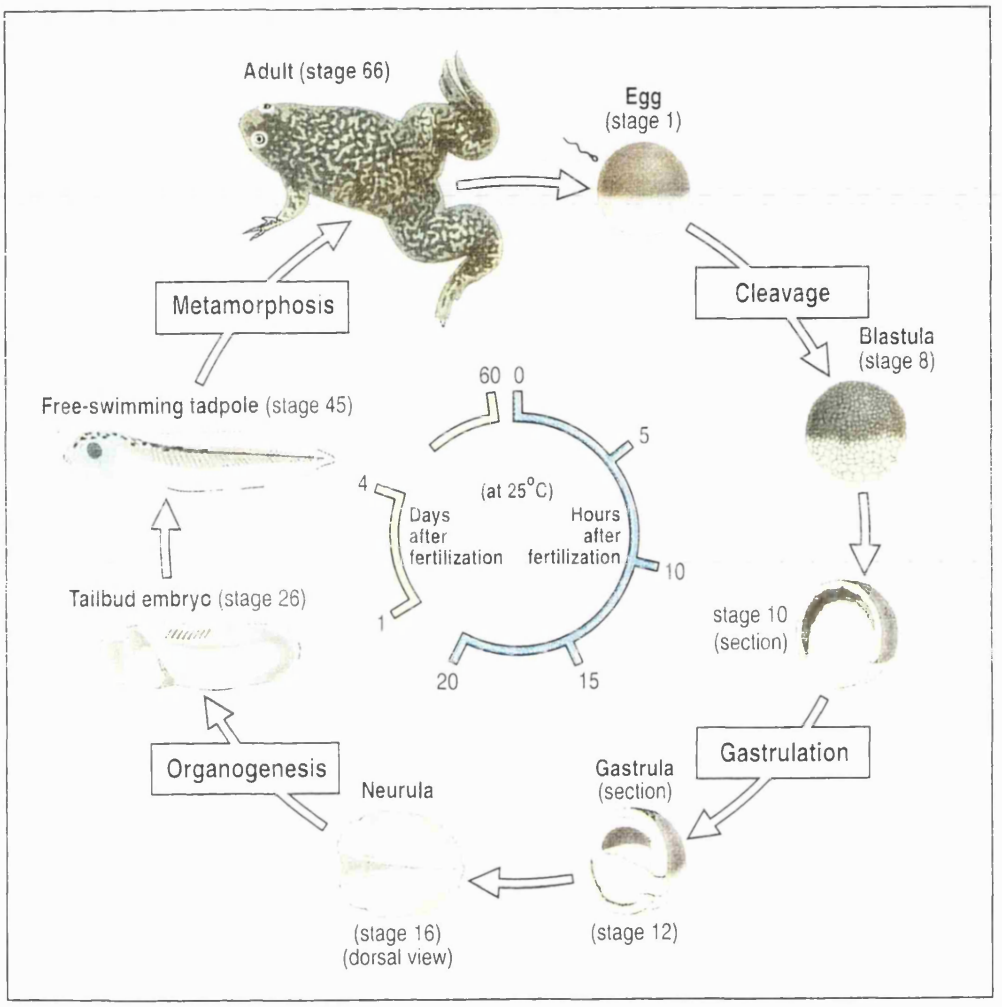

Fig. 1.1 Life cycle of the African claw-toed frog *Xenopus laevis*. The stages are according to Nieuwkoop and Faber (Nieuwkoop and Faber, 1975). From Wolpert (1998).

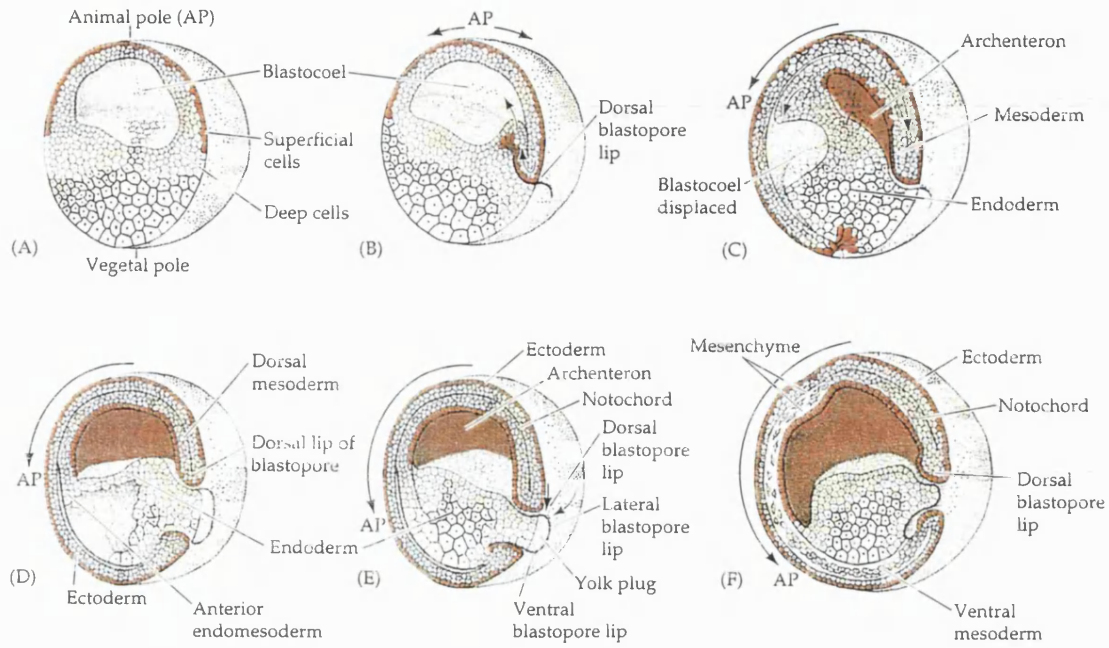

Fig. 1.2 Cell movements during *Xenopus laevis* gastrulation. The sections are cut through the middle of the embryo and are positioned so that the vegetal pole is tilted towards the observer and slightly to the left. The major cell movements are indicated by arrows and the superficial animal hemisphere cells are coloured so that their movements can be followed. (A,B) Early gastrulation. (C,D) Mid-gastrulation. (E,F) Late gastrulation. See text for details. From Gilbert (1994).

Axis specification

The first evidence for axis organizer activity within the *Xenopus* embryo came with the discovery of Spemann's organizer by Spemann and Mangold in 1924 (reviewed by Smith, 1989). The Spemann's organizer corresponds to the dorsal marginal region of a gastrula embryo, which when transplanted into the ventral region of a host gastrula generates the formation of two complete dorsal axes, with both the graft and the host cells contributing to the ectopic axis. Thus, this region is able to induce the differentiation of most tissues of the embryo and to place them in their correct positions according the anterior-to-posterior and ventral-to-dorsal axes of the embryo. Conversely, early organizer removal leads to the development of an embryo lacking axial structures (a 'Bauchstück' or belly piece) (Stewart and Gerhart, 1990). Thus, the organizer is both sufficient and necessary for axial development and acts by recruiting (organising) neighbouring cells.

An earlier-acting organiser region was originally identified in experiments performed initially by Nieuwkoop, but later revisited by other authors. In this work, the most dorsal vegetal blastomeres of a blastula stage embryo were transplanted to the ventral side of a normal embryo. The embryo receiving the explant formed a complete secondary axis (suggesting that an organizer was formed) without the contribution of the dorsal blastomeres themselves to the tissues of the secondary axis (Gimlich and Gerhart, 1984). This experiment was a clear demonstration of induction since the signalling cell instructs the neighbouring cells to change their fate but does not itself participate in the differentiation of dorsal mesoderm. This organizer-inducing dorsal vegetal region of the blastula was named the Nieuwkoop centre (Harland and Gerhart, 1997).

Taken together, these pioneering experiments not only demonstrated the existence of embryonic induction, but also laid the groundwork for subsequent work to understand how the embryonic axes are specified.

Other experiments in which vegetal blastomeres at the 16-32 cell stage were juxtaposed with animal pole explants showed that dorsal vegetal blastomeres were able to induce explanted tissue to form dorso-anterior cell types such as notochord, muscle

and head endoderm (Boterenbrood and Nieuwkoop, 1973). Similarly, intermediate vegetal blastomeres induced intermediate types of mesodermal derivatives (muscle) and ventral vegetal blastomeres induced ventral mesoderm derivatives (blood and mesenchyme) in the animal pole explants (Boterenbrood and Nieuwkoop, 1973). These results revealed the existence of a dorsal to ventral gradient of activity inducing progressively more ventral mesodermal fates.

One later interpretation of these experiments, together with results from other grafting experiments, evoked the existence of three qualitatively different signals to explain axis formation in the *Xenopus* embryo (Smith, 1989). In this model, two signals would emanate from dorsal and ventral vegetal blastomeres to divide the marginal zone into two distinct territories: the future Spemann's organizer dorsally, and the remainder of the mesoderm, ventrally and laterally. A third signal from the organizer region would then impose more dorsal and intermediate fates on the neighbouring ventral mesoderm during gastrula stages. This signal was therefore called the dorsalisation signal (Smith and Slack, 1983).

The three-signal model was originally focused on the induction and patterning of mesoderm, however many of the molecular candidates for inducers of mesoderm also have a role in endoderm induction (see below). To remain relevant, the three-signal model needs to be reformulated to include a generic meso-endodermal signal on which a dorsal-modifying signal is superimposed (Harland and Gerhart, 1997). Next, I review evidence supporting this model.

Germ layer specification

Germ layer specification seems to occur independently of axis specification in the embryo. This idea first emerged from experiments that prevent dorsal axis formation using ultraviolet light (UV) radiation (see later), thus allowing the uncoupling of the two events. Embryos irradiated with UV, either at the oocyte or fertilised egg stage, develop as cylindrical masses with no dorsal structures but containing the three primary germ layers – endoderm on the inside, mesoderm in between, and ectoderm on the outside (reviewed in Heasman, 1997).

The view that germ layer specification occurs via a generic meso-endodermal inducer, produced by vegetal blastomeres, was initially suggested by Nieuwkoop and colleagues (reviewed in Harland and Gerhart, 1997). Evidence supporting the idea came from comparisons between the fate map of cleavage stage *Xenopus* embryos, which shows the normal fate of a particular region of the embryo, and the specification map, which shows the fate of explants cultured in isolation (Slack, 1994). The fate map of a *Xenopus* blastula indicates that mesoderm is formed on the marginal zone of the embryo. However, animal hemispheres from blastula-staged embryos cultured in isolation generated epidermis, while vegetal explants, cultured under the same conditions, either did not generate any recognisable tissue or generated posterior endodermal tissue. These experiments suggested that contact between animal and vegetal explants was necessary to generate mesoderm in the marginal zone of the blastula embryo (Slack, 1994). When animal explants were grafted onto vegetal explants, both mesoderm and pharyngeal endoderm were induced from animal cells (Harland and Gerhart, 1997). This result clearly demonstrated the existence of mesoderm induction (and also of endoderm induction), which Nieuwkoop named meso-endoderm induction. The mesoderm component of this induction has been the main focus of attention for several years due to the lack of endodermal molecular markers, but this has changed recently.

Attempts to determine when meso-endoderm induction occurs involved grafting progressively older animal caps onto early vegetal inducing cells. These experiments showed that animal caps lose the competence to respond to vegetal signals at early gastrula stages (Gurdon et al., 1985; Jones and Woodland, 1987). Conversely, combining progressively younger vegetal blastomeres with early gastrula animal caps, which have only a brief period of competence left, showed that vegetal cells are signalling as soon as it is feasible to isolate them, at the 16 to 32 cell stage (Jones and Woodland, 1987). Since zygotic transcription only starts after the mid-blastula transition, one implication of the latter result is that meso-endoderm induction relies on maternal material (mRNA or protein) deposited in the oocyte (Harland and Gerhart, 1997).

This idea has been challenged by more recent experiments involving heterochronic recombination using a dorsal mesoderm marker (*XmyoD*) and a ventral

and lateral mesoderm marker (*Xwnt-8*), which showed that vegetal masses do not release mesoderm-inducing signals until after the mid-blastula transition. Although based on only two molecular markers this experiment raises the possibility that mesoderm-inducing genes may be acting zygotically (Wylie et al., 1996). More extensive marker analysis should be performed to elucidate this issue.

Together, these results suggest that meso-endoderm formation is controlled by processes involving induction, thus cell-to-cell communication. However, at least one study contradicts this idea and suggests that germ layer specification may occur cell-autonomously in response to determinants asymmetrically laid along the animal to vegetal axis of the *Xenopus* oocyte. In particular, experiments in which embryos were dissociated show that the most dorsal and the most ventral equatorial blastomeres initiate expression of dorsal and ventral mesodermal genes, respectively, even in the absence of cell-to-cell contact (Lemaire and Gurdon, 1994). However, the same genes are not activated in embryos where cell-to-cell signalling by some members of the Transforming Growth Factor family (TGF-β; see later) is inhibited (Hemmati-Brivanlou and Melton, 1992). Although this result supports the idea that meso-endoderm requires cell surface receptors and, thus, occurs by induction, it does not rule out the possibility that germ layers are established cell-autonomously. This could occur if the activity of localised determinants required autocrine signalling from members of the TGF-β family.

Most candidates for endogenous meso-endoderm-inducing factors belong either to the Fibroblast Growth Factor (FGF) or to the TGF-β families of growth factors (for reviews see Isaacs, 1997; Kingsley, 1994; Massague, 1998). However, to date none of the candidate factors fulfils three general criteria that have been used to judge potential candidates for endogenous meso-endoderm inducers (Heasman, 1997). These criteria include localisation of maternal RNA and/or protein to the vegetal hemisphere of the embryo, ectopic induction of mesoderm and endoderm if mis-expressed, and inhibition of this induction by using dominant-negative approaches in the embryo (Slack, 1994). However, recently a transcription factor from the T-box family, named VegT (Zhang and King, 1996), also known as Xombi (Lustig et al., 1996), Antipodean (Stennard et al., 1996) and Brat (Horb and Thomsen, 1997) has been identified which may be a cell

autonomous component of the pathway leading to meso-endoderm induction in the embryo. In the next sections I will present some of the best known candidate meso-endoderm inducers, and discuss the relevance of VegT for germ layer specification.

Fibroblast Growth Factors (FGFs)

Basic FGF (bFGF) was the first purified molecule able to induce ventral mesodermal tissues from isolated animal pole tissue (Kimelman and Kirschner, 1987; Slack et al., 1987). FGF activity was detected in an animal cap assay. This assay has been widely used to detect mesoderm-inducing activity and consists in explanting the animal pole region of the *Xenopus* blastula followed by culture in medium containing the factor to be assayed. The untreated cap will round up and eventually form epidermis, whereas an induced cap forms mesoderm, which can be detected either by histological criteria or by the expression of mesoderm marker genes. The typical mesoderm-induced caps morphology corresponds to elongation of the explants, thought to mimic gastrulation-like movements of involuting presumptive mesodermal cells (Symes and Smith, 1987).

Models to explain the role of FGF in early *Xenopus* development have, however, been extensively modified since its discovery and the current view supports the idea that FGFs may be involved in maintenance, rather than in induction, of dorsal and ventral types of mesoderm.

Four members of the FGF family (bFGF, FGF-3, eFGF and FGF-9) have been identified in the *Xenopus* embryo (for a review see Isaacs, 1997). Their expression patterns do not support an early role in mesoderm induction *in vivo* because their expression does not commence until after the blastula stage (Isaacs, 1997). Moreover, bFGF is unlikely to be a secreted factor *in vivo* because its lacks a secretory signal sequence (Kimelman et al., 1988). However, studies in which the activity of the FGF receptor at late blastula and gastrula stages was assayed by the activity of MAP kinase, an intracellular mediator of FGF signalling (LaBonne and Whitman, 1997), indicated that slightly higher levels of activity in the vegetal pole. This is consistent with a role for FGFs in meso-endoderm induction.

The main evidence for a role of FGFs in mesoderm formation, both of ventral and dorsal character, comes from interference with FGF signalling. In particular, over-expression of a truncated dominant-negative FGF receptor, by mRNA injection in *Xenopus* embryos, resulted in blockage of most kinds of mesoderm formation, including the dorsal mesoderm derivatives muscle and notochord. Only parts of the head mesoderm derivatives developed in the absence of FGF signalling (Amaya et al., 1991; Amaya et al., 1993; Kroll and Amaya, 1996). Furthermore, experiments involving interference with FGF signalling downstream of the receptor have also suggested that the FGF signal transduction pathway is required for production or maintenance of most of the mesoderm (LaBonne et al., 1995; Umbhauer et al., 1995; Whitman and Melton, 1992). Experiments in which transient expression of mesodermal genes (such as *Xbra*) is induced after injection of embryos with truncated FGF receptor favours the idea that FGFs are necessary for mesoderm maintenance rather than mesoderm induction (Isaacs et al., 1994; Schulte-Merker and Smith, 1995).

Interestingly, inhibition of FGF signalling prevents continued expression of mesodermal markers such as *Xbra* in response to the secreted factor activin (see below), suggesting that FGFs may be involved in the maintenance of an activin-like meso-endoderm inducing signal (LaBonne and Whitman, 1994).

Transforming Growth Factor-β (TGF-β) factors

Activin, a member of the TGF-β class of growth factors, was first implicated in mesoderm formation by the discovery that the mesoderm-inducing activity present in the supernatant of a *Xenopus* cell line (Smith, 1987) was due to a homologue of activin A (Asashima et al., 1990; Smith et al., 1990). Around the same time activin B, another activin isotype, was also shown to be a potent mesoderm inducer in animal cap assays (Thomsen et al., 1990). Recently, activin was also shown to have endoderm inducing properties (Gamer and Wright, 1995; Henry et al., 1996).

Several other members of the TGF-β superfamily have been shown to be potent inducers of a full range of endodermal and mesodermal tissues. These include *Vg-1* (Thomsen and Melton, 1993) and the *Xenopus nodal-related* 1 to 4 (*Xnr-1 to 4*; Jones et

al., 1995; Joseph and Melton, 1997; Smith et al., 1995). The *Xenopus* nodal-related genes are unlikely to be involved in the early events of meso-endoderm induction because they start to be expressed only after the onset of zygotic transcription. They will be discussed briefly later, in the context of VegT inducing properties. Bone morphogenetic proteins (Bmps) are involved in inducing ventral mesoderm and will be considered in more detail later.

Activin

The distribution of activin mRNA and protein has been analysed in the *Xenopus* embryo. Transcripts of *activin A* and *B* have been found in the follicle cells around *Xenopus* oocytes, but not in oocytes or fertilised eggs, and then later in blastula stages (for *activin B*) or late gastrula stages (for *activin A*) (Dohrmann et al., 1993; Thomsen et al., 1990). Despite the absence of maternal *activin* transcripts, three forms of activin protein (A, AB and B) are present in early *Xenopus* embryos (stage 1 to 5) at least in part as a complex with follistatin, an activin-binding protein (Fukui et al., 1994). Furthermore, activin D, a recently described isotype which is a less potent mesoderm inducer than activin A or B, is expressed during early *Xenopus* development (Oda et al., 1995). Taken together, these results suggest that activin stored in the egg and the embryo, and perhaps activin D during cleavage stages, may have a role in mesoderm induction in the *Xenopus* early embryo. However, it is less clear what is the role for follistatin in the complex with activin. Fukui and collaborators (1994) suggest that follistatin may have a dynamic regulatory role in modulating activin's activity through out developmental changes (Fukui et al., 1994).

Over-expression of follistatin in the embryo does not however block mesoderm induction (Schulte-Merker et al., 1994). This argues against a role for activin as an endogenous mesoderm inducer. Interestingly, although truncated versions of activin receptors also block signalling by other TGF-β family members, and therefore lack specificity (Schulte-Merker et al., 1994), a secreted version of a type II receptor does show specificity for activin and expression of this construct causes defects in mesoderm formation (Dyson and Gurdon, 1997).

Vg-1

There is extensive evidence for the involvement of Vg-1 in mesoderm induction. *Vg-1* is maternally expressed and localised to the vegetal pole of *Xenopus* oocytes and cleavage stage embryos (Mowry and Melton, 1992; Rebagliati et al., 1985). As a member of the TGF-ß family, Vg-1 is expected to form disulphide-linked dimers that are subsequently cleaved to release a mature C-terminal peptide as a secreted active dimer (Kingsley, 1994). The Vg-1 precursor protein is abundantly detected in the early *Xenopus* embryo but the cleaved mature form has not been found (Dale et al., 1993; Thomsen and Melton, 1993). An artificially-created mature Vg-1, constructed by fusing the N-terminal pro-region and the cleavage site of a Bmp to the C-terminal mature region of Vg-1, induced dorsal (but not ventral) mesoderm in animal caps (Dale et al., 1993; Thomsen and Melton, 1993). The fact that ventral mesodermal tissue, such as blood, was not induced in this experiment suggests that additional factors are required during normal development to induce mesoderm around all the circumference of the embryo. Another artificially created mature version of Vg-1, constructed by using an activin B instead of a Bmp pro-region, corroborates these results (Kessler and Melton, 1995). More recently, studies using a dominant-negative Vg-1 ligand suggested that Vg-1 is essential for the specification of meso-endodermal fates *in vivo* (Joseph and Melton, 1998). However, the possibility that this dominant-negative also interferes with *derriere*, a novel TGF-beta family member that is closely related to *Vg1* (Sun et al., 1999), cannot be excluded.

T-box family: VegT

VegT belongs to the T-box family of genes, of which the only amphibian member known until recently was the pan-mesodermal marker *Xbra* (Smith et al., 1991). Members of this family are putative transcription factors that contain a conserved DNA-binding sequence - the T-box (Muller and Herrmann, 1997; for a review see Smith, 1999). *VegT* was cloned simultaneously by many groups (Horb and Thomsen, 1997; Lustig et al., 1996; Stennard et al., 1996; Zhang and King, 1996) and it appears first as a maternal mRNA localised to the vegetal hemisphere of the oocyte and early embryo. Later, zygotic transcripts localise to the dorsal marginal zone of the late blastula/early

gastrula, and then more laterally and ventrally as gastrulation proceeds. Ectopic expression studies show that *VegT* can induce both mesoderm and endoderm (Horb and Thomsen, 1997; Lustig et al., 1996; Stennard et al., 1996; Zhang and King, 1996), whereas a dominant-negative construct consisting of *VegT* fused to the *engrailed* repressor inhibits mesoderm formation and severely disrupts normal development (Horb and Thomsen, 1997).

A major breakthrough in the understanding of germ layer formation came from studies which allowed the separation between the maternal and zygotic functions of *VegT* (Zhang et al., 1998). This was done by injecting antisense *VegT* oligonucleotides into *Xenopus* oocytes. The oligonucleotides hybridise to endogenous *VegT* RNA, which is then cleaved by endogenous RNase H (Zhang et al., 1998). Surprisingly, maternal *VegT* mRNA was shown to be important for germ layer formation in general, as embryos presented a shift in the fate map towards the vegetal pole. In particular, in *VegT*-depleted embryos the marginal zone generated exclusively ectodermal derivatives (epidermis and neural tissue) whereas the vegetal pole generated both ectodermal and mesodermal derivatives, but no endoderm (Zhang et al., 1998). When the mesoderm-inducing properties of the *VegT* vegetal masses were tested by recombining vegetal and animal explants, *VegT*-depleted vegetal masses were unable to secrete a mesoderm-inducing signal, although very weak induction of the mesodermal marker *Xbra* was still observed. *VegT*-depleted animal caps could still be induced to form mesoderm by untreated vegetal tissue (Zhang et al., 1998). These results show that VegT is essential for the release of the mesoderm-inducing signal, but is not required to receive it (Kimelman and Griffin, 1998).

Several models have been proposed to explain these findings. The simplest model is to assume a morphogenetic gradient of VegT protein. At high levels in the vegetal mass, VegT activates endoderm and represses mesoderm, whereas at low levels in the marginal zone, it activates mesoderm (Zhang et al., 1998). If *VegT* were incompletely depleted in the vegetal hemisphere, this model would explain why depletion of maternal *VegT* shifts the pattern of primary germ layer derivatives toward the vegetal pole. However, the localisation of the protein is still unknown and the

mRNA is uniformly distributed in the vegetal hemisphere of the embryo.

Another model assumes that VegT is only required in the vegetal mass to specify endoderm and to generate mesoderm-inducing signals. Here, the lack of mesoderm formation in the marginal zone of *VegT*-depleted embryos would be a consequence of the lack of mesoderm-inducing signals produced by the vegetal mass (Zhang et al., 1998). However, to explain why mesoderm forms ectopically in the vegetal pole of *VegT*-depleted embryos, a weak mesoderm-inducer of unknown identity must also exist vegetally, with effects that are too weak to be detected when maternal *VegT* is present (Kimelman and Griffin, 1998). Consistent with this is the observation of very low levels of *Xbra* in the marginal zone of *VegT*-depleted embryos and in animal caps conjugated with *VegT*-depleted vegetal tissue (Kimelman and Griffin, 1998).

While VegT may have a role in meso-endoderm induction its identity as a transcription factor indicates that it must exert its effects after the onset of zygotic transcription. One possibility is that VegT activates the transcription of a TGF-β signal or processes the release of an existing signal, such as Vg-1. In this respect, the nodal-related genes *Xnr-1/2* (Jones et al., 1995) are possible targets of VegT, as is the *Vg-1*-related zygotically-expressed TGF-β family member *derriere* (Sun et al., 1999).

Finally, the fact that a transcription factor such as VegT is involved in meso-endoderm induction may explain the results of experiments with dissociated embryos suggesting that germ layers form cell-autonomously (Lemaire and Gurdon, 1994). Thus, maternal *VegT* RNA may act cell-autonomously to mediate the induction of mesodermal markers in cells from dissociated embryos.

Dorso-ventral axis specification

Understanding how dorsal specification occurs in the embryo starts with the search for the earliest signs of dorsal determinant activity, which will lead to the formation of the Nieuwkoop centre and later, Spemann's organizer. I next review experiments that led to the discovery of the molecular players involved in establishing the Nieuwkoop centre and Spemann's organizer activities. Later, I analyse how the ventral signalling pathway is established in the early *Xenopus* embryo and how it

antagonises dorsalising signals.

Dorsal specification: the Nieuwkoop centre

Embryos irradiated vegetally with ultra-violet light (UV) prior to fertilisation (in the oocyte) reveal the existence of at least one oocyte component necessary for dorsal specification, which is localised to the cortex of the vegetal pole before maturation (reviewed by Elinson and Pasceri, 1989). Although this oocyte determinant has not been characterised molecularly, its vegetal localisation was confirmed by cytoplasmic transfer experiments (Holowacz and Elinson, 1995). This vegetal activity is irreversibly lost once it is disrupted with UV irradiation (Sive, 1993).

Fertilisation triggers dorsal development, as the future dorsal side of the embryo always arises opposite the point of sperm entry in the oocyte. This point defines the axis of cortical rotation, a process taking place within 15 minutes of fertilisation during which the cortex of the egg rotates in relation to the inner cytoplasmic mass of the egg (Vincent and Gerhart, 1987). This rotation involves the establishment of a parallel array of microtubules in the vegetal hemisphere between the cortex and the inner cytoplasm, presumably to provide the tracks upon which the cortex moves. When the formation of microtubules is disrupted by vegetal UV irradiation of the fertilised egg (as opposed to the oocyte), cortical rotation does not occur and the embryo lacks a dorsal-ventral axis (for a review see Gerhart et al., 1989). However, the effects of UV irradiation at this stage are reversible as cortical rotation can be artificially induced by applying centrifugal force during the first cell cycle (Gerhart et al., 1989). This procedure mimics cortex/inner cytoplasm movements occurring during cortical rotation.

The microtubule-rich zone formed in the vegetal pole of *Xenopus* embryos after cortical rotation is a transport zone (Rowning et al., 1997). Therefore, the cortex rotation may be a device to align microtubules into a single parallel array used for efficient transport of a maternal determinant from the vegetal pole to the location of the future Nieuwkoop centre (Rowning et al., 1997). Experiments supporting this idea include inhibition of axis formation by ablations of vegetal cytoplasm adjacent to the cortex of the egg performed before (but not after) cortical rotation (Sakai, 1996). In addition,

transplants of vegetal cytoplasm or the cortex of the egg induce secondary axis formation (Fujisue et al., 1993; Kageura, 1997; Yuge et al., 1990).

After cortical rotation, the axis inducing activity of the cortex was found broadly distributed over the dorsal side of the embryo, reaching as far as the upper animal hemisphere (Kageura, 1997). In experiments in which pairs of dorsal blastomeres from 32-cell stage embryos were transplanted into UV-ventralised embryos or into the vegetal side of a normal embryo, the highest (primary or secondary) axis forming activity was observed in the most dorsal vegetal cells (tier 4) (Gallagher et al., 1991; Gimlich, 1986; Kageura, 1990). These cells will normally populate the endoderm just below the dorsal blastopore lip (Bauer et al., 1994). However, a substantial amount of activity was also found in dorsal cells which go on to populate the dorsal blastopore lip (tier 3). Some activity was even detected in cells from the dorsal animal part of the embryo (tier 1 and 2). The region of strongest axis inducing activity, in the dorsal vegetal blastomeres, corresponds to the Nieuwkoop vegetal organising centre (Gerhart et al., 1989). However, the broad distribution of the dorsalising activity at blastula stages (Gallagher et al., 1991; Gimlich, 1986; Kageura, 1997; Kageura, 1990) indicates that cells giving rise to the Spemann organizer may also be able to contribute to dorsal cell fate through self-induction. Thus, although the Nieuwkoop centre is activated before Spemann's organizer, the two signalling centres may physically overlap (Kimelman et al., 1992).

Molecular players: β-catenin and upstream pathway components

Several strategies have been used to identify the molecular nature of the dorsalising activity of the Nieuwkoop centre, including over-expression studies and rescue of UV-ventralised embryos. Secreted molecules able to induce complete secondary axes include Xwnt-8 (Christian et al., 1991; Smith and Harland, 1991), *Xwnt-8b (Cui et al., 1995), Noggin (Smith and Harland, 1992), Chordin (Sasai et al., 1994), Xnr1 and 2 (Jones et al., 1995) and modified *Vg-1 (Thomsen and Melton, 1993). However, there is little evidence that any of these molecules is a true dorsal determinant (reviewed by Harland and Gerhart, 1997; Heasman, 1997; Moon and Kimelman, 1998). Most of these molecules are absent or only weakly expressed during cleavage states (exceptions are marked *) and their activities, when over-expressed

ectopically, may reflect an ability to trigger a dorsal pathway in early pluripotent blastomeres which would not normally be activated in undisturbed embryos. Dominant-negative constructs with high specificity for the desired endogenous molecule are necessary to elucidate this subject further.

A large body of evidence implicates the Wnt pathway in the specification of the dorsal axis (Fig. 1.3). The components of this signalling pathway have best been established in *Drosophila* (for a review see Cadigan and Nusse, 1997). Briefly, the wingless (wg) ligand is likely to bind and activate the Frizzled receptor, which subsequently activates a cytoplasmic protein, Dishevelled. Dishevelled causes the repression of Zeste White-3 (ZW3 or Shaggy) by an unknown mechanism. Although there may be several intervening proteins, ZW3 is a kinase that represses the accumulation of Armadillo by promoting its degradation. In the presence of active Wg signalling, ZW3 is repressed and Armadillo accumulates. As it accumulates, it is likely to form complexes with the HMG box transcription factor Pangolin, thus leading to the regulation of target genes.

β-catenin (the vertebrate homologue of Armadillo) is present in the *Xenopus* egg and early embryo (DeMarais and Moon, 1992; Fagotto and Gumbiner, 1994) and its over-expression in *Xenopus* embryos is sufficient to induce a complete secondary axis (Guger and Gumbiner, 1995). More importantly, depletion of *β-catenin* maternal transcripts resulted in the inhibition of dorsal specification (Heasman et al., 1994). *β-catenin* depleted embryos develop without dorsal structures, including somites, notochord and neural tubes, and resemble the most severe cases of UV-ventralised embryos (Heasman et al., 1994).

β-catenin protein has an interesting spatial and temporal distribution in the embryo. Starting with the first round of division, the dorsal side of the embryo becomes progressively enriched in cytoplasmic β-catenin. By the 16 to 32-cell stage, β-catenin translocates to the nuclei of dorsal blastomeres and remains nuclear until after the onset of zygotic transcription, but it disappears before gastrulation starts (Larabell et al., 1997; Schneider et al., 1996). These results support the idea that β-catenin is involved in dorsal specification.

Experiments examining GSK-3, the vertebrate homologue of ZW3 (Fig. 1.3; Siegfried et al., 1992) also support the involvement of this kinase in dorsal specification. A dominant-negative form of GSK3 causes an increase in β-catenin ventrally (Larabell et al., 1997) and induces ectopic axis formation in *Xenopus* (Dominguez et al., 1995; He et al., 1995; Pierce and Kimelman, 1995), but it is unable to rescue β-catenin-deficient embryos (Wylie et al., 1996). Conversely, over-expression of GSK3 reduces β-catenin levels dorsally and ventralises embryos (He et al., 1995; Larabell et al., 1997). This defines GSK3 as a negative regulator of β-catenin, as its counterpart ZW3 is to Armadillo in *Drosophila.*

In vitro evidence suggests that GSK3 functions by directly phosphorylating β-catenin at a specific amino terminal site (Yost et al., 1996). When this site is left intact, and active GSK3 is present, β-catenin is targeted to the ubiquitin proteasome degradation pathway; however if this site is mutated and GSK3 is present, β-catenin is not degraded (Aberle et al., 1997). Taken together, these results led to the proposal of a model in which a lower activity of GSK3 on the dorsal side of the embryo would result in dorso-ventral asymmetries in β-catenin phosphorylation and, hence, stability (for a review see Moon and Kimelman, 1998). It remains to be determined how the levels or activity of GSK3 become asymmetric, since *GSK3* RNA was found ubiquitously distributed in the early embryo (Dominguez et al., 1995; Pierce and Kimelman, 1995). One candidate to regulate levels of GSK3 is GBP, an inhibitor of GSK3 that prevents GSK3-dependent phosphorylation and increases β-catenin levels (Yost et al., 1998). However, GBP does not seem to be localised asymmetrically in the early embryo either. There are several other proteins, such as Axin and the tumour suppressor protein APC (adenomatous polyposis coli), that form a multiprotein complex with β-catenin and GSK3 and may play important roles in regulating β-catenin or GSK3 activity locally (Ikeda et al., 1998; Rubinfeld et al., 1995; Sakanaka et al., 1998; Zeng et al., 1997).

By analogy to the *Drosophila* Wg pathway, maternal *Xenopus* Wnts could act upstream of β-catenin to control its dorsal accumulation. The observation that *Xwnt-8* or *Xwnt-8b* over-expression generates complete secondary axis (Cui et al., 1995; Smith and Harland, 1991) supports this idea. However, *Xwnt-8* is not expressed during cleavage

stages (Christian et al., 1991; Smith and Harland, 1991) and, although *Xwnt-8b* is present at the right time to control the pathway leading to dorsal β-catenin accumulation, dominant-negative experiments with several Wnt signalling components argue that this is not the case. In particular, ectopic expression of dominant-negative mutants of Wnt, Frizzled or Dishevelled, do not block endogenous axis formation in *Xenopus* even though they inhibit ectopic axis formation in response to mis-expression of a Wnt ligand (Deardorff et al., 1998; Hoppler et al., 1996; Moon and Kimelman, 1998; Sokol, 1996). These results raise the possibility that the Wnt pathway could be activated independently of Wnt ligands in the early embryo.

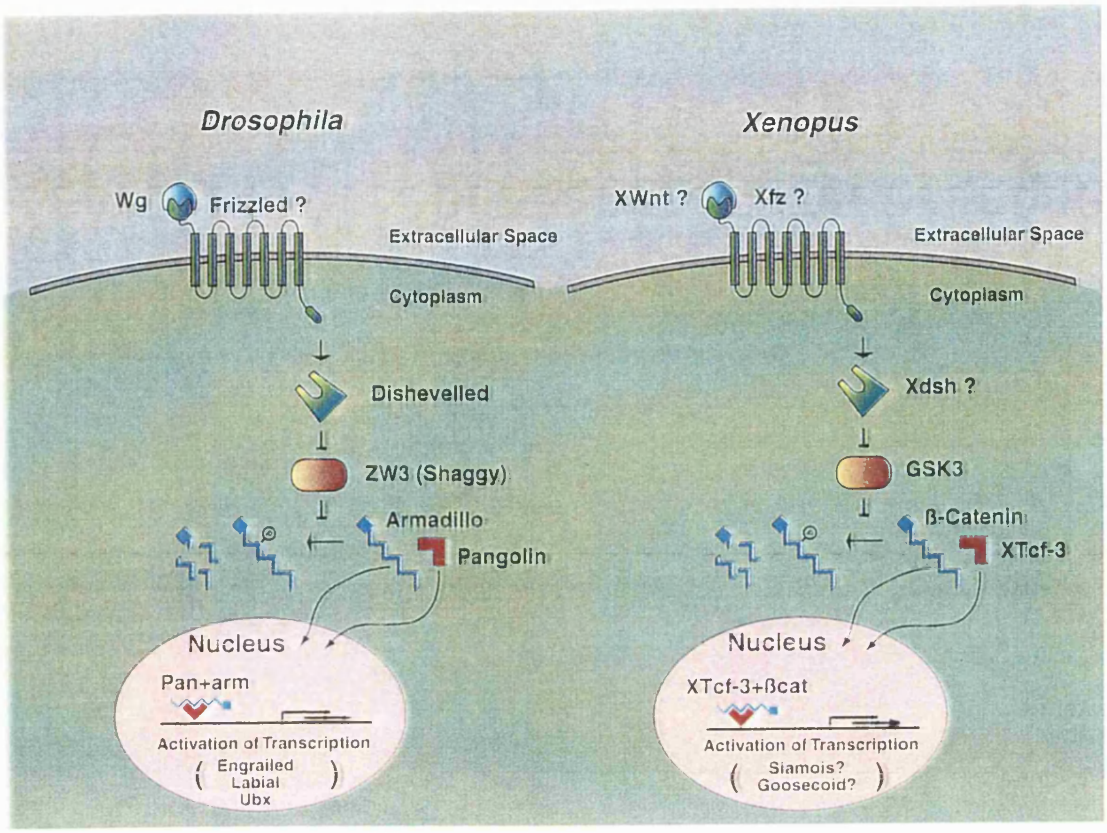

Fig. 1.3 A comparison of the *Drosophila* and *Xenopus* Wg/Wnt signal transduction pathways. See text for details. Reproduced from Heasman (1997).

β-catenin in the nuclei

β-catenin nuclear localisation occurs via interaction with members of the LEF/Tcf class of high mobility architectural (HGM box) transcription factors (Behrens et al., 1996; Molenaar et al., 1996). The *Xenopus* homologue of Tcf-3, XTcf-3, is expressed maternally but is not localised within the early embryo and, when over-expressed, causes translocation of β-catenin to the nucleus (Molenaar et al., 1996). However, XTcf-3 does not cause axis duplication when over-expressed into the embryo (Molenaar et al., 1996). This might suggest that β-catenin, but not XTcf-3, acts as a limiting factor (Molenaar et al., 1996). Further studies demonstrate that XTcf-3 is not only a transporter for β-catenin but also acts in transcriptional regulation. XTcf-3/β-catenin forms complexes on target DNA (Behrens et al., 1996; Huber et al., 1996) which, unlike XTcf-3 alone, are able to activate a reporter construct containing Tcf/LEF binding sites upstream of a minimal promoter (Molenaar et al., 1996). In the absence of β-catenin, Tcf factors may act as transcriptional repressors through interaction with members of the Groucho family of transcriptional repressors (Roose et al., 1998).

Candidates for genes directly regulated by β-catenin include the related homeobox containing genes *siamois* and *twin* (Lemaire et al., 1995; Laurent et al., 1997) and a gene encoding the TGF-β family member, *Xnr-3* (Smith et al., 1995). *Siamois* is expressed in dorsal vegetal and equatorial cells, before the expression of organizer genes such as *goosecoid*, and is necessary for the formation of the organizer and the embryonic axis (Fan and Sokol, 1997; Kessler, 1997; Lemaire et al., 1995). Expression of *siamois* is induced in animal pole explants by components of the Wnt signalling pathway (Carnac et al., 1996; Yang-Snyder et al., 1996), including β-catenin (Brannon and Kimelman, 1996; Fagotto et al., 1997). Analysis of the *siamois* promoter revealed that it contains three LEF/Tcf-3 consensus binding sites, and mutation of these sites eliminates β-catenin inducibility (Brannon et al., 1997). Thus, XTcf-3 is likely to repress *siamois* expression throughout the embryo with the exception of the dorsal region, where β-catenin interacts with XTcf-3 to activate *siamois* transcription (reviewed in Moon and Kimelman, 1998). The promoter of *twin* is very similar to that of *siamois*, as it also contains the three LEF/Tcf sites albeit with a different orientation and spacing. It is too

regulated by Wnt/β-catenin (Laurent et al., 1997). *Xnr-3* is expressed in the embryo in a similar pattern to *siamois*, although it is restricted to epithelial cells (Smith et al., 1995). Like *siamois*, *Xnr-3* is induced by Wnt (McKendry et al., 1997). The *Xnr-3* promoter contains two LEF/Tcf sites required for its expression that function together with an homeobox binding site (McKendry et al., 1997).

The Spemann organizer

Several lines of evidence show that the organizer is a non-homogeneous population of cells in terms of inductive properties, morphogenetic activities and developmental fate (reviewed by Harland and Gerhart, 1997). A complete organizer induces a complete secondary embryonic axis, with head, trunk and tail. However, the anterior half of the organizer (prospective pharyngeal endoderm and prechordal mesoderm) induces only head structures and the posterior part of the organizer (notochord territory) induces only tail-trunk structures (Zoltewicz and Gerhart, 1997). These partial regions of the early gastrula Spemann organizer have also been named the head and trunk organizer, respectively (Harland and Gerhart, 1997).

The heterogeneity of the organizer is also reflected in the genes that are specifically expressed in the organizer. Organizer-specific genes encoding transcription factors include *siamois* (Lemaire et al., 1995), *goosecoid* (Cho et al., 1991) and *XFKH1/Pintallavis* (Dirksen and Jamrich, 1992; Knochel et al., 1992; Ruiz i Altaba and Jessell, 1992); genes encoding secreted proteins include *noggin* (Smith and Harland, 1992), *chordin* (Sasai et al., 1994), *follistatin* (Hemmati-Brivanlou et al., 1994), *cerberus* (Bouwmeester et al., 1996) and *Xnr-3* (Smith et al., 1995). Several of these genes are expressed at higher levels in the head organizer or trunk-tail organizer, implying that the organizer is a spatially differentiated cell population, although in most cases the localisation of the respective proteins is unknown (Harland and Gerhart, 1997).

These regional differences raise the question of how signals from the Nieuwkoop centre can generate the full pattern of the organizer. In embryos in which cortical rotation has been blocked by UV radiation, the direct targets of the Wnt/β-catenin pathway (*siamois*, *twin* and *Xnr-3*) are not suppressed but are instead activated

ectopically at the vegetal pole (Brannon and Kimelman, 1996; Darras et al., 1997). This observation suggests that the Wnt/β-catenin pathway remains active at the vegetal pole in the absence of cortical rotation and that some component of the pathway may be physically translocated during cortical rotation to the marginal zone (Sokol, 1999). The lack of other organizer genes in UV-ventralised embryos, such as *chordin* and *goosecoid*, indicates that the Wnt signalling pathway, on its own, is not sufficient to trigger all dorsal development at the vegetal pole. It has therefore been proposed that TGF-β-related factors cooperate with Wnts to induce the organizer in the marginal zone (Harland and Gerhart, 1997; Sokol, 1999). Consistent with this idea, *goosecoid*, *chordin* and *siamois* have been shown to be sensitive to the dominant-negative activin receptor (Crease et al., 1998).

The *goosecoid* (*gsc*) promoter illustrates how the synergism between the Wnt/β-catenin pathway and TGF-β signalling may work at the molecular level. Analysis of the *gsc* promoter revealed the presence of a Wnt-response element, the proximal element (PE), and an Activin/Vg-1 response element, the distal element (DE) (Watabe et al., 1995). The *gsc* promoter is unlikely to be directly regulated by β-catenin/XTcf-3 complexes, because the Wnt-responsive element does not bind LEF-1 (Brannon et al., 1997); rather it may be regulated by *siamois* or *twin* at the PE (Fan and Sokol, 1997; Kessler, 1997; Laurent et al., 1997). The DE is sufficient to respond to the general endo-mesoderm inducing signal (activin/Vg-1-like signals) active throughout the vegetal hemisphere of the embryo, but both the PE and DE are necessary for high levels of transcription of *gsc* in the dorsal marginal zone (Watabe et al., 1995). Consistent with the Wnt/TGF-β synergism model, ectopic expression of *Xwnt-8* in animal pole explants, which do not contain Activin/Vg-1 activity, fails to induce *gsc*. By contrast *Xwnt-8* injected in the marginal zone strongly induces *gsc* (Sokol and Melton, 1992; Steinbeisser et al., 1993). In ventral and lateral regions, *gsc* expression is likely to be down-regulated by the presence of other signalling factors such as Bmps (see below) (Watabe et al., 1995).

Ventral specification

Ventral phenotypes were initially believed to be a default differentiation

pathway. Experiments supporting this idea include UV irradiation of *Xenopus* embryos. The mesoderm of these embryos does not form muscle or notochord, but contains mesenchyme, mesothelial tissue and blood and the ectoderm forms epidermis instead of neural tissues (Cooke and Smith, 1987). Thus, the embryos lack a dorsal/ventral axis and this suggests that the differentiation of ventral phenotypes occur in the absence of dorsal signalling by neighbouring tissues.

The idea that ventral phenotypes occur as a default differentiation pathway, although prevalent since Spemann's organizer transplant experiments, has now changed. Experiments involving culture and dissociation of animal caps cells illustrate this point. If intact animal pole explants were cultured in the absence of any treatment they differentiated into atypical epidermis, a tissue derived from ventral ectoderm. However, if the explants were dissociated and cultured as isolated cells, both neural differentiation and expression of neural markers were detected in reaggregates (Godsave and Slack, 1989; Grunz and Tacke, 1989), suggesting that the ventral fate requires cell-to-cell interactions. Experiments aimed at identifying the molecular signals involved in patterning the mesoderm and in neural induction have revealed that the specification of ventral fates (both mesodermal and ectodermal) requires active signalling. Below I review some of the molecules implicated in ventral signalling.

Xwnt-8 and Bmps

Xwnt-8, which encodes a secreted factor belonging to the Wnt family, was the first gene to be isolated possessing ventralising properties (Christian et al., 1991; Christian and Moon, 1993). However, the behaviour of this factor is not fully understood since it only ventralises embryos if injected as DNA cloned upstream of a cytoskeletal actin promoter, thus mimicking a zygotic effect (Christian and Moon, 1993). When *Xwnt-8* is injected as RNA (mimicking a maternal effect) it induces a secondary axis (Christian et al., 1991; Smith and Harland, 1991), and thus behaves as a dorsalising factor. *Xwnt-8* is expressed in a manner consistent with a function in ventralisation because transcripts are present in the ventral and lateral margin of the embryo at early gastrula stage, and are not detected during cleavage stages. Therefore, the dorsalising effects of *Xwnt-8* RNA may mimic the effects of another maternally expressed Wnt

gene, such as *Wnt-11* (Ku and Melton, 1993) or mimic activation of the Wnt pathway by another means. The evidence supporting a role of Wnts in ventral specification is, however, still contradictory, since a number of Xwnt-8 inhibitors such as *Dickkopf-1* (Glinka et al., 1998) failed to induce dorsal fates in ventral blastomeres, indicating that Xwnt-8 is not necessary for the maintenance of ventral fates (Sokol, 1999). By contrast, partial axis induction has been observed after ventral injection of *WIF-1*, another Wnt antagonist (Hsieh et al., 1999).

The relation of Xwnt-8 with Bone morphogenetic protein signalling, also involved in establishing ventral tissue identity in the *Xenopus* embryo (see below), is not very well understood at present. Surprisingly, *Bmp-4* was shown to repress *Xwnt-8* expression (Schmidt et al., 1995). However, as the opposite experiment has not been performed it remains unclear if they act in the same or parallel pathways (Lemaire, 1996).

Immediate-early responses to Bmps that mediate the establishment of ventral fates include *Xom*, the function of which is the main focus of this thesis. Therefore, Bmp signalling will be considered in detail next.

Bmp signalling

Bmp-2, Bmp-4 and Bmp-7

Bmps were originally identified by their bone and cartilage inducing properties, but have since been shown to be multifunctional proteins with a wide range of biological activities on various cell types. They regulate growth, differentiation, chemotaxis and apoptosis and play crucial roles in the morphogenesis of various tissues and organs, in both invertebrates and vertebrates (for a review see Hogan, 1996; Kawabata et al., 1998). Bmps are secreted molecules belonging to the TGF-β family of growth factors. The various members of this family are initially synthesised as larger precursor molecules with an amino-terminal signal sequence and a pro-domain of varying size. This precursor protein is usually cleaved at a RXXR site to release a mature carboxy-terminal segment which will make up the active signalling molecule, generally as a

homo or hetero-dimer (Kingsley, 1994).

Bmp-2 and *Bmp-4*, which encode very similar proteins, and *Bmp-7*, which is slightly more divergent, are expressed in *Xenopus* embryos. *Bmp-4* RNA is uniformly distributed throughout the *Xenopus* embryo at early gastrula stages (Dale et al., 1992). However, during gastrulation *Bmp-4* becomes restricted to the animal pole, ventral and lateral regions of the marginal zone, and is excluded from the organizer region and the prospective neural plate (Fainsod et al., 1994; Hemmati-Brivanlou and Thomsen, 1995). This expression pattern is consistent with a role in ventral specification. Less consistent with such a role are the expression patterns of *Bmp-2* and *Bmp-7*, which are present ubiquitously in ectoderm and mesoderm at blastula and gastrula stages, including the organizer (Clements et al., 1995; Hemmati-Brivanlou and Thomsen, 1995). The localisation and activity of Bmp proteins in *Xenopus* embryos is, however, unknown.

Over-expression of *Bmp-4* in early *Xenopus* embryos converts presumptive dorsal mesoderm into more ventral fates, including formation of blood and expression of ventro-lateral molecular markers (Dale et al., 1992; Jones et al., 1992; Schmidt et al., 1995). In ectodermal explants of embryos injected with *Bmp-4* RNA, epidermal differentiation is induced at the expense of neural structures (Sasai et al., 1995; Wilson and Hemmati-Brivanlou, 1995). Mis-expressed *Bmp-2* and *Bmp-7*, like *Bmp-4*, ventralise mesoderm and induce epidermal differentiation in ectoderm (Clements et al., 1995; Hemmati-Brivanlou and Thomsen, 1995).

Interestingly, direct exposure of explanted tissue to Bmp-2, Bmp-4 or Bmp-7 provided as homodimeric proteins function poorly in inducing ventral mesoderm. However, a purified recombinant heterodimer of *Xenopus* Bmp-4 (or Bmp-2) and Bmp-7 has potent mesoderm inducing activity at physiological concentrations, in addition to ventral mesodermal patterning activity (Nishimatsu and Thomsen, 1998). Based on the expression patterns of Bmp-2, Bmp-4 and Bmp-7, it is likely that Bmp-2(or 4)/7 heterodimers are produced in lateral and ventral tissues of the *Xenopus* early gastrula.

In contrast, inhibition of Bmp signalling causes ventral mesoderm to adopt dorsal fates. This has been shown by loss-of-function approaches using truncated forms of a Bmp type I receptor (Graff et al., 1994; Maeno et al., 1994; Schmidt et al., 1995; Suzuki

et al., 1994), antisense *Bmp-4* RNA (Steinbeisser et al., 1995), or dominant-negative forms of Bmp-4, Bmp-7 and Bmp-2 (Hawley et al., 1995; Suzuki et al., 1997). Interestingly, loss-of function experiments do not block induction of mesoderm (assessed by expression of the pan-mesodermal marker *Xbra*), suggesting that, in the embryo, Bmp signalling patterns mesoderm without inducing it. Studies of inhibition of Bmp-2/4/7 function in animal caps, using either a truncated type I Bmp receptor (Sasai et al., 1995), a truncated activin type II receptor (which also blocks Bmp-4; Wilson and Hemmati-Brivanlou, 1995) or a truncated type I activin receptor (which also blocks Bmp-7; Suzuki et al., 1997), show that ectoderm is induced to form neural tissue at the expense of epidermis.

The ability of Bmp-4 to ventralise mesoderm only becomes apparent once gastrulation has started and the organizer is induced. Evidence supporting this comes from the observation that over-expression of *Bmp-4* mRNA does not significantly block the initial induction of organizer specific genes, such as *goosecoid* and *Xnot*. However, after gastrulation has started, the expression of organizer markers rapidly disappears in *Bmp-4* injected embryos (Jones et al., 1996).

Bmp antagonists

Chordin(Sog)/Bmp(Dpp) antagonism

The existence of molecules that antagonise Bmp-4 function was hypothesised from the analysis of *Drosophila melanogaster* mutants. In *Drosophila*, the amount of neurogenic tissue is regulated by a dorso-ventral system of positional information in which the product of two genes, *decapentaplegic* (*dpp*) and *short-gastrulation* (*sog*), play antagonistic roles (Ferguson and Anderson, 1992; Francois et al., 1994; Holley et al., 1995). The vertebrate homologue of *dpp* is either *Bmp-4* or *Bmp-2* (Padgett et al., 1987) and the homologue of *sog* is *chordin* (Francois and Bier, 1995; Holley et al., 1995). *chordin* encodes a large secreted protein that possesses dorsalising and neuralising properties when over-expressed in the *Xenopus* embryo and at gastrula stages, *chordin* is expressed in the organizer region and prospective neural plate (Sasai et al., 1995; Sasai et al., 1994). The functions of *sog* and *chordin* are interchangeable

(Francois and Bier, 1995; Holley et al., 1995; Schmidt et al., 1995), so that *chordin* will rescue the *sog* mutation in *Drosophila* and *sog* will induce a secondary axis in *Xenopus* embryos. Furthermore, the *Drosophila sog/dpp* double mutant has the same phenotype as *dpp* alone, indicating that Sog acts through Dpp and has no additional effect of its own (Ferguson and Anderson, 1992; Holley et al., 1996).

Interestingly, the Bmp/Dpp interaction with Chordin/Sog may reflect an ancient means of dorso-ventral patterning predating the evolutionary branching of Arthropods and Chordates. However, an inversion in this signalling system seems to have occurred, so that Chordin specifies dorsal fates (and Bmp, ventral) in Chordates, whereas its homologue Sog specifies ventral fates (and Dpp, dorsal) in Arthropods. Based solely on morphological criteria, E. G. Saint-Hilaire in 1822 predicted the inversion in ventral/dorsal tissues in vertebrate and arthropod species (DeRobertis and Sasai, 1996; Jones and Smith, 1995).

Bmp-4 RNA can rescue dorsalised phenotypes created by injection of *chordin* RNA (Sasai et al., 1995) and the interaction between these two secreted factors is specific and direct. Chordin was shown to bind *in vitro* with high affinity to Bmp-4 (K_d=3x10^{-10}M), Bmp-2 and Bmp-4/Bmp-7 heterodimers, but not to activin or TGF-β1. It has been suggested that through this direct interaction Chordin specifically blocks the ability of Bmps to recognise their receptor (Fig. 1.4; Piccolo et al., 1996). Several other secreted factors expressed in the *Xenopus* organizer at gastrula stages have been demonstrated, like Chordin, to sequester Bmps. These include Noggin (Smith and Harland, 1992) and Follistatin (Hemmati-Brivanlou et al., 1994).

Noggin and Follistatin

noggin encodes a secreted polypeptide with no known homologues in *Drosophila* (Smith and Harland, 1992). Over-expression of *noggin* induces neural tissue in isolated explants of presumptive ectoderm and causes ventral marginal zone tissue to adopt dorsal fates (Lamb et al., 1993). Furthermore, co-injection of *noggin* with *Bmp-4* mRNA inhibits *noggin*-elicited neuralisation of animal caps (Xu et al., 1995). Biochemical studies have shown that Noggin is secreted as a dimer that binds Bmp-2 and Bmp-4 (K_d=2x10^{-11}M) with high affinity, binds Bmp-7 with slightly less affinity, but

does not bind to TGF-β (Zimmerman et al., 1996). Follistatin was previously characterised as an activin-binding factor but has been recently shown also to interact with Bmps (Fainsod et al., 1997).

It has been suggested that all these antagoniser molecules inhibit Bmp signalling by blocking interaction of Bmps with their receptors (Fig. 1.4), yet they are unrelated to each other at the primary sequence level. Their molecular contacts with Bmps may, therefore, differ (Cho and Blitz, 1998). Regardless of the mode of interaction with Bmps, their localised expression and Bmp antagonising activities suggests that at least one of their roles is to ensure the development of dorsal structures in the embryo.

Bmp-4 was shown to ventralise mesoderm in a dose-dependent manner along the dorsal-ventral axis, but no graded distribution of *Bmp-4* RNA has been found. A model has been proposed to explain these observations in which a gradient of Bmp-4 activity is regulated by long-range inhibition by Chordin and Noggin (Dosch et al., 1997; Jones and Smith, 1998). At present it is not known whether a gradient of Bmp morphogenetic activity corresponds to a gradient of protein concentration because it has not proved possible to quantify *in situ* the local concentration of Bmp protein.

The astacin family of metalloproteases

Genetic analysis of *dpp* signalling in *Drosophila* has identified *tolloid* as a potential regulator of Bmp signalling (Shimell et al., 1991). Tolloid is a member of the astacin family of metalloproteases that includes the only non TGF-β member of the Bmp family, Bmp-1. Recent genetic epistasis studies, together with biochemical analyses, have demonstrated that Tolloid functions upstream of Sog, and cleaves Dpp-Sog complexes (Marques et al., 1997). RNAs encoding Xolloid and Z-tld, the Tolloid-like metalloproteases identified in *Xenopus* and zebrafish respectively, are expressed ubiquitously at the beginning of gastrulation and the encoded proteins are able to cleave Chordin/Bmp complexes, thus releasing active Bmps (Blader et al., 1997; Piccolo et al., 1997). One difference in the proteolytic cleavage activity of *Drosophila* Tolloid and the two vertebrate proteases is that *Drosophila* Tolloid cleaves only the Dpp-Sog complex, whereas unbound *Xenopus* or zebrafish Chordin can be also proteolytically cleaved.

Taken together, the data suggest that the function of the 'Tolloid-like' members of the astacin metalloprotease family is, ultimately, to regulate the amount of free Bmp/Dpp at the cell surface by controlling the availability of Chordin/Sog. In support of this view, *Xolloid* over-expression inhibits development of dorso-anterior structures in whole embryos (Goodman et al., 1998). Furthermore, dorsal injections of *Xolloid* RNA into *Xenopus* embryos block secondary axis formation caused by *chordin*, but not by *noggin*, *follistatin*, or dominant-negative Bmp receptor injections (Piccolo et al., 1997).

Bmp receptors

Members of the TGF-β family, including Bmps, bind to two different types of serine-threonine kinase receptors, type I and type II, both of which are required for signal transduction (Fig. 1.4). Overall the structures of the type I and type II receptors are similar; they both have a relatively short extracellular domain with some conserved cysteine residues, a single transmembrane domain and an intracellular domain containing a serine-threonine kinase region. However, a unique feature of type I receptors is a highly conserved 30-amino acid region immediately preceding the kinase domain, termed the GS domain, which contains a characteristic SGSGSG sequence (Kawabata et al., 1998; Massague, 1998).

The first *Xenopus* TGF-β family receptor to be cloned was an activin type II receptor (Hemmati-Brivanlou and Melton, 1992), but others have since been identified. Table 1.1 shows vertebrate type I and type II TGF-β receptors, grouped by similarities in the kinase domains and by signalling activities.

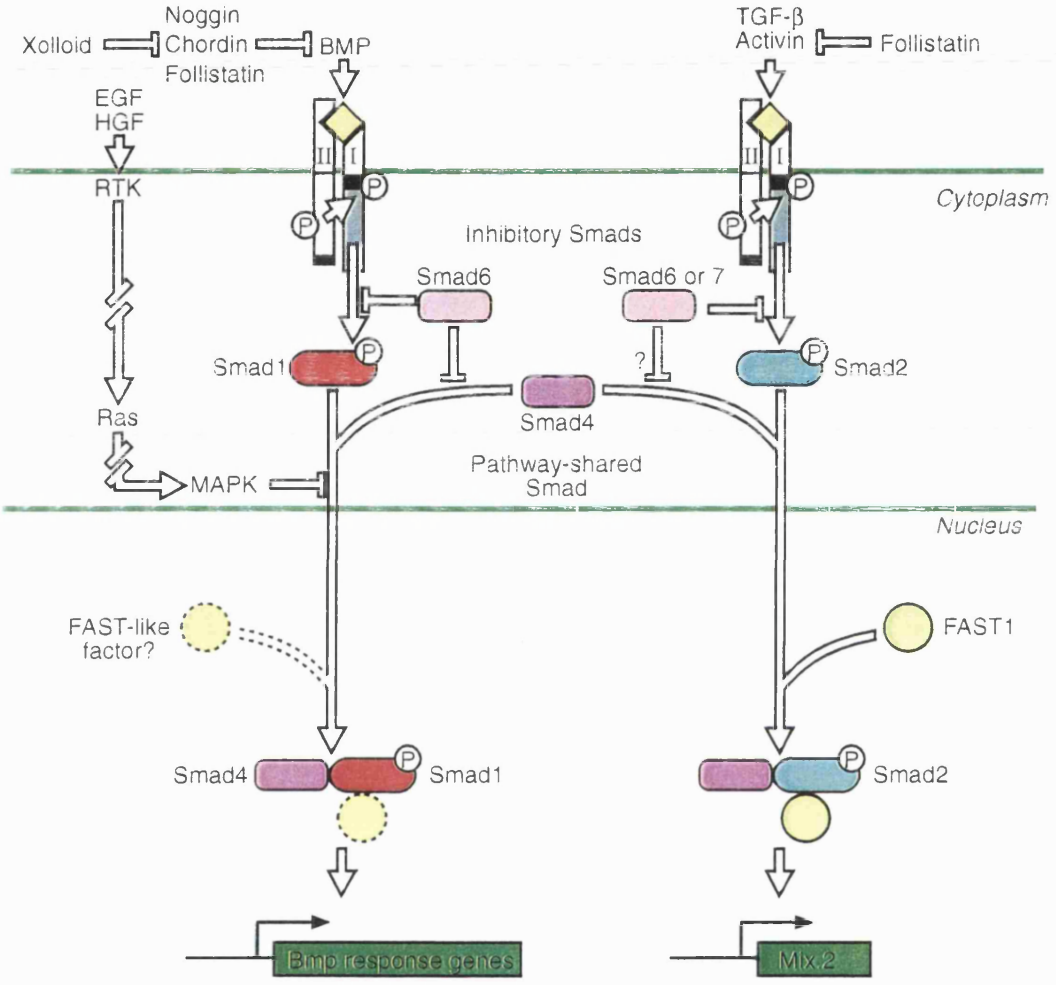

Fig. 1.4 TGF-β family signalling pathway illustrating several inhibitory mechanisms, which occur within and outside the cell and serve to control the extent of Bmp/TGF-β/Activin signalling. This diagram illustrates results obtained from experiments performed in cell culture and in the *Xenopus* embryo. See text for details. Adapted from Kretzschmar and Massague (1998).

Table 1.1. Mammalian TGF-β receptors and its homologues in *Xenopus laevis*.

	Mammals	*Xenopus laevis*
Type I	TβR-I (ALK5) ActR-IB (ALK4) ALK7	X-ActR-IB (Chang et al., 1997) X-TrR-I (Mahony and Gurdon, 1995)
	BMPR-IA (ALK3) BMPR-IB (ALK6)	X-BMPR-I A (Graff et al., 1994)
	ALK1 ActR-I (ALK2)	X-ActR-I (Suzuki et al., 1997)
Type II	TβR-II BMPR-II AMHR	X-BMPR-II (Frisch and Wright, 1998)
	ActR-II ActR-IIB	X-ActR-II (Hemmati-Brivanlou and Melton, 1992)

Models for ligand-mediated activation of the Bmp receptor, based on studies of the receptors for TGF-β, stipulate that the ligand recognises the intrinsically active type II receptor serine/threonine kinase. Then, the type I receptor, which is unable to bind ligand in the absence of the type II receptor, is recruited to the complex formed by the ligand and the type II receptor. This mode of binding to the receptor is characteristic of TGF-β and activin ligands (reviewed in Heldin et al., 1997), but it differs slightly for Bmps, where both type I and type II Bmp receptors can bind the ligand. This was shown by comparing the affinities of binding of Bmp to type I and type II Bmp receptors expressed together or separately. High affinity binding was observed when the two types of receptors are expressed together whereas low affinity binding occurs when they are expressed separately (Heldin et al., 1997; Liu et al., 1995).

Regardless of the specific mode of interaction with the ligand, binding always induces the formation of a heteromeric complex of type I and type II receptors. Given the dimeric nature of the ligands, each ligand monomer might contact one type I and one type II receptor, thereby generating a heterotetrameric receptor complex. Indeed, analysis of ^{125}I-labelled TGF-β1 crosslinked to its receptors has suggested that the signalling complex is a heterotetramer consisting of two type I receptors and two type II

receptors (Yamashita et al., 1994).

Following ligand-induced association of the two receptor classes, the type II receptor phosphorylates the type I receptor on glycine and serine residues in the GS domain, and this phosphorylation event activates the type I receptor, which then mediates downstream signalling (Massague, 1998; Wrana et al., 1994). This receptor activation model predicts that the type II and type I receptors act in sequence. A role for type I receptor in downstream signalling is shown by the finding that a single amino acid substitution in the GS domain of type I receptors results in constitutive ligand-independent activation of the downstream signalling cascade (Attisano et al., 1996; Wieser et al., 1995).

The specificity of signalling by Bmps can be partly explained by the specificity and binding affinity of Bmp ligands for Bmp receptors. However, ligand specificities and affinities of ligands for receptors within the TGF-β family are often promiscuous.

Within the Bmp type I receptors, binding affinities for BMPR-IA and IB are different for different Bmps (ten Dijke et al., 1994), but they remain restricted to Bmp ligands and thus are Bmp-specific receptors. In the same way, BMPR-II is the type II Bmp-specific receptor. However, the activin type I receptor, ActR-I (ALK2) exemplifies a case of promiscuity. This receptor binds with higher affinities to activin, but it also interacts with Bmp7 and probably other Bmps (ten Dijke et al., 1994). The *in vivo* relevance of ActR-I binding to Bmps is still debatable and the identity of its physiological ligands remains to be determined. Another example concerns the type II activin receptors (ActRII and ActR-IIB). Either of these receptors can bind certain members of the Bmp family (Bmp-2 and Bmp-7) when expressed in concert with Bmp type I receptors or ActR-I, although binding affinities for Bmps are lower than those for activins (Heldin et al., 1997; Liu et al., 1995; Yamashita et al., 1995). This situation is summarised in the table below.

Table 1.2 Bmp and activin ligands and respective type I and type II receptors.

Type I	Type II	Ligands
BMPR-IA/BMPR-IB	BMPR-II	Bmps
	ActRII/ActRIIB	
ActRI	BMPR-II	
	ActRII/ActRIIB	Bmps Activin
ActRIB	ActRII/ActRIIB	Activin

In conclusion, the combination of the number of different Bmp ligands, their multiple possible heterodimer combinations, and the different type I / type II receptor combinations to which they can bind, generate a vast range of different signalling activities. In particular, this poses problems to approaches involving inhibition of Bmp function by the use of dominant-negative versions of the Bmp receptors or ligands, and results should be analysed with caution.

Since the type I receptor transduces the TGF-β family signals, the intracellular region of this type of receptor should be able to transfer the specificity of the signal to the intracellular components of the respective transducing pathway. Experiments to identify the regions that control receptor signalling specificity have been conducted in the constitutively activated ActR-I (ALK-2) and ActR-IB (ALK-4) and have implicated the loop between kinase subdomains IV and V (the β4-β5 loop) in mediating the strong dorsal gene inducing properties of ALK-4 when over-expressed in *Xenopus* embryos. The 7 amino acids that make up this loop are capable, when transferred from constitutively activated ALK-4 to ALK-2, of carrying with them the ability to induce dorsal markers (Armes et al., 1999). An analogous result has been obtained using the TGF-β receptor TβR-I (ALK-5) and ALK2 in a tissue culture system (Feng and Derynck, 1997). It is therefore possible that the same loop transduces Bmp responses in the type I Bmp receptor.

Intracellular Bmp signalling: Smads

A breakthrough towards the understanding of the TGF-β family signalling pathway came from genetic screens conducted in two different organisms. *Mothers against dpp* (*Mad*) and *Medea*, were isolated in an attempt to identify enhancers of *dpp* mutations in *Drosophila* (Sekelsky et al., 1995) and *Sma-2-3* and *-4* were identified in *Caenorhabditis elegans* as genes whose mutations show identical phenotypes to a type II serine threonine kinase receptor of *C. elegans*, *daf-4* (Savage et al., 1996). Analysis of *Sma* genes revealed that they code for homologous Mad-related proteins, named therein Smads, which act downstream of the serine-threonine kinase receptor (Savage et al., 1996).

To date, several different vertebrate Smads have been identified and these can be classified into three major classes according to structural and functional criteria: pathway-restricted Smads, pathway-shared Smads and inhibitory Smads (for a review see Cho and Blitz, 1998; Kretzschmar and Massague, 1998). Among the first group, Smad1 and presumably its close homologues Smad5 and Smad8, are mediators of Bmp signalling, whereas Smad2 and Smad3 mediate TGF-β and activin signals in vertebrates. *Xenopus Smad1* and *Smad8* (*XSmad1* and *XSmad8*) have been identified and their transcripts are present ubiquitously during blastula and early gastrula stages, and *XSmad8* becomes restricted to the ventral side during gastrula stages (Graff et al., 1996; Nakayama et al., 1998). *Smad5* has not yet been identified in *Xenopus* but mouse *Smad5* was shown to have ventralising effects when over-expressed in *Xenopus* embryos (Suzuki et al., 1997). Two pathway shared Smads have been identified in *Xenopus*, XSmad4-α and XSmad-β which can both cooperate with Smad1 or Smad2 to mediate signalling responses (Masuyama et al., 1999). Inhibitory Smads, Smad6 and Smad7 have also recently been found in *Xenopus* embryos (Casellas and Brivanlou, 1998; Nakayama et al., 1998).

Smads transduce Bmp signals from the membrane to the nucleus

Current models propose that pathway-restricted Smads associate with type I receptors following activation of type I-type II receptor complexes in response to ligand stimulation. The Smads are then phosphorylated on specific serine residues and released

from the type I receptor to form a stable complex with a common-mediator Smad, Smad4. This complex translocates from the cytoplasm to the nucleus where it regulates transcriptional responses to TGF-β ligands (Fig. 1.4). Evidence that has led to the formation of this model, in particular involving the Smads that transduce Bmp signals, is described below (for reviews see Heldin et al., 1997; Kretzschmar and Massague, 1998).

Smad1 was shown to be a direct substrate of BMPR-I *in vitro*, as incubation with the BMPR-I kinase domain led to phosphorylation at specific serines at the C-terminus of Smad1 (Kretzschmar et al., 1997). Phosphorylation occurs at a serine motif SS(V/M)S, which is present in other pathway-specific Smads but is not present in Smad4 (Fig. 1.5). This is consistent with the failure of this Smad to undergo Bmp or TGF-β-induced phosphorylation *in vivo* (Lagna et al., 1996; Zhang et al., 1996). The transient nature of the receptor/Smad complex did not allow its detection for BMPR-I and Smad1, but such a complex has been observed for Smad2 and Smad3 and the TGF-β receptor (Macias-Silva et al., 1996; Zhang et al., 1996). This interaction required the activation of the receptor by the ligand (Macias-Silva et al., 1996).

Smad4, originally identified as the product of the *DPC4* tumour suppressor gene (Hahn et al., 1996), was shown to be a common mediator of the TGF-β family signalling pathway due to its association with Smad1 or Smad2 upon activation of the respective receptors (Lagna et al., 1996). Furthermore, the requirement of Smad4 for activin and Bmp responses in *Xenopus* embryo suggested that this Smad participated in both TGF-β/activin and Bmp signalling pathways (Lagna et al., 1996). In particular, the interaction between pathway-specific Smads and Smad4 is mediated by their carboxyl domains (Fig. 1.5; Hata et al., 1997) and mutation of the carboxy-terminal serines of Smad1 that are phosphorylated in response to Bmp signalling prevents its association with Smad4 (Kretzschmar et al., 1997).

Smad1 was shown to translocate to the nucleus of cells in response to a Bmp signal (Hoodless et al., 1996; Liu et al., 1996). In particular, mutations in the C-terminal serine residues of Smad1 and Smad2 prevent nuclear translocation, suggesting that this event is depend upon receptor-mediated phosphorylation of Smad1 and Smad2 (Kretzschmar et al., 1997; Macias-Silva et al., 1996). Furthermore, these mutations

prevent the ligand-dependent activation of transcriptional responses via Smad1 (Kretzschmar et al., 1997) or Smad2 (Macias-Silva et al., 1996).

The transcriptional activity of Smad1 and Smad4 was first detected in a reporter assay using Gal4-Smad fusion constructs (Liu et al., 1996). However, an important contribution towards our understanding of the role of Smads in transcriptional regulation came with the identification of Smads as components of the 'activin-response-factor' (ARF) which binds the promoter of the immediate-early activin response gene *Mix.2* in *Xenopus* (Chen et al., 1996; Chen et al., 1997). ARF is a DNA-binding complex that assembles onto the *Mix.2* promoter in response to activin, TGF-β and Vg-1. The complex contains Smad2, Smad4 and the winged-helix transcription factor FAST-1 (Chen et al., 1996; Chen et al., 1997; Liu et al., 1997). FAST-1 is a DNA-binding nuclear protein that associates with the C-terminus of Smad2 in response to TGF-β/activin signalling (Fig. 1.5; Chen et al., 1997; Liu et al., 1997). Transcriptional activation of a reporter construct containing the activin-response element of the *Mix.2* promoter is dependent on Smad4 since it occurs in Smad4 defective cells only after transfection with Smad4 (Liu et al., 1997). Interestingly, both the carboxy and the amino terminal regions of Smad4 are essential for activation of the *Mix.2* promoter, apparently contributing both to DNA-binding and transactivation functions (Liu et al., 1997). These observations suggest that after receptor-mediated phosphorylation, Smad2/Smad4 association in the cytoplasm and nuclear translocation, the complex forms transcriptionally active complexes with DNA-binding subunits such as FAST-1 to regulate transcription of response genes (Liu et al., 1997). A similar model may be applicable to Smad1-mediated transcriptional regulation of Bmp response genes (Fig. 1.4).

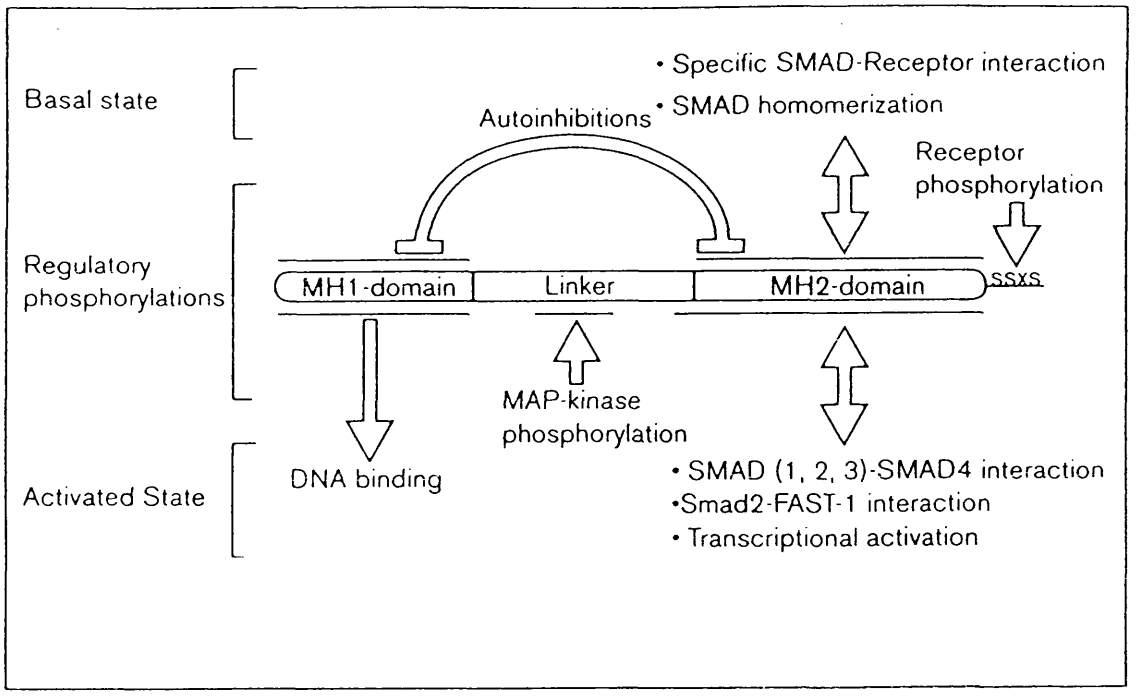

Fig. 1.5 Smad protein domains and their functions. Smad proteins can generally be divided into three different domains: the amino-terminal or MH1-domain, the linker domain and the carboxy-terminal or MH2-domain. The MH1 and the MH2 domains are highly related in sequence amongst the Smads, and the linker domain is usually more divergent. The model shows the known functions of the domains in the absence of signalling (basal state, shown on the top) or in the presence of signalling (activated state, shown on the bottom). Not all functions or phosphorylation sites are found or have been demonstrated for all Smads. See text for details. From Kretzschmar and Massague (1998).

Smad protein domains and their functions

Smad proteins consist of three regions, in particular two highly conserved regions – named the N-terminal and C-terminal domains or MH1 and MH2 domains, respectively – and a linker region, which is variable in sequence and length (Fig. 1.5).

The MH2 domain is regarded as the Smad effector domain because it contains the sites for receptor-mediated phosphorylation and activation (Kretzschmar et al., 1997; Macias-Silva et al., 1996), it displays transcriptional activity when fused to the heterologous DNA binding domain of Gal4 (Liu et al., 1996) and it mediates homomeric and heteromeric interactions between Smad4 and the pathway restricted Smads (Hata et al., 1997; Wu et al., 1997). The latter finding has been confirmed by the recent solving of the crystal structure of the Smad4 MH2 domain (Shi et al., 1997). The MH2 domain forms homotrimers, the key residues of which are conserved among Smads and are mutated in the majority of tumourogenic Smad4 mutants. This suggests that formation of homotrimers via the MH2 domains is essential for Smad function and thus likely to occur in all Smads. Interestingly, mutations in one loop protruding to the surface of Smad4 MH2, the so-called L3 loop, prevent interaction with Smad2. This suggests that the three protruding L3 loops in the Smad4 trimer are the site of interaction with pathway-restricted Smads (Lo et al., 1998; Shi et al., 1997).

In the absence of TGF-β family signalling, the MH1 domain inhibits the transcriptional activity of the Smad1 MH2 region (Liu et al., 1996), and the MH1 domains of Smad2 and Smad4 prevent the interaction of their associated MH2 domains by direct physical interference (Hata et al., 1997). Furthermore, additional experiments show that the MH1 domain of *Drosophila* Mad has specific DNA-binding activity which is required for Dpp-induced activation of the *vestigial* wing-patterning gene, and which, interestingly, can be inhibited by the presence of the Mad MH2 domain (Kim et al., 1997). Taken together, the available evidence suggests that, in the absence of signalling, the MH1 and MH2 domains interact with each other acting as reciprocal inhibitors. Upon receptor-mediated phosphorylation, this interaction may be altered and each domain can exert its respective activities (Kretzschmar and Massague, 1998).

The linker region, the most divergent of the Smads regions, may contain

phosphorylation sites important for regulation via MAP kinases activated by tyrosine kinase activated receptors (see below).

Smad-mediated regulation of the Bmp signalling

Pathway-restricted Smads and the pathway-shared Smad4, as crucial mediators of Bmp signalling, are likely to be subjected to tight regulation. To date, four different intracellular mechanisms involving Smads are known to regulate Bmp signalling (and TGF-β signalling in general). Two of these regulatory mechanisms occur via the inhibitory Smads - Smad6, Smad7 and the *Drosophila* product of *Daughters against dpp* gene (*Dad*). Inhibitory Smads include the most divergent members of the Smad family which, like Smad4, lack the carboxy-terminal SSXS phosphorylation motif (Hata et al., 1998; Hayashi et al., 1997; Imamura et al., 1997; Nakao et al., 1997; Tsuneizumi et al., 1997). Smad6 can inhibit both Bmp and TGF-β signalling in cultured cells (Imamura et al., 1997) as well as Bmp signalling in *Xenopus* embryos (Hata et al., 1998). Smad7 was shown to inhibit TGF-β signalling in mammalian cells (Hayashi et al., 1997; Nakao et al., 1997) and TGF-β/activin signalling in *Xenopus* embryos (Nakao et al., 1997). The *Dad* gene inhibits patterning by *dpp* in the *Drosophila* imaginal wing disk (Tsuneizumi et al., 1997).

Smad6 and Smad7, unlike Smad4, interact with type I receptors, as demonstrated by the association of Smad6 with several different type I receptors, including TGF-β and Bmp receptors, and the association of Smad7 with the TGF-β receptor (Hata et al., 1998; Hayashi et al., 1997; Imamura et al., 1997; Nakao et al., 1997). The interaction of Smad6/7 with the type I receptors is more stable than that of the pathway-restricted Smads, presumably because, without the carboxy-terminal phosphorylation site, release of a phosphorylated Smad from the activated receptor cannot occur. Thus, the inhibitory Smads may act by competing with pathway-restricted Smads for binding to the type I receptor (Fig. 1.4). Consistent with this idea, Smad6 inhibits Bmp or TGF-β- mediated phosphorylation of Smad1 or Smad2 (though not Smad3), respectively (Imamura et al., 1997). Furthermore, Smad7 inhibits phosphorylation of Smad2 and Smad3 by the activated TGF-β receptor (Hayashi et al., 1997; Nakao et al., 1997).

In addition, inhibitory Smads may sequester pathway-specific Smads (Fig. 1.4). This model has been suggested in response to two observations. First, full-length Smad6 is able to interact specifically with Smad1 (but not with Smad2) to form an inactive Smad1/6 complex, therefore competing with Smad4 for binding to Smad1 (Hata et al., 1998). Second, Smad6, which is unique in that it seems to lack an MH1 domain, can form stable complexes with Smads 1, 2, 4 and 7 (Topper et al., 1997).

It is necessary to stress that the issue of specificity of the inhibitory Smads is unclear at present. Moreover, over-expression approaches are not adequate to solve this issue since endogenous concentrations of type I receptors, pathway-restricted Smads and inhibitory Smads, which may be crucial for inhibition *in vivo* by the inhibitory Smads, will be altered by over-expression of a component of the pathway (Whitman, 1997). However, it will be important to distinguish whether inhibitory Smads are specific inhibitors, controlling one developmental pathway at the expense of another, or whether they are general inhibitors, acting in a feedback loop of autoregulation general to all TGF-β signalling pathways.

A third mechanism of regulation of the Bmp/TGF-β signalling pathway is centred on Smad4 itself. Candia and collaborators (1997) proposed that the intracellular abundance of Smad4 protein may be limiting, and simultaneous activation of Bmp and activin/Vg-1 signalling in *Xenopus* embryos may result in competition for binding Smad4 by different pathway-specific Smads. The outcome of this competition will determine the relative strengths of the competing signals, ultimately leading to specification of more dorsal or more ventral types of mesodermal tissues (Candia et al., 1997). Intracellular levels of Smad4 in response to TGF-β signals are, however, unknown at present.

The fourth mechanism to regulate the Smad1/Bmp signalling pathway was recently revealed following the discovery of *in vivo* phosphorylation sites other than those targeted by the receptors, which are localised in the linker region of Smad1 (Kretzschmar et al., 1997). These sites are subjected to regulation *in vivo* and *in vitro* by the Erk subfamily of MAP kinases after its activation by mitogenic factors – such as epidermal growth factor (EGF) or hepatocyte growth factor (HGF) – which signal

through receptor tyrosine kinases. This regulation is independent of the carboxy-terminal Bmp receptor-mediated phosphorylation and does not directly control the association of Smad1 with Smad4 (Kretzschmar et al., 1997). Instead, phosphorylation in the linker region of Smad1 inhibits nuclear accumulation of Smad1 in the presence of activated Bmp receptors (Fig. 1.4; Kretzschmar et al., 1997). The precise mechanism by which this occurs, however, requires further elucidation since in the absence of Bmp signalling, mutation of the linker serines in Smad1 causes nuclear localisation, while the wild type protein is cytoplasmic. This suggests that linker phosphorylation also has a role in maintaining Smad1 in the cytoplasm in the absence of Bmp signalling.

Other mediators of Bmp signalling

Another pathway that acts downstream of the Bmp type I receptor involves TAB1 (Shibuya et al., 1996), a protein that binds to and regulates the activity of a MAP kinase kinase kinase (MAPKKK) protein called TAK1 (Yamaguchi et al., 1995). It has been demonstrated that TAK1 is involved in at least one TGF-β-induced transcriptional response, and its kinase activity is stimulated in response to TGF-β or Bmp-4 (Yamaguchi et al., 1995). The *Xenopus* homologue of TAK1, XTAK1, induces cell death. However, co-injection of both *XTAK1* and *XTAB1* (*Xenopus TAB1*) together with the apoptosis inhibitor *bcl-2* in dorsal blastomeres not only rescued the cells from death but also induced differentiation of ventral mesoderm in *Xenopus* animal pole explants (Shibuya et al., 1998). Furthermore, expression of a 'kinase dead' version of XTAK1 reduces ventral mesoderm induction by Smad1, Smad5 and Bmp-4 and partially rescues phenotypes generated by a constitutively active BMPR-IA (Shibuya et al., 1998). Thus, XTAK1 and XTAB1 may function in the Bmp signal transduction pathway in *Xenopus*, possibly in cooperation with Smad signalling.

Recently, the human X-chromosome-linked inhibitor of apoptosis protein (XIAP) was isolated as a TAB1-binding protein, which also associates with Bmp receptors in mammalian cells (Yamaguchi et al., 1999). Injection of *XIAP* mRNA into dorsal blastomeres enhanced the ventralisation of *Xenopus* embryos in a TAB1/TAK1-dependent manner, whereas a truncated form of XIAP lacking the TAB1-binding domain partially blocked the expression of ventral mesodermal marker genes induced by

a constitutively active Bmp type I receptor. These results suggest that XIAP is a positive regulator of the Bmp signalling pathway, mediating an interaction between the Bmp receptor and TAB1 (Yamaguchi et al., 1999). Moreover, these results support the idea of a need for inhibition of apoptosis in order for specification of ventral fates to occur.

Bmp signalling in other vertebrate systems: zebrafish and mouse

The *Xenopus laevis* embryo is unsuitable for genetical analysis. However, genetic evidence for a role of the Bmp signalling pathway in establishing the embryonic axis can be found in other vertebrates, such as the zebrafish (*Danio rerio*) and the mouse (*Mus musculus*).

The zebrafish egg undergoes cleavage differently from *Xenopus*, however gastrulation shares many features in common with *Xenopus*. Just before gastrulation, the zebrafish embryo consists of two layers of cells (the blastoderm), which expand over the yolk cell in the direction of the vegetal pole (epiboly). Gastrulation begins at 50% epiboly with the prospective endoderm and mesoderm of the deep layer of cells turning inwards. This process is very similar to dorsal involution in *Xenopus* in all but one respect, which is that it occurs all around the periphery of the blastoderm at about the same time. The equivalent of the *Xenopus* organizer - the embryonic shield – is visible as a thickening of the dorsal blastoderm margin. The remaining gastrulation movements in zebrafish are similar to those occurring in *Xenopus* (Solnica-Krezel, 1999; Wolpert, 1998).

Mutations define at least 9 genes, summarised in the table below, that affect dorsal/ventral patterning during zebrafish gastrulation (for a review see Solnica-Krezel, 1999).

Table 1.3 Zebrafish mutations affecting dorsal/ventral axis specification.

Locus	Molecule encoded	Mutation	Phenotype	Reference
chordino *mercedes* *ogon*	Chordin unknown unknown	Null	Ventralised: more blood and pronephros, multiple ventral fin folds, increased expression of the ventral marker *eve1*; concomitant decrease in dorso-lateral fates, mostly somites and neurectoderm.	(Hammerschmidt et al., 1996; Schulte-Merker et al., 1997; Solnica-Krezel et al., 1996)
swirl *somitabun* *snailhouse* *lost-a-fin* *piggytail* *mini-fin*	zBmp-2 zSmad5 unknown unknown unknown z-Tolloid	Not null Antimorphic Not null	Dorsalised: expansion of somites and neurectoderm and variable degrees of reduction of ventral and posterior fates, such as lack of caudal fin, deletions of trunk and tail, reduction in amount of blood and pronephros.	(Connors et al., 1999; Hild et al., 1999; Kishimoto et al., 1997; Mullins et al., 1996; Nguyen et al., 1998; Solnica-Krezel et al., 1996).

Mutants are divided into two groups. One class of mutants presumably lacks the function of genes required for dorsal determination and therefore exhibits an increase in ventral fates (blood, pronephros, multiple ventral fin folds), and a concomitant decrease in dorso-lateral fates, mostly somites and neurectoderm. These include *chordino*, *mercedes*, and *ogon* (Table 1.3). The ventralised mutant *chordino* carries a null mutation in the zebrafish homologue of *chordin* and this gene is expressed dorsally at the embryonic shield stage in wild type fish (Schulte-Merker et al., 1997). Conversely, another class of mutants appear dorsalised and therefore may lack the function of genes involved in ventral specification. The mutant *swirl*, *somitabun*, *snailhouse*, *lost-a-fin*, *piggytail* and *mini-fin* belong to this class of mutants (Table 1.3). The encoded molecules have been identified for some of these mutations and, in all cases so far, they correspond to homologues of components of the Bmp signalling in *Xenopus*. Taken together, these results strongly support a role of the Bmp signalling pathway (and its antagonisers) in dorso-ventral patterning of the vertebrate embryo.

Mouse embryos arrive at gastrulation in a very different state than those of *Xenopus* and zebrafish because they first differentiate extraembryonic tissue necessary for their survival *in utero*. As a result, the mouse embryo at the start of gastrulation

(approximately 6,5 days postcoitum (dpc)) comprises a cup-shaped epithelial layer of cells (the epiblast) connected at its proximal end (the top of the cup) to extraembryonic ectoderm, and surrounded by extraembryonic visceral and parietal endoderm (Beddington and Robertson, 1999). At this stage the primitive streak forms at the future posterior pole of the embryo, which is where epiblast cells undergo an epithelial-mesenchyme transformation to generate mesoderm. The node, the equivalent of the organizer in *Xenopus*, forms at the most anterior part of the streak. However, the node is only able to induce a partial secondary axis lacking the most anterior structures such as the forebrain (Beddington, 1994). This activity mimics only partially the properties of the *Xenopus* organizer and resembles instead the activity of the trunk *Xenopus* organiser (Harland and Gerhart, 1997). Interestingly, recent evidence has emerged for a patterning activity in the extraembryonic anterior visceral endoderm (AVE), which occurs before the formation of the primitive streak, and which is responsible for inducing the most anterior structures of the embryo (reviewed in Beddington and Robertson, 1998; Beddington and Robertson, 1999). The AVE is likely the equivalent of the head organizer in *Xenopus* (Beddington and Robertson, 1999).

The phenotypes of mice bearing knockouts in some of the Bmp signalling pathway components are summarised on the table below.

Table 1.4 Mouse targeted mutations in some locus coding for Bmp signalling pathway components.

Locus	Molecule encoded	Mutation	Phenotype	Reference
Bmp-4	Bmp-4	Null	Variable; most homozygous arrest development at the egg cylinder stage and do not develop mesoderm	(Winnier et al., 1995)
BMPR-I	BMPR-I	Null	Homozygous die between 7 dpc and 9.5 dpc; small in size and with no mesoderm	(Mishina et al., 1995)
Smad4/DPC4	Smad4	Null	Homozygous die at approximately 7,5 dpc; small in size and with no mesoderm; other defects	(Sirard et al., 1998; Yang et al., 1998)

Targeted mutation of the *Bmp-4* locus generated variable phenotypes, of which the most frequent was arrest at the egg cylinder stage (6.5 dpc), a time which correlates with the first detection of low levels of *Bmp4* transcripts in the posterior primitive streak of the embryo (Winnier et al., 1995). Homozygous embryos did not form mesoderm as assessed by the expression of the mesodermal marker *T* (*Brachyury*). More advanced mutant phenotypes ranged from the neural-fold/early somite stage to a few embryos that had undergone turning and beating of the heart. All embryos were smaller and retarded in comparison to their littermates and had disorganised or truncated posterior structures (Winnier et al., 1995). These results suggest that Bmp-4 in the mouse is first required just before gastrulation, perhaps for proliferation and survival of the epiblast cells, for survival of newly formed mesodermal cells or, alternatively, for mesoderm induction (although in this case the embryos would be predicted to develop excessive ectoderm). The variability of the observed phenotypes can be explained by a requirement of Bmp-4 at different developmental stages. Therefore, in the presence of rescuing factors (perhaps maternal Bmps or embryonic Bmp-2, which is transcribed from 6.5 dpc), development might proceed beyond 6.5 dpc, although at a slower rate than normal, until the next step at which Bmp-4 is required.

Smad4 transcripts are uniformly distributed throughout development and, at 7 dpc, *BMPR-IA* transcripts are also detected homogeneously throughout the epiblast and

mesoderm (Mishina et al., 1995; Sirard et al., 1998; Yang et al., 1998). The phenotypes observed for targeted null mutations in *BMPR-IA* (*ALK3*) and *Smad4* (Mishina et al., 1995; Sirard et al., 1998; Yang et al., 1998) present many similarities with the earliest phenotypes of Bmp-4 homozygous embryos. Both are small in size and do not form mesoderm, as judged by the absence of a number of early mesodermal markers, including *T* (Mishina et al., 1995; Sirard et al., 1998; Yang et al., 1998). The fact that *BMPR-IA* homozygous mice do not develop beyond the egg cylinder stage, a phenotype more severe than that observed for *Bmp-4* homozygous mice (Winnier et al., 1995) can be explained by the fact that *BMPR-I* mutant embryos impair signalling from all known Bmps present at those stages (Bmp-2, -4 and –7).

An implication of the mouse, *Xenopus* and zebrafish studies presented is that the Bmp pathway is conserved in vertebrates. The mouse mutational studies, however, suggest that Bmp signalling is required for formation of all mesoderm whereas the *Xenopus* work indicates that it is necessary just for dorso-ventral patterning. This difference is unlikely to be due to a lack of genetical approaches in *Xenopus,* because zebrafish bearing mutations in the Bmp pathway, and in particular the mutant *chordino* which carries a null mutation, also show defects just in the dorso-ventral patterning. Therefore, Bmp signalling in mouse appears to act before mesoderm formation, which is consistent with the expression pattern of Bmp in the mouse embryo (Winnier et al., 1995), whereas in *Xenopus* and zebrafish Bmp signalling is essential for dorso-ventral patterning of the embryo.

Potential Bmp response genes

The Bmps mediate ventral patterning of the embryo by activating several response genes, which can act as immediate-early responses when their activation occurs in the absence of *de novo* protein synthesis and cell-to-cell signalling. In addition to *Xom* (Ladher et al., 1996), several other homeobox-containing genes that act as potential Bmp response genes have been identified in *Xenopus*. These include *Xvent-2* (Onichtchouk et al., 1996), *Xvent-2B* (Rastegar et al., 1999), *Xbr-1* (Papalopulu and Kintner, 1996), *Vox* (Schmidt et al., 1996), *Xvent-1* (Ault et al., 1996), *Xvent-1B* (Rastegar et al., 1999), *PV.1* (Gawantka et al., 1995), *Xmsx-1* (Maeda et al., 1997; Suzuki et al., 1997) and *Xvex-1*

(Shapira et al., 1999). Another family of putative transcription factors shown to be regulated by Bmp-4 includes the zync finger transcription factors of the GATA family. In particular *XGATA-1* and *XGATA-2* (Zon et al., 1991) mediate the effect of Bmp-4 in stimulating erythropoiesis (Kelley et al., 1994; Maeno et al., 1996; Walmsley et al., 1994; Xu et al., 1997; Zhang and Evans, 1996; Zhang and Evans, 1994). However, it has not been established whether these GATA factors act as immediate-early response genes to Bmp-4.

Xmsx1, the *Xenopus* homologue of the *Drosophila muscle segment* gene (*msh*), is an homeobox gene unrelated to *Xom* which is induced in an immediate-early fashion in response to Bmp-4 signalling. Evidence for this comes from several different observations. First, *Xmsx1* is induced by Bmp signalling in *Xenopus* ectoderm and mesoderm and, in particular, induction of *Xmsx1* expression by Bmp-4 in dissociated ectodermal cells occurs in the presence of a protein synthesis inhibitor (cycloheximide) (Maeda et al., 1997; Suzuki et al., 1997). Second, *Xmsx1* rescues neuralisation of animal caps by a dominant-negative Bmp type I receptor (Suzuki et al., 1994; Suzuki et al., 1997) and the gene is expressed at the right place and time to be a mediator of Bmp signalling effects in both the ectoderm and the mesoderm (Maeda et al., 1997; Suzuki et al., 1997). *Xmsx-1* does not mimic, however, all activities of Bmp-4 in the embryo since it acts in the marginal zone to specify dorso-lateral derivatives (such as muscle) while it suppresses ventral specification (as detected by the expression of α-globin ventral marker; Maeda et al., 1997). The role of *Xmsx-1* is however still controversial since previous studies report dorsal expression and axis-inducing activity for this gene (Chen and Solursh, 1995; Su et al., 1991).

Xvex-1 shares low amino acid identity at the level of the homeodomain with Xom (55%). It exhibits a ventral pattern of expression similar to *Xvent-1* but its temporal pattern of expression resembles that of *Xom* (see below). *Xvex-1* expression is regulated by the Bmp-4 signalling pathway during gastrulation, over-expression of *Xvex-1* results in ventralisation of *Xenopus* embryos and partial loss of *Xvex-1* function by injection of antisense RNA causes slight dorsalisation of the embryos and expansion of organizer genes like *goosecoid* (Shapira et al., 1999).

The remaining homeobox-containing genes presented above share high homology at the level of the homeodomain. For this reason they were included in the same family – the Xvent family of genes (Rastegar et al., 1999). The amino acid sequence of Xom and of its related counterparts is depicted in Fig. 1.6. The sequences can clearly be subdivided into two groups, which share high homology at the level of the homeodomain (approximately 80%), but lack any apparent homology in the N- and C-terminal flanking regions. The first subgroup includes *Xom*, *Xvent-2*, *Xvent-2B*, *Vox*, and *Xbr1* and the second subgroup contains *Xvent-1*, *Xvent-1B* and *PV1*. Within each subgroup, individual members share 92%-100% identity in the homeodomain region and 82%-99% identity over the entire sequence (Rastegar et al., 1999).

Due to the pseudotetraploid nature of *Xenopus laevis* genome, some members of each subgroup may be pseudoallelic versions of the same gene that arose during the global duplication of the genome (Kobel and Du Pasquier, 1986). According to Saha and Grainger (1993) pseudoallelic pairs of other *Xenopus* cloned genes share 95-98% of nucleotide identity within the coding region (Saha and Grainger, 1993). *PV.1* and *Xvent-1* share only 85% of nucleotide identity thus, by this criterion, they are not considered pseudoallelic pairs (Ault et al., 1997). The same is likely to be applicable to several members of the Xom subgroup of genes. However for simplification, in this thesis I consider all members of one subgroup as the same gene. This seems appropriate since, in addition to their high amino acid identity, members of each subgroup also share identical expression patterns. Expression patterns differ, however, between members of different gene subgroups. From now on, I will consider *Xom* and *Xvent-1* as representative members of each subgroup, and other members will be referred only to describe particular experiments in which their activities differ.

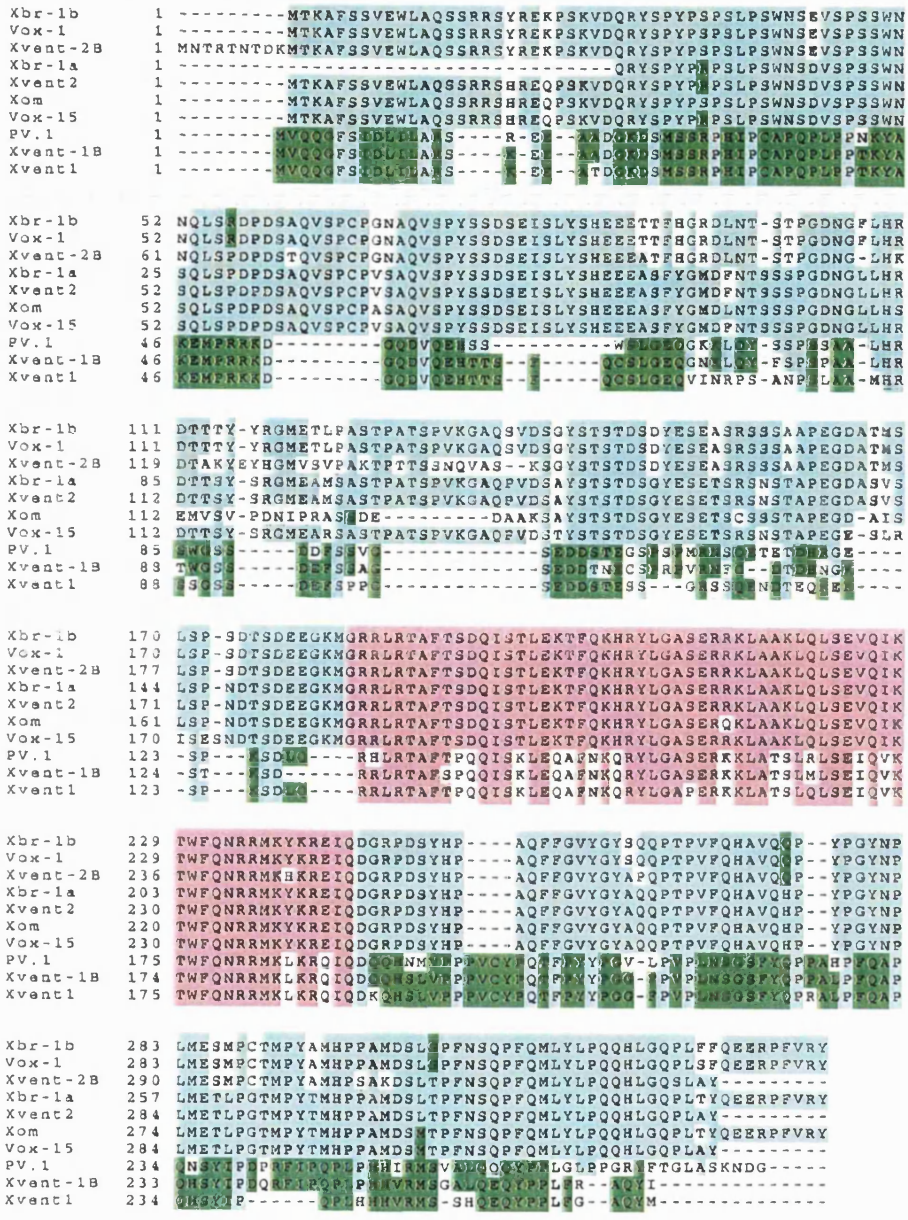

Fig. 1.6 Amino acid sequence alignment of the Xvent family of genes: *Xom* (Ladher et al., 1996), *Xvent-2* (Onichtchouk et al., 1996), *Xvent-2B* (Rastegar et al., 1999), *Xbr-1a* and *Xbr-1b* (Papalopulu and Kintner, 1996), *Vox-1* and *Vox-15* (Schmidt et al., 1996), *Xvent-1* (Ault et al., 1996), *Xvent-1B* (Rastegar et al., 1999), *PV.1* (Gawantka et al., 1995). *Xbr-1a* and *Vox-15* correspond to *Xbr-1* and *Vox*, respectively, in the main text. Amino acid identity is shaded red within the homeodomain of all proteins, blue within the *Xom* subgroup and green within the *Xvent-1* subgroup. Identical amino acids in all sequences, located outside the homeodomain, are also shaded in blue. Alignments were done using the ClustalW Multiple Sequence Alignment tool (http://dot.imgen.bcm.tmc.edu:9331/).

Xom is expressed throughout the *Xenopus* embryo at early gastrula stage, with the exception of the dorsal marginal zone. Its expression pattern resembles that of *Bmp-4* (Fainsod et al., 1994; Hemmati-Brivanlou and Thomsen, 1995), Bmp-4 induces ectopic expression of *Xom* in an immediate-early fashion (Ladher et al., 1996; Rastegar et al., 1999), and inhibition of Bmp signalling inhibits expression of *Xom* (Ladher et al., 1996; Onichtchouk et al., 1996). Furthermore, over-expression of *Xom*, like over-expression of *Bmp-4* (Dale et al., 1992; Jones et al., 1992), causes loss of dorso-anterior structures (Ladher et al., 1996; Onichtchouk et al., 1996; Rastegar et al., 1999; Schmidt et al., 1996), and can rescue the phenotype generated by inhibition of Bmp-4 signalling (Onichtchouk et al., 1996). Together these experiments suggest that *Xom* mediates the ventralising effects of Bmp-4 in an immediate-early manner.

As with *Xom*, *Xvent-1* expression is induced by mis-expression of *Bmp-4* RNA and, conversely, it is abolished by over-expression of a truncated type I Bmp receptor (Ault et al., 1996; Gawantka et al., 1995). Furthermore, mis-expression of *Xvent-1* results in a phenotype similar to that caused by over-expression of *Bmp-4* (Ault et al., 1996; Gawantka et al., 1995). However, the expression patterns of *Xvent-1* and *Xom* differ. *Xvent-1* and *Xom* are co-expressed ventrally and laterally in the marginal zone of early gastrula stage *Xenopus* embryos, but *Xvent-1* transcripts do not extend as dorsally those of *Xom*. Therefore *Xvent-1* expression differs from that of *Bmp-4* at this stage (Onichtchouk et al., 1996).

Recently, a homologue of the *Xvent* genes, *Tlx-2* (Tang et al., 1998), has been identified in the mouse embryo. Bmp-2 treatment of 6.5 dpc mouse embryos in culture rapidly activated *Tlx-2* expression in the epiblast, while in P19 cells a *Tlx-2* promoter element responded to Bmp-2, and this response was mediated by the type I Bmp receptor and Smad1 (Tang et al., 1998). These results indicate that *Tlx-2* is a potential target for Bmp signalling in the mouse. Furthermore, *Tlx-2*, like *Bmp-4*, is expressed in the primitive streak of 7 dpc mouse embryos and becomes restricted to the posterior part of the streak as gastrulation takes place. *Tlx-2* mutants are able to initiate mesoderm formation at the posterior end, so Tlx-2 does not seems to be involved in proliferation/survival of the epiblast or mesoderm induction, as for Bmp-4 or BMPR-IA (Mishina et al., 1995; Winnier et al., 1995). However, mesodermal cells remain

restricted to this posterior region and formation of the primitive streak is disrupted, with cells displaying a disorganised, multilayer morphology and embryos arresting development at 7 to 7.5 dpc. Thus, *Tlx-2* mediates a subset of Bmp functions during gastrulation (Tang et al., 1998).

The conservation of the *Bmp/Tlx-2* and *Bmp/Xvents* pathways in mouse and *Xenopus*, respectively, together with the homology between *Tlx-2* and *Xvents* homeodomains, suggest the existence of an evolutionarily conserved pathway involving *Xvents(Tlx-2)* and *Bmp* that is essential for vertebrate development.

Homeodomain-containing proteins

The *Xvent* genes are homeobox-containing genes which encode a highly conserved, and unusual, homeodomain (Fig. 1.6; see Chapter 3). The homeodomain is one of the most common domains found in eukaryotic transcriptional regulators. It is formed by a 60 amino-acid motif involved in binding DNA in a sequence-specific manner (for a review see Gehring et al., 1994 and Mann, 1995 #1067; Mann, 1995). Structurally, it consists of an N-terminal arm and three alpha helices (Fig. 1.7). The first and second helices are separated by a 5-amino-acid loop that includes several solvent-exposed amino acids. The second and third helices, together with a 4-amino-acid turn that connects them, form a structure that is very similar to the helix-turn-helix motif present in prokaryotic repressor proteins. DNA contacts are mediated by the third alpha helix, also called the recognition helix, which sits on the major groove of the DNA, and by an N-terminal arm, which makes specific base-contacts in the minor groove (Mann, 1995).

The majority of homeodomain proteins act as transcription factors. As with many other transcription factors, their regulatory function arises from the specificity of interactions with DNA, and from subsequent interactions with components of the basal transcriptional machinery (Laughon, 1991). This putative modular nature, likely to be the case with Xom, is at the basis of the first two sets of experiments in this thesis. First, I address the DNA binding specificity of Xom and then, the behaviour of Xom in the regulation of transcription.

Insights into the DNA binding properties of Xom can be gained by understanding how homeodomains, in general, contact DNA. Structural studies of several homeodomain-DNA complexes reveal highly conserved homeodomain/DNA interactions (for a review see x. Despite this conservation, in vivo 'swap' experiments in which the homeodomain of one protein is replaced by that of another, demonstrate that the specificity of *in vivo* function is determined by the homeodomain and sequences immediately flanking it (Mann, 1995). Consequently, it is difficult to imagine how the homeodomain can be responsible for a wide range of functional specificity.

One possibility is that, in addition to the binding affinity of a homeodomain monomer for DNA, other mechanisms may exist to create additional specificity in the DNA-homeodomain interaction. Evidence for homo and hetero-dimerisation of homeodomains has been provided for many homeodomain proteins (Pomerantz and Sharp, 1994; Wilson et al., 1993). In addition, co-operative interaction of the homeodomain with other regulatory proteins has been shown for the Hox proteins and another class of homeodomains, Extradenticle (Exd) in *Drosophila* or Pbx in mammals (Scott, 1999). Exd and Pbx enhance the specificity and affinity of Hox proteins via protein-protein interactions that result in cooperative DNA binding. Structural studies of Ubx-Exd-DNA and HoxB1-Pbx1-DNA co-crystals have shown that cooperative binding between the Hox and Exd/Pbx proteins relies on a hexapeptide amino-terminal to the homeodomain of Hox proteins (Passner et al., 1999; Piper et al., 1999). This hexapeptide reaches Exd or Pbx1 bound to the opposite side of the double helix of DNA, inserting itself into a special pocket in Exd or Pbx1 formed partially by a tripeptide loop specific to the Exd/Pbx type of homeodomains. Because both complexes make sequence-specific contacts with DNA, the specificity and binding affinity of the whole complex is enhanced (Scott, 1999). Binding to yet other co-factors could also be involved to in determining Hox-DNA binding specificities (Mann and Affolter, 1998; Scott, 1999).

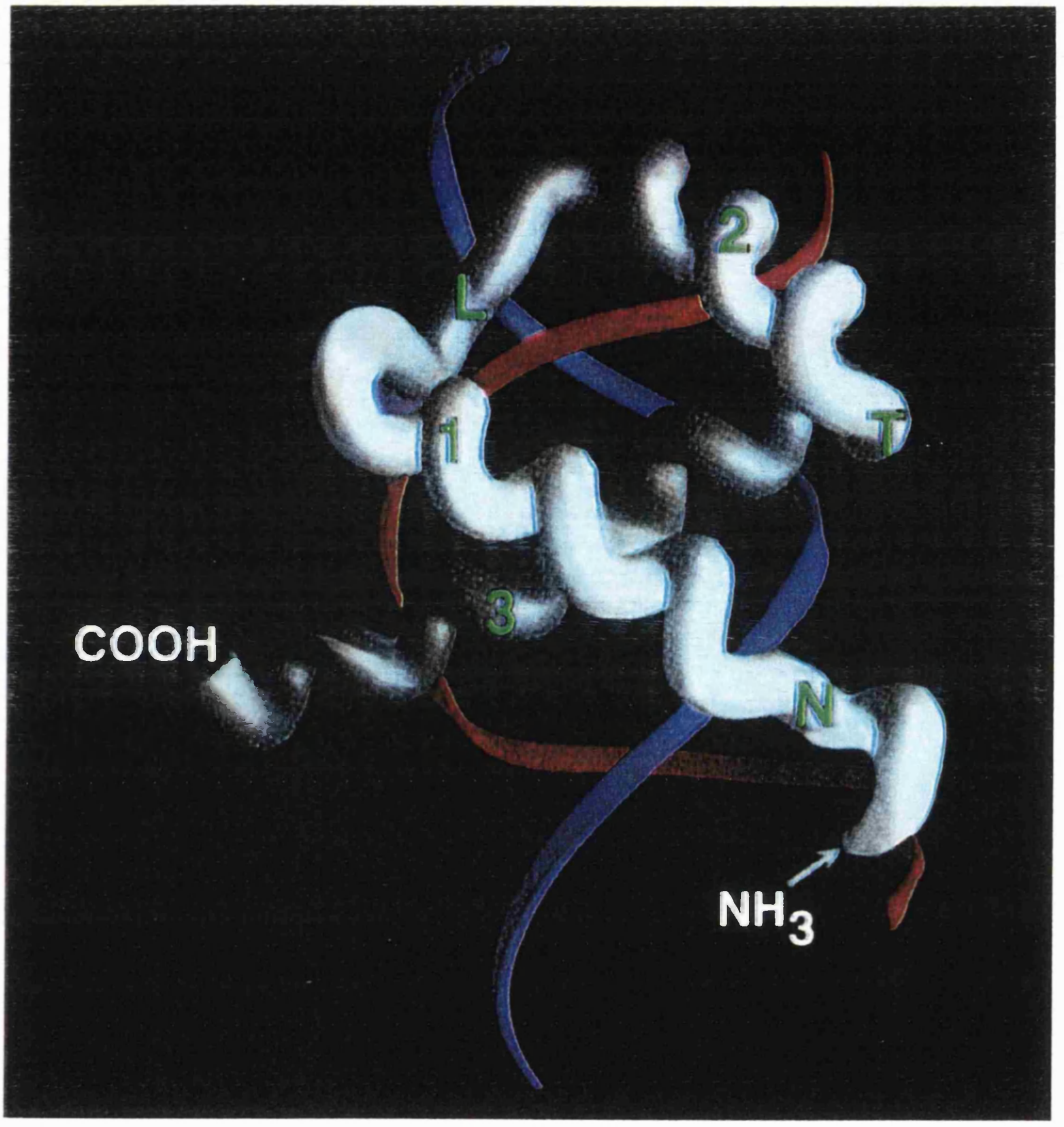

Fig. 1.7 The three-dimensional structure of the Antennapedia homeodomain bound to DNA. For the homeodomain, only the alpha carbon backbone is shown (in grey and white). The two strands of DNA are shown as red and blue ribbons. The structural components of the homeodomain, N-terminal arm (N), helix 1(1), loop (L), helix 2 (2), turn (T) and helix 3/4 (3) are labelled in green. Modified from Mann (1995).

Transcription factors

Homeodomain proteins have been shown to act both as activators and repressors of transcription and in this study, the role of Xom in transcription was also analysed (Chapter 4).

The regulation of transcription is carried out by a number of regulatory proteins that can bind at great distances from the start of transcription of a particular gene, and act by modulating the activity of RNA polymerase II (pol II). This RNA polymerase is one of three different polymerases that exist in an eukaryotic cell to carry out transcription. However, it is the RNA polymerase II that is responsible for the synthesis of all messenger RNA of the cell (and also certain small nuclear RNAs) accounting for approximately 20-40% of the total RNA polymerase activity (Gilbert, 1994).

Three distinct groups of DNA sequence elements direct transcription by pol II. The first group includes the core, or basal, promoter elements found near the site where pol II initiates transcription, such as the TATA element located upstream of the transcription start site (consensus TATAa/tAa/t) and the Initiator motif, a pyrimidine-rich sequence (consensus PyPyA_{+1}NT/APyPy) encompassing the transcription start site (for review see Orphanides et al., 1996). These elements serve to nucleate the formation of an initiation complex, although some cellular promoters can contain only one element or even neither. Two other groups of cis-regulatory elements are the promoter-proximal elements, situated 50 to a few hundred base pairs upstream of the start site, and the promoter-distal-elements (enhancers) found up to tens of thousands of base pairs away from the transcription start site (Mitchell and Tjian, 1989; Ptashne, 1988). Both of these elements contain binding sites for proteins that modulate transcription.

Fractionation of nuclear extracts has led to the identification of six fractions, in addition to pol II, which are sufficient to reconstitute transcription by pol II *in vitro*. The same six fractions, most containing multisubunit proteins, were found in organisms as diverse as human, rat, *Drosophila* and yeast, and are collectively known as General Transcription Factors (GTF). They include TFIIA, TFIIB, TFIID, TFIIE, TFIIF and TFIIH, named according to their chromatographic elution profiles and order of discovery (Orphanides et al., 1996). An important example is the multisubunit TFIID,

which contains the TATA-binding protein (TBP) and at least 8 TBP associated factors ($TAF_{II}s$). The purification of the GTFs as separate entities with unique functions and the observation that they can assemble at the promoter in a specific order *in vitro* suggested that a preinitiation complex is built in a ordered stepwise manner (Orphanides et al., 1996).

Recent genetical and biochemical data challenged this model by revealing that a subset of GTFs exists in a large pre-assembled complex with pol II and other novel transcription factors, the SRB proteins. The pol II holoenzyme complex was first discovered in yeast and later in higher eukaryotes (for a review see (Greenblatt, 1997). Its precise GTF content *in vivo* is however uncertain since it varies with the source of the holoenzyme and the method used in its purification (Greenblatt, 1997).

Transcription initiation starts with the formation of a preinitiation complex onto DNA, followed by separation of the DNA strands (promoter melting) to grant the polymerase access to the nucleotides of the template strand, and then by formation of the first phosphodiester bond of the RNA transcript. Extension of the RNA transcript results in disruption of the polymerase contacts with the initiation complex (promoter clearance) and entry into the elongation phase of transcription in which the nascent RNA is extended as the polymerase embarks on its journey along the template (Orphanides et al., 1996). The polymerase then releases the DNA strand when it finds specific terminator sequences and the primary transcript is cleaved (Ogbourne and Antalis, 1998).

In a cell, transcription is a tightly regulated process that must be triggered by activator proteins and is, therefore, called activated transcription (Orphanides et al., 1996). These proteins bind to specific DNA sequences and induce the expression of a gene or sets of genes, to overcome a general repressed state of DNA, due to packaging into chromatin (for review see Kingston et al., 1996). Activator proteins can act, in theory, at any step of transcription: formation of the preinitiation complex, promoter clearance, elongation and termination.

In prokaryotes, the formation of the preinitiation complex has two limiting steps, the recruitment of a preinitiation complex to a 'closed' configuration onto DNA and an

ATP-dependent step which triggers a conformational change in the polymerase generating the 'open complex', ready to initiate elongation (Orphanides et al., 1996). Thus, prokaryote activators can act in either of these two steps. In eukaryotes, the discovery of the pol II holoenzyme unravelled resemblances between prokaryote and eukaryote activator mechanisms, since it became possible that a single activator-holoenzyme interaction recruits the entire initiation machinery to a promoter, in much the same way that a prokaryote activator recruits the polymerase to the closed complex (reviewed in Ptashne, 1988). Although the composition of the holoenzyme is still a matter of intense debate, different subsets of holoenzyme complexes seem to be recruited by different promoters (Greenblatt, 1997). Therefore, there are several potential recruiting steps at which eukaryotic activators might act. The binding of TFIID to DNA, for example, seems to be the earliest step in the majority, if not all, eukaryotic promoters and thus, might be subject to regulation. In addition to recruitment, activators can induce conformational changes or covalent modifications in the pre-initiation complex required for the complex to undertake promoter clearance and enter into the elongation phase (Orphanides et al., 1996). The mode of termination of transcription by pol II is not very clear at present and thus the mechanisms to overcome termination are less studied (Ogbourne and Antalis, 1998).

Transcriptional repression can be achieved by many different mechanisms. Possible mechanisms to repress transcription include repressors involved in inducing an inactive chromatin structure at the regulated promoter, active repression and passive repression (Hanna-Rose and Hansen, 1996). Repressors involved in inducing inactive chromatin structures are currently under intense investigation and act by interaction with specific chromatin components, presumably by mediating, directly or indirectly, deacetylation reactions on DNA (for a review see Kingston et al., 1996). Active repression mechanisms include direct repression and quenching repression. Direct repression involves interference with the formation and activity of the basal transcription complex, thereby inhibiting transcription (Hanna-Rose and Hansen, 1996). This could occur through interaction with any of the basal transcription factors, with pol II itself or with a co-repressor that ultimately targets the basal machinery. Quenching repression includes interference with transcriptional stimulation by an activator that is also bound

to the promoter. Quenching could be accomplished by direct interaction with an activator protein, by interaction with a co-activator specific to the activator, or by interaction with the basal transcription machinery that is responsive to a particular class of activators. Finally, passive repression includes competition with activators or basal transcription factors for access to the DNA (Hanna-Rose and Hansen, 1996).

For homeodomain-containing proteins, in particular Hox proteins, there is evidence that their transcriptional regulation properties may be influenced by other proteins. Exd, in addition to its proposed role in conferring additional DNA-binding selectivity to Hox proteins (see above), is also likely to change Hox proteins from repressors to activators (Biggin and McGinnis, 1997; Mann and Affolter, 1998; Pinsonneault et al., 1997). This has been suggested by the observation that most of the Exd- and Hox-regulated enhancers activate transcription while enhancers repressed by Hox proteins appear to do so without Exd (Pinsonneault et al., 1997). However, the number of well characterised Hox-regulated promoters is still very small, so this conclusion can hardly be taken as a generalisation.

This study

This thesis describes a functional analysis of Xom. First, Xom DNA binding sequences were determined by performing an *in vitro* binding site selection procedure (Pollock and Treisman, 1990) and the ability of Xom to bind potential binding sequences *in vitro* was tested in electrophoretic mobility shift assays. Together, these results showed that the sequence CTAATT(A/G) is critical for Xom binding DNA, but that binding is greatly enhanced by the presence of an ATTA motif 6 or 7 nucleotides upstream of the core TAAT. A cell culture assay further demonstrated that Xom interacts with a potential Xom binding sequence. These experiments are described in Chapter 3.

In Chapter 4, the ability of Xom to regulate transcription was analysed by fusing Xom to the Gal4 heterologous yeast DNA binding domain. Xom was shown to behave as a repressor of transcription in *Xenopus* embryos and its repressing activity was mapped to the N-terminal and C-terminal regions flanking the homeodomain. Similar

results were obtained using a cell culture system.

Xom's transcriptional repressing activity, together with its ventral expression pattern and ventralising activity in the early *Xenopus* embryo, suggested that Xom might function by down-regulating the expression of genes that are required for dorsal development in *Xenopus*. Moreover, over-expression of *Xom* RNA or of a dominant-negative version, indicated that Xom down-regulates *goosecoid*, an homeobox gene expressed in the organizer capable of partially mimicking organizer's activity (Blumberg et al., 1991; Cho et al., 1991; Niehrs et al., 1993). These experiments are described in Chapter 5.

Finally, to test whether Xom acts by directly repressing *goosecoid* transcription, reporter constructs containing a *goosecoid* promoter fragment containing or lacking point mutations in potential Xom binding sites, were co-injected with different effector RNAs in *Xenopus* embryos (Chapter 6). These experiments suggested that at least part of Xom's repressing effect is direct and a possible site to which Xom binds was identified.

CHAPTER 2

MATERIALS AND METHODS

Abbreviations

BSA	Bovine serum albumin
CHAPS	3-[(3-cholamidopropyl)-dimethylammonio]-1-propanesulfonate
dH_2O	Distilled water
DTT	Dithiothreitol
EDTA	Ethylene-diamine-tetra-acetate
EGTA	Ethylene glycol-bis(β-aminoethylether)-N,N,N',N'-tetraacetic acid
HEPES	N-2-hydroxyethylpiperazine-N'-2-ethanesulfonic acid
IPTG	Isopropylthio-β-D-galactosidase
MOPS	3-(N-morpholino)-propanesulfonic acid
PCR	Polymerase chain reaction
PEG	Polyethylene glycol
SDS	Sodium lauryl sulfate
X-Gal	5-bromo-4-chloro-3-indolyl-β-D-galactosidase
ATP	Adenosine 5'-triphosphate
CTP	Cytidine 5'-triphosphate
UTP	Uridine 5'-triphosphate
GTP	Guanidine 5'-triphosphate
TTP	Thymidine 5'-triphosphate

Molecular Biology Techniques

Preparation and storage of competent bacteria

The DH5α strain of *Escherichia coli* was rendered competent for transformation by treatment with $CaCl_2$. A single colony was placed in 50 ml of L-broth and shaken at

37°C overnight. 10 ml of this culture was inoculated into 100 ml of P-medium (15.9 mM K_2PO_4, 6.3 mM KH_2PO_4, 15 mM $(NH4)_2SO_4$, 10 mM $MgSO_4$, 1.8 mM $FeSO_4$, 1% casamino acids and 0.2% glucose) and cells were grown to an optical density of 0.3 at 600 nm. After washing in 100 ml of 10 mM NaCl at 4°C, cells were repelleted. Bacteria were resuspended in 100 ml of 50 mM $CaCl_2$ and incubated at 4°C for 15 minutes. Finally bacteria were pelleted and resuspended in 10 ml of 50 mM $CaCl_2$, 16% (v/v) glycerol, aliquoted and quickly frozen in dry ice before being stored at -80°C.

To render CMK cells competent, 0.5 ml of cells was diluted into 50 ml of 2X TY and incubated at 37°C with shaking for 1 hour and 30 minutes until optical density (550 nm) became 0.4 or 0.5. Then, cells were spun in a 50-ml tube at 3000 rpm for 10 minutes. After centrifugation, the supernatant was poured off and 17 ml of Hanaham Transformation Buffer (HTB; 10 mM $CaCl_2.6H_2O$, 45 mM $MnCl_2$, 100 mM RbCl, 3 mM hexamino III cobalt chloride, 10 mM MES pH 6.3) was added. The tube was swirled gently (or vortexed softly) to disperse cells and then incubated on ice for approximately 30 minutes. The previous centrifugation was repeated for 5 minutes, the supernatant poured off, 4 ml of HTB medium was added and cells were left on ice for 5 to 10 minutes. While keeping cells on ice, 140 µl of dimethyl-formamide was added and incubated for 5 to 10 minutes, followed by 140 µl of 2.2 M DTT/40 mM potassium acetate pH 6 for 5 to 10 minutes and finally, 140 µl of dimethyl-formamide. Cells were kept at 4°C and remained competent for transformation until the following day.

Plasmid transformation of competent bacteria

Frozen DH5-α competent bacteria were thawed on ice. Up to 100 ng of DNA was added to 100 µl of cells in Falcon 2059 tubes (Becton Dickinson). The bacterial cells were kept on ice for 15-30 minutes and then heat shocked at 42°C for 45 seconds followed by cooling on ice for 30 minutes to 2 hours. After this period, 200 µl of LB was added and the mixture was incubated at 37°C for 15 minutes. Bacteria were then plated out onto LB plates containing 100 mg/ml ampicillin and placed in a 37°C incubator overnight.

Alternatively, 100 to 1000 ng of DNA were added to 100 µl of pre-thawed DH5-

α competent bacteria. The mixture was kept on ice for 20 minutes and then at room temperature for 10 minutes, 200 µl of LB was added and the mixture was plated out and incubated as above.

For defined plasmid recovery, 10µl of competent DH5-α bacteria was added to 500 ng of plasmid DNA and placed at 37°C for 90 seconds, then 100 µl of L-broth was added to the mixture and this was plated out onto LB plates containing 100 mg/ml ampicillin. Plates were placed at 37°C overnight.

CMK bacterial cells, rendered competent on the previous day and stored in the fridge, were incubated with various dilutions of ligation reaction for 30 minutes on ice. Heat shock at 42°C for 2 minutes was performed. Immediately after, cells were mixed with melted top-agar (previously heated 10 minutes in a microwave oven and kept in a 42°C bath), 4.5 µl of IPTG (0.2g/ml) and 44 µl of X-Gal (20 mg/ml in dimethylformamide) in a 10 ml tube. While still warm, this mixture was plated onto LB plates (no ampicillin is necessary for M13 phage vectors) and incubated overnight at 37°C.

Small scale preparation of plasmid DNA

From a 3.5 ml overnight culture of transformed DH5-α bacteria in LB, 1.5 ml was transferred to a 1.5 ml microfuge tube and spun for 20 seconds. The supernatant was removed completely and the pellet resuspended in 300 µl of Resuspension Buffer (Qiagen; 10 mM EDTA, 50 mM Tris.HCl pH 8.0, 100µg/ml RNAse). 300 µl of Lysis Buffer (Qiagen; 0.2 M NaOH, 1% SDS) was added, mixed and left for 2 minutes at room temperature to allow alkaline lysis of the cells. Lysis solution was then neutralised by adding 300 µl of ice cold Neutralisation Buffer (Qiagen; 3 M KOAc pH 5.5) and mixing carefully by inverting the tube a few times followed by 10 minutes on ice. The tube was spun for 15 minutes at room temperature. 700 µl of the supernatant was transferred into a fresh microfuge tube and phenol/chlorophorm extraction was performed (see below). DNA was precipitated from the aqueous upper layer by adding 650 µl of isopropanol, leaving 15 minutes and then spinning for 15 minutes, all at room temperature. After centrifugation the pellet was washed in 70% ethanol, dried and

resuspended in distilled water with 0.1 mg/ml RNase A (Sigma).

Alternatively, DNA was often prepared by a more rapid procedure called a TENS prep. The pellet from centrifugation of a 1.5 ml overnight culture was resuspended by vortexing in the LB (~50 µl) remaining after turning the tube upside down. 300 µl of TENS solution (0.1 M NaOH, 0.5% SDS) was added and the tube was shaken briefly. 150 µl of 3M NaOAc (pH 5.5) was then added and shaking was repeated. After a two minute centrifugation at room temperature in a microfuge the supernatant was removed (450 µl) and 900 µl of 100% ethanol was added. After a further 2 minute centrifugation the pellet was washed once in 70% ethanol and resuspended in distilled water with 0.1 mg/ml RNase A (Sigma).

Phage DNA was recovered from CMK bacteria by performing a phage miniculture followed by polyethylene glycol (PEG) precipitation. Tubes containing 1.5 ml 2X TY with a 1:100 dilution of CMK cells (rendered competent on the previous day and stored at 4°C) were prepared. Then, individual white plaques (corresponding to slow-growing bacteria infected with phage) were picked up with a toothpick under a magnifier and added to each tube. This mixture was then cultured for 5 hours and 30 minutes at 37°C with shaking at 300 rpm. The cultures were transferred to microfuge tubes and spun for 5 minutes. The supernatant was removed (bacteria remains in the bottom of the tube whereas the phages stay in the supernatant) and added to new tubes containing 200 µl of PEG 20%/2.5 M NaCl. The solution was mixed well and left for 10 to 15 minutes at room temperature to allow DNA to precipitate. Two sets of 10-minute centrifugations were performed, aspirating off the supernatant between centrifugations, and the pellet was resuspended in low TE. After PEG precipitation, phenol/chlorophorm extraction and an ethanol precipitation were performed and the pellet was resuspended in 35 µl of low TE.

Medium and large scale preparation of plasmid DNA

0.1 to 1 ml of plasmid bacterial culture was placed in 100 ml of LB containing 100 mg/ml ampicillin, and shaken at 37 °C overnight. The Qiagen midi or maxi-prep kit (Qiagen) was then used to isolate the DNA, according to the QIAfilter Midi or QIAfilter

Maxi protocol, respectively, as suggested by the manufacturers.

DNA quantification and manipulation

DNA and RNA were quantified by spectrophotometry at 260 nm (optical density, OD=1 equates to 50 µg/ml double stranded DNA, 35 µg/ml single stranded DNA and 40 µg/ml RNA). The ratio between the readings at 260 nm and 280 nm provided an estimate of the purity of the nucleic acid preparation (pure preparations of DNA and RNA should have OD_{260}/OD_{280} values of 1.8 and 2.0, respectively).

Phenol/Chlorophorm extraction

To remove proteins from nucleic acid solutions, a mixture of phenol:chlorophorm:isoamyl-alcohol (25:24:1 volume ration) was added in a 1:1 volume ratio to the DNA solution and vortexed for 1 minute. After a 3 minute centrifugation, the upper (aqueous) layer was transferred into a new microfuge tube and extracted with an equal volume of chloroform.

Precipitation

Concentration of DNA was performed by ethanol precipitation. 3 M NaOAc pH 5.5 (to a final concentration of 0.3 M) and 2.5 volumes of 100% ethanol were added to a DNA solution and left on dry ice for approximately 20 minutes. 1 µl of 10 mg/ml glycogen was often used as a carrier if the DNA amount to be purified was too small to be visualised as a pellet at the bottom of the tube. Centrifugation at >20 000 g for 5-20 minutes was performed and the DNA pellet was then washed in 70% ethanol, dried and resuspended in TE or distilled water.

PEG precipitation was carried out by adding 30 µl of 20% PEG/2.5 M NaCl to 50 µl of DNA solution, followed by incubation on ice for 30 minutes and centrifugation for 10 minutes at 4°C. The pellet was washed in 70% ethanol, dried and then resuspended in a suitable volume of distilled water or TE.

Restriction digestions

Restriction enzyme digests were performed at either 37°C or room temperature for approximately 1 hour using commercially supplied restriction enzymes and buffers (Promega, New England Biolabs). The enzyme component of the reaction never comprised more than 10% of the reaction volume. For enzyme digests using more than one restriction enzyme, the buffer suggested by the manufacturer was used.

Ligation and dephosphorylation reactions

Intermolecular ligations were performed in small volumes, generally 20 µl for a total DNA content of 0.5 µg. Ligations were performed overnight at 14°C using T4 DNA polymerase (Gibco BRL) and the appropriate ligation buffer (Gibco BRL).

When the plasmid was capable of self-ligation, the compatible ends were dephosphorylated before use. Dephosphorylation of approximately 1 µg DNA was performed using alkaline phosphatase 0.1 u/µl (Boehringer) and alkaline phosphatase buffer (Boehringer) in 50 µl total volume. The reaction was incubated at 37°C for 20-30 minutes, followed by phenol/chlorophorm precipitation and was further purified using the QIAquick Gel Extraction Kit protocol (without electrophoresis of the DNA).

5' phosphorylation of oligonucleotides

Commercially obtained oligonucleotides generally are not 5' phosphorylated and thus cannot be used directly in ligation reactions. Oligonucleotides were 5' phosphorylated in the following reaction:

5 µl	sense strand 1 µg/µl
5 µl	antisense strand 1µg/µl
5 µl	10X kinase buffer (NewEnglandBiolabs)
5 µl	rATP 10 mM
2 µl	T4 polynucleotide kinase 10u/µl (NewEnglandBiolabs)
28µl	dH_2O

This mixture was incubated for 30 minutes at 37°C followed by 10 minutes at 80°C to heat inactivate the enzyme, with slow cooling down on the bench top to allow annealing of the two strands. Alternatively, the reaction was done independently for each strand with an additional step of annealing after mixing the two reactions.

Agarose gel electrophoresis of DNA and RNA

DNA separation and size estimation were performed by agarose gel electrophoresis. Gels were prepared by dissolving agarose in 0.5 x TAE to a final concentration of 0.8% to 2% depending on the expected size of the DNA fragment. To visualise the DNA, 0.5 mg/ml ethidium bromide was added to the gel. DNA samples were mixed with 6X gel loading buffer and electrophoresis was performed at 5 to 20 V/cm of gel length, until the appropriate resolution was achieved. The resolved DNA was visualised using ultraviolet light at 340 nm, and the size was estimated by comparison with known size markers such as the 1 kb size markers (Gibco BRL).

Purification of specific DNA fragments from gels

In order to purify DNA fragments of interest, DNA was subjected to agarose gel electrophoresis and the region of the gel containing the appropriate band was excised under ultra-violet light (365 nm). DNA was purified using the QAIquick Gel Extraction Kit protocol using a microcentrifuge, according to the instructions of the manufacturer (Qiagen).

Polymerase Chain Reaction (PCR)

PCR reactions were carried out using different versions of the *Thermus aquaticus* (Taq) DNA polymerase (AmpliTaq or KlenTaq; Perkin Elmer and Clontech, respectively), Vent (NewEnglandBiolabs) or Pfu (Stratagene) DNA polymerases according to the manufacturer's recommendations. Pfu DNA polymerase has a very low error rate and thus it was preferably used for applications requiring high-fidelity DNA synthesis, such as cloning. The reactions were set up using the buffers supplied in a total volume of 50 µl. dNTPs were added to a final concentration of 0.2 mM each, and primers were added to a final concentration of 0.4 µM. The reaction mix was overlaid

with mineral oil (Sigma) to prevent evaporation. PCR reactions were performed on a Perkin-Elmer Thermal Cycler or Stratagene Robocycler 40. Details of specific primers and conditions used are given in the 'Plasmid Construct' and 'Binding Site Selection' sections of this chapter.

DNA Sequencing

All DNA sequence analysis was performed by the dideoxy chain termination method using a sequencing kit (Sequenase v.2, USB). 1 to 5 μg of DNA was denaturated for 5 minutes at room temperature in 0.2 mM EDTA/ 200 mM NaOH in 20 μl, followed by neutralisation with 2 μl of 2 M ammonium acetate pH 4.6 and precipitation with 60 μl of 100% ethanol. After centrifugation, the pellet was washed with 70% ethanol and resuspended in a suitable volume to be used in annealing and subsequent labelling and termination reactions of the sequencing procedure, which were performed according to the manufacturer's instructions. Sequencing reactions were loaded onto a sequencing gel (6% acrylamide/bis-acrylamide (19:1), 7 M urea, 0.8 or 1-fold TBE, 7 μl/ml of 10% ammonium persulfate and 0.35 μl/ml of TEMED) and run at 50 W, for approximately 2 hours. After electrophoresis, the gel was fixed in 10% methanol (or ethanol)/10% acetic acid for approximately 20 minutes. The fixed gel was dried on a vacuum drier and autoradiographed overnight at room temperature.

Generally, sequencing was performed with DNA obtained after medium or large-scale preparation of plasmid DNA. However, if the DNA used had been prepared by small-scale preparation then a PEG precipitation was performed before sequencing to ensure removal of contaminant RNA.

In vitro transcription

RNA was transcribed from constructs containing a promoter from bacteriophage SP6 or T7, which are highly specific promoters. The transcription method used allowed the synthesis of capped RNA, which is necessary for efficient translation. Transcription reactions were performed as described below (see also Smith, 1993):

10 μl	5 X Transcription buffer (Promega)

5 µl	0.1 M DTT
5 µl	10 mM rATP
5 µl	10 mM rCTP
5 µl	10 mM UTP
5 µl	1 mM rGTP
5 µl	5 mM Cap analogue (m7-G; New England Biolabs)
2.5 µl	RNase inhibitor (Promega)
5 µl	Linearised template DNA (1 µg/µl)
2.5µl	20 u/µl SP6 (Boehringer) or T7 (Promega) RNA polymerase

The reaction mixture was incubated at 37°C for 30 minutes, after which 2.5 µl of 10mM rGTP was added and the reaction was incubated for a further 60 minutes at 37°C. 5 µl of RNase-free DNase I (Promega) was added to this reaction, to degrade the DNA template, and the reaction was further incubated at 37°C for 15 minutes. The mixture was then subjected to phenol/chloroform extraction followed by size exclusion chromatography using Nu-Clean R50 spin columns (Kodak) or Chroma Spin-30+DEPC-H_2O columns (Clontech) to remove free nucleotides. Finally, the flow-through was ethanol precipitated, the pellet was resuspended in a suitable volume (generally 20 µl) and the RNA concentration was determined by spectophotometry.

To determine the efficiency of translation of the synthesised RNA, synthetic RNA was usually translated using the rabbit reticulocyte system (Promega) and ^{35}S-methionine-labelled protein products were analysed by polyacrylamide gel electrophoresis.

In vitro synthesised RNAs were used for injection into *Xenopus* embryos or as a template for synthesis of *in vitro* translated protein for binding site selection or gel mobility shift assays.

Constructs used as templates for *in vitro* transcription in this thesis are listed in the table below, with specific indications of which restriction enzymes and RNA

polymerases were used for linearisation and RNA synthesis, respectively.

Table 2.1. Constructs used as templates for *in vitro* transcription.

Gene	Expression plasmid	Linearisation site	RNA pol	Reference
Xom-HA	pSP64T	*HincII*	SP6	This thesis
Xom^{L213P}-HA	pSP64T	*HincII*	SP6	This thesis
XomVP16	pCS2+	*NotI*	SP6	This thesis
ΔXom-HA	pT7	*PstI*	T7	This thesis
Gal4.Xom(1-327)	pCS2+	*ApaI**	SP6	This thesis
Gal4.Xom(235-327)	pCS2+	*ApaI**	SP6	This thesis
Gal4.Xom(1-173)	pCS2+	*ApaI**	SP6	This thesis
Gal4	pCS2+	*ApaI**	SP6	This thesis
Mouse Activin βA	pSP64T	*SmaI*	SP6	(Albano et al., 1993)
β-globin	pT7A90	*Xba I*	T7	Gift from Richard Treisman
PV1	pSP64R1	*BamHI*	SP6	(Ault et al., 1996)

* after linearisation, these constructs were made blunt by filling with T4 DNA polymerase (New England Biolabs).

In vitro protein synthesis

Two approaches were used for *in vitro* translation: a system using RNA templates (Rabbit Reticulocyte Lysate System Nuclease Treated, Promega) or a system using DNA templates (T7/SP6 TNT Coupled Reticulocyte Lysate System, Promega). Small-scale ^{35}S-methionine labelled or large-scale unlabelled *in vitro* translations were performed for analytical or preparative purposes, respectively. Reaction conditions were as follows:

	Labelled	Unlabelled
RNA-based *in vitro* translation:	**Small-scale**	**Large-scale**
Denaturated RNA 1µg/µl or dH_2O	0.2 µl	2 µl
RNase inhibitor 40 u/µl (Promega)	0.4 µl	1 µl
1 mM amino acids minus methionine (Promega)	0.4 µl	1 µl
Redivue L-^{35}S-methionine >1000Ci/mmol	1.6 µl	_
1 mM amino acids minus leucine (Promega)	_	1 µl
Reticulocyte lysate, nuclease treated (Promega)	14 µl	35 µl
Distilled water	3.4 µl	10 µl
DNA-based *in vitro* translation		
DNA 2 µl/µl or dH_2O	0.5 µl	1 µl
RNase inhibitor (Promega)	0.4 µl	1 µl
1 mM amino acids minus methionine (Promega)	0.4 µl	1 µl
Redivue L-^{35}S-methionine >1000Ci/mmol	1.6 µl	_
1 mM amino acids minus leucine (Promega)	_	1 µl
TNT Reaction Buffer (Promega)	0.8 µl	2 µl
TNT T7 or SP6 RNA polymerase (Promega)	0.4 µl	1 µl
TNT Reticulocyte lysate (Promega)	10 µl	25 µl
Distilled water	5.9 µl	18 µl

All reactions were incubated at 30°C for 1 to 2 hours. Small-scale labelled reactions were mixed with 5 µl 5X Sample Buffer and typically 2.5 µl of reaction were analysed by SDS-PAGE electrophoresis along with RPN 756 Rainbow™ coloured protein molecular weight markers (Amersham). Large-scale unlabelled reactions were aliquoted in smaller volumes and frozen at -70°C.

Western blot

Protein extracts were analysed in 10.0-17.5% acrylamide SDS-PAGE electrophoresis gels and subsequently blotted on a polyvinylidene difluoride membrane (Sequi-Blot™ PVDF protein sequencing membrane, Bio-Rad), previously permeabilised by immersion in methanol. The electrophoretic transfer was performed in 1X CAPS

Buffer/10% methanol (10X CAPS Buffer stock contains: 22.1 g of 3-(cyclohexylamino)-1-propanesulfonic acid (CAPS) in 900 ml water, titrated to pH 11 with 2 N NaOH and filled up to 1 l with water) for 30 minutes at 200 mA constant current.

The PVDF membrane was pre-blocked with 5% milk powder (Marvel) in PBS for 1 hour at room temperature with moderate shaking. Then, it was incubated with 5 to 10 μg/ml of primary antibody in 0.5% milk powder/PBS overnight at 4°C. Anti-HA mouse monoclonal antibody (Boehringer), anti-Myc mouse monoclonal antibody (9E10; gift from Gerard Evan) or anti-Gal4 DNA binding domain mouse monoclonal (RK5C1; Santa Cruz Biotechnology) were used as primary antibodies. A series of 4 washes of 15 minutes each were performed using 0.1% Tween 20/PBS followed by a 1 to 2 hour incubation with the secondary antibody. Anti-mouse IgG (whole molecule) alkaline phosphatase conjugate (Sigma) was used as the secondary antibody in a 1:1000 dilution. The membrane was placed for approximately 2 minutes in Reaction Buffer (100 mM Tris pH 9.5, 100 mM NaCl, 5 mM $MgCl_2$). Detection of alkaline phosphatase activity was assayed by overlaying the membrane with 3 or 4 ml of BM Purple Substrate (Boehringer), which contains the substrates of the alkaline phosphatase reaction (Nitro Blue Tetrazolium Chloride (NBT) and 5-bromo-4-chloro-3-indolyl phosphate (BCIP)). The membrane was kept in the dark for 10 to 40 minutes until the staining developed. The reaction was terminated with Stop Buffer (100 mM Tris, 100 mM NaCl, 10 mM EDTA) and washed in distilled water to avoid formation of salt crystals on the membrane.

Site-directed Mutagenesis

The introduction of specific mutations into plasmids was performed using the Chameleon™ Double Stranded Site-directed Mutagenesis System (Stratagene) or the GeneEditor™ *in vitro* Site-directed Mutagenesis System (Promega) according to the manufacturer's instructions.

The principle behind the Chameleon™ Double Stranded Site-directed Mutagenesis kit (Stratagene) is based on the annealing of two oligonucleotide primers to double stranded denaturated target plasmid DNA: the selection primer, which changes

one nonessential unique restriction site to a new restriction site and the mutagenesis primer, which encodes a specific mutation in the gene of interest. Primers are extended around the template plasmid to create a new strand containing the desired mutation but no longer containing the unique restriction site. The unmutated parental plasmid is then digested with the restriction enzyme unique to this plasmid. Subsequently, the digestion reaction is transformed into a repair-deficient *Escherichia coli* strain, which cannot distinguish the original unmutated strand from the newly created strand thus randomly selecting one of the strains of the plasmid to be repaired. As a consequence, half of the plasmids contain the desired mutation and the other half converts back to the original plasmid. A second round of digestion and transformation (into an *E. Coli* strain with normal repair machinery) will favour the mutants. Finally, DNA is isolated from individual clones and the mutant plasmids are identified by restriction digestion with the restriction enzyme corresponding to the selection primer.

The GeneEditor™ *in vitro* Site-Directed Mutagenesis System uses antibiotic selection to obtain specific mutations. The selection oligonucleotide provided encodes mutations which alter the ampicillin resistance gene, creating new additional resistance to the GeneEditor™ Antibiotic Selection Mix (Promega). The selection oligonucleotide is annealed to a single- or double-stranded DNA template at the same time and in the same strand as a mutagenetic oligonucleotide. Subsequent synthesis and ligation of the mutant strand links the two oligonucleotides. The new resistance encoded by this mutant DNA strand facilitates selection of the desired mutation.

Binding site selection

Binding site selection was carried out using *in vitro* translated protein as described by Pollock and Treisman (1990) with modifications introduced by Tim Mohun. This technique allows the *in vitro* selection of DNA sequences to which a given protein binds with high affinity. Briefly, a random pool of oligonucleotides is incubated with *in vitro* translated protein and then the protein/DNA complexes are immunoprecipitated. Bound oligonucleotides are eluted from the protein and are amplified by the PCR to use in the next round of binding, immunoprecipitation, elution and amplification. After several rounds of selection, the pool of oligonucleotides

obtained is tested for its ability to bind *in vitro* translated protein in a gel mobility shift assay. DNA is recovered from a specific shifted band sliced from the gel, and then PCR amplified, cloned and sequenced.

The oligonucleotide (R76) used to initiate the selection rounds is flanked by *EcoR1* and *BamH1* and contains a random 26 base sequence flanked by two known sequences for PCR amplification: 5'CAGGTCAGTTCAGCGGATCCTGTCG $(A/G/T/C)_{26}$GAGGCGAATTCAGTGCAACTGCAGC-3'. Primers used in PCR were: primer F (Forward): 5'-GCTGCAGTTGCACTGAATTCGCCTC-3'; Primer R (Reverse): 5'-CAGGTCAGTTCAGCGGATCCTGTCG-3'.

The detailed protocol for binding site selection is described next.

1)Preparation of double stranded R76

R76, primer F and primer R were gel purified before use on a 10% native acrylamide gel by loading approximately 20 μg of DNA. After running and ultra-violet shadowing, bands were cut corresponding to the full-length oligonucleotides and they were eluted overnight at 37°C in elution solution. Ethanol precipitation was performed after adding 1 μg of glycogen carrier (Boehringer) and DNA was resuspended in TE. Assuming 60% recovery, dilutions were performed in order to obtain a working concentration of 50-100 ng/μl. R76 oligonucleotide was rendered double strand by preparing a PCR mixture as indicated below. The 5X Hot PCR contains 250 μM dATP, 250 μM dTTP, 250 μM dGTP, 250 mM KCl, 7.5 mM $MgCl_2$, 50 mM TRIS pH 8.3.

2μl	R76 (50 ng/μl), a kind gift from Tim Mohun
4μl	5X Hot PCR
1μl	AmpliTaq polymerase 1 u/μl (Perkin Elmer)
2μl	dCTP 40 μM
5μl	α^{32}P dCTP 3000 Ci/mM
1.5μl	primer F 100 ng/μl
1μl	BSA 10 μg/μl

3.5µl dH_2O

One cycle of PCR (1 minute at 94°C, 3 minutes at 62°C, 5 minutes at 72°C) was performed with this reaction mix. After PCR, the volume was increased to 150 µl with low TE, phenol/chlorophorm extraction and ethanol precipitation (with glycogen as carrier) were performed and the pellet was resuspended in 10 µl of low TE with 1 µl of 10X native gel loading buffer. Then, the amplified product was run on a 8% acrylamide native gel in 1X TBE at 10 W for 2 to 3 hours. To localise the DNA on the gel, autoradiography was performed exposing the gel for 2 seconds. The band was cut out from the gel and DNA was eluted overnight at 37°C in 0.4 ml of Normal Elution Buffer (0.5 M NH_4OAc, 10 mM MgAc, 1 mM EDTA, 0.1% SDS). Eluted DNA was concentrated by ethanol precipitation (using glycogen) and resuspended in 26 µl of low TE. 2 µl were taken for quantification in a Cerenkov scintillation counter and the yield was calculated using the approximation $4X10^6$ cpm = 50 ng of double stranded R76 (the calculation procedure is presented below). The probe was diluted to 0.4 ng/µl to use in the first round of binding site selection.

Quantitation of oligonucleotides

The reaction for preparation of double stranded R76 has a hot/cold dCTP ratio such that on average 2.5 hot dCTP molecules will be incorporated per molecule of dsR76. If the specific activity of $\alpha^{32}P$ dCTP is 3000 Ci/mM then the specific activity of dsR76 will be 2.5 X 3000 Ci/mM = 7500 Ci/mM. Note that time should be taken into account when calculating specific activity. Therefore, the specific activity of R76 at a given time point, N, is calculated by $N = N_0 . e^{-0.0495.t}$ (where t = time in days since the labelled CTP is synthesised).

Assuming that 1 X 10^6 cpm by Cerenkov counting is approximately equal to 1 µCi then it is possible to convert counts into moles of dsR76. Subsequently moles can be converted into ng knowing that the molecular weight of R76 is 76 X 635 g = 48260 g.

Quantification after PCR amplification of selected DNA follows the same procedure except that the ratio of hot:cold dCTP is such that, on average, one hot dCTP will be incorporated per molecule of double stranded R76. Therefore, the specific activity of dsR76 is 3000 Ci/mM.

2)Binding reaction

The following reaction mix was added to 0.4 ng of double stranded R76 probe (approximately $5X10^9$ molecules), on the first round of selection, or 0.2 ng for the

following rounds. Buffer E (1X) corresponds to 1X Dignam's Buffer (20 mM HEPES pH 7.9, 100 mM KCl, 0.2 mM EDTA, 0.2 mM EGTA, 20% glycerol) containing protease inhibitors (2 μg/ml of aprotinin and 0.2 mM of Phenylmethylsulfonylfluoride (PMSF; Sigma), 0.1% NP40, 50 μg/ml BSA (Sigma)).

20 μl	1X Buffer E
1 μl	Appropriate cold *in vitro* translated Xom-HA or dH_2O
1 μl	Poly dIdC 200ng/μl (Pharmacia)
1 μl	anti HA antibody 1 μg/ml (Boehringer)
1 μl	0.4 ng/μl R76 probe in the first round
	or 0.2 ng/μl in the next rounds
1 μl	dH_2O

This reaction was incubated on ice for 30 minutes to allow DNA/protein/antibody complexes to form.

3) Immunoprecipitation

Meanwhile, Protein A-Sepharose 6 MB beads (Pharmacia), to use in the immunoprecipitation step, were prepared. 25 μl of Protein A beads, previously swollen in an equal volume of distilled water, were placed in a 1.5 ml microfuge tube by pipetting using tips with the edges cut out. The beads were equilibrated in cold Dignam's Buffer by adding 250 μl of buffer, mixing, spinning for 15 seconds and aspirating off the buffer using a duck billed tip. The binding reaction was then added to the Protein A-Sepharose beads (accumulated at the bottom of the tube) with gentle mixing (pipetting up and down) on ice. The mixture was placed rotating gently on a rotator in the cold room for 2 to 3 hours (or overnight) to allow for the antibody to bind the beads. The immune complexes were washed twice by addition of 250 μl of cold Dignam's Buffer containing 0.1% NP40 by briefly vortexing and inverting twice and then pulse microcentrifugating for 20 seconds and aspirating the supernatant.

4) Elution

Elution was accomplished by adding 200 µl of Protein A-Sepharose elution buffer (5 mM EDTA, 0.5% SDS, 100 mM NaOAc pH 5.6, 50 mM Tris pH 8.0) and incubating at 45°C for 30 minutes. This was followed by phenol/chlorophorm extraction and ethanol precipitation (using glycogen as a carrier). The pellet was resuspended in 4 µl of low TE from which 2 µl were used for PCR amplification as template while the remainder was stored at - 20°C.

5) PCR amplification of selected pool of oligonucleotides

PCR reaction conditions were as follows:

2 µl	recovered DNA
4 µl	5X Hot PCR (see above)
1 µl	α^{32}-P dCTP 3000 Ci/mM
1 µl	AmpliTaq polymerase (Perkin and Elmer)
1.5 µl	primer F 100 ng/µl
1.5 µl	primer R 100ng/µl
2 µl	cold dCTP 40 µM
2 µl	BSA 1 mg/ml
5 µl	dH_2O

PCR conditions were as follows: denaturation for 1 minute at 94°C, annealing for 1 minute at 62°C and extension for 1 minute at 72°C. This cycle was repeated for 15 times followed by a 5 minutes extension period at 72°C. After removal of the mineral oil, the PCR reaction was diluted to 100 µl, it was phenol/chlorophorm extracted, ethanol precipitated (with glycogen) and the pellet was resuspended in 10 µl of low TE plus 1 µl of 10X native gel loading buffer. This mixture was run on a 8% acrylamide native gel in 1X TBE at 12 W for approximately 2 hours. To purify the fragment from the gel, autoradiography was performed (2 seconds of exposure) to localise the desired band on the gel. The band was removed and DNA was eluted overnight at 37°C in 0.4 ml

of Normal Elution Buffer. Eluted DNA was concentrated by ethanol precipitation (using glycogen) and resuspended in 22 µl of low TE. The DNA yield was calculated as previously using a scintillation Cerenkov counter and it was diluted to 0.2 ng/µl to use in the next round of binding site selection.

Steps 2, 3, 4 and 5 were repeated for 5 rounds within the next 7 days to further restrict the pool of selected sequences. The probes from each round were stored at -20°C.

6) Electrophoretic mobility shift assay (EMSA)

After 5 rounds of binding site selection, an EMSA was performed using the selected probes from each round of selection. The reaction conditions were as follows:

1 µl *in vitro* translated Xom-HA or dH_2O

6 µl 2X Buffer E (see above)

1 µl Poly dIdC 1 µg/µl (Pharmacia)

2 µl dH_2O

15 minutes incubation at room temperature

2 µl selected probe 20000 cpm/µl

25 minutes incubation at room temperature

1 µl of anti-HA antibody (Boehringer) 1 mg/ml or H_2O

15 minutes incubation at room temperature

1 µl 10X native loading buffer

The mixture was loaded without delay on a 6% acrylamide native protein gel, which had been pre-run at 100 mV constant voltage in 0.5X TBE for approximately 1 hour in the cold room. The gel was then run under the same conditions for approximately 2 to 3 hours, dried in a vacuum dryer and autoradiographed overnight at -70°C between two enhancing screens. The band corresponding to a specific complex obtained in the last round performed was cut out from the dry gel and DNA was recovered for further amplification by cold PCR.

7) Cold PCR

Half of the dried gel slice containing the desired band was used directly in a PCR amplification as follows. The 5X buffer comprised: 250 mM KCl, 50 mM Tris.HCl pH 8.4, 12.5 mM $MgCl_2$, dNTPs 1 mM each, BSA 0.85 mg/ml.

20 µl	5X buffer
10 µl	20 µM Primer F
10 µl	20 µM Primer R
2 µl	AmpliTaq polymerase (Perkin and Elmer)
48 µl	dH_2O

PCR reaction conditions were: 18 cycles of 1 minute denaturation at 94°C, 1 minute annealing at 62°C and 1 minute extension at 72°C, with one extra step of extension of 5 minutes at 72°C. After carefully removing the mineral oil, the PCR products were diluted to 150 µl with low TE, vortexed strongly and spun for a few minutes to bring down the paper and gel slice. From this solution, 8 µl were run on a analytical 2% agarose gel (a 76 bp band was detected) while the rest was phenol/chlorophorm extracted, ethanol precipitated (with glycogen as carrier) and the pellet was resuspended in 50 µl of TE.

8) Cloning the final pool of selected oligonucleotides

10 µl of solution containing the amplified final pool of selected oligonucleotides was digested with *BamHI* and *EcoRI* in a total volume of 50µl. To purify the 42 base pair fragments the digestion reaction was loaded onto an 8% native acrylamide gel mounted on the Biorad Mini Gel Apparatus (Biorad) and run for approximately 30 minutes at a fixed current of 20 mA (approximately 130 mV). The gel was then stained with 1:1000 ethidium bromide in water for 5 minutes and the band was excised under ultra-violet light. DNA was eluted from the acrylamide gel slice with 0.4 ml Normal Eluting Solution for approximately 2 hours at 50°C. Alternatively, the digestion solution was phenol/chlorophorm extracted, ethanol precipitated, the pellet was resuspended in 30 µl of distilled water and 5 µl was used for ligation. The 42 bp fragments were ligated

to *BamHI*-digested and 5' phosphorylated M13 mp19 phage vector (a kind gift of Nicole Civill). Cloning into a *BamH1*-digested vector results in the formation of concatamers of two or multiples of two copies of *BamHI/EcoRI*-digested 42 bp selected sequence, which facilitates the sequencing step since it allows one to sequence multiple oligonucleotides in just one sequencing reaction. The ligation reaction was then transformed into CMK competent cells, phage minicultures were prepared and DNA was purified by PEG precipitation followed by ethanol precipitation.

9) Sequencing of final pool of selected oligonucleotides

DNA sequence analysis was performed using the dideoxy chain termination method provided by a sequencing kit (Sequenase v2; USB), according to the manufacturer's instructions.

10) Analysis of sequences

The sequences of 111 clones were compiled in a word processor file (Microsoft Word, version 6.0.1) and a consensus binding site was established by using the command 'find' to look for repeated motifs and by manually ordering the sequences. As the motif TAAT was revealed to be the most frequent, sequences were aligned by TAAT motifs and then ordered firstly, by the distance between two TAAT motifs and secondly, by the similarity of the nucleotides flanking one TAAT motif. Whenever a clone contained more than two core sequences, the minimum distance between any two antiparallel sites was chosen for scoring. Sequences were also analysed by MEME motif discovery tool (version 2.2), which is software designed to identify frequent motifs in biopolymers (http://www.sdsc.edu/MEME; Bayley, 1994).

Electrophoretic Mobility Shift Assays (EMSA)

Proteins used in EMSA were usually prepared by *in vitro* translation from synthetic capped RNA, as described above. Alternatively, *in vitro* translated protein was produced from DNA using the TNT *in vitro* translation kit (Promega). Binding reactions contained 1 μl of *in vitro* translated protein, 1X buffer, 1-2 μg Bluescript plasmid digested with *AluI* (Boehringer), 50,000-100,000 cpm probe and, when indicated, a 50-

100 fold excess of unlabelled specific or non-specific oligonucleotide, in a total volume of 12 µl. The 1X buffer was either (i) 100 mM KCl, 0.2 mM EDTA, 0.2 mM EGTA, 20% glycerol, 50 µg/ml BSA, 0.4 mM Phenylmethylsulfonyl fluoride (PMSF), 4 µg/ml aprotinin, 20 mM HEPES pH 7.9 or (ii) 50 mM KCl, 1 mM EDTA, 10% glycerol, 100 µg/ml BSA, 0.4 mM PMSF, 4 µg/ml aprotinin, 1 mM DTT, 20 mM HEPES pH 7.9. Complexes were allowed to form at room temperature for 10-15 min before adding probe and were incubated for 15-20 min after addition of probe. For antibody shift analyses, 1 µg of monoclonal anti-HA antibody (Boehringer), 12CA5, or anti-Myc antibody, 9E11, was added to the reactions and incubation was continued for an additional 10-15 min. Complexes in Fig. 3.4 and 6.4 were resolved on 4.5–5% polyacrylamide gels and those in Fig. 3.6 on 3% polyacrylamide gels. Gels were run initially at 300 mV for 10 minutes and then at 100-200 mV for 2-3 hours at 4°C. Oligonucleotides used in EMSA were annealed for 10 minutes at 70°C and cooled slowly to room temperature; they were then labelled by 3' filling with ^{32}P-dCTP (3,000 Ci/mmol) using the Klenow fragment (Promega). The top strands of probes A-I are shown below and are summarised in Fig. 3.4A (TAAT/ATTA core motifs are underlined, nucleotide substitutions are bold):

A: CTAGGTCGGGTGCTAATTGAGTCATTAGGGATACG;

B: CTAGGTCGGGTGCTA**C**TTGAGTC**G**TTAGGGATACG;

C: CTAGGTCGGGTGCTA**C**TTGAGTCATTAGGGATACG;

D: CTAGGTCGGGTGCTAATTGAGTC**G**TTAGGGATACG;

E: CTAGGTCGGGTGATAATT**C**AGTCATTAGGGATACG;

F: CTAGGAGTCGGGTGCTAATTTCATTAGGGATACAG;

G: CTAGGATCGGGTGCTAATTGGTCATTAGGGATACG;

H: CTAGGTCGGGTGCTAATTGANGTCATTAGGGATAG;

I: CTAGGTGGGTGCTAATTGANNNGTCATTAGGGATG;

J: CTAGCCTGTCGCTAATTAACCGATTAGGCCTGTTC.

Plasmid Constructs

For RNA injections into Xenopus embryos and/or EMSA

Xom-HA.pSP64T and **Xom^{L213P}-HA.pSP64T** were made by inserting a *BamHI/EcoRV* fragment comprising the entire open reading frame of Xom or Xom^{L213P} into *BglII/EcoRV*-digested pSP64T-HA, a vector based on pSP64T (Kreig and Melton, 1984) which also contained two copies of the hemaglutinin (HA) epitope followed by an in-frame stop codon. An *EcoRV* site was introduced at the 3' end of the Xom open reading frame using the Chameleon™ Site-Directed Mutagenesis Kit (Stratagene) to eliminate the stop codon and allow in-frame cloning with the HA epitope (mutagenesis primer: 5'-GCATTGGCTTCATATTGATATCTAACAAATGG-3'). Xom^{L213P} carries a point mutation in which a leucine at amino acid 213 (amino acid 40 of the homeodomain) is mutated to proline. Mutagenesis was carried out using the Chameleon™ Double Stranded Site-directed Mutagenesis Kit (Stratagene). The successful introduction of the L213P mutation in Xom^{L213P}-HA.pSP64T was verified by sequencing.

The **XomVP16.pCS2+** construct consists of the entire open reading frame of Xom fused at its C-terminus to a VP16 activation module (which contained two copies of: the λ repressor linker region (amino acids 92-132) fused to a minimal VP16 activation domain (amino acids 423-454)), all of which was inserted into pCS2+ (kind gift of Josh Brickman; (Emami and Carey, 1992). This construct was made in two steps: an *EcoRI/BamHI*-digested Xom fragment obtained by PCR was inserted in frame upstream of the module described above and cloned into pBXG1 (a kind gift of Josh Brickman); secondly, a fragment containing the resulting XomVP16 fusion was inserted into *EcoRI/XbaI*-digested CS2+ (Rupp et al., 1994). The primers used to obtain Xom full-length flanked by *EcoRI* and *BamHI* were: G1-5'GTCGGAATTCACCATGGTGACTAAAGCTTTCTCCTC3' (sense) and G2-5'CGCGGGATCCATATCTAACAAATGGCCT3' (antisense).

Gal4.Xom(1-327).CS2+, Gal4.Xom(235-327).CS2+ and **Gal4.Xom(1-173).CS2+** constructs were obtained following triple ligation of the following DNA

fragments: *BglII/EcoRI*-digested Gal4 (comprising amino acids 1-147) derived from the vector pBXG1, *EcoRI/XbaI*-digested Xom (comprising amino acids 1-327, 1-173 or 235-327), and *BamHI/XbaI*-digested pCS2+ (Rupp et al., 1994). Xom fragments used in this ligation were derived by PCR and cloned into pBXG1. The primers used were: G1 and G2 (see the cloning of XomVP16.pCS2+) for Xom(1-327), G4 (5'GTCGGAATTCACCATGGTGGATGGCAGACCAGACTC3') and G2 for Xom(235-327), and G1 and G3 (5'CGCGGGATCCCATCTTGCCCTCTTCATC3') for Xom(1-173). These DNA fragments were first digested with *EcoRI* and *BamHI*, cloned into pBXG1 (kind gift of Josh Brickman), and re-digested with *EcoRI* and *XbaI*. **Gal4.CS2+** was made by ligating *BglII/XbaI*-digested Gal4 (comprising amino acids 1-147) and *BamHI/XbaI*-digested CS2+. The orientation of the inserted fragment was verified by restriction digestion and sequencing.

ΔXom-HA.pT7 contains Xom (comprising amino acids 114 to 291) cloned in frame upstream of the three HA epitopes of the HA.pT7 vector (a kind gift from Tim Mohun). The Xom fragment was obtained by PCR using 5'-CTCTGCCATGGTTTCAGTGCCAG-3' as the sense primer and T7 as the antisense primer. This fragment was then digested with *NcoI* and inserted into *NcoI*-digested HA.pT7. The orientation of the insert was verified by restriction digestion and the in frame insertion of the DNA fragment was verified by *in vitro* translation and immunoprecipitation.

Unless otherwise stated, in frame insertions were verified by sequencing in all constructs. Additionally, RNA translation efficiency of the constructs was tested by *in vitro* translation using ^{35}-S labelled methionine followed by SDS-PAGE electrophoresis.

For expression of recombinant protein

Six histidine affinity tags were fused in frame at the N-terminus of Xom-HA by inserting a *PstI*-digested Xom-HA fragment from pSP64T into pQE30 plasmid (Qiagen), previously digested with *PstI* and treated with alkaline phosphatase. Sequencing was performed at the histidine-Xom junction.

Luciferase-based vectors

The **A_0.E4.luc** reporter construct (G_0E4.luc; a gift of Josh Brickman) contains an E4 minimal promoter driving the expression of *Photinus pyralis* (firefly) luciferase. This promoter drives weak constitutive expression in a variety of cell types.

The **A_5.E4.luc** reporter construct contains 5 copies of a consensus Xom binding sequence (5'-CTAGGTCGGGTGC**TAATTGAGTCATTA**GGGATACG-3'; also referred as oligonucleotide A, see Fig. 3.4) inserted upstream of the E4 minimal promoter in G_0E4.luc (which for our purposes is referred to as A_0.E4.luc). Double stranded oligonucleotide A was 5' phosphorylated and inserted (in several dilutions) into pBLCAT3T (a gift from Tim Mohun), previously digested with *XbaI* and treated with alkaline phosphatase. A fragment containing 5 copies of oligonucleotide A was then digested with *BamHI* and *SalI* and inserted into Bluescript.II.KS (Stratagene). Finally, a *KpnI/SacI*-digested 5 copy-fragment was inserted into A_0E4.luc. Sequencing was performed using primer GL3 (Promega) to confirm the number of tandem oligonuclotides inserted.

The **G_0p.luc** reporter construct (pGL3.luc; Promega) contains the SV40 enhancer/promoter region driving the expression of firefly luciferase. This enhancer/promoter region provides strong constitutive expression in a variety of cell types.

G_2p.luc and **G_5p.luc** reporter constructs (a gift of Josh Brickman) contains 2 or 5 copies, respectively, of the Gal4 17-mer binding site cloned upstream of the SV40 enhancer/promoter in pGL3.luc (which for our purposes is referred to as G_0p.luc).

The **-300gsc.luc** reporter construct (a gift of Niall Armes and Masazumi Tada) consists of 300 base pairs of the *goosecoid* promoter (Watabe et al., 1995) cloned into pGL3.Basic (Promega), driving the expression of firefly luciferase.

-300gsc.luc$^{-201/2}$ and -300gsc.luc$^{-145/-136}$ are versions of -300gsc.luc which contain point mutations in the indicated nucleotides (see Fig. 6.3). Point mutations were inserted using the GeneEditor™ *in vitro* Site-directed Mutagenesis System (Promega) according to the manufacturer's recommendations. The mutagenesis oligonucleotides used were:

5'CTAAAGGTTTTCCTACTGGAGTGGGTTAGTTTGATTAC3' for -300gsc.luc$^{-145/-136}$ and 5'GATTAACGGTGAGCAGGTAGCTCCTGTGAATAAC3' for -300gsc.luc$^{-201/2}$. Successful introduction of point mutations was confirmed by sequencing.

pRL-TK and **pRL-SV40** (Promega) were used as internal reference plasmids in luciferase assays. Both drive constitutive expression of a Renilla luciferase reporter gene cloned from the anthozoan coelenterate *Renilla reniformis,* with some minor modifications (Dual-Luciferase™ Reporter Assay System, Promega). Luciferase expression is directed by the herpes simplex virus thymidine kinase promoter region in the pRL-TK vector, or by the SV40 enhancer/promoter region, in the pRL-SV40 vector.

Mammalian expression vector- based constructs

XomVP16-Myc/His.pcDNA3 and **Xom^{L213P}VP16-Myc/His.pcDNA3** were used as effector DNAs in transient transfections in cultured cells. An *EcoRI/BamHI*-digested Xom (or Xom^{L213P}) fragment was inserted in frame upstream of the VP16 module (see above) cloned in pBXG1-VP16 (a kind gift of Josh Brickman). Then, the Xom (or Xom^{L213P})-VP16 fusion was digested with *EcoRI* and *XbaI* and inserted into pcDNA3.1-Myc/His (Invitrogen). The Xom/VP16 fusion region was sequenced. XomVP16-Myc/His.pcDNA3 was also used as a template for RNA synthesis and protein translation for EMSA.

Xom/Gal fusion constructs were cloned into pBXG1 (a gift of Joshua Brickman) to be used in transient transfection assays. Xom fragments used in this ligation were derived by PCR using primers G1 and G2 (to amplify Xom full length), or G4 and G2 (to generate a fragment comprising amino acids 235 to 327), or G1 and G3 (to generate a fragment comprising amino acids 1 to 173). See above for the sequence of the primers. These DNA fragments were digested with *EcoRI* and *BamHI* and cloned into pBXG1 to generate **G4.Xom(1-327).pBXG1, G4.Xom(235-327).pBXG1** and **G4.Xom(1-173).pBXG1**.

Xom-HA.pcDNA3 and **Xom^{L213P}-HA.pcDNA3** were made by inserting a *BamHI/EcoRV* fragment comprising the entire open reading frame of Xom or Xom^{L213P}, respectively, into pcDNA3 (Invitrogen).

Embryos and Embryo Manipulations

Obtaining Xenopus embryos

Xenopus embryos were obtained by artificial fertilisation as described by Smith and Slack (1983). Briefly, *Xenopus* embryos were obtained from adult females that had been injected 12 hours previously with 500-1000 units of human chorionic gonadotrophin, and transferred to a 90 mm Petri dish. The eggs were fertilised by rubbing them with testes dissected from a sacrificed male. Males were sacrificed by decapitation and disruption of the spinal cord. Testes were dissected and submersed in L15 media (Sigma) at 4°C for 2 or 3 days. Five minutes after fertilisation the eggs were flooded with 10% Normal Amphibian Medium (NAM; Slack, 1984). The embryos were de-jellied using 2% cysteine hydrochloride (pH 7.9-8.1), and staged according to Nieuwkoop and Faber (1975).

Microinjection of Xenopus embryos

De-jellied embryos were transferred into 75% NAM containing 4% Ficoll in 35 mm Petri dishes lined with 1% agarose. Transfer was done by aspirating the embryos immersed in solution into glass Pasteur pipettes sectioned at a suitable diameter. Embryos were injected using an nitrogen (N_2)-driven injection system (Narishige IM 300 Microinjector, Japan) with the aid of a micromanipulator (Oxford manipulator, Micro Instruments). Typically, volumes of 10 nl per injection were delivered into one blastomere of two or four-cell stage embryos using a capillary glass needle. The injection volume was calculated by injecting the liquid into oil and measuring the diameter of the drop using a graticule. By treating the drop as a sphere, the injected volume was determined. For dorsal or ventral injections, the dorsal and ventral halves of the 4-cell stage embryo were distinguished due to the lighter pigmentation and bigger size frequent in dorsal blastomeres. Embryos that were not used for animal cap assays were transferred to 10% NAM before gastrulation, generally at stage 8 (mid-blastula). Non-specific death of embryos before stage 8 was not included in the scoring of phenotypes.

Animal cap dissection

Animal pole explants, usually called animal caps, were dissected from embryos at blastula stage 8-9 in 75% NAM. The vitelline membrane surrounding the embryo was removed manually using sharpened number 5 watchmakers forceps (supplied by BDH). A square of tissue from the animal-most 20-25% region was cut by using the forceps as scissors. The tissue was placed in 75% NAM on agarose-coated dishes until sibling embryos had reached the desired stage.

For luciferase assay experiments, animal caps were cultured for 3 hours and 30 minutes from the time the last animal cap was cut. An average of 150 animal caps were cut per experiment (approximately 1 hour and 15 minutes of dissection) and 2 replicas of 10 animal caps per experimental group were taken for analysis.

For RNase protection analyses, animal caps were treated with 10 u/ml of activin and 0.1% bovine serum albumin for approximately 4 hours after dissection (to the equivalent of stage 10.5 to 11). After this period, the solution was aspirated from the tube and the caps were frozen at –70°C until further analysis.

Luciferase assays on animal cap or whole embryo lysates

Animal caps were lysed in 3.3 µl/cap of 1X Passive Lysis buffer (Dual-Luciferase™ Reporter Assay System, Promega) and centrifuged for 5 min at 4°C. The amount of luciferase activity present in the supernatant was determined according to the manufacturer's instructions (Dual-Luciferase™ Reporter Assay System, Promega) and results were quantified using a luminometer. Whole embryos at the desired stage were lysed in 33 µl/embryo of 1X Passive Lysis buffer and treated as above.

Whole mount in situ hybridization

Whole mount *in situ* hybridization was modified from the protocol of Harland (1991). Gastrula stage embryos were removed from their vitelline membranes, a hole was made in the blastocoel to improve penetration of solutions, and they were fixed for 2 hours at 4°C in MEMFA (fresh formaldehyde at 3.7% in 1X MEM salts) before being transferred to methanol for long-term storage at -20°C. All procedures were performed in

5-ml screw top glass vials (Phase Separation). In all solutions containing water, water filtered to 0.2 micron (SPH_2O, Romil Ltd.) was used.

Embryos were rehydrated by taking them through a methanol/water (and PBS) series starting with 75% methanol in water, 50% methanol in water and then 25% methanol in PBS for about 5 minutes each. Embryos were then washed 3 times in PBS/Tween 0.1%. Proteinase K (Boehringer) at 5 µg/ml is then added, to increase penetration by degradation of surface proteins, and embryos were left for 10 to 20 minutes at room temperature. The timing of proteinase treatment was monitored carefully, because long exposures can damage the embryos. Embryos were again washed in PBS/Tween 0.1% and then treated with 4 ml of 0.1M triethanolamine pH 7.7, 5 minutes twice, to acetylate proteins (0.1 M triethanolamine solution was prepared previously by diluting the suitable amount of triethanolamine, adjusting the pH with HCl and then filtering with a Sartolab V500 filter). Without removing the triethanolamine solution, 10 µl of acetic anhydride was added and incubated for 5 minutes twice. This treatment blocks the activity of endogenous phosphatases. Again, the embryos were washed with PBS/Tween 0.1% for 5 minutes twice. To fix, embryos were treated with freshly prepared 4% paraformaldehyde in PBS for 20 minutes. To prepare 30 ml of this solution, 1.2 g of paraformaldehyde was mixed with 27 ml of water and 10 µl of NaOH, shaken and dissolved in the microwave oven (series of 5 seconds until the mix was dissolved), and then 3 ml of a 10X PBS stock solution and one drop of concentrated H_3PO_4 were added. The embryos were washed 5 times with PBS/Tween 0.1%, pre-hybridised with 1 ml of Hybe solution for 2 hours at 60°C and, finally, they were hybridised overnight at 60°C in 500 µl of this solution with 2 µl of denaturated dioxigenin (DIG)-labelled probe. The Hybe solution was: 50% deionised formamide, 5X SSC pH 6, 200 µg/ml t-RNA, 100 µg/ml heparin, 1X Denhard'ts (50X stock contains 1 g polyvinylpyrrolidone, 1 g Ficoll and 1 g BSA made up to 100 ml with SPH_2O), 0.1% Tween 20, 0.1% CHAPS and 5 mM EDTA.

On the next day, the embryos were washed using a series of washing solutions with decreasing amounts of formamide: 50% formamide/5X SSC/0.1% CHAPS (10 minutes at 60°C), 25% formamide/2X SSC/0.1% CHAPS (10 minutes at 60°C), 2X

SSC/0.1% CHAPS (30 minutes at 60°C twice), 0.2X SSC/0.1% CHAPS (30 minutes at 60°C twice). After the washes, embryos were treated with maleic acid buffer (150 mM NaCl, 0.1 M maleic acid pH 7.5) in 0.1% triton (MABT) for 5 minutes at room temperature twice. The MABT solution has a suitable pH for incubation with anti-DIG antibody and should be prepared with a non-ionic detergent such as Triton to avoid nonspecific interference with the antibody binding reaction. Before adding antibody, the embryos were treated with freshly prepared 2% blocking reagent (Boehringer)/10% lamb serum (heat inactivated)/MABT, for 1 hour at room temperature. Finally, embryos were incubated overnight at 4°C with gentle rotation with a 1:4000 dilution of anti-dioxigenin (DIG) Fab fragments conjugated with alkaline phosphatase 150u/200µl (Boehringer).

On the following day, embryos were washed 4 times for 1 hour at room temperature in MABT. Then, they were treated with alkaline phosphatase buffer (0.1 M Tris.HCl pH 9.5, 0.1 M NaCl, 50 mM $MgCl_2$, 0.1% Tween 20 and 2 mM levamisol freshly added) followed by 1 ml of BM purple alkaline phosphatase substrate (Boehringer). The staining reaction was carried out for approximately 5 hours and 30 minutes at room temperature with *goosecoid* probe and 2 hours 30 minutes for the *XFDH1* probe. After staining was complete, the embryos were washed in alkaline phosphatase buffer twice and staining was fixed by a 1 hour treatment with MEMFA at 4°C with gentle rotation. Then, embryos were washed in methanol twice and bleached in 70% methanol/10% H_2O_2 (30% of a 30% stock H_2O_2) to remove the normal pigmentation of the embryos and reduce nonspecific staining. Finally, the embryos were stored in methanol at 4°C or used in whole mount antibody staining. To make *goosecoid* probe, pΔgsc subclone (Cho et al., 1991) was linearised with *XhoI* and transcribed with T7 RNA polymerase in the presence of DIG-RNA Labelling Mix (Boehringer). *XFKH1* probe was made by linearising XFKH1.pGEM4Z (a kind gift from Caroline Hill) with *EcoRI* and transcribing with T7 RNA polymerase.

Whole mount antibody staining

Immunolocalisation of the lineage tracer fluorescein dextran (Molecular Probes) was carried as described Jones and Smith (1998). Embryos stained previously for

alkaline phosphatase activity (in whole mount *in situ* hybridization) were re-hydrated in a series of solutions with decreasing methanol concentration: 75% methanol in PBS, 50% methanol in PBS, 25% methanol in PBS, PBS and PBT (PBS/ 0.2% BSA/0.1% Triton X-100). All procedures were performed in 5-ml screw top glass vials (Phase Separation). Non-specific epitopes were then blocked by incubating the embryos in 10% heat inactivated lamb serum (Gibco BRL) mixed with PBT for 1 hour before the incubation with primary antibody. For this study, Fab fragments coupled with alkaline phosphatase and recognising fluorescein (Boehringer) were used at a 1:2000 dilution in PBT and 10% lamb serum. Incubation with this antibody was performed overnight at 4°C.

The primary antibody was rinsed by washing 6 times, 15 minutes each, in PBT and one time in 0.1 M Tris pH 8.2/Tween 0.1%. The staining of bound antibody was detected using a solution comprising 1 tablet of Fast Red Staining (Boehringer)/4 ml of 0.1 M Tris pH 8.2. Incubation was performed on ice for approximately 30 minutes until red staining was visible. The reaction was stopped in PBS and staining was fixed for 1 hour at 4°C in MEMFA. The embryos were photographed and transferred into methanol for long-term storage at -20°C.

Immunolocalisation of notochord or muscle tissue was carried out by a different procedure from the one described above. Embryos were collected at tadpole stage 35, fixed in MEMFA for 1 hour at 4°C, washed twice in methanol and stored at 4°C until further use. Embryos were re-hydrated in a series of solutions with decreasing methanol concentration: 75% methanol in water, 50% methanol in water, 25% methanol in PBS, PBS and they were then left in PBS for 30 minutes. Next, they were bleached in 10% H_2O_2/PBS overnight (or several hours) over a light box and washed in PBT (PBS/ 0.2% BSA/0.1% Triton X-100) 4 times for 5 minutes each, and then twice for half an hour each. Non-specific epitopes were blocked by incubating the embryos in 5% heat inactivated lamb serum (Gibco BRL) mixed with PBT (PBTN) for 30 minutes before incubation with the primary antibody. Monoclonal antibody 12/101 (Kintner and Brockes, 1984), specific for muscle, was used at a 1:200 dilution in PBTN, whereas monoclonal MZ15 antibody (Smith and Watt, 1985), specific for notochord, was used at

a dilution of 1:400 in PBTN, and both were incubated overnight at 4°C. On the following day, embryos were washed in PBT for 5 minutes (3 times) and for 30 minutes (4 times) and non-specific binding was blocked by an incubation of 30 minutes in PBTN, as previously described. Incubation with anti-mouse peroxidase coupled antibody (Amersham), diluted 1:200 in PBTN, was performed for 2 hours at room temperature. The embryos were washed again in PBT for 5 minutes, 3 times, and 30 minutes, 4 times. The staining of bound antibody was detected by incubating with Developing Solution for 10 to 20 minutes in the dark. The Developing Solution was prepared by dissolving a 10 mg Diaminobenzidine Tetrahydrochloride (DAB) tablet (Sigma) in 30 ml of PBS, filtering to take out the remaining precipitate, adding Triton to make 0.1% and $NiCl_2$ to a final concentration of 0.3 mg/ml. To start staining reaction, H_2O_2 to make 0.03% was added and the embryos were submersed by this solution. The staining reaction was stopped with 2 mM EDTA. The embryos were then dehydrated by a series of solutions with increasing methanol concentration: 25% methanol/PBS, 50% methanol/PBS, 75% methanol/PBS and stored in methanol at 4°C.

RNAse Protection

RNA was isolated from *Xenopus* whole embryos or animal caps using the acid phenol/guanadinium isothiocyanate procedure (Chomczynski and Sacchi, 1987). Briefly, tissue was homogenised in a solution of guanadinium isothiocyanate (4M guanadinium isothiocyanate; 25 mM sodium citrate pH 7; 0.5% sarcosyl; 0.7% β-mercaptoethanol freshly added), acid-phenol (1:1 volume) and 0.2 M sodium acetate. 20 to 30 animal caps or 3 whole embryos were used per 500 µl of guanadinium solution. The phases were separated by adding 0.2 volumes of chloroform. The aqueous upper phase was then precipitated using an equal volume of isopropanol, after which the pellet was washed in 70% ethanol.

To guard against RNAase activity, water filtered to 0.2 micron (SPH_2O; Romil Ltd.) was used in all solutions, which were then autoclaved.

The constructs used to make probes for RNAase protection analysis are listed in the table below.

Table 2.2. Constructs used as templates for RNAase protection probes

Gene	Linearisation site	RNA Polymerase	Probe length	Protected Length	Reference
EF-1α	*Hinf I*	SP6	150	114	(Krieg et al., 1989)
goosecoid	*Xba I*	T3	440	367	(Cho et al., 1991)

A probe template construct was linearised with the appropriate restriction enzyme and the probe transcription reaction was set up at room temperature, as follows (see also Tada et al., 1997).

4 µl	5 X Transcription buffer (Promega)
2 µl	0.1M DTT
2 µl	5 mM nucleotides (-UTP)
1.2 µl	UTP 200 µM
1 µl	RNAse inhibitor (Promega)
5 µl	^{32}P-UTP
0.8µl (0.8µg)	Linearised template DNA
1 µl	RNA polymerase (Promega)
3 µl	SPH_2O

The reaction was incubated for 1 hour at 37°C, after which 1 µl of RQ1-DNAse was added to degrade the DNA template and incubation was continued for 20 more minutes at 37°C. Then, 20 µl of formamide-containing loading dye was added. The reaction was denatured by heating to 80°C for 2 minutes and then size fractionated using a short polyacrylamide gel (6% polyacrylamide, 7M Urea). This gel was run at 35 W for approximately 1 hour, until the xylene cyanol dye had migrated two-thirds of the distance of the gel. The gel was wrapped in cling film and the desired band was cut out from the gel after being visualised with a 15 second exposure to X-ray film. The gel

piece was eluted in 500 µl of elution buffer (0.1% SDS, 1 mM EDTA, 0.5 M ammonium acetate) for 2–3 hours at 50°C. The eluate was then precipitated (using t-RNA as carrier) and resuspended so that 1 µl of probe contained at least 5 X 10^5 counts.

Labelled probes were added to RNA (isolated from *Xenopus* whole embryos or animal caps) that was dissolved in 50% formamide and 1 X Hyb salts (5 X Hyb Salts: 2M NaCl, 0.2M PIPES (pH 6.4), 5 mM EDTA). This mix was then heated to 85°C for 5 minutes to denaturate the RNA and hybrids were allowed to form for 8-14 hours at 55-60°C. After hybridisation, non-homologous sequences were degraded by digestion with RNAase T1 10 u/ml at room temperature for 30 minutes in RNase Buffer (10 mM Tris.HCl pH 7.5, 5 mM EDTA, 300 mM NaCl). RNAase T1 was then destroyed by incubation with 0.1 mg/ml proteinase K (Boehringer) for 15 minutes at 37°C in RNase Buffer/0.5% SDS. The whole reaction was then subjected to phenol/chloroform extraction followed by ethanol precipitation. The resulting pellet was resuspended in 2 ml of SPH_2O. Formamide-containing loading dye was then added to the solution and the mixture was loaded on a large 6% polyacrylamide gel containing 7 M urea. The gel was run until the xylene cyanol had migrated 75% of the total gel length. The gel was then fixed using a solution containing 10% methanol and 10% acetic acid in water, after which it was dried and exposed to X-ray film at -70°C, with intensifying screen.

Photography

To visualise staining in internal tissues, embryos were dehydrated in methanol and placed in Murray's Clear (2 volumes of benzyl benzoate, 1 volume of benzoic acid), which renders them transparent, and placed in glass Petri dishes with a rounded bottom (Murray's Clear has to be handled with glass). Photographs were taken using a Wild m8 stereomicroscope and camera. Embryos were also photographed in aqueous solution, after being re-hydrated in a series of solutions with decreasing methanol concentration. After photography, embryos were again dehydrated in a series of solutions with increasing concentration of methanol and stored in methanol at 4°C.

Cell Culture

Handling culture cells

COS cells were stored in liquid Nitrogen in 10% DMSO/complete DMEM medium in vials of 1.5 ml. Complete DMEM, which can be stored at 4°C for 15 days, contained Dulbecco's Modified Eagle Medium (Sigma), 10% Newborn Calf Serum (PAA Laboratories) and 200 mM L-Glutamine (Sigma) at 1:100 dilution.

Cells were thawed at 37°C (but not to completion), transferred to 9 ml of complete DMEM medium and centrifuged at 4°C for 5 minutes at 1000 rpm. The supernatant was removed and cells were resuspended in the medium remaining in the tube. 10 ml of complete DMEM was added to the cells, which were then cultured at 37°C in 80 cm^2 cell culture flasks (Nunc). When cells reached 70% confluency (approximately 1 or 2 days later under these conditions), they were split at a 1:2 dilution and cultured again to use in transient transfections. To subculture cells, they were rinsed with PBS-Ca^{++}-Mg^{++}-free and treated with trypsin-EDTA 1X (0.5 g porcine trypsine and 0.2 g EDTA.4Na per litre; Sigma) by adding 2 ml of trypsin-EDTA 1X to cells, taking off the excess and leaving for 5 minutes. Then, the flask containing the trypsinised cells was hit with the hand to loosen cells adherent to the flask wall, and they were resuspended in 10 ml of newly added complete DMEM. A suitable volume of trypsinised cells in 10 ml of complete DMEM, generally diluted to 1:10, was then used to start a new culture of cells.

During the first cycles of splitting/transfection, cells were grown to 70% confluency to re-freeze for long-term storage. Cells were trypsinised as above and spun down in 10 ml tubes for 5 minutes at 1000 rpm and at 4°C. The supernatant was poured off and cells were resuspended in the medium remaining in the tube. 2 ml of freezing solution kept on ice (complete DMEM/10% DMSO) was added and aliquots of 1 ml were transferred to 1.5 ml tubes suitable for liquid nitrogen freezing, and placed on ice. The freezing procedure should take place very slowly to prevent damage of cells. Therefore, cells were placed into an ice-cold isopropanol-insulated container. This container was then placed at -70°C for at least 4 hours before cells were transferred to

liquid nitrogen. 10 ml of cell at 70% confluency contains approximately 2 to $5X10^6$ cells, thus each vial of frozen cells contained approximately 1 to $2.5X10^6$ cells/ml.

Lipofectamine-based transient transfection method

70% confluent COS cells were trypsinised as above and counted in an haematocytometer (25 unitarian squares=$1X10^{-4}$ cm^3). Cells were diluted in complete DMEM medium into 6-well polystyrene cell culture plates (Costar). Each well contained $1.2X10^5$ cells in 2 ml medium.

On the following day, cells were re-fed by replacing the medium with 2 ml of new complete DMEM medium. Cells were then incubated at 37°C for 2 to 3 hours before transfection. Meanwhile, DNA mixtures for transfection were prepared. Each DNA mixture contained variable amounts of effector DNA, 100 ng of firefly luciferase reporter construct, 100 ng of reference plasmid and variable amounts of plasmid DNA to a total of 800-1000 ng DNA. All DNA used in transient transfections was obtained by midi-preparation (Qiagen) followed by phenol/chlorophorm extraction and ethanol precipitation. Each DNA sample was added to 100 µl of Optimem 1-glutamax (Gibco BRL, the commercial equivalent of DMEM/2 mM glutamine). In parallel, 10 µl of lipofectamine™ reagent 2 mg/ml (Gibco BRL) was added to 100 µl of Optimem 1-glutamax in 24-well plates (Costar). Each DNA sample was then combined with the lipofectamine on the 24 well-plates with thorough mixing. This solution was incubated for 30 minutes at room temperature. Meanwhile, cells were rinsed with filtered PBS and then rinsed with 1 ml of Optimem 1-glutamax. To start transfection, the previous wash medium was removed from cells, 0.8 ml of Optimem 1-glutamax was added to the 200 µl DNA/lipofectamine mixture and mixed gently and then cells were overlayed with the 1 ml DNA/lipofectamine/Optimem mixture and incubated at 37°C for 4 hours. After this serum deprivation period, 1 ml of Optimem 1-glutamax/20% newborn calf serum was added to each well (to a total of 2 ml of medium and 10% of serum concentration), and left overnight in the 37°C incubator. On the following day, the medium was replaced by 2 ml of complete DMEM per well. Cells were harvested approximately 48 hours after transfection.

Mouse fibroblast NIH3T3 cells were used in transient transfection experiments to assay the subcellular localisation of proteins encoded by transfected constructs (see Fig. 4.3). In these experiments, the transfection procedure was similar to that for COS cells with the following modifications: cells were cultured on circular coverslips, smaller amounts of DNA were used for transfection (0.4 to 0.6 μg per transfection), cells were serum-starved for 6 hours after transfection and 2.5 ml of complete DMEM medium (with antibiotics) was added to each well to allow culture until cells were harvested.

Luciferase assays

Cells were rinsed with 2 ml of PBS and lysed with 1 ml/well of 1X Lysis buffer (Dual-Luciferase™ Reporter Assay System, Promega) by incubating 30 minutes at room temperature with gentle shaking. As cell membranes remain adherent to the well, the supernatant containing the cytoplasmic contents was recovered to a microfuge tube, spun at 4°C for 5 minutes to further remove the cell debris and, finally, used for assaying luciferase activity.

Promega's Dual-Luciferase™ Reporter Assay System combines the simultaneous expression and measurement of two individual reporter enzymes within a single system. Typically, the experimental reporter (firefly or *Photinus pyralis* luciferase) reflects the effect of specific experimental conditions on the level of gene expression, while the activity of the co-transfected control reporter (*Renilla reniformis* luciferase) provides an internal control by which each value within the experimental set can be normalised. This eliminates inherent variability (such as the efficiency of transfection and lysis) that can decrease experimental accuracy. Since firefly and *Renilla* luciferase are of distinct evolutionary origins, they have dissimilar enzyme structures and substrate requirements. These differences make it possible to selectively discriminate between their respective bioluminescence reactions.

The firefly luciferase reporter assay is initiated by adding a 2 μl aliquot of the lysate to 50 μl Luciferase Assay Reagent 2. Quenching of firefly luciferase luminescence, and concomitant activation of *Renilla* luciferase, is accomplished by adding 50 μl of Stop & Glo™ Reagent (S&G) to the sample tube immediately after

quantification of the firefly luciferase reaction. The luminescence signal is quenched at least by a factor of 10^5 within 1 second following the addition of S&G and complete activation of *Renilla* luciferase is also achieved within this period. Determination of *Renilla* and firefly luciferase activities was performed according to the manufacturer's instructions using a luminometer.

Preparation of protein extracts for Western blot analysis

For Western blot analysis, COS cells were transiently transfected with 1 μg of DNA encoding the desired protein. Approximately 48 hours after transfection, cells were washed with PBS and lysed in 150 μl of RIPA Buffer (PBS, 1% NP40, 0.5% sodium deoxycholate, 0.1% SDS and freshly added proteinase inhibitors (15 μl of 1 tablet proteinase inhibitor cocktail (Boehringer)/2 ml RIPA Buffer)). Cells were scraped from the wells and placed into a microfuge tube. 100 μl of RIPA Buffer with proteinase inhibitors were added to the wells and the scraping procedure was repeated. The 250 μl solution containing the cells was then aspirated into a 1 ml syringe and passed through a 23 gauge needle approximately 10 times to shear DNA. 5 μl of 0.2 mM phenylmethylsulfonyl fluoride (PMSF) was added (this proteinase inhibitor was not in the original cocktail) and lysed cells were left for 30 minutes on ice. Finally, cells were spun for 20 minutes at 4°C and 200 μl of supernatant was added to 40 μl of 5X Sample Buffer. 25 μl of protein extract was boiled for 5 minutes to denaturate before use while the remaining extract was stored at -20°C.

Immunocytochemistry: Russell's protocol

After transfection, 3T3 fibroblast cells stuck to coverslips were washed by handling the coverslip with forceps and diving it carefully into a 1 l beaker filled with PBS. The following treatments were done with the coverslips standing on clean parafilm wrapped around a glass plate and cells were kept wet at all times. A Pasteur pipette was used to deliver a few drops of the solution in use on the cells, and solutions were removed using the vacuum pump.

Cells were fixed with 3% paraformaldehyde in PBS for 30 minutes and then

washed in PBS using the 1 l beaker. To permeabilise cells, 0.1% Triton/PBS was used for 5 minutes followed by a new wash in PBS. Blocking solution (0.25% gelatin/PBS) was added for 20 minutes, removed, and the primary antibody solution was added, which contained 1 mg/ml of anti-HA monoclonal antibody (Boehringer) into the previous solution, and left overnight at 4°C. At this point, coverslips were placed into 6-well cell culture dishes lined with humid paper towels to prevent evaporation. On the following day, cells were washed in PBS, covered with blocking solution again and incubated with the secondary antibody (FITC-conjugated anti-mouse IgG (Sigma) at 1:40 dilution in blocking solution) for 1 hour at room temperature. Finally, cells were washed twice in PBS. To mount, coverslips (with cells facing down) were put over one drop of mounting medium (citifluor) surrounded by three drops of nail varnish to hold the coverslip. Then, the coverslip was gently pressed down and sealed all around with more nail varnish. PBS crystals were cleaned from the top of the coverslip with a humid cotton bud and cells were ready for observation in a fluorescence microscope.

Statistical Analysis

t- test

The t-test performed was a two-sample test assuming unequal variances of both ranges of data (heteroscedastic test). See Microsoft Excel (1998) for the respective mathematical equations.

Formulation of Frequently Used Solutions

PBS	137 mM NaCl, 2.7 mM KCl, 4.3 mM $Na_2HPO_4.7H_2O$, 1.4 mM KH_2PO_4
TE	1 mM EDTA, 10 mM Tris.HCl pH 8.0
low TE	0.1 mM EDTA, 10 mM Tris.HCl pH 8.0
TAE	40 mM Tris.acetate, 2 mM $Na_2EDTA.2H_2O$ (pH 8.5)
TBE	89 mM Tris-Base, 89 mM Boric acid, 2 mM EDTA pH 8.0
20X SSC	3 M NaCl, 0.3 M Na_3citrate.$2H_2O$, adjust pH to 7.0 with 1 M HCl
6X gel loading buffer	6X TAE, 50% v/v glycerol, 0.25% w/v bromophenol blue
10X native gel loading buffer	50% glycerol, 10 mM Tris.HCl pH 8.0, traces of bromophenol blue and xylene cyanol
5X sample buffer (for SDS-PAGE)	15% w/v SDS, 15% v/v β-mercaptoethanol, 50% v/v glycerol, 1.5% w/v bromophenol blue
Formamide-containing loading dye	10 mM NaOH, 1 mM EDTA, 80% v/v formamide, 0.02% w/v bromophenol blue, 0.02% w/v xylene cyanol
10X NAM (1 litre)	110 M NaCl, 2 M KCl, 1 M $Ca(NO_3)_2$, 1 M $MgSO_4$, 0.1 M Na_2EDTA
10% NAM (500 ml)	5 ml 10X NAM, 10 ml 0.1M Na phosphate (pH 7.4), 2.5 ml 10 mg/ml gentamycin
75% NAM (500 ml)	37.5 ml 10X NAM, 10 ml 0.1M Na phosphate (pH 7.4), 5 ml 0.1M $NaHCO_3$, 2.5 ml 10 mg/ml gentamycin
2% cysteine hydrochloride pH 7.9-8.1 (200 ml)	4.4 g L-cysteine hydrochloride monohydrate, 1.33 to 1.36 g NaOH pellets, fill up to 200 ml distilled water
10 X MEM salts	1 M MOPS, 20 mM EGTA, 10 mM $MgSO_4$
MEMFA (50 ml)	5 ml 10X MEM salts, 5 ml 37% formaldehyde

Formulation of Frequently Used Bacterial Growth Media

LB (L-Broth)	1% w/v bacto-tryptone, 0.5% w/v bacto-yeast extract, 1% w/v NaCl
L-agar	L-Broth supplemented with 1.5% bacto-agar
2X TY	1.6% w/v bacto-tryptone, 1% w/v bacto-yeast extract, 0.5% w/v NaCl
LB Top-agar	1% w/v tryptone, 0.5% w/v yeast extract, 0.5% w/v NaCl, 0.7% w/v agar

CHAPTER 3

DNA binding properties of Xom

INTRODUCTION

Despite the vast number of biological functions of homeoproteins, nearly all homeodomains bind to DNA sequences containing the TAAT core motif (Gehring et al., 1994; Laughon, 1991). Based on structural studies, sequence comparisons and *in vitro* binding studies, Wilson and collaborators (Dear et al., 1993; Wilson et al., 1996) suggested the existence of an amino acid consensus sequence for the recognition of the TAAT motif by homeobox containing genes. This includes 5 amino acid positions interacting with the core DNA itself, 12 that make the hydrophobic core, and 8 involved in making DNA phosphate contacts, in a total of 22 important residues (Fig. 3.1 A). All these positions are conserved in the Xom homeodomain except at position 47, where it contains a threonine instead of the more frequent isoleucine or valine (Ladher et al., 1996). Analysis of several homeodomain-DNA structures, such as those of *engrailed*, *evenskipped* and *Antennapedia*, show that the frequent isoleucine or valine at position 47 establishes a hydrophobic interaction with the methyl group of the second thymidine of the TAAT core (Fig. 3.1 B; for a review see Wilson et al., 1996). Therefore, the identity of the residue at position 47 may be important for DNA binding specificity.

In addition to Xom, Xvent-1 and Tlx-2, other homeodomain containing proteins such as human HOX11 (Kennedy et al., 1991), *Drosophila* BarH1 (Higashijima et al., 1992) and *Drosophila* Oml D (Tanda and Corces, 1991) also have a threonine at position 47 of the recognition helix. For the HOX11 homeodomain, this substitution was shown to affect DNA binding specificity. *In vitro* binding site selection showed that the preferred sequences of HOX11 exhibited a motif consisting of TAAC, TAAT or both (Dear et al., 1993). The same analysis performed with a mutant HOX11 protein containing a isoleucine at position 47 invariably generated the TAAT motif (Dear et al., 1993), showing that position 47 in the recognition helix indeed has an important role in establishing the identity of the most 3' nucleotide of the TAAT motif.

However, a study in which a sequence containing a 5'-AAAT-3' motif, which corresponds to the Oct-1 POU homeodomain consensus binding site, was used to screen

a Oct-1 POU homeodomain bacterial expression library in which residues 47 and 51 had been randomised, generated a large variability of residues at position 47 relative to position 51 (Pomerantz and Sharp, 1994). This suggested that the residue at position 47 has only a minor contribution to the DNA binding specificity of the POU homeodomain (Pomerantz and Sharp, 1994). Based on this and other results, Pomerantz and Sharp (1994) argue that, at position 47, side chains other than valine or isoleucine may be capable of making similar hydrophobic/van der Walls contacts with the second thymidine of the TAAT motif (or AAAT, in this case). Alternatively, amino acid residues at other positions, such as the conserved asparagine at position 51, may specify the identity of this base pair through water mediated contacts (Pomerantz and Sharp, 1994).

This is consistent with the findings of Kalionis and O'Farrell (1993), who used the oligonucleotide 5'-TCAATTAATTGA-3' (containing two overlapping palindromes of the TAAT core motif) as a probe to screen a cDNA expression library from *Drosophila*. Although this oligonucleotide corresponds to an *engrailed* homeodomain binding site (underlined), this approach lead to the identification of 17 unrelated homeodomains proteins including the *Drosophila* BarH1 protein, which shares 59% amino acid identity with Xom and Xvent-1 and, like Xom and Xvent-1, has the threonine at position 47 of the homeodomain. Although a stronger binding signal was observed using the sequence 5'-TCATTTAAATGA-3' (Kalionis and O'Farrell, 1993), which contains the sequence 5'-TAAA or 5'-AAAT instead of the 5'-TAAT core motif, this study shows that the non-conservative threonine substitution at position 47 allows binding to TAAT motifs *in vivo*.

The homeodomain preference for specific nucleotides adjacent to TAAT core sequences may also be mediated by differences in the primary structure of the homeodomain. In particular, the identity of the amino acid at position 50 may specify the identity of two nucleotides 3' of the TAAT core (Wilson et al., 1996). This amino acid is very polymorphic amongst different homeodomains although it is conserved between homologues of different species. When position 50 is occupied by a glutamine (as in Xom), and the remaining residues important for binding the core motif are conserved (Fig. 3.1), the predicted binding sequence is TAAT(C/T)N. An exception is

Fushi tarazu, which has a glutamine on position 50 and binds preferentially to TAATG (Wilson et al., 1996). A possible explanation for a single amino acid being able to confer a variety of distinct DNA binding preferences may lie in its particular structural relationship with the DNA bases. Indeed, position 50 of the recognition helix is not in intimate contact with the bases of the major groove, which allows for a diverse range of side chains to be accommodated. Each side chain then favours a particular sequence of DNA bases to which it can form relatively long range contacts, perhaps van der Walls or water mediated hydrogen bonding (Wilson et al., 1996).

In this Chapter, the specific DNA binding preferences of Xom were analysed. To that aim, an *in vitro* PCR-based binding site selection analysis was performed and binding to intact and mutagenised potential Xom binding sequences was analysed *in vitro* by electrophoretic mobility shift assays (EMSA). In addition, the ability of a Xom fusion construct to interact with this sequence was further analysed by transient transfection in mammalian cultured cells.

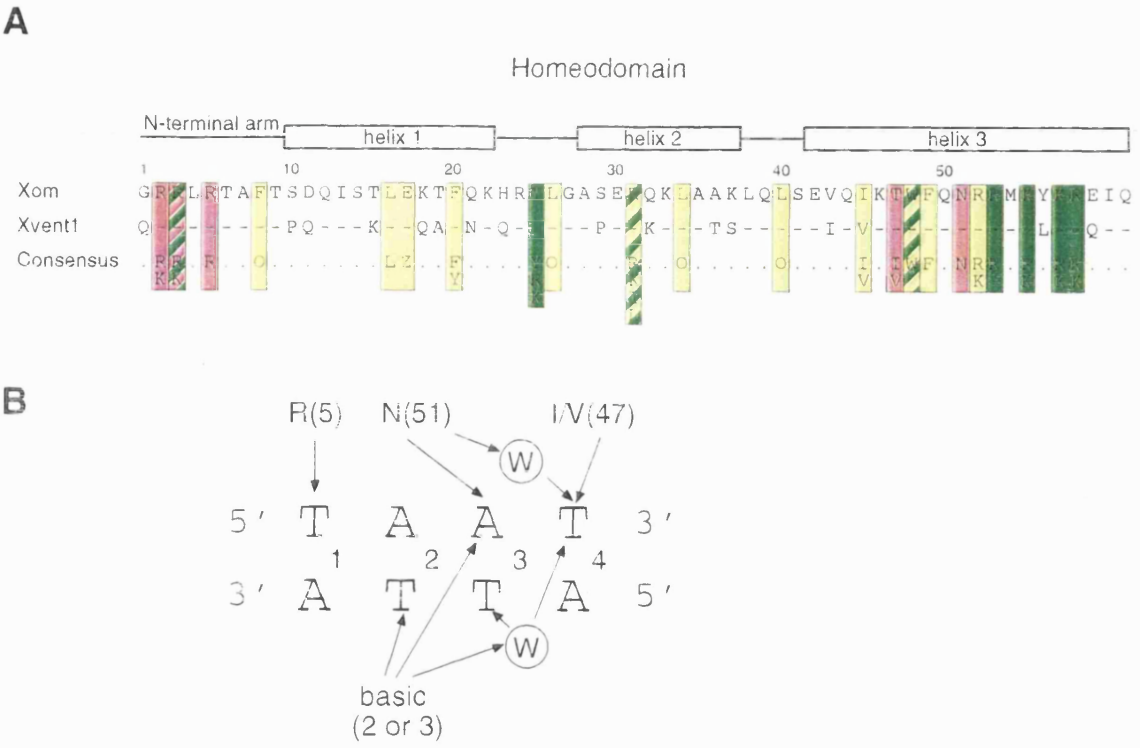

Fig. 3.1. (A) Amino acid sequence alignment of Xom and Xvent-1 homeodomains showing potentially important residues for the recognition of a TAAT core motif. Below the two homeodomain sequences is the TAAT-binding consensus of amino acids as described by Wilson et al. (1996). Note that Xom and Xvent-1 are conserved at the amino acid consensus positions, except at position 47. Residues in the consensus that make DNA phosphate contacts are in green, those that contact bases making up the TAAT motif are in red and those that contribute to the hydrophobic core are in yellow. O, hydrophobic residue; Z, charged residue; the remaining letters correspond to the universal one-letter code for amino acids. The position of the residues in the secondary structure of the homeodomain is indicated at the top. (B) Base-specific contacts between amino acids represented in the TAAT-binding consensus and base-pairs making up the TAAT motif. Water molecules are represented by an encircled w. Adapted from Wilson et al. (1996).

RESULTS

Determination of the binding preference of Xom

To determine the binding preference of Xom, a PCR-based target site selection procedure was used as described in Materials and Methods (Chapter 2). This technique allows the selection of DNA sequences to which a given protein binds with high affinity. A random pool of oligonucleotides is incubated with protein, followed by immunoprecipitation of protein/DNA complexes, elution of bound oligonucleotides and re-use of the PCR-amplified oligonucleotide pool in the next round of selection. This procedure is repeated several times, until a highly selected pool of oligonucleotides is cloned and sequenced.

In vitro translated proteins (Xom-HA, ΔXom-HA or unprogrammed reticulocyte lysate) were used as the source of DNA binding activity. ^{35}S-labelled Xom-HA (Fig. 3.2) migrated with a molecular weight of approximately 50 kDa in SDS-PAGE electrophoresis. This migration is approximately 12 kDa slower than that predicted by its amino acid sequence (38 kDa); the reason for this discrepancy is unknown. It is interesting to note that the truncated version of Xom containing the homeodomain and part of its flanking sequences also migrated approximately 10-15 kDa slower than expected based on its amino acid sequence (22 kDa). This suggests that post-translation modifications may occur within the truncated Xom version. Although unlikely in the *in vitro* conditions used, phosphorylation could explain the protein mobilities observed for Xom-HA and ΔXom-HA since ΔXom retains a threonine/serine-rich region on the N-terminal region of Xom. In addition, the same migration pattern for Xom-HA was observed when this construct was transiently transfected in cultured cells (not shown).

After five rounds of binding site selection, the selected pools were used in electrophoretic mobility shift assay (EMSA). The pool selected with Xom-HA, but not with ΔXom-HA, formed a specific complex on the gel, in the presence of antiserum (see below). DNA corresponding to the specific band was isolated, the oligonucleotide fragments were cloned and 111 were sequenced.

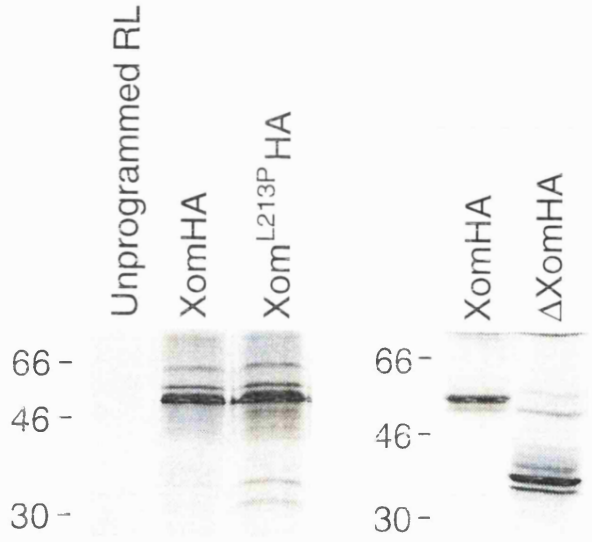

Fig. 3.2 *In vitro* translated proteins used as the source of DNA binding activity in binding site selection analysis and/or in electrophoretic mobility shift assays. SDS PAGE electrophoresis performed with *in vitro* translated ^{35}S-labelled Xom-HA, Xom^{L213P}-HA, ΔXom-HA or unprogrammed reticulocyte lysate.

A consensus binding sequence was established manually by ordering the sequences stepwise. Analysis of 111 sequences revealed primarily a TAAT/ATTA motif which was present in all but one sequence. This motif corresponds to the consensus core binding sequence for the vast majority of homeobox proteins (Gehring et al., 1994; Laughon, 1991). In 82% of the cases, the sequences contained two or more core motifs, usually in antiparallel orientation (75% of all sequences). As this motif proved to be very frequent, sequences were aligned by TAAT motifs and then ordered firstly, by the distance between two antiparallel TAAT motifs and, secondly, by the similarity of the nucleotides flanking one TAAT motif. Whenever a clone contained more than two core sequences, the minimum distance between any two antiparallel sites was chosen for scoring. This alignment showed that in most cases the core sequences were separated by six or seven nucleotides (30% and 25%, respectively, of the sequences with antiparallel cores). A consensus binding sequence was thus established which contains two antiparallel core motifs separated by six nucleotides (Fig. 3.3), as follows: CTAATT(A/G)(A/G/C)(G/C)(T/C)(G/A/C)ATTAN. I note that the first TAAT motif is frequently flanked 5' by C and 3' by T.

A computer-based analysis of the same 111 sequences, which finds out frequent motifs in biopolymers (see Materials and Methods), did not identify two antiparallel core motifs, but yielded three consensus sequences containing a TAAT core. In order of frequency of appearance these were: G(C/G)**TAATTA**, A(C/T)**TAATT**(G/A)GT and (A/G)AGC(G/A)**ATAATC**(G/A). These results are consistent with the manual analysis. The first two sequences contain the TAAT core flanked by at least three preferred nucleotides also present in the consensus established manually and, in particular, they emphasise the presence of a C 5' and a T 3' of the core TAAT motif.

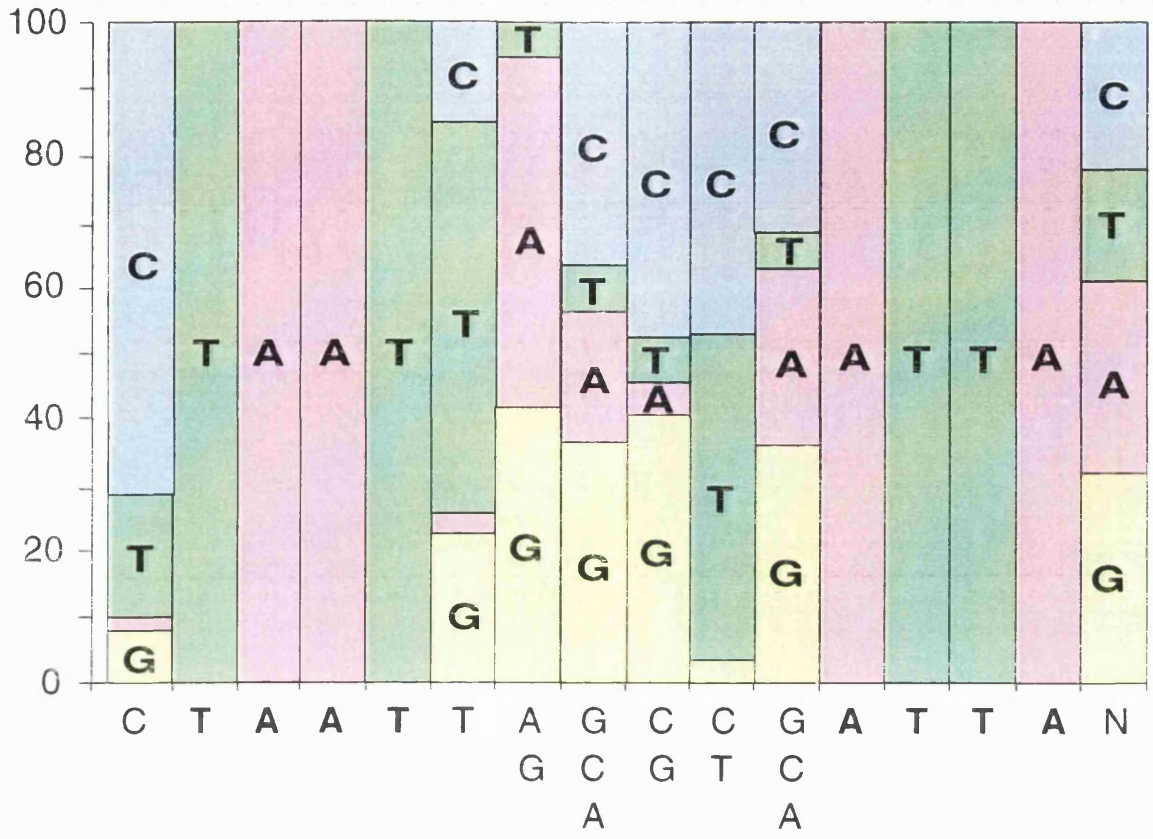

Fig. 3.3 Schematic representation of the consensus binding sequence derived from a PCR-based target site selection analysis (Pollock and Treisman, 1990) performed with *in vitro* translated Xom protein. Sequences containing two (or more) TAAT motifs in antiparallel orientation (75% of the 111 sequences analysed) were aligned with reference to the TAAT motifs. The % frequency with which a nucleotide (G, A, T or C) appeared in the same position was scored. Of these sequences, most had 6 or 7 nucleotides separating the two TAAT antiparallel motifs (30% and 25%, respectively). A consensus binding sequence was established which contains two antiparallel core motifs separated by six nucleotides and flanked by the indicated preferred nucleotides.

Does Xom bind to its consensus binding sequence?

In vitro analysis

A set of oligonucleotides containing mutated and non mutated combinations of the consensus binding sequence (Fig. 3.3) was tested in EMSA (Fig. 3.4 A). HA-tagged Xom (Xom-HA), prepared by *in vitro* translation, formed a specific complex with probe A, but only in the presence of anti-HA antibody, which appeared to stabilise binding of Xom-HA to its consensus sequence (compare lanes 3 to 6, Fig. 3.4 B). The same result was observed with probe J (data not shown, see Materials and Methods). Probes A and J correspond to two independent clones sequenced from the final pool of oligonucleotides obtained from the binding site selection procedure. Binding to probe A was abolished by a 100-fold molar excess of unlabelled oligonucleotide, but not by a similar excess of oligonucleotide B, in which both core motifs are mutated (Fig. 3.4 B lanes 7 and 8). Further evidence for specificity comes from the observation that Xom^{L213P}-HA, in which the leucine at position 40 of the homeodomain is replaced by a proline, does not bind probe A (Fig. 3.4 B, lane 9 and 10); such a mutation is thought to interfere with homeodomain conformation and thereby to prevent DNA binding (Le Roux et al., 1993; Mead et al., 1996). Together, these results confirm that Xom binds its consensus sequence *in vitro*.

Although binding of Xom-HA to its consensus site in EMSA gels was detected in the presence of anti-HA antibody (lanes 3 to 6, Fig. 3.4 B), binding of probe A to a modified version of Xom, XomVP16 (see below), can be detected in the absence of antiserum (compare lanes 3 to 5, arrow, Fig. 3.6). XomVP16 comprises the Xom open reading frame fused to a module containing two VP16 activation domains followed by Myc and His tags (see Materials and Methods). Specificity of XomVP16 binding to probe A was demonstrated by supershifting the specific complex following incubation with anti-Myc antibody (lane 6, asterisk, Fig. 3.6). Furthermore, competition with a 100-fold molar excess of unlabelled probe A, but not with unlabelled probe B, prevented formation of the specific complex (lanes 7 and 8, Fig. 3.6).

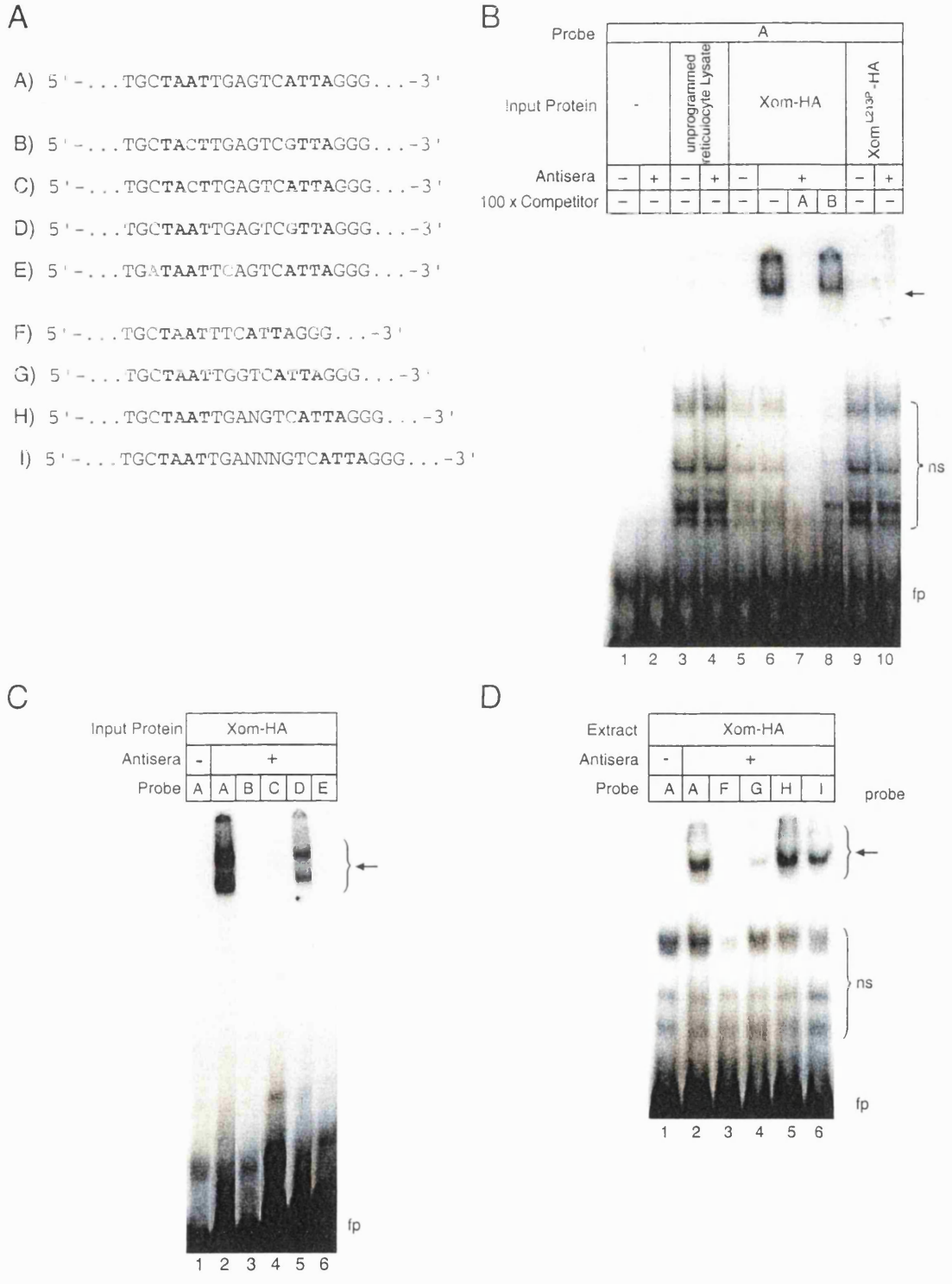
A
A) 5'-...TGCTAATTGAGTCATTAGGG...-3'
B) 5'-...TGCTACTTGAGTCGTTAGGG...-3'
C) 5'-...TGCTACTTGAGTCATTAGGG...-3'
D) 5'-...TGCTAATTGAGTCGTTAGGG...-3'
E) 5'-...TGATAATTCAGTCATTAGGG...-3'
F) 5'-...TGCTAATTTCATTAGGG...-3'
G) 5'-...TGCTAATTGGTCATTAGGG...-3'
H) 5'-...TGCTAATTGANGTCATTAGGG...-3'
I) 5'-...TGCTAATTGANNNGTCATTAGGG...-3'
B
Probe
A
Input Protein
-
unprogrammed reticulocyte Lysate
Xom-HA
Xom L213P-HA
Antisera
100 x Competitor
A
B
ns
fp
1 2 3 4 5 6 7 8 9 10
C
Input Protein
Xom-HA
Antisera
Probe
A A B C D E
fp
1 2 3 4 5 6
D
Extract
Xom-HA
Antisera
Probe
A A F G H I
probe
ns
fp
1 2 3 4 5 6

Fig. 3.4 Electrophoretic mobility shift assays (EMSA) define the Xom DNA binding site. (A) Probes used in (B-D). See also Materials and Methods. (B) Probe A forms a specific complex with Xom (lanes 5, 6) but not with unprogrammed reticulocyte lysate (lanes 3, 4). Complex formation is competed with a 100-fold excess of probe A (lane 7) but not with a similar concentration of probe B (lane 8). Complex formation requires the addition of anti-HA antiserum (lanes 5, 6). Xom^{L213P}-HA, in which the leucine at position 40 of the homeodomain is replaced by proline, does not bind the consensus binding site (lanes 9, 10). Specific complexes are indicated by an arrow and non-specific (ns) complexes due to components of the reticulocyte lysate are indicated. These complexes are not present when water or antiserum is incubated with the probe (lanes 1 and 2, respectively). fp indicates free probe. (C) Complex formation using probes A–E. (D) Complex formation using probes A and F–I. 5% acrylamide gels are shown.

Probe				Binding
A	C **T A A T** T G	N_4	**A T T A**	+++
H	. . . . .	N_5	. . . .	+++
I	. . . . .	N_7	. . . .	++
G	. . . . .	N_3	. . . .	+
D	. . . . .	N_4	G . . .	++
C	. . . C . . .	N_4	. . . .	0
B	. . . C . . .	N_4	G . . .	0
E	A C	N_4	. . . .	0
F	. . . . . T	N_1	. . . .	0
Consensus	C **T A A T** T A/G	N_{4or5}	**A T T A**	

Fig. 3.5 Summary of the results of *in vitro* binding analyses presented in Fig. 3.4. Probes correspond to sequences shown in Fig. 3.4 A. The number of +'s represents the intensity of binding of the specific complexes detected in EMSAs. The consensus sequence is as in Fig. 3.3.

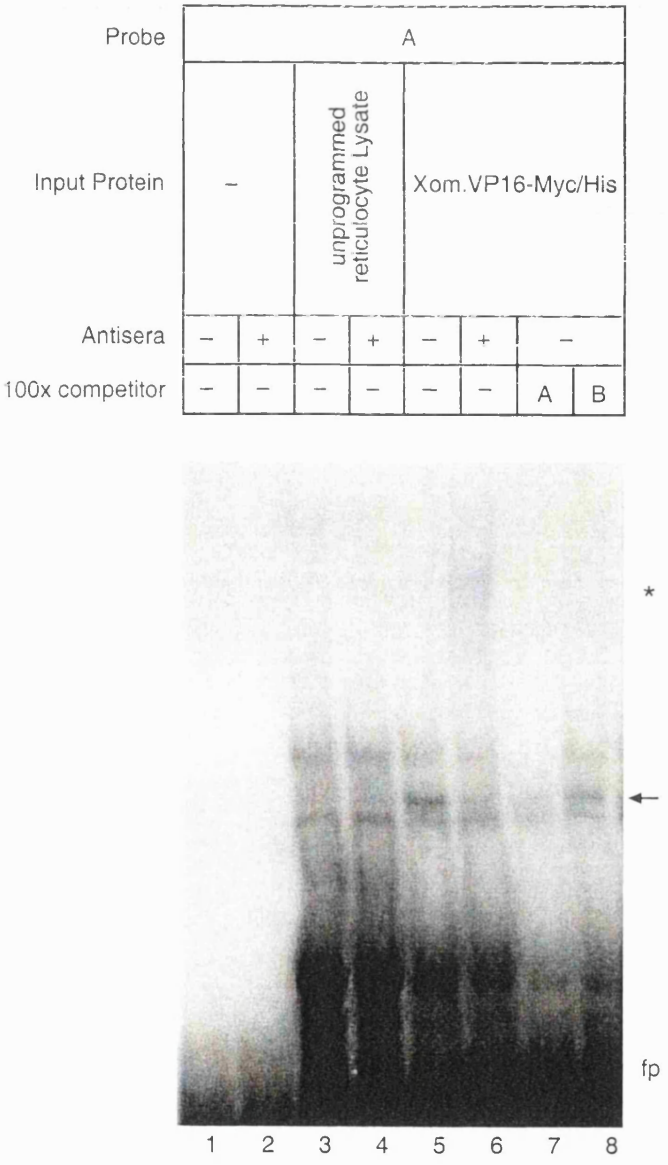

A) 5'-...TGC**TAAT**TGAGTC**ATTA**GGG...-3'

B) 5'-...TGC**TA**C**T**TGAGTCG**TTA**GGG...-3'

Fig. 3.6 XomVP16 binds the Xom consensus binding sequence in electrophoretic mobility shift assays. XomVP16-Myc/His forms a complex with probe A in the absence of antiserum (lane 5). Binding is competed with an excess of probe A (lane 7) but not with probe B (lane 8). Arrow indicates specific complex. Asterisk indicates supershifted complex formed following addition of 9E11 anti-Myc antibody (lane 6). Specific complexes are not observed with water (lanes 1, 2) or unprogrammed reticulocyte lysate (lanes 3, 4). A 3.5% acrylamide gel is shown.

The requirement for integrity of the core motifs, for specific nucleotides flanking the first core motif, and for a particular spacing between the two core motifs for Xom binding was tested by use of probes B to I (Fig. 3.4 A). Mutation of both core sequences (probe B, Fig. 3.4 C lane 3) or of the first core sequence (probe C, Fig. 3.4 C lane 4) abolish binding. Mutating just the second core motif does not prevent binding although it substantially reduces the intensity of the specific complexes (probe D, Fig. 3.4 C lane 5). This mutation retains the TAAT core motif which, in the binding site selection procedure was preferentially flanked 5' by C and 3' by T and (A/G), and indeed mutation of the 5' C to A and the most 3' G to C prevents binding (probe E, Fig. 3.4 C lane 6).

The above observations indicate that the critical nucleotides determining the specificity of Xom binding consist of the first core TAAT flanked by a 5' C and a 3' T and (A/G), and that this motif is sufficient for Xom binding (probe D, Fig. 3.4 C lane 5). The manual ordering of sequences obtained by binding site selection, however, yielded a consensus sequence which comprised two antiparallel TAAT motifs separated by six or seven nucleotides. To investigate the requirement for such spacing we made use of probes F-I. As predicted from the results of the binding site selection, optimum binding is obtained with a spacing of 6 or 7 nucleotides (probes A and H, Fig. 3.4 D lanes 2 and 5), and binding is greatly reduced with spacings of 5 (probe G), or 9 (probe I) nucleotides (Fig. 3.4 D lanes 4 and 6, respectively). No binding was observed with probe F, where the core motifs are separated by 3 nucleotides, but this is likely to be due to the replacement of the preferred G, present two positions 3' of the core TAAT, by a T.

Together, these results show that the sequence **CTAATTG** is critical for Xom binding, but that binding is enhanced by the presence of a ATTA motif 6 or 7 nucleotides 3' of the core TAAT. A summary of the results of the *in vitro* analysis of Xom/DNA binding properties is presented in Fig. 3.5.

Interestingly, a truncated version of Xom-HA (ΔXom-HA), which contains the homeodomain but lacks the most N- and C- terminal regions, did not generate specific bands in EMSAs when incubated with probe A and anti-HA antibody (data not shown). This result suggests that under these conditions, the homeodomain and part of its

flanking sequences may not be sufficient for the detection of specific binding on EMSA gels. This is discussed below.

Cell culture analysis

To ask whether Xom is able to bind its consensus sequence in an *in vivo* context, an approach involving transient transfections in mammalian cell culture was adopted. First, a XomVP16-Myc/His construct was made in which the open reading frame of Xom was fused to a module containing two copies of a fusion of the λ repressor linker region and the VP16 activation domain, followed by Myc and His tags (Materials and Methods and Fig. 3.7 A). The addition of λ repressor linker regions separating the two VP16 activation domains has been shown to increase the potency of VP16 as a transcriptional activator (Emami and Carey, 1992; Ohashi et al., 1994). This may be due to an increase in spacing and flexibility, allowing the VP16 activation domains more readily to access the transcriptional machinery. Since VP16 is a very potent activator, the fusion of this module to Xom should convert it into a transcriptional activator.

The ability of Xom to interact with DNA in an *in vivo* context was tested by transiently transfecting XomVP16-Myc/His into mammalian tissue culture cells (COS cells) along with a reporter construct carrying five copies of the Xom consensus sequence (oligonucleotide A; Fig. 3.4 A) upstream of the E4 minimal promoter (Fig. 3.7 A). If Xom is able to bind oligonucleotide A, as predicted from the previous EMSA results, the VP16 activation module tethered to Xom should be able to activate transcription. Consequently, an increase in levels of luciferase reporter activity, relative to those of the reporter construct alone, should be observed. On the other hand, if Xom does not bind to oligonucleotide A in the context of cultured COS cells (or if the reporter does not contain Xom consensus sequences) the levels of reporter activity should remain unchanged. Fig. 3.7 B shows that XomVP16-Myc/His activates transcription in a dose-dependent and site-dependent manner. Moreover, fusion of the VP16 activation domain to Xom^{L213P} (which does not bind oligonucleotide A; see Fig. 3.4 B, lanes 9 and 10) does not result in transcription activation, even though it is translated to similar levels as XomVP16-Myc/His (Fig. 3.7 B inset). These results confirm that, in a cell context, Xom can interact with the consensus sequence identified by the PCR-based binding site

selection procedure.

DISCUSSION

In this chapter I have investigated the DNA binding preferences of Xom using a PCR-based binding site selection procedure and showed that the sequence CTAATT(A/G) is critical for Xom to bind DNA in EMSAs (Fig. 3.5). Furthermore, binding is enhanced by the presence of an ATTA motif 6 or 7 nucleotides 3' upstream of the core TAAT (Fig. 3.5). EMSA analysis was carried out in the presence of anti-HA antibody, which appears to stabilise binding of Xom-HA to probes carrying Xom preferred sequences (compare lanes 5 and 6, Fig. 3.4 B). However, binding of XomVP16 can also be detected in the absence of antiserum (Fig. 3.6, lane 5). Finally, Xom was shown to interact with a potential binding sequence in the context of mammalian cultured cells (Fig. 3.7 B).

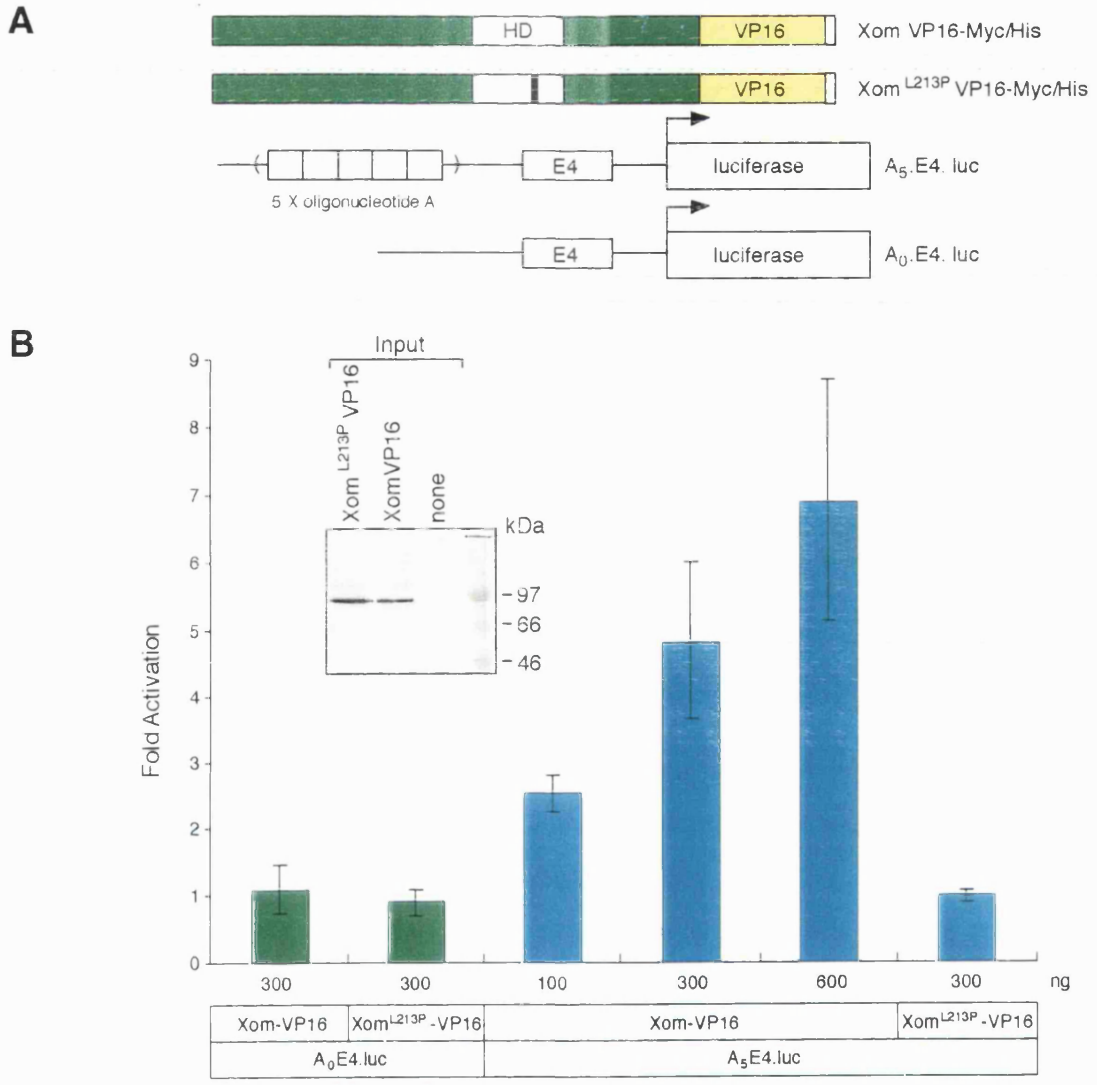

Fig. 3.7 XomVP16 requires the Xom consensus sequence to activate transcription. (A) Representation of effector and reporter DNAs. XomVP16-Myc/His effector plasmid comprises the Xom open reading frame fused to a VP16 activation module and Myc and His tags (see text for details). Xom^{L213P}VP16-Myc/His is identical except that it contains a proline residue at position 40 of the homeodomain rather than a leucine. Reporter constructs A_5.E4.luc and A_0.E4.luc have five or no copies, respectively, of the Xom consensus binding sequence (oligonucleotide A in Fig. 3.4 A). (B) COS cells were transiently transfected with the indicated amounts of effector DNA, 100 ng of reporter construct, 100 ng of reference plasmid (pRL-TK) together with plasmid pcDNA3 to make a total of 800-1000 ng DNA. Two replicas of each experimental group were performed per experiment. Cells were harvested and luciferase activities were normalised to the activity of reporter construct alone (A_5.E4.luc or A_0.E4.luc). Data are derived from at least three independent experiments and are expressed as the mean fold activation +/- standard deviation. (Inset) Western blot analysis on COS cells transfected with 1 μg of DNA encoding XomVP16-Myc/His and Xom^{L213P}VP16-Myc/His, using anti-Myc mouse monoclonal antibody 9E10.

Xom binding specificity

All potential Xom binding sites derived from binding site selection analysis contained at least one TAAT core motif, and this core motif was shown to be necessary for binding Xom in EMSAs. Thus, in contrast to predictions from the results of Dear et al. (1993) the threonine present at position 47 of the Xom recognition helix does not alter the preference for binding to the consensus homeodomain binding core TAAT.

The Xom consensus binding sequences (with the exception of the third computer-derived consensus sequence) show a marked preference for a T residue 3' of the first TAAT core motif. This finding is consistent with predictions based on comparisons of the binding preferences of related homeodomains which show that position 50 in the homeodomain (a glutamine in Xom) influences the choice of nucleotide in this position (Wilson et al., 1996). Interestingly, Xom also displays a strong preference for a C 5' of he TAAT core motif, which was not predicted by the studies above mentioned.

Binding site selection with Xvent-1, which shares 73% amino acid identity with Xom, including all positions directly or indirectly involved in recognition of the TAAT motif (Fig.3.1 A), revealed three consensus binding sequences (Friedle et al., 1998) none of which contain a TAAT motif. From the most preferred to the least preferred, these were 5'-CTATTTG-3' (≅60% of the cases), 5'-TGCATTTTG-3' (25%) and 5'-TTGATC-3' (10%). Interestingly, the most common Xvent-1 consensus binding sequence isolated has the same flanking nucleotides as that of Xom but the TAAT core is replaced by TATT. Thus, with the exception of this one nucleotide (underlined), Xom and Xvent-1 bind the same sequence.

It is likely that the differences in the i*n vitro* binding properties of Xom and Xvent-1 depend on amino acids within the homeodomain, since binding site selection with Xvent-1 was performed using only the homeodomain (Friedle et al., 1998). Interestingly, sequence comparison studies in Hox genes suggest that differences of DNA binding specificity in this class of related homeodomains may be due to residues within the homeodomain that mediate protein-protein interactions (Sharkey et al., 1997).

In the above studies it was found that most of the residues conserved within a given paralogous gene (conserved across different species), but different in all other paralogous groups, are solvent exposed and facing away from the DNA, free for interaction with potential protein partners. Similar sequence comparisons between Xom and Xvent-1 homeodomains show that all residues involved in the interaction with the TAAT motif are conserved whereas some of the divergent residues correspond to residues facing away the DNA in the homeodomains of the Hox cluster (Fig. 3.1 A). Given the high degree of conservation of the interaction with DNA in all homeodomains (Gehring et al., 1994), the divergent residues between Xom and Xvent-1 homeodomains may also be facing away the DNA and thus, differences *in vitro* specificity may be due to protein-protein interaction.

Does Xom form dimers?

Binding to palindromic sites has been reported for the paired/pax family of homeodomains, which bind co-operatively to DNA sequences containing two or three (but not more) nucleotides separating TAAT motifs (Wilson et al., 1993). Co-operative binding is said to occur when the binding of one homeodomain molecule can increase the affinity of binding of a second molecule (Wilson et al., 1993). By analogy, Xom may bind to a suitable palindromic sequence co-operatively by forming dimers on the DNA. This possibility is supported by the finding that Xom binds more strongly to a palindromic probe containing two TAAT motifs (probe A) than to a probe containing only one TAAT motif (probe D), and that the spacing between core motifs affects binding (Fig.3.5). However, specific binding, albeit weaker, still occurs with probe D, and also with probes G and I (Fig 3.5), which have the spacing altered but retain a single TAAT motif with the appropriate flanking nucleotides. These results suggest that formation of dimers may occur although it is not necessary for Xom to bind DNA. Consistent with this suggestion, I note that the computer-based analysis of the binding site selection data did not reveal a requirement for palindromic TAAT cores.

The number and mobilities of the bands in the EMSA shown on Fig. 3.4 do not resolve this question. Although the number of specific complexes varied from experiment to experiment, they did not depend on whether the probes contained two

TAAT core motifs or just one. The variability from experiment to experiment may depend on the composition of the reticulocyte batch, which may contain proteins that interfere with Xom binding to DNA. However, the unchanged pattern of bands whether palindromic (probe A) or nonpalindromic (probe D) probes were used, suggests two possibilities.

First, dimers may form in solution rather than onto the DNA. In this scenario, two predominant bands of similar mobility should be detected with either a palindromic (A) or a nonpalindromic probe (D). When a palindromic probe is used, the two predominant bands would correspond to a Xom dimer/probe and a Xom monomer/probe. Alternatively, when a non palindromic probe was used, the two bands would correspond to a Xom dimer/two probes (each monomer bound to the preferred TAAT motif) or a Xom dimer/one probe (one Xom monomer would bind to the degenerate Xom site) and Xom monomer/probe. All complexes would be stabilised by binding to antiserum.

Second, the formation of homodimers may be induced by the anti-HA antibody. Each Fab fragment of anti-HA monoclonal antibody may recognise one tag in each Xom monomer thus one anti-HA antibody would bind to two Xom monomers. This pair of monomers, held by the antibody and perhaps further stabilised by protein-protein interactions, would bind to a palindromic probe in a stable way and, possibly, be capable of inducing binding to sequences containing a degenerated second site, such as probe D. According to this model, the appearance of several specific complexes in EMSA gels corresponds to complexes containing different molar ratios of Xom, probe and antibody.

Finally, a combination of the two models presented may operate to generate the pattern of bands observed in EMSAs of Fig. 3.4.

The formation of specific complexes in EMSAs using XomVP16 (Fig. 3.6) might be stabilised by a different mechanism not involving the induction of dimer formation (see below). Induced dimerisation is unlikely since neither the VP16 domain nor the λ repressor linker region of the VP16 fusion module contain dimerisation domains (Emami and Carey, 1992). Consistent with this is the observation that only one specific complex is observed on Fig. 3.6 (lane 5).

Interestingly, Xom binds preferentially to a sequence with the unusual distance of 6 or 7 nucleotides separating the TAAT motifs, which corresponds to a 10 nucleotide separation from centre to centre of TAAT core motifs. Since a complete turn in the DNA helix takes 10 nucleotides, two Xom homeodomains would be bound, theoretically, to two adjacent sites on the DNA helix. Depending on the structure of bound Xom, such a positioning could facilitate a direct interaction between Xom proteins bound to DNA.

The requirement for antibodies to detect Xom-DNA complexes in EMSA gels is bypassed by XomVP16

The *in vitro* binding analysis performed shows that the detection of specific complexes on the gel required co-incubation with anti-HA antibody (Fig. 3.4). Oddly this was not the case when XomVP16 and probe A were incubated in EMSA (Fig. 3.6 lane 5). Since the VP16 activation module lacks DNA-binding activity, Xom mediates the observed interaction between XomVP16 and probe A. Additional support is given by cell culture experiments, which show that XomVP16 requires the Xom consensus binding sequence to activate transcription of a reporter gene (Fig. 3.7 B).

The precise role of the antibody or of the VP16 module fused to Xom in allowing detection of specific complex formation under *in vitro* conditions is unknown. Stability of Xom may be enhanced due to a masking effect of putative degradation target sites, possibly localised to the C-terminus of Xom, since the VP16 module (and also the HA tag) were fused to the C-terminus of Xom. Consistent with this Xom translates less efficiently than XomVP16, when the same amount of DNA is transiently transfected in cell culture and analysed by Western blot (not shown). Alternatively, the VP16 module may influence the conformation of Xom to induce the formation of high-order complexes that stabilise Xom binding to DNA. This is consistent with the observation XomVP16/probe A specific complex migrate slower than Xom/probe A complexes, supershifted with anti-HA, on EMSA gels (not shown).

The homeodomain is necessary but perhaps not sufficient for DNA binding

The Xom homeodomain is necessary for binding its consensus binding sequence

because binding to probe A does not occurs with Xom^{L213P}, which has an amino acid substitution thought to disrupt homeodomain conformation (Fig. 3.4 B). However, the issue of whether the homeodomain is sufficient for binding is less clear. ΔXom, a truncated version of Xom containing the homeodomain flanked by 60 amino acids on the N-terminus and 57 amino acids on the C-terminus, does not bind to probe A in EMSA (not shown). This result suggests that residues outside the homeodomain may be important for binding DNA or, alternatively, for stabilisation of the complex in EMSA gels.

Interestingly, the homeodomain of *Drosophila* BarH1, which shares 56% identity with Xom, also does not seem to be sufficient for binding DNA. Using a series of deletion mutants, the DNA binding region of BarH1 was crudely mapped to the sequences upstream of the homeodomain, the homeodomain and part of the sequences downstream of the homeodomain, partially including the conserved Bar domain (Akimaru and Saigo, 1991). Although the sequences of BarH1 and Xom are unrelated outside the homeodomain, the fact that the BarH1 homeodomain alone is not sufficient for binding DNA, suggests that this may be a characteristic of Xom related homeodomains.

Future prospects

To analyse further, and to clarify, some aspects of Xom/DNA interactions, a source of purified Xom protein should be used. In particular, purified Xom protein would allow the determination of Xom/DNA binding affinities, through the calculation of dissociation constants, and this would allow one to better assess the existence of co-operative binding effects on sequences bearing palindromic motifs versus non-palindromic motifs. Moreover, studies involving immunoprecipitation would become possible to address the putative homo or heterodimeric nature of Xom, in solution or bound to DNA. As a long-term goal, the determination of the Xom crystallographic structure would be desirable.

Given these considerations, I carried out preliminary attempts to obtain recombinant Xom protein using His-tagged Xom and a Ni-NTA resin affinity-

chromatography purification system (QIAgen). Unfortunately, I was unsuccessful in inducing expression of Xom from the bacterial strain chosen. In addition, small-scale partial purification using the Ni-NTA resin from transformed bacteria did not reveal signs of induction of Xom in any of the bacterial fractions, either soluble, insoluble or periplasmic. The reasons for these difficulties are unknown. It may be necessary in the future to use alternative systems such as GST-fusions or even to use expression in eukaryotic cells.

CHAPTER 4

Role of Xom in regulation of transcription

INTRODUCTION

Xvent genes encode homeobox-containing genes that elicit ventralisation and loss of anterior structures when mis-expressed in *Xenopus* embryo (Ault et al., 1996; Gawantka et al., 1995; Ladher et al., 1996; Onichtchouk et al., 1996; Schmidt et al., 1996) Rastegar, 1999). The Xvent genes might exert their effects by repressing the expression of dorsal genes thereby allowing ventral gene expression, or by activating directly the expression of ventral genes. In this chapter, I ask whether Xom behaves as an activator or as a repressor of transcription, or neither.

Recently, Xvent-1 was shown to repress expression of the dorsally-expressed gene *XFD-1'* (Dirksen and Jamrich, 1992; Knochel et al., 1992; Ruiz i Altaba and Jessell, 1992) in a direct manner and the repression activity was mapped to the N-terminus (Friedle et al., 1998). In line with this finding, injection of a mutant encoding the N-terminus and the homeodomain of Xvent-1 led to ventralisation of the embryos, whereas a mutant containing just the homeodomain and the C-terminal region, did not (Friedle et al., 1998). Xvent-1 contains a conserved hexapeptide similar to the engrailed homology sequence thought to be involved in repression of transcription by recruiting the Groucho co-repressor to target promoters (Goriely et al., 1996; Jaynes and O'Farrell, 1991; Jimenez et al., 1999; Mailhos et al., 1998). Since this hexapeptide is localised N-terminally of Xvent-1, this suggests that this sequence may be involved in mediating Xvent-1 repression of *XFD-1'*.

In contrast to Xvent-1, Xom does not contain the engrailed-homology sequence nor, apparently, any clearly recognisable activator or repressor domain motifs. In this chapter I address the function of Xom in regulation of transcription in an effort to understand how Xom causes ventralisation of *Xenopus* embryos.

RESULTS

Xom is a transcriptional repressor

To address the function of Xom in transcription I made use of various Xom protein fusions with the yeast Gal4 DNA binding domain (Fig. 4.1 A). Effector RNA encoding Gal4-Xom fusions was injected into both blastomeres of two-cell stage *Xenopus* embryos along with reporter and reference DNA (Fig. 4.1 B). Reporter DNA comprised 5 copies of the Gal4 17-mer binding site cloned upstream of a minimal promoter driving the expression of the luciferase reporter (G_5p.luc). In control experiments a similar construct was injected which lacked Gal4 binding sites, G_0p.luc (Fig. 4.1 A). In the reference plasmid pRL-SV40, the SV40 promoter drives the expression of Renilla luciferase. After injection, embryos were allowed to develop to stage 8.5 (blastula), when animal caps were dissected and cultured for 3.5 hr, to the equivalent of stage 10-10.5, and then assayed for firefly and Renilla luciferase activities (Fig. 4.1 B). In this assay, the high affinity interaction between the Gal4 binding domain of the fusion protein and its 17-mer binding site should result in the tethering of Xom to the promoter region of the reporter. By these means the effects of Xom (or truncation versions) in regulating the transcription of the reporter gene can be addressed.

Fig. 4.1 C shows that RNA encoding Gal4 binding domain fused to either full-length, N-terminal region or C-terminal region of Xom (Fig. 4.1 A) significantly reduces luciferase activity compared with that of Gal4 alone when co-injected with G5p.luc (which is considered as 100% activation). For all three effector constructs, the repression effect was dependent on the presence of Gal4 binding sites. Note that the range of effector RNA concentrations used in these experiments may be reaching saturation levels because increasingly higher doses of G4Xom(1-327) or G4Xom(235-327) caused only minor reduction in luciferase activity levels. In independent experiments considered separately, however, a dose-dependent effect was present when different amounts of effector RNA were used. Taken together, these results show that Xom is a repressor of transcription, with repressor function localised to both the C-terminal and N-terminal regions of the molecule.

Transient transfection experiments performed in COS cells also indicate that Xom is able to act as a transcriptional repressor, but in this system Xom behaves slightly differently (Fig. 4.2). Cells co-transfected with a reporter construct containing 2 or 5 copies of the Gal4 17-mer binding site and the effector construct G4Xom(235-327), generated a 2 to 5-fold decrease in luciferase activity compared with the activity of Gal4 alone (Fig. 4.2 A). However, no repression was observed using G4Xom(1-327) or G4Xom(1-173) under the same conditions. Furthermore, the repression effect of G4Xom(235-327) seems to be independent of the presence of Gal4 binding sites in the reporter construct because a decrease in luciferase activity was also observed in one experiment using a reporter lacking such sites, G_0p.luc (Fig. 4.2 A). Differences in observed luciferase activity levels were not due to different amounts of protein in the cells since the transfection of Gal4-Xom fusions into COS cells results in similar translation efficiencies, as detected by Western blot (Fig. 4.2 B).

Taken together, the results show that Xom works as a repressor of transcription, and that this repression activity is context dependent.

Xom is present in the nucleus

The subcellular localisation of Xom was analysed in transient transfection assays. Fibroblast cells (3T3) were transiently transfected with full-length Xom, Xom^{L213P}, or vector alone (pcDNA3) and the localisation of the respective proteins was detected by immunocytochemistry with anti-HA antibody. Figure 4.3 shows that Xom was found mainly in the nuclei of cultured cells but sometimes also in the cytoplasm. The same was observed for and Xom^{L213P}, although the Figure 4.3 C only shows staining in the nuclei. By contrast, pcDNA3 vector alone did not generated any detectable protein (Fig. 4.3). These results show that Xom (and Xom^{L213P}) are localised in the correct compartment of the cell to behave as transcription factors.

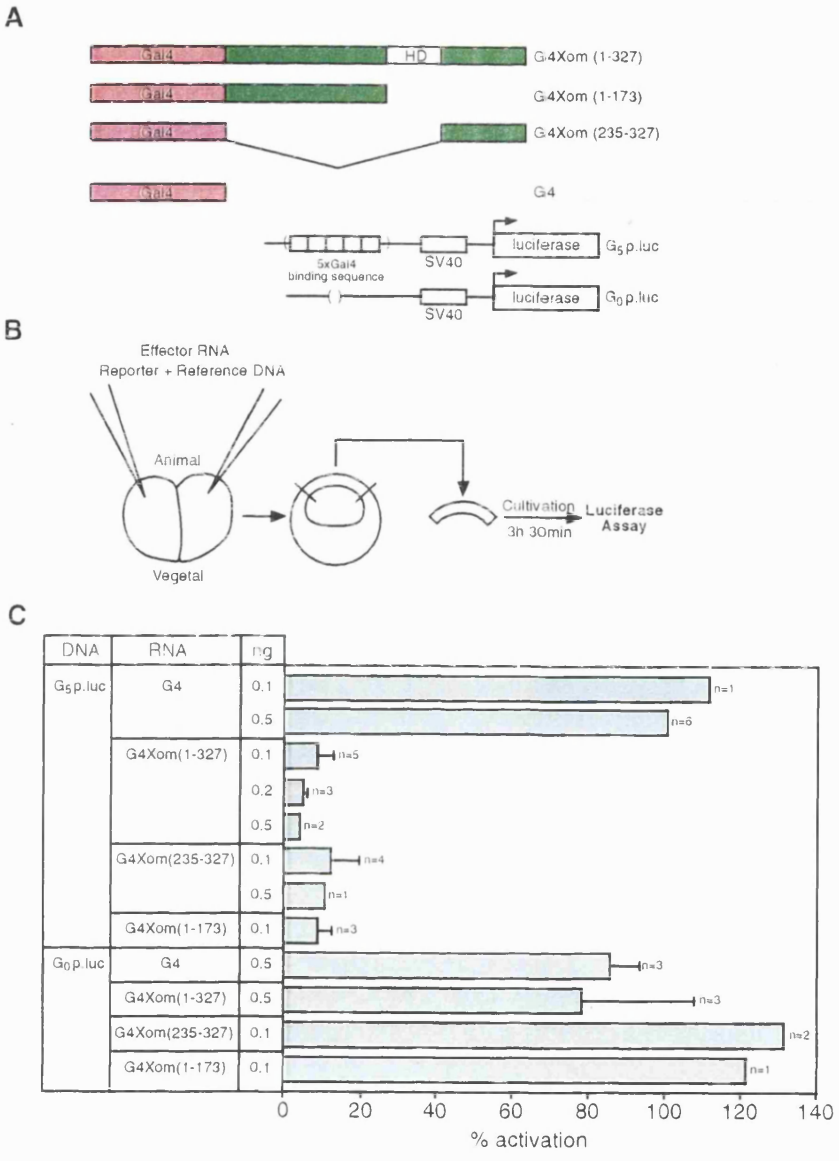

Fig. 4.1. Xom represses transcription in *Xenopus* embryos. (A) Representation of the effector RNAs and reporter constructs used in *Xenopus* luciferase assay experiments. Effector RNAs include the Gal4 binding domain alone (G4) or Gal4 fused to different portions (as indicated; numbers represent amino acids) of Xom. HD: homeodomain. Reporter constructs are as indicated. (B) Design of the *Xenopus* luciferase assay experiment. Both blastomeres of *Xenopus* embryos at the 2-cell stage were injected with 10 nl effector RNA, firefly luciferase reporter DNA and reference plasmid (pRL-SV40). Animal pole regions were dissected at blastula stage 8.5 and cultured for 3.5 hr before harvesting for determination of luciferase activity. (C) The indicated reporter constructs were co-injected with reference plasmid and the indicated RNAs into *Xenopus* embryos as described in (B). Luciferase activity in each experiment was normalised to the activity of 0.5 ng Gal4 RNA co-injected with G5p.luc (= 100% activation) and is expressed, when three or more experiments were carried out (n), as mean +/- standard deviation.

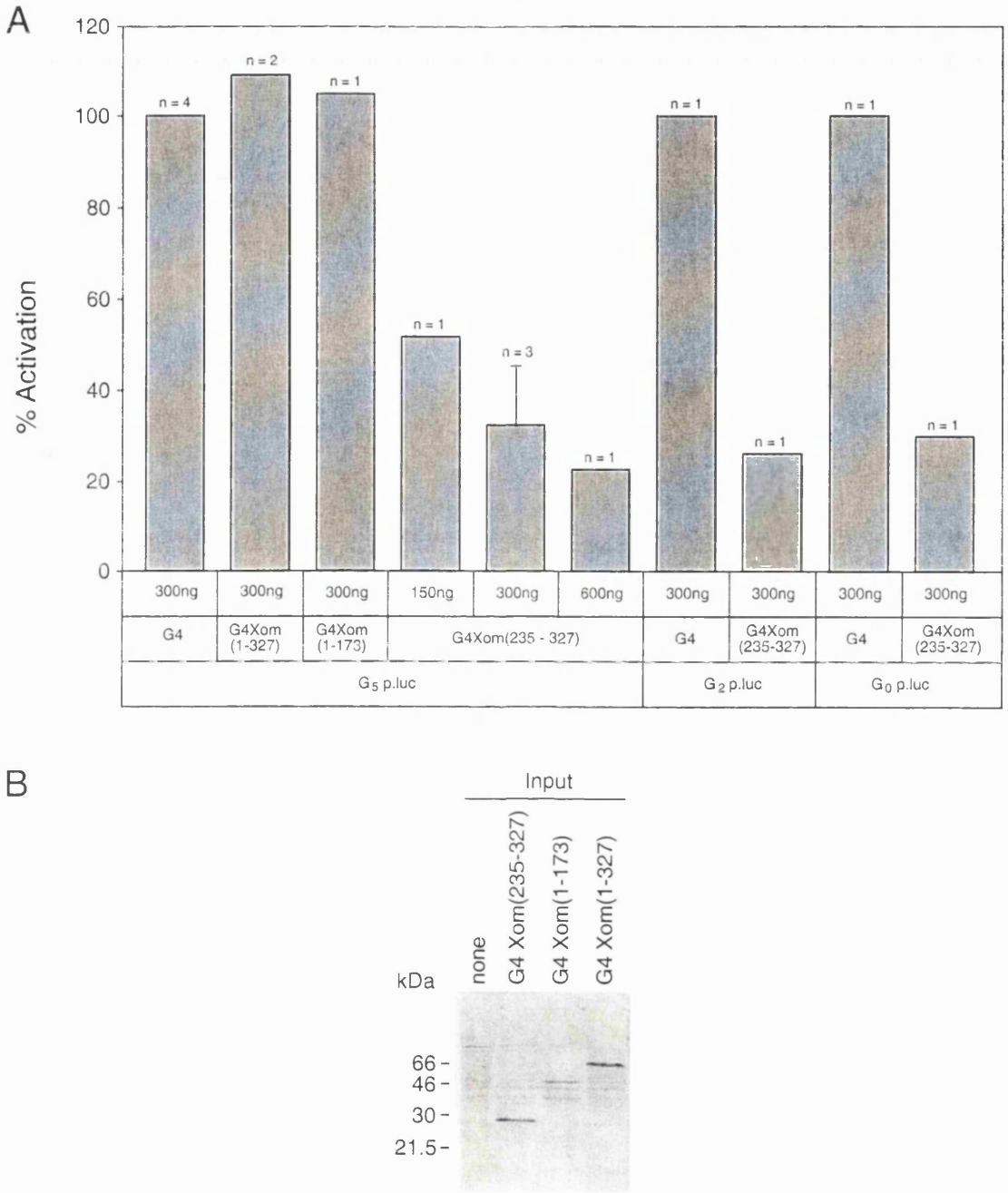

Fig. 4.2 The C-terminal region of Xom mediates repression of transcription in cell culture. (A) COS cells were transiently transfected with the indicated amounts of effector DNA, 100 ng of reporter construct, 100 ng of reference plasmid (pRL-TK) and plasmid pBXG1 to make a total of 800-1000 ng DNA. Two replicas of each experimental group were performed per experiment. Cells were harvested and luciferase activities were normalised to the activity of Gal4 alone transfected with reporter construct (G_5p.luc, G_2p.luc or G_0p.luc) which was considered 100% activation. Data derived from at least three independent experiments is expressed as the mean fold activation +/- standard deviation; n indicates the number of experiments carried out. (B) Western blot analysis of COS cells transiently transfected with 1 μg of the indicated input DNAs. Anti-Gal4 antibody was used to detect Gal4-Xom fusions.

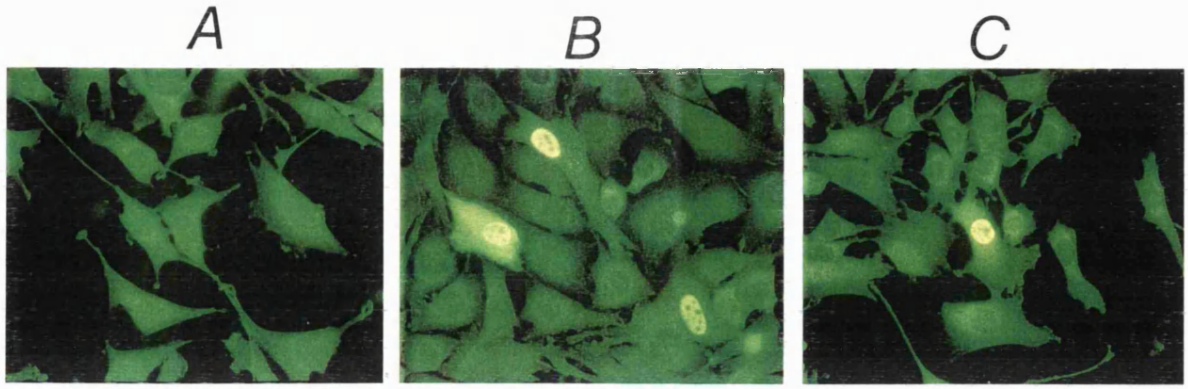

Fig 4.3. Subcellular localisation of Xom-HA and Xom^{L213P}-HA in cultured cells. Fibroblast cells (3T3) were transiently co-transfected with empty plasmid (pcDNA3) (A), Xom-HA (B) or Xom^{L213P}-HA (C) and immunocytochemistry was performed using anti-HA monoclonal antibody. Xom^{L213P}-HA has a leucine at position 40 of Xom homeodomain replaced by proline.

DISCUSSION

In this chapter, I have shown that Xom has repressor activity when fused to a heterologous binding DNA domain. In *Xenopus* embryos, the repressor activity is detectable both in the C-terminal and N-terminal regions of the molecule whereas in cell culture, only the C-terminal region of Xom has repression activity. Interestingly, this latter repression activity appears to be independent of the presence of binding sites on the reporter construct. Finally, full-length Xom localises mainly to the nucleus of cultured cells.

Xom repression activity is context-dependent

The comparison between results of experiments performed in *Xenopus* animal caps and in cell culture reveals that Xom represses transcription in a context-dependent manner. When Xom RNA is injected uniformly into *Xenopus* embryos, exogenous Xom protein is presumably available from early cleavage stages to after the mid-blastula transition, for a period which depends on Xom protein stability. Therefore, exogenous Xom should be present at approximately the same time and place as endogenous Xom, and thus it should be exposed to a similar set of factors as endogenous Xom protein. In contrast to the *Xenopus* experiments, in cultured mammalian cells only the C-terminal region of Xom retains repression activity whereas Xom N-terminal region may require interaction with other factors, absent from COS cells but available in the embryo. This suggests that the N-terminal and C-terminal parts of Xom may repress transcription by different mechanisms.

Alternatively, interaction with specific proteins in *Xenopus* may result in a conformational effect on Xom, which exposes both the N- and C-terminal regions towards the surface of the protein, able to interact with other proteins to achieve repression of transcription. In cultured cells, the conformational effect might not take place and the N-terminal region might remain inaccessible.

Although preliminary, the site-independent repression effect obtained in one experiment using the C-terminal region of Xom in cell culture experiments (Fig. 4.2), suggests that this region does not need to be tethered to a particular promoter and thus

may interact directly with the transcriptional machinery. This requires further experiments.

Structural basis for a role of Xom in transcriptional repression

The finding that both N- and C-terminal regions of Xom have repressing activity in *Xenopus* embryos (Fig. 4.1 C) suggests two possibilities. One is that Xom has scattered residues in both the N- and C-terminal regions, which confer repression activity after correct folding of the protein. The total number of residues involved in repression, however, might not be crucial. Instead, a minimum number of residues necessary to confer repressing activity should exist in both N- and C-terminal parts of the molecule. This would account for the observation that a similar level of repression is detected with both full-length and deleted versions of Xom (Fig. 4.1 C). The second possibility is that Xom contains two (or more) discrete repressing domains separated by the homeodomain. Similarly, the discrete repressing domains on the N- and C-terminal region of Xom would work independently but redundantly, in order to generate a non synergistic and non additive effect.

Analysis of the Xom amino acid sequence reveals stretches of residues rich in proline. In particular, the N-terminal region (excluding the homeodomain) has a region of 52 amino acids (from amino acid 22 to 74) that contains 11 proline residues (Fig. 4.4). The Xom C-terminal region is also very rich in proline (Ladher et al., 1996), containing 16 proline residues scattered over the 93 amino acids from the end of the homeodomain to the end of the protein (Fig. 4.4). Proline-rich regions of this sort have been associated with repression of transcription (Hanna-Rose and Hansen, 1996) although the frequency of proline residues in Xom is lower than in well characterised proline-rich repressor domains, such as Even-skipped, Paired or the artificial repressor peptide FS1 (Han and Manley, 1993). Nevertheless, the Xom amino acid sequence (excluding the homeodomain) does contain a significant proportion (12%) of prolines.

Fig. 4.4 Xom amino acid sequence. The homeodomain is boxed; prolines (P) are highlighted in red; serines (S) and threonines (T) are highlighted in blue and acidic residues (D and E) are highlighted in violet.

Proline-rich regions have, however, also been associated with domains of activation of transcription and the only difference between these and proline-rich repression domains is the frequent association of proline-rich activation domains with regions rich in serine and threonine (Hanna-Rose and Hansen, 1996). Within the proline-rich region of the Xom N-terminal region there are several serine residues. Furthermore, adjacent to this region there is a serine/threonine-rich region (comprising amino acids 132 and 152) (Fig. 4.4). Although it is difficult to assess the relevance of these observations without further experiments, they suggest that the N-terminal proline-rich region of Xom is not involved in the repression activity of this part of the protein.

Another common feature of repression domains is the presence of highly charged residues (Hanna-Rose and Hansen, 1996). In yeast, a selection for potent transcriptional repression activity from random sequences yielded a basic polypeptide (Saha et al., 1993), which led to the conclusion that charged repression regions consist largely of basic residues. However, this is not always the case and there are examples of potent repressor domains bearing acidic residues that are important for the repression activity. Such is the case of the highly conserved motif named the Kruppel-associated box (KRAB) (Witzgall et al., 1994). Acidic regions have also been associated with activators (Ptashne, 1988). In the case of Xom, there are few basic residues and these are uniformly distributed along its length. However, the Xom N-terminal region is clearly highly acidic (Ladher et al., 1996) and this may be involved in repression activity.

In summary, the ability of Xom to repress transcription can be a consequence of some of its amino acid sequence features. Xom N-terminal region may repress transcription through its acidic residues. In contrast, the Xom C-terminal region proline residues may be important features. If this is the case, the residues involved in Xom-mediated repression seem to be spread out along the length of Xom. This observation tends to favour a model in which repression is mediated by scattered residues within Xom's amino acid sequence, which may form a domain of interaction upon correct folding of the protein (as discussed above). I note that these conclusions should be tested by further studies involving detailed deletion analysis and mutagenesis of target residues.

Xom does not repress transcription by competition for access to DNA

As described earlier in the general introduction (Chapter 1), the mechanisms by which a repressor may act include active repression (direct or by quenching), passive repression (competition for access to DNA) and mechanisms to render chromatin inactive at a particular promoter (Hanna-Rose and Hansen, 1996). The results presented in this chapter cannot address which of these repression mechanisms Xom employs. However, fusions of Xom (or truncations of Xom excluding the homeodomain) to the Gal4 heterologous DNA-binding domain, repress transcription in *Xenopus* embryos (Fig. 4.1). This suggests that Xom does not act by competition for sites on DNA and, thus, is unlikely to act by a passive mechanism.

CHAPTER 5

Function of Xom in the *Xenopus* embryo

INTRODUCTION

In the previous chapters, I have shown that Xom acts as a repressor of transcription in *Xenopus* embryos and that it interacts with a consensus DNA binding sequence *in vitro* and in cultured cells. The question now arises of how Xom functions in the embryo and which genes are under its transcriptional control, that is, which are its natural target genes.

One approach to finding candidate target genes for the Xvent family has been to analyse the effect of injection of mRNA encoding Xvents, or dominant-negative versions of Xvents, into the *Xenopus* embryo. This has been followed by the analysis of the expression of several known genes.

Previous over-expression experiments using Xvent genes show that this family generates embryos with increased ventral and posterior tissues at the expense of dorsal and anterior tissues (Ault et al., 1996; Gawantka et al., 1995; Ladher et al., 1996; Onichtchouk et al., 1996; Schmidt et al., 1996; Rastegar et al., 1999). However, when analysed in more detail, reports from different authors describe different phenotypes with similar doses of injected RNA. At present, it is unclear whether the differences are due to particular experimental conditions or whether they represent differences in function between Xom-like and Xvent-1 like genes. This is described in more detail below.

Within the Xom subgroup of genes, embryos injected at the 4-cell stage with a high dose (4 ng) of *Xom* RNA into the dorsal side presented anterior/dorsal deficiencies in 65% of cases, of which 48% had no notochord (Ladher et al., 1996). Other authors, however, have described more severe phenotypes in similar experiments using *Xvent-2*, *Vox* or *Xvent-2B*, including the'Bauchstück' phenotypes (Onichtchouk et al., 1996; Rastegar et al., 1999; Schmidt et al., 1996) characteristic of maximally ventralised embryos (Kao and Elinson, 1988).

For the Xvent-1 subgroup, embryos injected radially with 0.6 to 0.8 ng of *Xvent-*

1 mRNA show anterior truncations, loss of prechordal plate mesoderm and sometimes notochord, but always retain a clearly recognisable embryonic axis (Gawantka et al., 1995). However, it has also been reported that dorsal injections of *PV.1* (1 ng) or *Xvent-1B* RNA can generate completely ventralised embryos, which do not have a clearly recognisable axis (Ault et al., 1996; Rastegar et al., 1999).

In an attempt to clarify some discrepancies in results from different groups and to determine the variability associated with this type of experiments, *Xom* and *PV.1* mis-expression experiments have been revisited in this chapter.

Ventralisation phenotypes in whole embryos are characterised by defects in dorso-anterior structures (such as the eyes and the cement gland) and/or in dorsal axial structures (such as notochord and muscle), which are generally accompanied by truncations of anterior structures (microcephaly or absence of the head). In the *Xenopus* gastrula, the head mesoderm originates from the prechordal mesoderm, which is the first part of the marginal zone to invaginate through the blastopore lip. Axial structures originate from the dorsal marginal zone that invaginates through the blastopore lip immediately after the prechordal mesoderm (Dale and Slack, 1987; Gilbert, 1994). The apparent relation between defects in anterior and in dorsal structures, due to over-expression of ventralising factors, is consistent with the idea that inhibition of ventralising signals is both necessary for the function of both the trunk and the head organiser (Glinka et al., 1997).

At the molecular level, the lack of anterior/dorsal structures in the *Xenopus* embryo correlates with an absence or reduction in transcripts of dorsal-lip specific early response genes and an up-regulation of ventrally and laterally expressed genes. In particular, truncation of anterior-dorsal structures as a result of *Bmp-4* over-expression inhibits the expression of dorsally-expressed genes such as *gsc* (Cho et al., 1991) *Xnot* (von Dassow et al., 1993) and *XFD-1/XFD-1'* (or *Pintallavis/XFKH1*) (Dirksen and Jamrich, 1992; Knochel et al., 1992; Ruiz i Altaba and Jessell, 1992) and stimulates the expression of ventral-lateral genes like *Xhox3* (Ruiz i Altaba and Melton, 1989) and *Xpo* (Fainsod et al., 1994; Jones et al., 1996; Re'em-Kalma et al., 1995; Sato and Sargent, 1991).

Since Xvents i) act downstream of Bmps to mediate ventral specification (Chapter 1), ii) are expressed ventrally and laterally at early gastrula stages (Chapter 1) and iii) act as repressors of transcription in *Xenopus* (Chapter 4; Friedle et al., 1998)), it is likely that they function by repressing the expression of organizer specific genes. Indeed, Xvent-1 has recently been shown to act as a direct repressor of the dorsal-lip-early-response gene XFD-1' (Friedle et al., 1998). However, nothing is known about targets of Xom. In an effort to address this question, the effects of Xom gain-of-function and loss-of-function on the expression of two organizer genes, *gsc* and *XFKH1(XFD-1')*, were analysed.

RESULTS

Mis-expression of *Xom* and *PV.1* in the embryo

Morphological and histological phenotypes

Two dorsal blastomeres of 4-cell stage embryos were injected with 4 ng of *Xom* RNA (Ladher et al., 1996) or 1 (or 2) ng of *PV.1* RNA (Ault et al., 1996), respectively, and the resulting phenotypes were analysed at stage 35. Each individual injection experiment was always performed with eggs from the same female. The results from 5 independent experiments are compiled in Table 5.1.

Table 5.1: Morphological phenotypes observed after five independent dorsal injections of *Xom* or *PV.1* in *Xenopus* embryo.

RNA	Phenotype (%), Stage 35					n
	Normal	Severe [a]	Mild[b]	Very Mild[c]	Gastrulation defects[d]	
Non injected	60	0	0	3	14(0)	30
Xom (4 ng)	12	32	22	16	18(12)	50
PV.1 (1 or 2 ng)	3	37	17	0	43(31)	35

[a] Severe phenotypes include embryos with no head or small heads, lacking cement gland and

eyes. [b] Mild phenotypes correspond to embryos with small head, small cement gland and no eyes or eye defects. [c] Very mild corresponds to embryos with eye defects only, or sometimes also with a small cement gland but always a normal sized head. Eye defects include: small eyes (on one side or both sides), one eye absent (on the right or the left side) and combinations of these phenotypes. [d] Gastrulation defects include embryos with different extents of non-closure of the blastopore lip; the number between brackets corresponds to the percentage of embryos with gastrulation defects lacking cement glands. n, total number of embryos.

Analysis of Table 5.1 indicates that *Xom* injections generated 32% of embryos that were severely ventralised, with no head or small heads, lacking cement gland and eyes. This phenotype, however, was not observed in all experiments performed. Mild and very mild ventralisation was observed in 22% and 16%, respectively, of *Xom* injected embryos. Figure 5.1 shows examples of very mild ventralisation as a result of mis-expression of *Xom*, whereas uninjected embryos are not ventralised (Fig. 5.1 A, B and inset). Occasionally, very mild phenotypes were accompanied by shortening and bending of the tail, which may indicate defects in convergence-extension movements, characteristic of gastrula stage dorsal involuting tissue. By contrast, *PV.1* injected embryos generated more embryos with a severe ventralised phenotype (37%), which were present in all experiments performed (Table 5.1 and Fig. 5.1 C). Embryos with a very mild ventralisation phenotype were never observed (Table 5.1). I note that in these experiments *PV.1* RNA was always used in lower doses than *Xom* RNA. In a substantial proportion of embryos presenting gastrulation defects, the cement gland was also missing in injected embryos (Table 5.1; Fig. 5.1 B and C), while control non-injected embryos still formed cement gland. This further indicates that patterning did not occurred normally in injected embryos. Taken together, these results indicate that in the range of concentrations used, Xom has a milder ventralising phenotype than PV.1.

Xom and *PV.1* injected embryos from one of the experiments described in Table 5.1 were further analysed by whole mount antibody staining using the antibody MZ15, which recognises the notochord, and the results are presented in Table 5.2.

Table 5.2. Whole mount antibody staining using MZ15 antibody.

RNA	Notochord staining (%), Stage 35			n
	Normal	Fragmented*	Absent	
Uninjected	100	0	0	10
Xom (4ng)	41	53	6	17
PV.1 (1 ng)	40	60	0	10

* Corresponds to MZ15 staining in fragments of notochord spread along the axis of the tadpole, which can cover from almost 100% to almost 0% of the length of the axis.

Mis-expression of *Xom* and *PV.1* RNA causes frequent disruption of the notochord, and in one case complete absence (Table 5.2 and 5.1 B, D and E). These results confirm that the ventralisation phenotypes observed in *Xom* and *PV.1*-injected embryos correlates with a disruption in dorsal structures, such as the notochord.

In summary, in my hands and in the range of concentrations used, *Xom* has a variable and, generally, milder ventralising phenotype than *PV.1*. However, neither *Xom* nor *PV.1* generated completely ventralised embryos, as has previously been reported (Ault et al., 1996; Onichtchouk et al., 1996; Rastegar et al., 1999; Schmidt et al., 1996). Similar phenotypes for *PV.1* (*Xvent-1*) injections as the ones presented here have been observed by Gawantka et al. (1995). It remains possible that higher doses of RNA will generate completely ventralised embryos, although increased concentrations of *Xom* cause embryos to die.

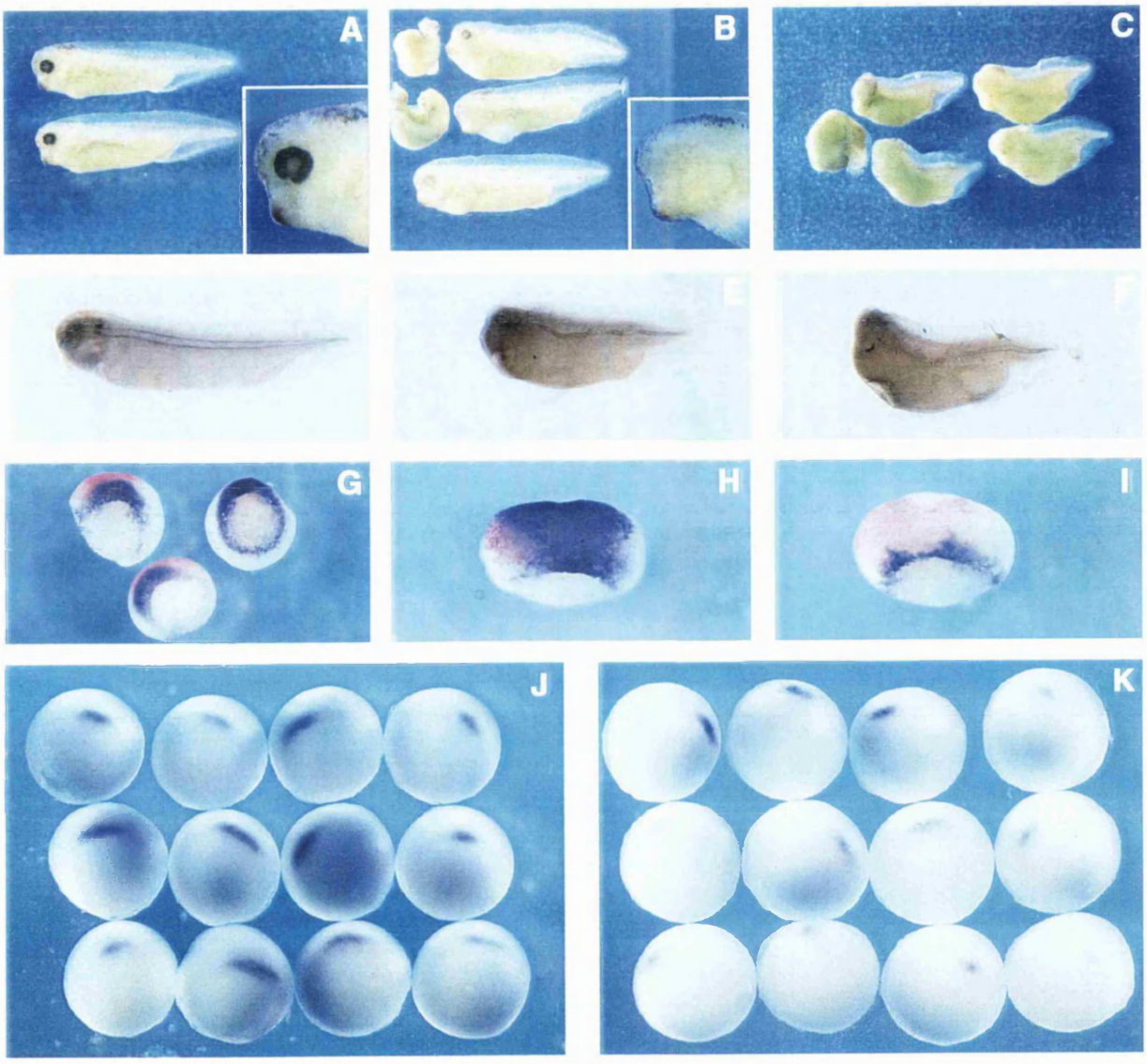
A
B
C
G
H
I
J
K

Fig. 5.1 Over-expression of *Xom* and *PV.1* causes ventralisation of *Xenopus* embryos and affects expression of dorsally-expressed genes. Phenotypes of uninjected embryos at tadpole stage (A) or of embryos injected dorsally at the 4-cell stage with 4 ng of *Xom* RNA (B) or 2 ng of *PV.1* RNA (C). In this experiment, *PV.1* injections generated severe ventralised embryos with no head or small heads and a shortened body, whereas *Xom* injections generated milder phenotypes, defective in the formation of the eyes and/or cement gland but with normal head and body size. Embryos with severely impaired gastrulation are also shown (B, C). The inset in (B) shows an embryo injected with *Xom* lacking one eye while the inset in (A) shows the normal head of an uninjected embryo. (D-F) Notochord staining of uninjected embryos (D) and dorsally injected embryos with 4 ng of *Xom* (E) or 2 ng of *PV.1* (F). Note discontinuous notochord staining in injected embryos. (G) *FRKH1* expression in control embryos at early gastrula stage 10.5 injected with the fluorescein dextran lineage marker and analysed by whole mount *in situ* hybridisation with a *FRKH1* probe and by whole mount antibody staining to show fluorescein dextran staining. Vegetal view of three embryos. (H, I) *FRKH1* expression in stage 10.5 embryos co-injected with fluorescein dextran and 4 ng of *Xom* (H) or 2 ng of *PV.1* (I). Dorso-vegetal view. Note up-regulation of *FRKH1* expression in *Xom*-injected embryos and *FRKH1* down-regulation in *PV.1*-injected embryos. *Goosecoid* expression in uninjected embryos (J) or in embryos injected in both blastomeres of 2-cell stage embryo with 4 ng *Xom* RNA (K) analysed by whole mount *in situ* hybridisation at stage 10.5. Vegetal views; dorsal to the top. Note down-regulation of *goosecoid* expression in injected embryos.

Molecular marker analysis

The effects of *Xom* and *PV.1* RNA injection on the expression of *forkhead-1* (*FRKH1*) (Dirksen and Jamrich, 1992; Knochel et al., 1992; Ruiz i Altaba and Jessell, 1992) at early gastrula stage 10.5 was analysed by whole mount *in situ* hybridisation. Control embryos, injected with fluorescein dextran lineage marker (Fig. 5.1 G) showed that endogenous *FRKH1* is restricted to the dorsal blastopore lip in most embryos, but expression can sometimes be detected all around the marginal zone in a ring which is thin laterally and ventrally, but much thicker dorsally. Six out of 11 embryos injected with 1 (or 2) ng of *PV.1* RNA together with fluorescein dextran locally reduced *FRKH1* expression, interrupting or forming a thinner ring of *FRKH1* expression on the injected side (Fig. 5.1 I). Similarly, Friedle *et al.* (1998) observed suppression of *FRKH1* (*XFD-1'*) expression in embryos injected dorsally with 1 ng of *Xvent-1* mRNA (Friedle et al., 1998).

Surprisingly, 16 out of 18 embryos injected with 4 ng of *Xom* together with fluorescein dextran presented an expansion of the endogenous *FRKH1* domain of expression. In most cases, the *FRKH1* expression domain extended towards the animal pole (Fig. 5.1 H), but elevated staining has also been detected in the animal-ventral and lateral parts of the embryo and, to a lesser extent, in the vegetal pole. All ectopic staining occurred within injected cells (or their progeny), which stained red due to fluorescein dextran, indicating that Xom acts cell autonomously. The effects of *PV.1* and *Xom* on *FRKH1* expression are discussed below.

The effect of *Xom* over-expression on *goosecoid* (*gsc*) (Cho et al., 1991) was analysed by whole mount *in situ* hybridisation and by RNAse protection at the gastrula stage. Whole mount *in situ* hybridisations at the early gastrula stage showed that embryos injected in both blastomeres at the two-cell stage with 4 ng of *Xom* RNA had a substantial reduction in *gsc* expression in comparison with uninjected embryos (Fig. 5.1 J and K). The reduction in the level of *gsc* transcripts was confirmed by RNAse protection in whole embryos at stage 10.5 (Fig. 5.2). In animal cap experiments, activin was used to induce expression of *gsc* because *gsc* has been shown to respond to activin in an immediate-early fashion (Cho et al., 1991). Injection of 4 ng *Xom* mRNA resulted

in down-regulation of activin-induced expression of *gsc* in animal caps.

Taken together, the results from whole mount *in situ* and RNAse protection experiments support the idea that Xom down-regulates *gsc* expression. Consistent with this, down-regulation of *gsc* expression was observed in dorsal marginal zones of *Xvent-2* injected embryos (Onichtchouk et al., 1998) and, locally, in injected LiCl-dorsalised embryos injected with *Xvent-2* (Onichtchouk et al., 1996). In another study, over-expression of *Vox* abolishes *gsc* expression in whole embryos (Schmidt et al., 1996). However, in my hands *gsc* expression was never completely abolished.

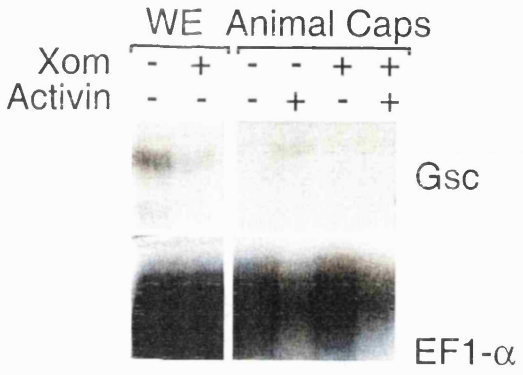

Fig. 5.2: Over-expression of *Xom* causes down-regulation of *goosecoid* expression in *Xenopus* embryos and in activin-induced animal caps. Embryos were left intact or injected with 4 ng of *Xom-HA* RNA into two dorsal blastomeres of 4-cell stage embryos and analysed by RNase protection at stage 10.5 with the indicated probes. Alternatively, embryos were left intact or injected with 4 ng *Xom-HA* RNA, animal caps were dissected at blastula stage and treated with 10 u/ml of activin for approximately 4 hours. After this incubation period, animal caps were analysed by RNase protection with the indicated probes at the equivalent of stages 10.5-11. WE, whole embryos.

Dominant-negative approaches

Xom^{L213P}

The first attempt to interfere with the function of Xom was performed by injecting RNA encoding Xom^{L213P}, which contains a mutation in which a proline replaces a leucine between helices two and three of the homeodomain (see Materials and Methods). This approach was based on the interfering Mix.1 construct used by Mead and colleagues, named M11 (Mead et al., 1996). This mutation is thought to disrupt the conformation of the homeodomain, thus interfering with binding to DNA. Indeed, binding to their respective consensus binding sequences was reduced, or abolished, when either M11 (Mead et al., 1996), $Antennapedia^{L213P}$ (Le Roux et al., 1993) or Xom^{L213P} (Fig. 3.4 B, Chapter 3) were used in electrophoretic mobility shift assays. The dominant-negative action of M11, is based on a putative dimerisation with endogenous Mix.1, which would prevent Mix.1 to bind its target genes and therefore, exerting its effects.

To test whether Xom^{L213P} is able to disrupt ventral specification, Xom^{L213P} RNA was injected in one ventral blastomere at the 32-cell stage and its effects were analysed in whole embryos. Embryos injected with 4 ng of Xom^{L213P} RNA formed partial secondary axes at low frequency (6%, n=195, 4 independent experiments), and different extents of disruption of blastopore closure (44%) (Fig. 5.3 B). Uninjected embryos (Fig. 5.3 A) or embryos injected ventrally with *Xom* RNA were normal. Three Xom^{L213P} RNA injected embryos, which formed partial secondary axes, were analysed by histology and contained ectopic muscle and neural tissue, but no notochord (not shown). Preliminary attempts to rescue Xom^{L213P} injection phenotypes by co-injecting equimolar amounts of Xom^{L213P} and *Xom* RNA into one ventral blastomere of 32-cell stage embryos were not successful.

Injections performed earlier, into two ventral blastomeres of 4-cell stage embryos, generated a slightly higher (16%) frequency of partial secondary axes, and the frequency of gastrulation defects was smaller (32%, n=38). In this experiment, all partial secondary axes contained ectopic muscle, which sometimes appeared disorganised and

diffuse, occupying a large ectopic area of the body of the embryo (Fig. 5.3 C, D and E). These results suggest that the Xom^{L213P} promotes dorsal specification in ventral cells, thus behaving in an opposite way to *Xom*.

Recently, two studies have shown that M11 may interact with the functions of other genes (Latinkic and Smith, 1999; Lemaire et al., 1998). Animal caps from embryos injected with RNA encoding M11 form cement gland and express the neural marker *N-CAM* (Latinkic and Smith, 1999; Lemaire et al., 1998). However, *Mix.1* is not present, to detectable levels, in the animal pole tissue (Rosa, 1989) suggesting that M11 interferes with the function of another gene product in animal caps. It is possible, therefore, that Xom^{L213P} also interferes with other gene products acting non-specifically. This observation, and the fact that, secondary axis formation induced by dorsal injection of Xom^{L213P} RNA occurred at low frequency and could not be rescued by wild type *Xom* RNA, led me to abandon the use of Xom^{L213P} as an inhibitor of Xom function.

I note, however, that Onichtchouk *et al.* (1998) obtained partial secondary axis formation in embryos injected ventrally with 5 ng of $Xvent\text{-}2^{L213P}$ RNA (35%; n=89), which was rescued by 2 ng injections of *Xvent-2* RNA (Onichtchouk et al., 1998) and similar results were obtained by Rastegar *et al.* (1999). Interestingly, a distinctive phenotype was not obtained for $Xvent\text{-}1^{L312P}$ injections (Onichtchouk et al., 1998).

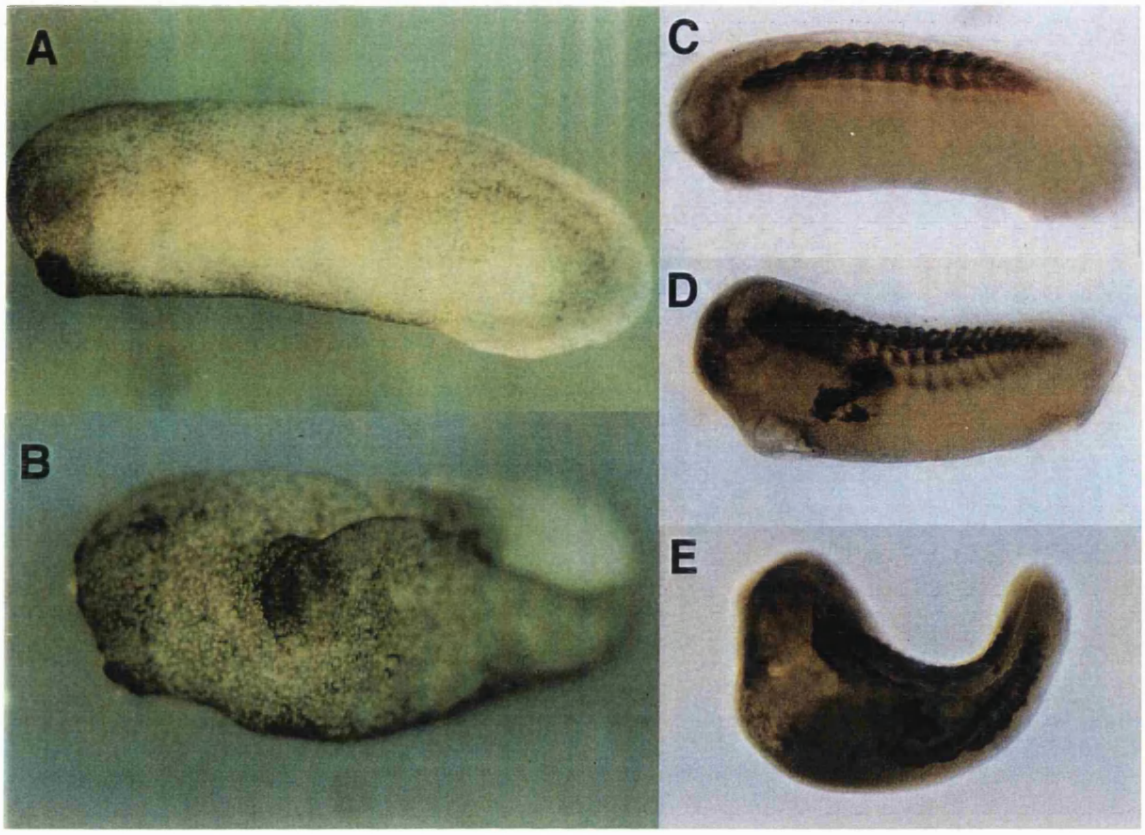

Fig. 5.3: Xom^{L213P} over-expression causes partial secondary axis formation and ectopic muscle differentiation. (A) Stage 27 uninjected embryo. (B) Stage 27 embryo injected with 4 ng of Xom^{L213P} RNA in one ventral blastomer at the 32-cell stage. Note the formation of a partial secondary axis. (C) Uninjected embryo analysed by whole mount antibody staining at stage 35 to detect muscle tissue. (D, E) Embryos injected into two ventral blastomeres of a 4-cell stage embryo with 4 ng of Xom^{L213P} RNA and analysed in the same way as in (C) show ectopic muscle formation.

XomVP16

A second approach to interfere with Xom function was based on XomVP16, which consists of full length Xom fused at its C-terminus to a VP16 activation module (see Materials and Methods and Fig. 3.7). VP16 is a very potent activator of transcription that, when fused to transcription factors, can override their normal function (Ferreiro et al., 1998; Latinkic and Smith, 1999). Other authors have recently used a similar construct in which a VP16 activation domain replaces the N-terminal portion of Xom and this appeared to act in a dominant-negative fashion (Onichtchouk et al., 1998). However, my XomVP16 construct retains the entire Xom open reading frame in an effort to avoid deleting any domain required for DNA or protein-protein interactions including, perhaps, dimerisation (see Discussion of Chapter 3). It should therefore be more specific in its effects.

To test whether XomVP16 is able to induce ectopic dorsal tissue, 4-cell stage *Xenopus* embryos were injected into two adjacent blastomeres with 2 or 4 ng RNA encoding XomVP16 together with fluorescein dextran lineage marker. When left to develop, such embryos sometimes died at late gastrula stages, but in one experiment where survival was high, partial secondary axes were observed in 15% of cases (n=26; data not shown). To test whether XomVP16 affected *gsc* expression, embryos were also analysed by whole mount *in situ* hybridisation at stage 10.5. All 15 embryos injected with 2 or 4 ng RNA showed cell-autonomous ectopic *gsc* in both the animal pole and marginal zone, whereas injections of 1 ng of XomVP16 did not induce ectopic expression of *gsc*. Fig. 5.4 illustrates two examples of injected embryos. These results further support the idea that *Xom* acts through down-regulating endogenous *gsc* expression.

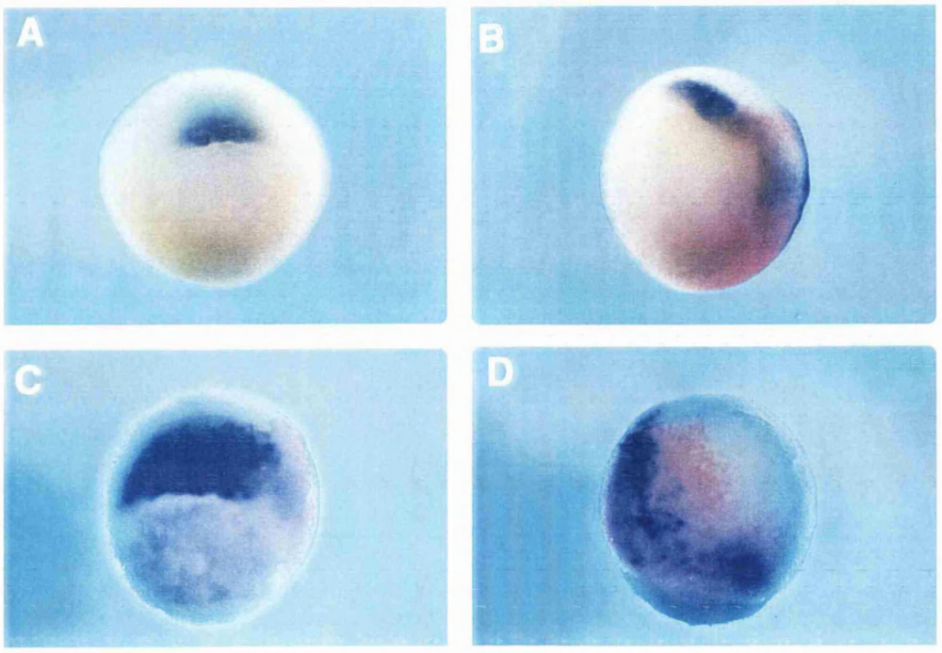

Fig. 5.4: Over-expression of *XomVP16* causes ectopic activation of *goosecoid*. (A) *goosecoid* expression in uninjected embryos at stage 10.5; vegetal view. (B, C, D) Two adjacent blastomeres of *Xenopus* embryos at the 4-cell stage were co-injected with 4 ng of *XomVP16* RNA and fluorescein dextran lineage marker and analysed by whole mount *in situ* hybridisation at early gastrula stage 10.5 to reveal *goosecoid* expression and whole mount antibody staining to show fluorescein dextran. (B) Vegetal view of an injected embryo with dorsal to the top. Expression of *goosecoid* is expanded laterally to the injected side. (C) Vegetal-dorsal view of an injected embryo with dorsal to the top. Expression of *goosecoid* is expanded towards the animal pole. (D) Ventral view of the same embryo as in (C) with the animal pole to the top. Ectopic expression of *goosecoid* occurs ventrally and laterally in the marginal zone and extends into the animal pole region.

DISCUSSION

In this chapter the function of Xom in the embryo was analysed by mis-expression and loss-of-function approaches. Dorsal injections of *Xom* RNA into *Xenopus* embryo cause different extents of anterior-dorsal defects affecting head, eyes, cement gland and notochord, but which are generally less severe than in *PV.1* injected embryos. However, in my hands neither the injection of *Xom* nor *PV.1* RNA generated completely ventralised embryos, as described in other studies (Ault et al., 1996; Onichtchouk et al., 1996; Rastegar et al., 1999; Schmidt et al., 1996). Analysis of the effects of mis-expression of *Xom* and *PV.1* on the expression of dorsal genes at stage 10.5 revealed that *PV.1* reduces *FRKH1* expression whereas *Xom* has the opposite effect, expanding *FRKH1* expression in whole mount *in situ* hybridisation experiments. In addition, *Xom* is able to down-regulate the expression of *gsc*, and this result has been supported by injections of *XomVP16* RNA, which induce *gsc* expression.

Possible explanations for discrepancies in the results of over-expression studies using Xvent genes

Several Xvent plasmids have been used in *Xenopus* over-expression studies, which when injected into the embryo generate transcripts containing the Xvent coding region flanked by RNA of different length and sequence (this thesis; Ault et al., 1996; Gawantka et al., 1995; Ladher et al., 1996; Onichtchouk et al., 1996; Rastegar et al., 1999; Schmidt et al., 1996). This flanking sequence may affect RNA stability and could account for the variability of phenotypes observed.

The discrepancy in the phenotypes obtained in over-expression experiments was particularly striking for *Xom* and the other genes of the same subgroup. Over-expression of *Xom* (this study; Ladher et al., 1996) caused markedly milder ventralised embryos than those obtained with *Vox* , *Xvent-2* and *Xvent-2B* (Onichtchouk et al., 1996; Rastegar et al., 1999; Schmidt et al., 1996). This is unlikely to be due to a difference in the plasmid used to transcribe *Xom,* since *Xom* RNA was transcribed from two different vectors (p64T and CS2+, data not shown) with similar results. Thus, the discrepancy between my results and those of Ladher et al. (1996) in comparison to other authors

could be due to a real difference in activity of Xom. Consistent with this possibility, Xom contains a stretch of 16 divergent amino acids and a deletion of 9 amino acids in its N-terminal region not present in Xvent-2B, Vox, Xbr1 or Xvent-2 (Fig. 1.6, Chapter 1).

For PV.1, the discrepancy in the phenotypes obtained in this and other studies is smaller than for the experiments with Xom. Very similar experiments to those described in this chapter performed by Ault *et al.* (1996) using presumably the same plasmid show maximally ventralised *PV.1*-injected embryos. Although in this study no maximally ventralised embryos were observed (n=35), only one normal embryo was detected in 5 independent experiments and no very mild ventralised phenotypes were ever observed. Therefore, the difference in phenotypes of PV.1 injections is small and might be due to undetermined experimental variability.

XomVP16 as a dominant-negative construct

A XomVP16 construct was used to test the effects of down-regulation of Xom. The use of this construct as a dominant-negative version of Xom is supported by several observations.

First, XomVP16 can bind specifically *in vitro* to a sequence containing a consensus Xom binding sequence (Chapter 3, Fig. 3.6) and to interact with this sequence in order to behave as a transcriptional activator in transient transfections in COS cells (Chapter 3, Fig. 3.7). Furthermore, XomVP16 also works as an activator in reporter studies performed in the embryo, whereas Xom works as a repressor (data not shown). This suggests that XomVP16 can bind the same targets as Xom *in vivo* and can activate transcription.

Second, Onichtchouk *et al.* (1998), using another VP16-based construct (VPXvent-2), obtained a slightly higher efficiency of secondary axis formation (24%, n=65) when 1 ng of *VPXvent-2* was injected ventrally into *Xenopus* embryos. These secondary axes contained muscle but only rarely notochord, and this phenotype was completely rescued by co-injecting 2 ng of Xvent-2 (Onichtchouk et al., 1998). This result shows that VPXvent-2 acts as a dominant-negative form of Xvent-2 (Xom), thus suggesting that XomVP16 also acts as a dominant-negative form of Xom.

Finally, VP16-fusion based strategies have been successfully used to disrupt the repression function of other proteins such as Gsc (Ferreiro et al., 1998; Latinkic and Smith, 1999). In particular, a construct containing *gsc* fused to an identical VP16 module as the one used in this thesis has been used as dominant-negative construct (Latinkic and Smith, 1999). Interestingly, in a slightly different approach, a construct containing the entire coding region of Vox fused at its carboxy-terminus to the Gal4 activation domain (VoxG4A), caused partial secondary axis formation when injected ventrally in *Xenopus* embryos, and this could be rescued by co-injection with wild type *Vox* (Melby et al., 1999).

Differential regulation of *XFKH1* by Xom and Xvent-1 (PV.1)

The effects of the *Xenopus* forkhead-like gene *XFKH1* (and its pseudoallele *Pintallavis*) are restricted to the notochord and patterning of the neural axis (Ruiz i Altaba and Jessell, 1992) and, in animal cap assays, *Pintallavis* is able to synergise with the pan-mesodermal marker *Xbra* to induce the formation of dorsal mesoderm (O'Reilly et al., 1995). Furthermore, disruption of a related gene in mouse, *HNF-3β*, results in more severe defects in forebrain or node and notochord formation (Ang and Rossant, 1994; Weinstein et al., 1994).

Results presented in this chapter show that Xom and Xvent-1 (PV.1) regulate *XFKH1* expression (Fig 5.1 G-I) in different ways. The inhibitory effect of Xvent-1 on *XFKH1* expression has previously been shown to be direct and the binding sites of Xvent-1 in the promoter of *XFKH1* have been determined (Friedle et al., 1998). In contrast, it is unlikely that the observed activation effect of Xom on *XFKH1* expression in whole mount *in situ* hybridisation is direct because Xom functions primarily as a transcriptional repressor. Furthermore, there are no Xom binding sites in the Bmp or Activin response elements mapped within the *XFKH1* promoter (Howell and Hill, 1997; Kaufmann et al., 1996).

The reciprocal regulation of *XFKH1* expression by Xom and Xvent-1 may be part of a mechanism to restrict *XFKH1* expression dorsally. Before stage 9, the expression pattern of *XFKH1* differs from that of its pseudoallele *Pintallavis* in that it is

expressed in a much wider area (>90° arc) of the dorsal marginal zone (Dirksen and Jamrich, 1992; Ruiz i Altaba and Jessell, 1992). Later *XFKH1* expression becomes more restricted dorsally, but its pattern of expression is never as restricted to the dorsal-most area of the embryo as that of *gsc*, for example. In my hands, *XFKH1* can sometimes be detected all around the marginal zone at stage 10-10.5. Early *XFKH1* expression could thus be under positive control by Xom, the first Xvent gene to be expressed (Gawantka et al., 1995). Later at stage 10, superimposition of *Xvent-1* expression could result in down-regulation of *XFKH1* laterally and ventrally, although Xom would still have a role in maintaining *XFKH1* expression levels in the dorso-lateral region where *Xom* is expressed but free of Xvent-1 transcripts. This model assumes that the proteins encoded by *Xom* and *Xvent-1* are active where the gene is transcribed, although this is unknown at present. Furthermore, double whole mount *in situ* hybridisations using *Xom* and *XFKH1* should be performed to test whether the expression of these two genes overlaps.

Xom down-regulates *goosecoid* expression

The dorsally expressed gene *goosecoid* behaves as an early-response gene to activin when assayed in the animal caps, possibly mimicking the early response to a TGF-β like signal acting in the embryo to specify the organizer region (Cho et al., 1991). *gsc* homologues have been cloned in mouse (Blum et al., 1992), chick (Izpisúa-Belmonte et al., 1993), human (Blum et al., 1994), and zebrafish (Schulte-Merker et al., 1994; Stachel et al., 1993) and in all of them *gsc* marks the equivalent of the *Xenopus* Spemann organizer. In *Xenopus*, ectopic expression of *gsc* mRNA mimics the activity of the organizer by inducing the formation of a partial secondary axis and by the ability to dorsalise ventral mesoderm explants (Cho et al., 1991; Niehrs et al., 1993; Niehrs et al., 1994). Furthermore, inhibition of *gsc* function causes dorso-anterior defects (Ferreiro et al., 1998; Latinkic and Smith, 1999; Steinbeisser et al., 1995).

gsc is a likely target of Xom. Consistent with this suggestion, I found that uniform over-expression of *Xom* in *Xenopus* embryos causes down-regulation of *gsc* (Fig. 5.1 J and K). A similar, but more extreme, down-regulation is observed in response to *Vox* (Schmidt et al., 1996), and *Xvent-2* has also been reported to cause down-regulation of *gsc* (Onichtchouk et al., 1996; Onichtchouk et al., 1998). Additional

experiments demonstrate that *Xom* also down-regulates activin-induced expression of *gsc* in isolated animal pole regions (Fig. 5.2).

Attempts to inhibit Xom function by expressing XomVP16 caused cell-autonomous ectopic expression of *gsc* in injected embryos (Fig. 5.4). In addition, mis-expression of a similar Xom interfering construct resulted in ectopic expression of *gsc* in animal caps (Onichtchouk et al., 1998). These experiments further support the idea that Xom regulates *gsc* expression. Interestingly, injection of a hormone-inducible version of a dominant-negative version of Xom, based on the fusion of Xom to a Gal4 activation domain, induces ectopic expression of *gsc* even in the presence of an inhibitor of protein synthesis, cycloheximide (Melby et al., 1999). This indicates that the up-regulation of *gsc* expression by this dominant-negative construct occurs independently of protein synthesis, suggesting that Xom down-regulates *gsc* expression in a direct fashion. This issue will be addressed on the next chapter.

Like *Xom*, *Xvent-1* also down-regulates *gsc* expression, in the early gastrula embryo, in marginal zone explants, and in activin-induced animal caps (Ault et al., 1996; Gawantka et al., 1995). As discussed in Chapter 3, the binding preference of Xvent-1 differs from that of Xom, and Xvent-1 binding sites are not present in a 300 nucleotide region of the *gsc* promoter (Friedle et al., 1998; Watabe et al., 1995). Thus, Xvent-1 may not regulate the expression of *gsc* directly and, in contrast to *Xom* and *gsc*, note that the expression domains of *Xvent-1* and *gsc* do not abut (Onichtchouk et al., 1996).

CHAPTER 6

Analysis of the effect of Xom on the *gsc* promoter

INTRODUCTION

Ectopic expression of *Xom* causes loss of dorso-anterior structures in the *Xenopus* embryo (Chapter 5; Ladher et al., 1996; Onichtchouk et al., 1996; Rastegar et al., 1999; Schmidt et al., 1996), and the demonstration that Xom functions as a transcriptional repressor (Chapter 4) suggests that it exerts its effects by down-regulating genes required for dorsal and anterior development. One likely target of Xom is *goosecoid* (*gsc*), a homeobox-containing gene expressed in the organizer of *Xenopus* embryos - the only region of the embryo where *Xom* itself is not activated (Cho et al., 1991; Ladher et al., 1996; Onichtchouk et al., 1996).

Two cis-acting growth factor-responsive elements have been identified within 300 nucleotides upstream of the *goosecoid* (*gsc*) transcription start site: the distal element (DE) and the proximal element (PE). These respond, respectively, to activin/BVg1 and to Wnt signalling (Watabe et al., 1995). The DE mediates activin induction in the absence of protein synthesis and responds to activin and BVg1 throughout the vegetal hemisphere and marginal zone but not in the animal hemisphere. Both DE and PE are essential for high-level transcription of the *gsc* gene, specifically in the dorsal mesoderm (Watabe et al., 1995). This is consistent with the idea that that TGF-β-related factors cooperate with Wnts to induce the organizer in the marginal zone (Harland and Gerhart, 1997; Sokol, 1999). Activin/BVg1-like activity is present throughout the marginal and vegetal regions, suggesting that endogenous *gsc* levels should be expressed at low levels in these regions. The fact that such transcripts are not observed in ventral and lateral regions of the embryo suggests that expression is down-regulated by the presence of other signalling factors such as Bmps (Watabe et al., 1995).

In this chapter, I investigate whether the repressing effect of Xom on the expression of *gsc* is direct by analysing the 300 nucleotides upstream of the start site of the *gsc* promoter, which contain the DE and the PE (Watabe et al., 1995). To that end, two mutated luciferase reporter constructs were generated which contain point mutations in potential Xom binding sites, one in the PE and another in the DE. They were used in

reporter studies in the embryo.

RESULTS

Xom represses activin-activated *gsc* promoter in reporter studies

To ask whether Xom repressor activity is mediated by a fragment containing 300 nucleotides 5' of the *gsc* transcription start site (Watabe et al., 1995), this promoter fragment was placed upstream of a luciferase reporter gene, thus creating -300gsc.luc. This reporter construct was co-injected with different effector RNAs, including RNA encoding activin, into both blastomeres of *Xenopus* embryos at the two-cell stage. Animal pole regions were dissected at stage 8.5, and luciferase activity was determined after a fixed incubation period. In an effort to detect repression effects, activin was used in these experiments to raise luciferase basal levels, since *gsc* responds to activin in an immediate-early fashion (Cho et al., 1991).

In contrast to the experiments of Watabe et al. (1995), I used RNA encoding activin rather than soluble activin protein. It was therefore necessary to optimise the time of cultivation of animal caps in order to obtain the desired activin stimulation of the *gsc* promoter. A preliminary time-course experiment was performed in which whole embryos were collected 2, 3 or 4 hours after stage 9, when, in a typical experiment, dissection of animal caps would have been completed (see Materials and Methods). Fig. 6.1 shows that from 3 hours onwards the -300gsc.luc reporter construct responded to activin with a 15 to 20-fold increase in luciferase activity compared with the activity of the reporter alone. These levels of activin-induced activation of *gsc* are suitable for the detection of inhibitory effects since injection of several concentrations of *Xom* RNA repressed activin-induced activation. This repression effect ranged from approximately 50% with 1 or 2 ng of *Xom* RNA to a complete inhibition of activation with 4 ng of *Xom* RNA at all time points assayed (Fig. 6.1). Co-injection of a non specific RNA (β-globin) together with activin RNA resulted in variable effects at early dissection times, but at 4 hours after dissection the effect of globin RNA on luciferase levels was indistinguishable from that of activin RNA injected alone (Fig. 6.1). These experiments show that any period between 3 and 4 hours after dissection is adequate to detect an

inhibitory effect of Xom on the activin-activated *gsc* promoter. Therefore, in the experiments performed next, animal caps were cultured for 3 hours and 30 minutes after dissection. After this period, they were generally equivalent to stage 10 and, occasionally, stage 10.5 embryos.

Animal caps were injected with the –300gsc.luc reporter construct together with different effector RNAs into both blastomeres of *Xenopus* embryos at the two-cell stage. Animal pole regions were then dissected at stage 8.5 and luciferase activity was determined 3.5 hours later. Under these experimental conditions, activin elicited a 19-fold activation of the -300gsc.luc reporter construct in animal caps (mean of 13 independent experiments; data not shown). To access the inhibitory effect of Xom, luciferase activities obtained in response to activin alone were defined as 100% activation and activities obtained in the presence of Xom were expressed relative to this. Fig. 6.2 shows that injection of RNA encoding Xom reduces activin-induced luciferase activity driven by the -300gsc promoter. No significant reduction in luciferase activity was observed when RNA encoding non-specific proteins (the Gal4 activation domain or β-globin) was injected (Fig. 6.2). These results show that Xom is able to repress the activin-stimulated transcription of *gsc* through the –300 base pair fragment of the *gsc* promoter.

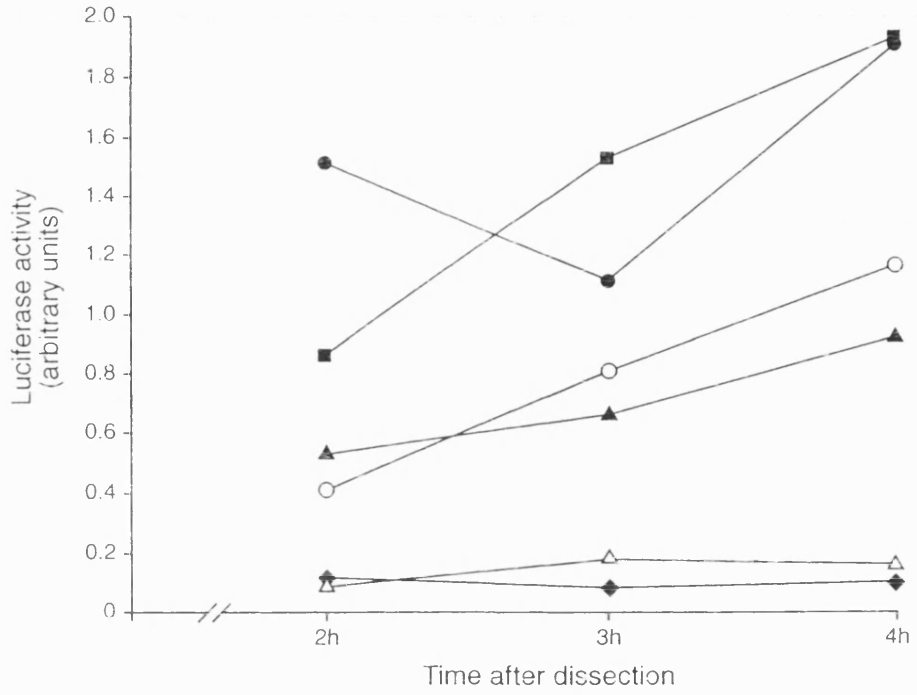

	RNA			DNA
	Xom	β-globin	Activin	-300 gsc.luc
◆	-	-	-	+
■	-	-	+	+
▲	1 ng	-	+	+
○	2 ng	-	+	+
△	4 ng	-	+	+
●	-	2 ng	+	+

Fig 6.1: Time course of Xom repressing effect on activin-induced activation of the *goosecoid* promoter. 2-cell stage *Xenopus* embryos were injected with the indicated amounts of effector RNAs and/or 50 pg of activin RNA, together with -300gsc.luc reporter DNA and reference plasmid pRL-TK. Whole embryos were collected 2, 3 or 4 hours after stage 9 and luciferase activities were determined. Note that from 3 hours onwards the -300gsc promoter responds to activin with 15 to 20-fold increase in luciferase activity compared with the activity of the reporter alone and that injection of several concentrations of *Xom* RNA repressed this effect.

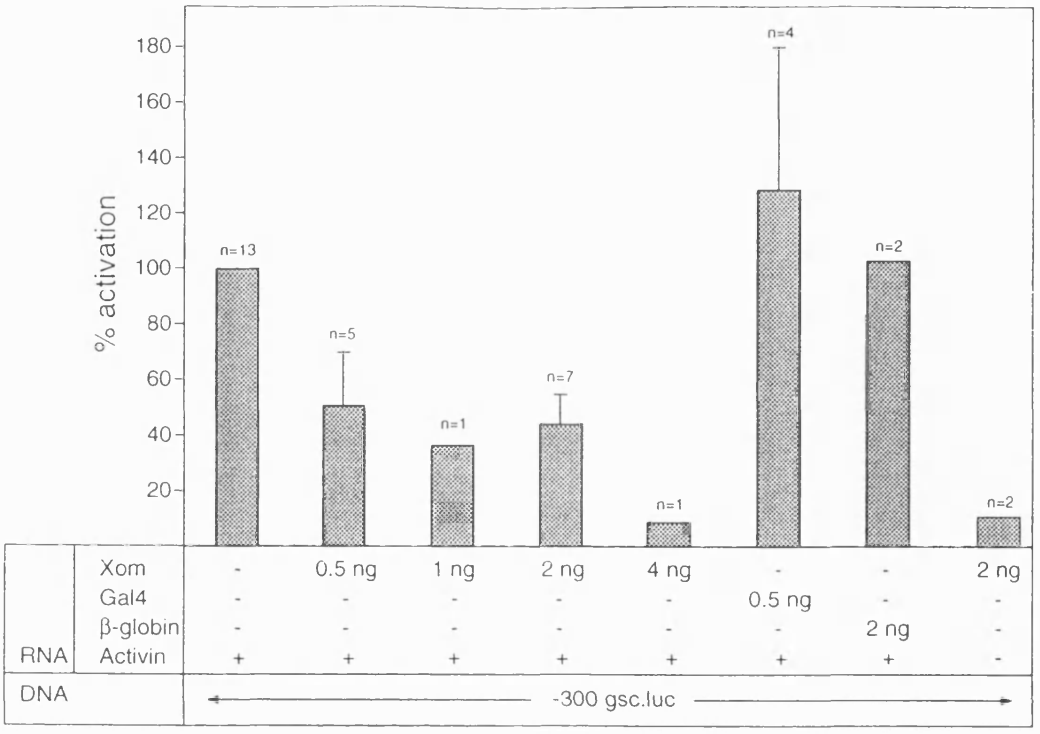

Fig. 6.2: Xom represses activin-induced activation of the *goosecoid* promoter. 2-cell stage *Xenopus* embryos were injected with the indicated amounts of effector RNAs and/or 50 pg of activin RNA, together with -300gsc.luc reporter DNA and reference plasmid pRL-TK. Animal pole regions were dissected at blastula stage 8.5 and cultured for 3.5 hr. Luciferase activities were determined in duplicate and expressed as a percentage of that obtained with activin alone. Values shown are means +/- standard deviation; n, number of experiments performed. This figure contains data which is also included in Table 6.1.

Analysis of point mutations in the *gsc* promoter

To test whether the ability of Xom to repress the -300.gsc activin-stimulated promoter is due to direct interaction with specific sites on the promoter, I analysed the sequence of this region of the *gsc* promoter and found that it contains two putative targets for Xom binding. The proximal element (PE) contains the sequence CTAATGGAGTGGATTAG, which resembles the Xom consensus sequence shown in Fig. 3.3 (Chapter 3) but differs in that the nucleotide 3' of the first core TAAT is G rather than T. The distal element (DE) contains the sequence GCAATTAG (complementary strand CTAATTGC), whose flanking nucleotides correspond precisely to those identified by binding site selection and which, according to the analysis in Fig. 3.4 (probe D), would be expected to bind Xom. In addition, there are scattered motifs in both the PE and DE which correspond to the core homeodomain DNA-binding consensus sequence TAAT (Gehring et al., 1994).

Two mutated -300gsc.luc reporter constructs were generated. -300gsc.luc$^{-145/136}$ contains two point mutations in the putative binding site in the PE while -300gsc.luc$^{-201/2}$ contains point mutations in the putative binding site in the DE (Fig. 6.3A). Preliminary experiments demonstrated that these constructs show a 3 or 6-fold (average for -300gsc.luc$^{-201/2}$ and -300gsc.luc$^{-145/136}$, respectively) higher basal level of luciferase activity in animal caps when compared with the wild type reporter construct (Fig. 6.3 B). This suggests that the mutations prevent the interaction of endogenous repressors, perhaps including Xom itself, with the –300gsc constructs.

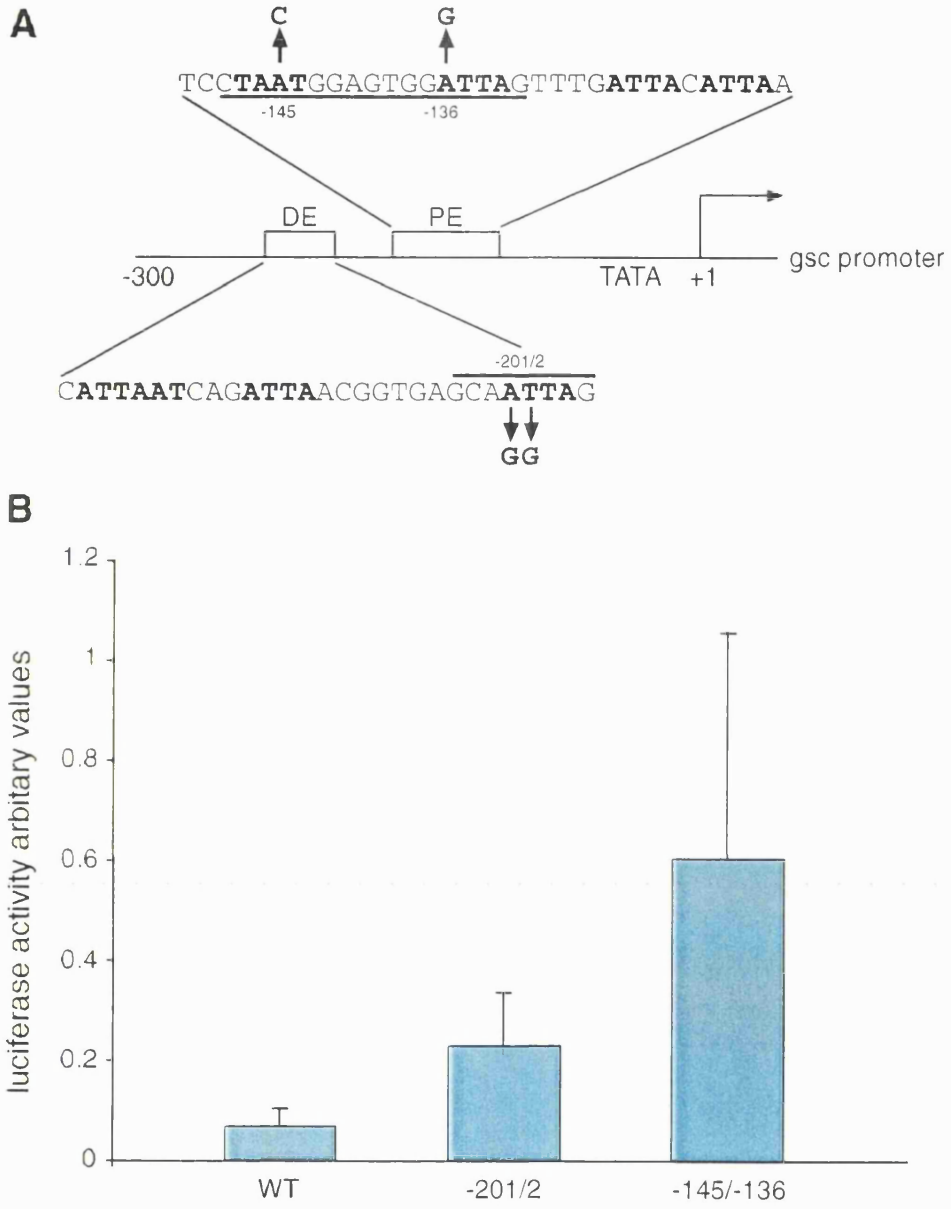

Fig. 6.3 Point mutations increase the basal activity of a *goosecoid* promoter reporter construct in *Xenopus* embryos. (A) Representation of the 300 nucleotides 5' of the *goosecoid* transcription start site. The sequences of the Distal Element (DE) and the Proximal Element (PE) (Watabe et al., 1995) are indicated. TAAT motifs are in bold, putative Xom binding sequences are highlighted, and the point mutations introduced into -300gsc$^{-201/2}$.luc and -300gsc$^{-145/-136}$.luc are shown. (B) *Xenopus* embryos at the 2-cell stage were injected with -300gsc.luc (WT), -300gsc$^{-201/2}$.luc (-201/2) or -300gsc$^{-145/-136}$.luc (-145/-136) reporter DNA and reference plasmid pRL-TK. Animal pole regions were dissected at blastula stage 8.5 and cultured for 3.5 hr. Luciferase activities were determined in duplicate for at least three independent experiments. Values shown are means +/- standard deviation.

Table 6.1 (below) summarises the results of 7 independent experiments of co-injections of the -300gsc.luc reporter construct and the mutated versions described above, with the indicated RNAs. Numbers 1-7 correspond to independent experiments. In each experiment, values were normalised to the luciferase activity of the respective reporter construct injected alone.

Table 6.1. Analysis of point mutations in the *goosecoid* promoter. Results from 7 independent experiments.

Reporter	RNA*	1	2	3	4	5	6	7	mean	sd
	None	1.0	1.0	1.0	1.0		1.0		1.0	0.0
-300gsc.luc	Activin (B)	16.0	15.3	16.0	16.7		11.3		15.1	2.2
	Activin+Xom (A)	12.7	8.4	8.1	4.9		4.2		7.7	3.4
	None		1.0			1.0		1.0	1.0	0.0
-300gsc$^{-145/-136}$.luc	Activin (B)		7.8			14.4		14.9	12.4	4.0
	Activin+Xom (A)		5.3			5.1		6.4	5.6	0.7
	None	1.0	1.0	1.0	1.0		1.0		1.0	0.0
-300gsc$^{-201/2}$.luc	Activin (B)	21.9	5.9	3.6	14.4		6.9		10.5	7.5
	Activin+Xom (A)	20.2	4.5	2.2	10.5		4.3		8.3	7.3

* The following RNA doses were used: *Activin* (50 pg) and *Xom* (0.5 ng). sd, standard deviation. (A) and (B) indicate lanes of values used in the calculations shown in Table 6.2.

The experiments summarised in Table 6.1 show that mutation of the Xom binding site contained within the DE (generating the construct -300gsc.luc$^{-201/2}$) interferes with the ability of Xom to repress activin-induced luciferase activity whereas the mutation within the PE has no effect. In particular, injection of 0.5 ng of *Xom* RNA was shown to decrease approximately by half the activin-induced luciferase activity of -300gsc.luc (Table 6.1 and Fig. 6.2). However, if -300gsc.luc$^{-201/2}$ was used, the repression effect of Xom was minor, while Xom repressed -300gsc.luc$^{-145/136}$ in a manner similar to that observed with –300gsc.luc.

Since levels of activation varied somewhat in these experiments, a t-test was

performed to determine whether the repressing effects of *Xom* were significantly smaller using the mutated (-300gsc.luc$^{-201/2}$) than using the wild type (-300gsc.luc) reporter construct. To that end, the value A/B was calculated for each experiment and reporter construct, in which A and B correspond to normalised luciferase activity values obtained by injections of *activin* and *Xom* (A) or *activin* alone (B), as indicated in Table 6.1. Table 6.2 (below) shows these calculations.

Table 6.2: Values for the t-test.

Reporter	Equation	1	2	3	4	5	6	7	mean	sd
-300gsc	A/B	0.794	0.549	0.506	0.293	-	0.372	-	0.503	0.192
-300gsc$^{-201/2}$	A/B	0.922	0.763	0.611	0.729	-	0.623	-	0.730	0.126
-300gsc$^{-145/-136}$	A/B	-	0.679	-	-	0.354	-	0.430	0.488	0.170

sd, standard deviation; A and B refer to lanes of values indicated in Table 6.1.

A t-test was performed comparing the means of the first and second rows of values in Table 6.2 which confirmed that mutation in nucleotides –201 and –202 significantly interferes ($p<0.05$) with the ability of Xom to repress activin-induced activation of the *gsc* promoter. Due to insufficient numbers of experiments, a t-test comparing the first and third rows was not performed. However, the results indicate that mutation of the putative binding site in the PE (generating -300gsc.luc$^{-145/136}$) had little effect on repression of luciferase activity by Xom, suggesting that this site plays no role in Xom-mediated repression *in vivo*.

DISCUSSION

In this chapter I analysed whether Xom has a direct effect in regulating *gsc* expression by analysing the *gsc* promoter. Reporter studies in animal caps using a construct containing 300 nucleotides upstream of the start site of the *gsc* gene fused to a luciferase reporter showed that Xom is able to repress the activin-stimulated transcription of *gsc* (Fig. 6.2). Two mutated -300gsc.luc reporter constructs were then generated bearing point mutations in potential Xom binding sites within the DE or the

PE of the *gsc* promoter. Preliminary experiments demonstrated that these constructs both show a 3 or 6-fold higher basal level of luciferase activity in animal caps when compared with the wild type reporter construct (Fig. 6.3 B), suggesting that the mutations prevent the interaction of endogenous repressors. Experiments summarised in Table 6.1 show that mutation of the Xom binding site contained within the DE (generating the construct -300gsc.luc$^{-201/2}$) interferes significantly with the ability of Xom to repress activin-induced luciferase activity. Mutation of the putative binding site in the PE (generating -300gsc.luc$^{-145/136}$), however, has little effect, suggesting that this site plays no role in Xom-mediated repression *in vivo*.

Xom represses *goosecoid* transcription

During development, *gsc* expression is very precisely controlled, both spatially and temporally. The *gsc* promoter presents unique features, since the signalling pathways controlling different developmental fates converge on this promoter to control the expression of a single gene, itself being a major player as a mediator of organiser function in the embryo. Current models postulate that dorsal mesoderm specification and the establishment of the *Xenopus* organiser require synergy between the TGF-β signalling pathway involved in dorsal mesoderm specification and the Wnt/β-catenin signalling pathway, and indeed the *gsc* promoter is a paradigm of this possibility. In addition, Bmps could play a role in preventing *gsc* expression in the ventral region of the embryo (Watabe et al., 1995). This aspect is of particular interest in this study since *Xom* is an immediate early-response to Bmp-4 (Ladher et al., 1996).

Few studies have addressed the question of how Bmp signalling controls the expression of *gsc*, but evidence argues against the existence of Bmp-specific elements in the *gsc* promoter. Results from experiments using a constitutively active type I Bmp receptor, which transduces Bmp-2/4 signals in a ligand-independent fashion (ΔE-CABR), suggest an intracellular bi-directional interference of Bmp 2/4 and Activin/BVg1 signalling on the regulation of transcription from the *gsc* promoter (Candia et al., 1997). In particular, initial characterisation of the activin/BVg1 response element (DE) revealed that 20 minutes after animal caps are treated with activin a specific binding complex (ABC), containing Smad2 and Smad4 proteins, assembles on

this element, which can be abolished by co-injection of activin and ΔE-CABR (Candia et al., 1997). Ultimately, the formation of this complex would depend on the availability of Smad4, which was hypothesised by the authors to be present in the embryo at limiting concentrations, and which would be regulated by the type of signalling operating in the cell.

It is possible that Xom represses *gsc* expression by displacing the ABC protein complex which forms on the DE of the *gsc* promoter upon stimulation with activin (Candia et al., 1997). However, this interaction would have to be transient because no protein complex bound to the DE was detected after co-injection of activin and the constitutively active Bmp receptor (Candia et al., 1997). It is unlikely however that the function of Xom on the DE is solely explained by a passive mechanism by which Xom competes for binding DNA, since Xom was shown to have repressing activity when fused to a heterologous DNA binding domain (Fig. 4.1, Chapter 4).

Recently, it has been shown that Bmp signalling can also interfere with Wnt signalling-mediated activation of *gsc* on the PE (Laurent and Cho, 1999). However, Bmp signalling does not interfere with the induction of *twin* (*Xtwn*) and *siamois* (*Xsia*) type homeobox-containing genes (Laurent and Cho, 1999), which activate the *gsc* promoter through the PE (Fan and Sokol, 1997; Kessler, 1997; Laurent et al., 1997; Laurent and Cho, 1999). This suggests a later role for Bmp signalling, possibly postzygotically during gastrula stages, to inhibit the maintenance of *gsc* expression (Laurent and Cho, 1999). The mechanism by which Bmp controls *gsc* expression through the PE is unknown at present and unlikely to involve Xom, since mutation of a Xom potential site on the PE does not affect the ability of Xom to repress activin-stimulated activation of the *gsc* promoter (Table 6.1).

Evidence that *gsc* can be expressed throughout the marginal and vegetal region of the *Xenopus* embryo, although it is normally prevented from doing so, was provided by injection of a reporter construct containing 6 copies of the DE alone (Watabe et al., 1995). In contrast, injection of a reporter construct containing the 300 nucleotide region, which contains the DE and the PE, is strongly induced only in dorsal blastomeres (Watabe et al., 1995). This suggests that the repression of *gsc* expression ventrally is

mediated by sequences that lie outside the DE although within the 300 nucleotide region of the promoter.

I have shown that the effect of Xom on *gsc* expression may be direct and occurring through the potential Xom binding sequence, GCAATTAG (complementary strand CTAATTGC) in the DE. With the exception of the potential Xom binding site on the PE of the *gsc* promoter, which was shown not to be involved in Xom-mediated repression of *gsc*, no other potential Xom sites were found within the –300 base pairs of the *gsc* promoter. Therefore, it is unlikely that Xom is one of the putative factors binding to sequences outside the DE but within the –300 base pairs *gsc* promoter fragment involved in down-regulating *gsc* expression laterally and ventrally (Watabe et al., 1995).

In this study, I have shown that Xom has a role in repression of *gsc*. However, Xom alone is unlikely to be able to account for the complete absence of *gsc* transcripts in the lateral and ventral region of the *Xenopus* gastrulating embryo. Consistent with this idea is the fact that *Xom* RNA injections do not completely abolish activin-induced luciferase activity of –300gsc.luc in reporter assays (Table 6.1), nor abolish endogenous expression of *gsc* in the embryo (Fig. 5.1 J and K), nor completely inhibit activin-induced endogenous *gsc* expression in whole embryos and animal caps (Fig. 5.2). Furthermore, the increase in basal reporter activity observed for the reporter construct bearing a mutation in the PE (-300gsc.luc$^{-145/136}$) is unlikely to involve Xom, raising the possibility that other homeodomain-containing proteins are also involved in *gsc* repression.

Activation of *goosecoid* transcription

Studies with the mouse *gsc* promoter, which contains two regions of high homology with the *Xenopus gsc* promoter corresponding to a DE and a PE (Watabe et al., 1995), have led to the identification of a TGFβ/Activin Response element (TARE) immediately downstream of the mouse DE and including part of the PE (Labbe et al., 1998). The TARE contains a binding site for a novel winged-helix/forkhead transcription factor, FAST-2, and two G-C rich Smad4 binding regions. These observations have led to a model in which activation of the *gsc* promoter and formation

of a TRF (TGFβ/activin Response Factor) on the TARE requires cooperativity between the FAST-2 binding site and a Smad binding site. FAST 2 recruits complexes of Smad 2/4 to the *gsc* promoter through its interaction with Smad 2 and this promotes Smad 4 binding to an adjacent site thus stabilising formation of a higher-order complex and enhancing ligand-dependent activation of the *gsc* promoter (Labbe et al., 1998).

In *Xenopus*, it possible that a *Xenopus* FAST-like protein binds a FAST-1/2 site in the *gsc* promoter and acts to recruit Smad 2/4 complexes to DNA, in the same way as in the mouse *gsc* promoter. Consistent with this idea is the fact that two FAST-type binding sites (one is degenerate) exist in the *gsc* promoter and a protein related to mouse FAST-2, FAST-1, has been identified and shown to bind the activin responsive element in the *Xenopus Mix.2* promoter (Chen et al., 1997). Although mouse Smad 4 binding sites are poorly conserved in *Xenopus*, there is a CAGA core sequence present in the *Xenopus* DE (Labbe et al., 1998) which was recently shown to bind Smad 4 (Dennler et al., 1998). However, the FAST-1/2 binding site in the *Xenopus gsc* promoter is localised in the PE and this is inconsistent with the idea that TGF-β/Activin responsiveness of *gsc* promoter is exclusively mediated by the DE (Watabe et al., 1995). Alternatively, a FAST-like factor could bind a degenerate FAST-type binding site adjacent 3' to the DE.

Xom is a repressor of *gsc* likely to act through an active repression mechanism, which may include inhibition of activators of *gsc* transcription. In this respect, an as-yet unknown *Xenopus* FAST-like factor and Smad2 and 4, may be candidates for interaction with Xom.

Other proteins involved in repressing *gsc* transcription

Other proteins have shown to repress *gsc* transcription in the *Xenopus* embryo. *XlPOU2* is a homeobox-containing gene able to suppress organizer genes, such as *gsc*, *noggin* or *chordin* when over-expressed in the embryo (Witta and Sato, 1997). *Gsc* is one potential target of XlPOU2 since XlPOU2 can bind specifically to the DE of the *gsc* promoter and it is able to repress activin-induced activity from this promoter in reporter studies in the *Xenopus* embryo (Witta and Sato, 1997). However, *XlPOU2* is expressed within the organizer itself at the early gastrula stage, making it an unlikely partner of

Xom in the repression of *gsc* expression. XlPOU2 may be part of a negative regulation mechanism operating within the organizer itself to assure that *gsc* is expressed in adequate levels (Witta and Sato, 1997).

Gsc itself is involved in a feedback regulatory mechanism to maintain *gsc* levels or to repress *gsc* expression at later stages (Danilov et al., 1998). This auto-regulatory effect is mediated through a paired type homeodomain binding site on the PE of the mouse and human *gsc* promoters, partially conserved in *Xenopus* (Danilov et al., 1998).

CHAPTER 7

General Discussion

The work presented in this thesis attempts to contribute to the understanding of the specification of ventral/dorsal tissues in the frog *Xenopus laevis* by the study of the homeobox-containing gene *Xom*.

Bmps instructs cells to become ventral

The notion that vertebrate embryos must be specified according to dorsal-ventral and anterior-posterior axes comes from direct observation of their ventral-dorsal and anterior-posterior asymmetries in the morphology of the tadpole or adult. It was the discovery of the Spemann organiser that first showed that a region of the embryo, localised dorsally, was able to develop into dorsal type of tissues and to influence the fate of other parts of the embryo. The inductive properties of the organizer led to the idea that dorsal fates were dominant over ventral. This notion lasted for more than half a century and was supported by initial experiments unveiling the molecular players of dorsal-ventral axis determination in *Xenopus*. More recently, experiments with dissociated embryos and the discovery of Bone morphogenetic proteins (Bmps) as a ventralising agent in *Xenopus* embryos (Dale et al., 1992; Grunz and Tacke, 1989; Jones et al., 1992; Klein and Melton, 1994) challenged this idea suggesting that dorsal cell fate specification is a default state, under control of permissive signals rather than instructive ones. In molecular terms, this means that dorsal cell fate specification is dependent upon signals that are not mediated through a receptor and that probably do not involve the activation of a signalling cascade (Hemmati-Brivanlou, 1998).

Bmp response genes mediate different subsets of Bmp functions

A simple way to understand how ventral specification takes place in the embryo is to assume two distinct functions for the Bmp signalling pathway. First, dorsal gene expression must be restricted to the organiser region. Second, ventral gene expression should be stimulated to allow the specification of distinct lineages that originate the range of tissues generated ventrally and laterally in the embryo, such as for example blood, smooth muscle and pronephros. To accomplish these functions Bmp activates

several response genes, each of which execute a particular subset of Bmp functions in the embryo. Therefore, Bmp-4 induces a large number of response genes, including homeobox and GATA-binding factors (see Chapter 1).

Recently, it was shown that the homeobox-gene *Xvent-1* (*PV.1*) acts in the patterning of ventral mesoderm by regulating Bmp-4 stimulation of erythropoiesis (Xu et al., 1999). Patterning of the mesoderm to form blood involves the specification of ventral blood islands (VBI) during gastrulation, which can be detected by the expression of *globin* (Dale and Slack, 1987). Bmp-4 stimulation of VBI formation occurs by up-regulation of *GATA-2*, a GATA-binding zinc finger transcription factor expressed ventral and laterally in ectoderm and mesoderm during gastrula stages (Maeno et al., 1996; Walmsley et al., 1994; Zhang and Evans, 1996). *Xvent-1*, which acts downstream of *Bmp-4*, inhibits *GATA-2* and *globin* expression in ventral marginal explants thus inhibiting erythropoiesis (Xu et al., 1999). It is likely that to accomplish this function *Xvent-1* responds, in addition to Bmp-4, to FGF since FGF inhibits erythropoiesis, stimulates formation of smooth muscle and up-regulates Bmp-mediated expression of *Xvent-1* in animal caps (Xu et al., 1999).

The immediate-early Bmp-4 response gene *Xmsx-1* may have a similar role to *Xvent-1* (*PV.1*) in erythropoiesis because *Xmsx-1* was shown to repress *globin* expression (Maeda et al., 1997). However, *Xom* is probably not involved in erythropoiesis because *Xom* does not affect *globin* expression and by contrast, over-expression of *GATA-2* or a GATA-activity interfering construct did not affect *Xom* (*Xvent-2*) expression (Ladher et al., 1996; Sykes et al., 1998).

In contrast, Xom is likely to have ventralising activity by restricting the expression of dorsal genes, such as *gsc*, to dorsal regions of the gastrula embryo. Similarly, *Xvent-1* acts directly in transcriptional repression of another organiser expressed gene, *XFKH1* (Friedle et al., 1998). It would be interesting to investigate how widespread is the repression of dorsally expressed genes and whether Xom and Xvent-1 still work as repressors in other dorsal gene promoters.

Xom (and Xvent-1) act downstream of Bmp-2/4

In *Xenopus*, ventralisation has been attributed to the action of Bmps (see Chapter 1). *Xom* is an immediate-early response to Bmp-2/4 since its expression is induced by Bmp-2/4 in dissociated embryos in the presence of cycloheximide (Ladher et al., 1996; Rastegar et al., 1999). On the other hand, *Xvent-1* is not activated directly by Bmp signalling (Rastegar et al., 1999).

In reporter studies, *Xom* (*Xvent-2B*) was shown to up-regulate both itself and *Xvent-1* (*Xvent-1B*) (Rastegar et al., 1999). This suggested that Xom could act upstream of Xvent-1, regulating its expression, and also to auto-regulate its own expression in the embryo. However, cycloheximide experiments revealed that *Xom* by itself is not sufficient to activate transcription of *Xvent-1* and additional factors synthesised after the midblastula transition are required (Rastegar et al., 1999). Moreover, the auto-activation of *Xom* may be an indirect consequence of up-regulation of *Bmp-4* since co-injection with a truncated Bmp receptor blocks the autoregulatory effect of Xom on its own promoter (Rastegar et al., 1999).

Xom mediates Bmp function by repressing *goosecoid*

In this thesis, I have shown that one homeobox gene of the Xvent family, *Xom*, acts directly on the *gsc* promoter to downregulate its expression in the embryo. As Xom acts downstream of Bmp signalling (see above), Bmp antagonists such as chordin and noggin should be able to down-regulate *Xom* and up-regulate *gsc* expression (Piccolo et al., 1996; Zimmerman et al., 1996). Indeed, over-expression of *noggin* or of a dominant-negative Bmp receptor were shown to cause down-regulation of *Xom* expression in whole embryos (Dosch et al., 1997; Ladher et al., 1996; Onichtchouk et al., 1996). In addition, *noggin* is able to counteract the *Bmp-4*-mediated down-regulation of *gsc* in dorsal mesodermal explants; conversely, *Bmp-4* is able to counteract *noggin*-mediated induction of *gsc* expression in ventral mesodermal explants (Dosch et al., 1997). In this respect, Chordin is unlikely to act endogenously to inhibit *gsc* expression because *chordin* starts to be expressed in the Spemann's organizer after the onset of *gsc* expression (Sasai et al., 1994).

Although over-expression of *Bmp-4* clearly abolishes *gsc* expression in the early embryo, injection of a dominant-negative version of the Bmp receptor into the embryos does not induce, or induces only slightly, ectopic *gsc* expression (Gawantka et al., 1995; Graff et al., 1994; Schmidt et al., 1995; Suzuki et al., 1994). This observation suggests that *gsc* may also be under transcriptional repression by factors not induced by the Bmp pathway. A possible candidate is the homeobox-containing gene *Xcad-2*. *Xcad-2* is able to ventralise *Xenopus* embryos and to repress *gsc* expression in the presence of a truncated Bmp receptor (Pillemer et al., 1998). It would be interesting to analyse in more detail the function of this gene in an effort to determine whether it works as a direct repressor of *gsc*, as *Xom* does, and whether it works as a partner of Xom in the repression of *gsc*. Interestingly, injections of synthetic RNA encoding the *Xenopus* truncated Bmp receptor (tBR) into zebrafish embryos led to the formation of ectopic domains of *gsc* expression (Neave et al., 1997).

Are there any other Xom targets?

One possible target for Xom function is *chordin* (Sasai et al., 1994). Evidence to support this comes from the observation that *Xom* (*Vox*) counteracts the up-regulation of *chordin* due to injection of dominant-negative Bmp receptor (Melby et al., 1999). Furthermore, an inducible Xom interfering construct induces *chordin* expression even in the presence of a protein synthesis inhibitor (cycloheximide) (Melby et al., 1999). Interestingly, *gsc* was shown to be a strong activator of *chordin* expression (Sasai et al., 1994) although this effect is possibly not direct since *gsc* acts as a repressor of transcription (Danilov et al., 1998). As *Xvent-2* (*Xom*) is downregulated by *gsc* (Ferreiro et al., 1998) it is likely that *gsc* represses *Xom*, which would then repress *chordin* at early gastrula *Xenopus* embryos (Melby et al., 1999).

References

Aberle, H., Bauer, A., Stappert, J., Kispert, A., and Kemler, R. (1997). beta-catenin is a target for the ubiquitin-proteasome pathway. Embo J *16*, 3797-804.

Akimaru, H., and Saigo, K. (1991). DNA binding activity of the BarH1 homeodomain of Drosophila. Nucleic Acids Symp Ser, 29-30.

Albano, R. M., Groome, N., and Smith, J. C. (1993). Activins are expressed in preimplantation mouse embryos and in ES and EC cells and are regulated on their differentiation. Development *117*, 711-723.

Amaya, E., Musci, T. J., and Kirschner, M. W. (1991). Expression of a dominant negative mutant of the FGF receptor disrupts mesoderm formation in Xenopus embryos. Cell *66*, 257-70.

Amaya, E., Stein, P. A., Musci, T. J., and Kirschner, M. W. (1993). FGF signalling in the early specification of mesoderm in Xenopus. Development *118*, 477-87.

Ang, S. L., and Rossant, J. (1994). HNF-3 beta is essential for node and notochord formation in mouse development. Cell *78*, 561-74.

Armes, N. A., Neal, K. A., and Smith, J. C. (1999). A short loop on the ALK-2 and ALK-4 activin receptors regulates signaling specificity but cannot account for all their effects on early Xenopus development. J Biol Chem *274*, 7929-35.

Asashima, M., Nakano, H., Shimada, K., Kinoshita, K., Ishii, K., Shibai, H., and Ueno, N. (1990). Mesodermal induction in early amphibian embryos by activin A (erythroid differentiation factor). Roux's Arch. Dev. Biol. *198*, 330-5.

Attisano, L., Wrana, J. L., Montalvo, E., and Massague, J. (1996). Activation of signalling by the activin receptor complex. Mol Cell Biol *16*, 1066-73.

Ault, K. T., Dirksen, M. L., and Jamrich, M. (1996). A novel homeobox gene PV.1 mediates induction of ventral mesoderm in Xenopus embryos. Proc Natl Acad Sci U S A *93*, 6415-20 .

Ault, K. T., Xu, R. H., Kung, H. F., and Jamrich, M. (1997). The homeobox gene PV.1 mediates specification of the prospective neural ectoderm in Xenopus embryos. Dev Biol *192*, 162-71.

Bauer, D. V., Huang, S., and Moody, S. A. (1994). The cleavage stage origin of Spemann's Organizer: analysis of the movements of blastomere clones before and during gastrulation in Xenopus. Development *120*, 1179-89.

Bayley, T. L. a. E., C. (1994). Fitting a mixture model by expectation maximization to discover motifs in biopolymers. In Second International Conference on Intelligent Systems for Molecular Biology (Menlo Park, California, USA: AAAI Press), pp. 28-36.

Beddington, R. S. (1994). Induction of a second neural axis by the mouse node. Development *120*, 613-20.

Beddington, R. S., and Robertson, E. J. (1998). Anterior patterning in mouse. Trends Genet *14*, 277-84.

Beddington, R. S., and Robertson, E. J. (1999). Axis development and early asymmetry in mammals. Cell *96*, 195-209.

Behrens, J., von Kries, J. P., Kuhl, M., Bruhn, L., Wedlich, D., Grosschedl, R., and Birchmeier, W. (1996). Functional interaction of beta-catenin with the transcription factor LEF-1. Nature *382*, 638-42.

Biggin, M. D., and McGinnis, W. (1997). Regulation of segmentation and segmental identity by Drosophila homeoproteins: the role of DNA binding in functional activity and specificity. Development *124*, 4425-33.

Blader, P., Rastegar, S., Fischer, N., and Strahle, U. (1997). Cleavage of the BMP-4 antagonist chordin by zebrafish tolloid. Science *278*, 1937-40.

Blum, M., De Robertis, E. M., Kojis, T., Heinzmann, C., Klisak, I., Geissert, D., and Sparkes, R. S. (1994). Molecular cloning of the human homeobox gene goosecoid (GSC) and mapping of the gene to human chromosome 14q32.1. Genomics *21*, 388-93.

Blum, M., Gaunt, S. J., Cho, K. W. Y., Steinbeisser, H., Blumberg, B., Bittner, D., and De Robertis, E. M. (1992). Gastrulation in the mouse: the role of the homeobox gene goosecoid. Cell *69*, 1097-1106.

Blumberg, B., Wright, C. V. E., De Robertis, E. M., and Cho, K. W. Y. (1991). Organizer-specific homeobox genes in Xenopus laevis embryos. Science *253*, 194-196.

Boterenbrood, E. C., and Nieuwkoop, P. D. (1973). Wilhelm Roux' Arch EntwMech Org. *173*, 319-332.

Bouwmeester, T., Kim, S., Sasai, Y., Lu, B., and De Robertis, E. M. (1996). Cerberus is a head-inducing secreted factor expressed in the anterior endoderm of Spemann's organizer. Nature *382*, 595-601.

Brannon, M., Gomperts, M., Sumoy, L., Moon, R. T., and Kimelman, D. (1997). A beta-catenin/XTcf-3 complex binds to the siamois promoter to regulate dorsal axis specification in Xenopus. Genes Dev *11*, 2359-70.

Brannon, M., and Kimelman, D. (1996). Activation of Siamois by the Wnt pathway. Dev Biol *180*, 344-7.

Cadigan, K. M., and Nusse, R. (1997). Wnt signaling: a common theme in animal development. Genes Dev *11*, 3286-305.

Candia, A. F., Watabe, T., Hawley, S. H., Onichtchouk, D., Zhang, Y., Derynck, R., Niehrs, C., and Cho, K. W. (1997). Cellular interpretation of multiple TGF-beta signals: intracellular antagonism between activin/BVg1 and BMP-2/4 signaling mediated by Smads. Development *124*, 4467-80.

Carnac, G., Kodjabachian, L., Gurdon, J. B., and Lemaire, P. (1996). The homeobox gene Siamois is a target of the Wnt dorsalisation pathway and triggers organiser activity in the absence of mesoderm. Development *122*, 3055-65.

Casellas, R., and Brivanlou, A. H. (1998). Xenopus Smad7 inhibits both the activin and BMP pathways and acts as a neural inducer. Dev Biol *198*, 1-12.

Chang, C., Wilson, P. A., Mathews, L. S., and Hemmati-Brivanlou, A. (1997). A Xenopus type I activin receptor mediates mesodermal but not neural specification during embryogenesis. Development *124*, 827-37.

Chen, X., Rubock, M. J., and Whitman, M. (1996). A transcriptional partner for MAD proteins in TGF-beta signalling [published erratum appears in Nature 1996 Dec 19-26;384(6610):648]. Nature *383*, 691-6.

Chen, X., Weisberg, E., Fridmacher, V., Watanabe, M., Naco, G., and Whitman, M. (1997). Smad4 and FAST-1 in the assembly of activin-responsive factor. Nature *389*, 85-9.

Chen, Y., and Solursh, M. (1995). Mirror-image duplication of the primary axis and heart in Xenopus embryos by the overexpression of Msx-1 gene. J Exp Zool *273*, 170-4.

Cho, K. W., and Blitz, I. L. (1998). BMPs, Smads and metalloproteases: extracellular

and intracellular modes of negative regulation. Curr Opin Genet Dev *8*, 443-9.

Cho, K. W., Blumberg, B., Steinbeisser, H., and De Robertis, E. M. (1991). Molecular nature of Spemann's organizer: the role of the Xenopus homeobox gene goosecoid. Cell *67*, 1111-20.

Chomczynski, P., and Sacchi, N. (1987). Single-step method of RNA isolation by acid guanidinium thiocyanate- phenol-chloroform extraction. Anal Biochem *162*, 156-9.

Christian, J. L., McMahon, J. A., McMahon, A. P., and Moon, R. T. (1991). Xwnt-8, a Xenopus Wnt-1/int-1-related gene responsive to mesoderm- inducing growth factors, may play a role in ventral mesodermal patterning during embryogenesis. Development *111*, 1045-55.

Christian, J. L., and Moon, R. T. (1993). Interactions between Xwnt-8 and Spemann organizer signaling pathways generate dorsoventral pattern in the embryonic mesoderm of Xenopus. Genes Dev *7*, 13-28.

Clements, J. H., Fettes, P., Knöchel, S., Lef, J., and Knöchel, W. (1995). Bone morphogenetic protein 2 in the early development of *Xenopus laevis*. Mech. Dev. *52*, 357-370.

Connors, S. A., Trout, J., Ekker, M., and Mullins, M. C. (1999). The role of tolloid/mini fin in dorsoventral pattern formation of the zebrafish embryo. Development *126*, 3119-3130.

Cooke, J., and Smith, J. C. (1987). The midblastula cell cycle transition and the character of mesoderm in u.v.-induced nonaxial Xenopus development. Development *99*, 197-210.

Crease, D. J., Dyson, S., and Gurdon, J. B. (1998). Cooperation between the activin and Wnt pathways in the spatial control of organizer gene expression. Proc Natl Acad Sci U S A *95*, 4398-403.

Cui, Y., Brown, J. D., Moon, R. T., and Christian, J. L. (1995). Xwnt-8b: a maternally expressed Xenopus Wnt gene with a potential role in establishing the dorsoventral axis. Development *121*, 2177-86.

Dale, L., Howes, G., Price, B. M., and Smith, J. C. (1992). Bone morphogenetic protein 4: a ventralizing factor in early Xenopus development. Development *115*, 573-85.

Dale, L., Matthews, G., and Colman, A. (1993). Secretion and mesoderm-inducing activity of the TGF-beta-related domain of Xenopus Vg1. Embo J *12*, 4471-80.

Dale, L., and Slack, J. M. (1987). Fate map for the 32-cell stage of Xenopus laevis.

Development *99*, 527-51.

Dale, L., and Slack, J. M. (1987). Regional specification within the mesoderm of early embryos of Xenopus laevis. Development *100*, 279-95.

Danilov, V., Blum, M., Schweickert, A., Campione, M., and Steinbeisser, H. (1998). Negative autoregulation of the organizer-specific homeobox gene goosecoid. J Biol Chem *273*, 627-35.

Darras, S., Marikawa, Y., Elinson, R. P., and Lemaire, P. (1997). Animal and vegetal pole cells of early Xenopus embryos respond differently to maternal dorsal determinants: implications for the patterning of the organiser. Development *124*, 4275-86.

Dear, T. N., Sanchez-Garcia, I., and Rabbitts, T. H. (1993). The Hox 11 gene encodes a DNA-binding nuclear transcription factor belonging to a distinct family of homeobox genes. Proc. Natn. Acad. Sci. USA *90*, 4431-4435.

Deardorff, M. A., Tan, C., Conrad, L. J., and Klein, P. S. (1998). Frizzled-8 is expressed in the Spemann organizer and plays a role in early morphogenesis. Development *125*, 2687-700.

DeMarais, A. A., and Moon, R. T. (1992). The armadillo homologs beta-catenin and plakoglobin are differentially expressed during early development of Xenopus laevis. Dev Biol *153*, 337-46.

Dennler, S., Itoh, S., Vivien, D., ten Dijke, P., Huet, S., and Gauthier, J. M. (1998). Direct binding of Smad3 and Smad4 to critical TGF beta-inducible elements in the promoter of human plasminogen activator inhibitor-type 1 gene. Embo J *17*, 3091-100.

DeRobertis, E. M., and Sasai, Y. (1996). A common plan for dorsoventral patterning in Bilateria. Nature *380*, 37-40.

Dirksen, M. L., and Jamrich, M. (1992). A novel, activin-inducible, blastopore lip-specific gene of Xenopus laevis contains a fork head DNA-binding domain. Genes Dev *6*, 599-608.

Dohrmann, C. E., Hemmati-Brivanlou, A., Thomsen, G. H., Fields, A., Woolf, T. M., and Melton, D. A. (1993). Expression of activin mRNA during early development in Xenopus laevis. Dev Biol *157*, 474-83.

Dominguez, I., Itoh, K., and Sokol, S. Y. (1995). Role of glycogen synthase kinase 3 beta as a negative regulator of dorsoventral axis formation in Xenopus embryos. Proc Natl Acad

Sci U S A *92*, 8498-502.

Dosch, R., Gawantka, V., Delius, H., Blumenstock, C., and Niehrs, C. (1997). Bmp-4 acts as a morphogen in dorsoventral mesoderm patterning in Xenopus. Development *124*, 2325-34.

Dyson, S., and Gurdon, J. B. (1997). Activin signalling has a necessary function in Xenopus early development. Curr Biol *7*, 81-4.

Elinson, R. P., and Pasceri, P. (1989). Two UV-sensitive targets in dorsoanterior specification of frog embryos. Development *106*, 511-8.

Emami, K. H., and Carey, M. (1992). A synergistic increase in potency of a multimerized VP16 transcriptional activation domain. Embo J *11*, 5005-12.

Fagotto, F., Guger, K., and Gumbiner, B. M. (1997). Induction of the primary dorsalizing center in Xenopus by the Wnt/GSK/beta-catenin signaling pathway, but not by Vg1, Activin or Noggin. Development *124*, 453-60.

Fagotto, F., and Gumbiner, B. M. (1994). Beta-catenin localization during Xenopus embryogenesis: accumulation at tissue and somite boundaries. Development *120*, 3667-79.

Fainsod, A., Deissler, K., Yelin, R., Marom, K., Epstein, M., Pillemer, G., Steinbeisser, H., and Blum, M. (1997). The dorsalizing and neural inducing gene follistatin is an antagonist of BMP-4. Mech Dev *63*, 39-50.

Fainsod, A., Steinbeisser, H., and De Robertis, E. M. (1994). On the function of BMP-4 in patterning the marginal zone of the Xenopus embryo. Embo J *13*, 5015-25.

Fan, M. J., and Sokol, S. Y. (1997). A role for Siamois in Spemann organizer formation. Development *124*, 2581-9.

Feng, X. H., and Derynck, R. (1997). A kinase subdomain of transforming growth factor-beta (TGF-beta) type I receptor determines the TGF-beta intracellular signaling specificity. Embo J *16*, 3912-23.

Ferguson, E. L., and Anderson, K. V. (1992). Decapentaplegic acts as a morphogen to organize dorsal-ventral pattern in the Drosophila embryo. Cell *71*, 451-61.

Ferreiro, B., Artinger, M., Cho, K., and Niehrs, C. (1998). Antimorphic goosecoids. Development *125*, 1347-59.

Francois, V., and Bier, E. (1995). Xenopus chordin and Drosophila short gastrulation

genes encode homologous proteins functioning in dorsal-ventral axis formation [letter]. Cell *80*, 19-20.

Francois, V., Solloway, M., O'Neill, J. W., Emery, J., and Bier, E. (1994). Dorsal-ventral patterning of the Drosophila embryo depends on a putative negative growth factor encoded by the short gastrulation gene. Genes Dev *8*, 2602-16.

Friedle, H., Rastegar, S., Paul, H., Kaufmann, E., and Knochel, W. (1998). Xvent-1 mediates BMP-4-induced suppression of the dorsal-lip-specific early response gene XFD-1' in Xenopus embryos. Embo J *17*, 2298-307.

Frisch, A., and Wright, C. V. (1998). XBMPRII, a novel Xenopus type II receptor mediating BMP signaling in embryonic tissues. Development *125*, 431-42.

Fujisue, M., Kobayakawa, Y., and Yamana, K. (1993). Occurence of dorsal axis-inducing activity around the vegetal pole of an uncleaved Xenopus egg and displacement to the equatorial region by cortival rotation. Development *118*, 163-178.

Fukui, A., Nakamura, T., Uchiyama, H., Sugino, K., Sugino, H., and Asashima, M. (1994). Identification of activins A, AB, and B and follistatin proteins in Xenopus embryos. Dev Biol *163*, 279-81.

Gallagher, B. C., Hainski, A. M., and Moody, S. A. (1991). Autonomous differentiation of dorsal axial structures from an animal cap cleavage stage blastomere in Xenopus. Development *112*, 1103-14.

Gamer, L. W., and Wright, C. V. (1995). Autonomous endodermal determination in Xenopus: regulation of expression of the pancreatic gene XlHbox 8. Dev Biol *171*, 240-51.

Gawantka, V., Delius, H., Hirschfeld, K., Blumenstock, C., and Niehrs, C. (1995). Antagonizing the Spemann organizer: role of the homeobox gene Xvent-1. Embo J *14*, 6268-79.

Gehring, W. J., Affolter, M., and Burglin, T. (1994). Homeodomain proteins. Annu Rev Biochem *63*, 487-526.

Gehring, W. J., Qian, Y. Q., Billeter, M., Furukubo-Tokunaga, K., Schier, A. F., Resendez-Perez, D., Affolter, M., Otting, G., and Wuthrich, K. (1994). Homeodomain-DNA recognition. Cell *78*, 211-23.

Gerhart, J., Danilchik, M., Doniach, T., Roberts, S., Rowning, B., and Stewart, R. (1989). Cortical rotation of the Xenopus egg: consequences for the anteroposterior pattern of

embryonic dorsal development. Development *107 Suppl*, 37-51.

Gilbert, S. F. (1994). Developmetal Biology, 5th edition Edition, S. F. Gilbert, ed.: Sinauer Associates, Inc. Publishers, Sundeland, Massachusetts).

Gimlich, R. L. (1986). Acquisition of developmental autonomy in the equatorial region of the Xenopus embryo. Dev Biol *115*, 340-52.

Gimlich, R. L., and Gerhart, J. C. (1984). Early cellular interactions promote embryonic axis formation in Xenopus laevis. Dev Biol *104*, 117-30.

Glinka, A., Wu, W., Delius, H., Monaghan, A. P., Blumenstock, C., and Niehrs, C. (1998). Dickkopf-1 is a member of a new family of secreted proteins and functions in head induction. Nature *391*, 357-62.

Glinka, A., Wu, W., Onichtchouk, D., Blumenstock, C., and Niehrs, C. (1997). Head induction by simultaneous repression of Bmp and Wnt signalling in Xenopus. Nature *389*, 517-9.

Godsave, S. F., and Slack, J. M. (1989). Clonal analysis of mesoderm induction in Xenopus laevis. Dev Biol *134*, 486-90.

Goodman, S. A., Albano, R., Wardle, F. C., Matthews, G., Tannahill, D., and Dale, L. (1998). BMP1-related metalloproteinases promote the development of ventral mesoderm in early Xenopus embryos. Dev Biol *195*, 144-57.

Goriely, A., Stella, M., Coffinier, C., Kessler, D., Mailhos, C., Dessain, S., and Desplan, C. (1996). A functional homologue of goosecoid in Drosophila. Development *122*, 1641-50.

Graff, J. M., Bansal, A., and Melton, D. A. (1996). Xenopus Mad proteins transduce distinct subsets of signals for the TGF beta superfamily. Cell *85*, 479-87.

Graff, J. M., Thies, R. S., Song, J. J., Celeste, A. J., and Melton, D. A. (1994). Studies with a Xenopus BMP receptor suggest that ventral mesoderm-inducing signals override dorsal signals in vivo. Cell *79*, 169-179.

Greenblatt, J. (1997). RNA polymerase II holoenzyme and transcriptional regulation. Curr Opin Cell Biol *9*, 310-9.

Grunz, H., and Tacke, L. (1989). Neural differentiation of Xenopus laevis ectoderm takes place after disaggregation and delayed reaggregation without inducer. Cell Differ Dev *28*, 211-7.

Guger, K. A., and Gumbiner, B. M. (1995). beta-Catenin has Wnt-like activity and mimics the Nieuwkoop signaling center in Xenopus dorsal-ventral patterning. Dev Biol *172*, 115-25.

Gurdon, J. B., Fairman, S., Mohun, T. J., and Brennan, S. (1985). Activation of muscle-specific actin genes in Xenopus development by an induction between animal and vegetal cells of a blastula. Cell *41*, 913-22.

Hahn, S. A., Schutte, M., Hoque, A. T., Moskaluk, C. A., da Costa, L. T., Rozenblum, E., Weinstein, C. L., Fischer, A., Yeo, C. J., Hruban, R. H., and Kern, S. E. (1996). DPC4, a candidate tumor suppressor gene at human chromosome 18q21.1. [see comments]. Science *271*, 350-3.

Hammerschmidt, M., Pelegri, F., Mullins, M. C., Kane, D. A., van Eeden, F. J., Granato, M., Brand, M., Furutani-Seiki, M., Haffter, P., Heisenberg, C. P., Jiang, Y. J., Kelsh, R. N., Odenthal, J., Warga, R. M., and Nusslein-Volhard, C. (1996). dino and mercedes, two genes regulating dorsal development in the zebrafish embryo. Development *123*, 95-102.

Han, K., and Manley, J. L. (1993). Transcriptional repression by the Drosophila even-skipped protein: definition of a minimal repression domain. Genes Dev *7*, 491-503.

Hanna-Rose, W., and Hansen, U. (1996). Active repression mechanisms of eukaryotic transcription repressors. Trends Genet *12*, 229-34.

Harland, R., and Gerhart, J. (1997). Formation and function of Spemann's organizer. Annu Rev Cell Dev Biol *13*, 611-67.

Harland, R. M. (1991). In situ hybridization: an improved whole mount method for Xenopus embryos. Meth. Enzymol. *36*, 675-685.

Hata, A., Lagna, G., Massague, J., and Hemmati-Brivanlou, A. (1998). Smad6 inhibits BMP/Smad1 signaling by specifically competing with the Smad4 tumor suppressor. Genes Dev *12*, 186-97.

Hata, A., Lo, R. S., Wotton, D., Lagna, G., and Massague, J. (1997). Mutations increasing autoinhibition inactivate tumour suppressors Smad2 and Smad4 [see comments]. Nature *388*, 82-7.

Hawley, S. H. B., Wünnenburg-Stapelton, K., Hashimoto, C., Laurent, M. N., Watabe, T., Blumberg, B. W., and Cho, K. W. Y. (1995). Disruption of BMP signals in embryonic

Xenopus ectoderm leads to direct neural induction. Genes Dev. *9*, 2923-2935.

Hayashi, H., Abdollah, S., Qiu, Y., Cai, J., Xu, Y. Y., Grinnell, B. W., Richardson, M. A., Topper, J. N., Gimbrone, M. A., Jr., Wrana, J. L., and Falb, D. (1997). The MAD-related protein Smad7 associates with the TGFbeta receptor and functions as an antagonist of TGFbeta signaling. Cell *89*, 1165-73.

He, X., Saint-Jeannet, J. P., Woodgett, J. R., Varmus, H. E., and Dawid, I. B. (1995). Glycogen synthase kinase-3 and dorsoventral patterning in Xenopus embryos [published erratum appears in Nature 1995 May 18;375(6528):253]. Nature *374*, 617-22.

Heasman, J. (1997). Patterning the Xenopus blastula. Development *124*, 4179-91.

Heasman, J., Crawford, A., Goldstone, K., Garner-Hamrick, P., Gumbiner, B., McCrea, P., Kintner, C., Noro, C. Y., and Wylie, C. (1994). Overexpression of cadherins and underexpression of beta-catenin inhibit dorsal mesoderm induction in early Xenopus embryos. Cell *79*, 791-803.

Heldin, C. H., Miyazono, K., and ten Dijke, P. (1997). TGF-beta signalling from cell membrane to nucleus through SMAD proteins. Nature *390*, 465-71.

Hemmati-Brivanlou, A. (1998). Should the master regulator Rest in peace? [news; comment]. Nat Genet *20*, 109-10.

Hemmati-Brivanlou, A., Kelly, O. G., and Melton, D. A. (1994). Follistatin, an antagonist of activin, is expressed in the Spemann organizer and displays direct neuralizing activity. Cell *77*, 283-95.

Hemmati-Brivanlou, A., and Melton, D. A. (1992). A truncated activin receptor inhibits mesoderm induction and formation of axial structures in Xenopus embryos [see comments]. Nature *359*, 609-14.

Hemmati-Brivanlou, A., and Thomsen, G. H. (1995). Ventral mesodermal patterning in Xenopus embryos: expression patterns and activities of BMP-2 and BMP-4. Dev Genet *17*, 78-89.

Henry, G. L., Brivanlou, I. H., Kessler, D. S., Hemmati-Brivanlou, A., and Melton, D. A. (1996). TGF-beta signals and a pattern in Xenopus laevis endodermal development. Development *122*, 1007-15.

Higashijima, S., Kojima, T., Michiue, T., Ishimaru, S., Emori, Y., and Saigo, K. (1992).

Dual Bar homeo box genes of Drosophila required in two photoreceptor cells, R1 and R6, and primary pigment cells for normal eye development. Genes Dev *6*, 50-60.

Hild, M., Dick, A., Rauch, G. J., Meier, A., Bouwmeester, T., Haffter, P., and Hammerschmidt, M. (1999). The smad5 mutation somitabun blocks Bmp2b signaling during early dorsoventral patterning of the zebrafish embryo. Development *126*, 2149-59.

Hogan, B. L. (1996). Bone morphogenetic proteins in development. Curr Opin Genet Dev *6*, 432-8.

Holley, S. A., Jackson, P. D., Sasai, Y., Lu, B., De Robertis, E. M., Hoffmann, F. M., and Ferguson, E. L. (1995). A conserved system for dorsal-ventral patterning in insects and vertebrates involving sog and chordin [see comments]. Nature *376*, 249-53.

Holley, S. A., Neul, J. L., Attisano, L., Wrana, J. L., Sasai, Y., O'Connor, M. B., De Robertis, E. M., and Ferguson, E. L. (1996). The Xenopus dorsalizing factor noggin ventralizes Drosophila embryos by preventing DPP from activating its receptor. Cell *86*, 607-17.

Holowacz, T., and Elinson, R. P. (1995). Properties of the dorsal activity found in the vegetal cortical cytoplasm of Xenopus eggs. Development *121*, 2789-98.

Hoodless, P. A., Haerry, T., Abdollah, S., Stapleton, M., O'Connor, M. B., Attisano, L., and Wrana, J. L. (1996). MADR1, a MAD-related protein that functions in BMP2 signaling pathways. Cell *85*, 489-500.

Hoppler, S., Brown, J. D., and Moon, R. T. (1996). Expression of a dominant-negative Wnt blocks induction of MyoD in Xenopus embryos. Genes Dev *10*, 2805-17.

Horb, M. E., and Thomsen, G. H. (1997). A vegetally localized T-box transcription factor in Xenopus eggs specifies mesoderm and endoderm and is essential for embryonic mesoderm formation. Development *124*, 1689-98.

Howell, M., and Hill, C. S. (1997). XSmad2 directly activates the activin-inducible, dorsal mesoderm gene XFKH1 in Xenopus embryos. Embo J *16*, 7411-21.

Hsieh, J. C., Kodjabachian, L., Rebbert, M. L., Rattner, A., Smallwood, P. M., Samos, C. H., Nusse, R., Dawid, I. B., and Nathans, J. (1999). A new secreted protein that binds to Wnt proteins and inhibits their activities. Nature *398*, 431-6.

Huber, O., Korn, R., McLaughlin, J., Ohsugi, M., Herrmann, B. G., and Kemler, R. (1996). Nuclear localization of beta-catenin by interaction with transcription factor LEF-1. Mech

Dev *59*, 3-10.

Ikeda, S., Kishida, S., Yamamoto, H., Murai, H., Koyama, S., and Kikuchi, A. (1998). Axin, a negative regulator of the Wnt signaling pathway, forms a complex with GSK-3beta and beta-catenin and promotes GSK-3beta- dependent phosphorylation of beta-catenin. Embo J *17*, 1371-84.

Imamura, T., Takase, M., Nishihara, A., Oeda, E., Hanai, J., Kawabata, M., and Miyazono, K. (1997). Smad6 inhibits signalling by the TGF-beta superfamily [see comments]. Nature *389*, 622-6.

Isaacs, H. V. (1997). New perspectives on the role of the fibroblast growth factor family in amphibian development. Cell Mol Life Sci *53*, 350-61.

Isaacs, H. V., Pownall, M. E., and Slack, J. M. (1994). eFGF regulates Xbra expression during Xenopus gastrulation. Embo J *13*, 4469-81.

Izpisúa-Belmonte, J.-C., De Robertis, E. M., Storey, K. G., and Stern, C. D. (1993). The homeobox gene goosecoid and the origin of organizer cells in the early chick blastoderm. Cell *74*, 645-59.

Jaynes, J. B., and O'Farrell, P. H. (1991). Active repression of transcription by the Engrailed homeodomain protein. EMBO J. *10*, 1427-1433.

Jimenez, G., Verrijzer, C. P., and Ish-Horowicz, D. (1999). A conserved motif in goosecoid mediates groucho-dependent repression in drosophila embryos [In Process Citation]. Mol Cell Biol *19*, 2080-7.

Jones, C. M., Dale, L., Hogan, B. L., Wright, C. V., and Smith, J. C. (1996). Bone morphogenetic protein-4 (BMP-4) acts during gastrula stages to cause ventralization of Xenopus embryos. Development *122*, 1545-54.

Jones, C. M., Kuehn, M. R., Hogan, B. L., Smith, J. C., and Wright, C. V. (1995). Nodal-related signals induce axial mesoderm and dorsalize mesoderm during gastrulation. Development *121*, 3651-62.

Jones, C. M., Lyons, K. M., Lapan, P. M., Wright, C. V. E., and Hogan, B. L. M. (1992). DVR-4 (Bone morphogenetic protein-4) as a posterior-ventralizing factor in *Xenopus* mesoderm induction. Development *115*, 639-647.

Jones, C. M., and Smith, J. C. (1998). Establishment of a BMP-4 morphogen gradient by

long-range inhibition. Dev Biol *194*, 12-7.

Jones, C. M., and Smith, J. C. (1995). Inductive signals. Revolving vertebrates. Curr Biol *5*, 574-6.

Jones, E. A., and Woodland, H. R. (1987). The development of animal caps cells in *Xenopus*: a measure of the start of animal cap competence to form mesoderm. Development *101*, 557-63.

Joseph, E. M., and Melton, D. A. (1998). Mutant Vg1 ligands disrupt endoderm and mesoderm formation in Xenopus embryos. Development *125*, 2677-85.

Joseph, E. M., and Melton, D. A. (1997). Xnr4: a Xenopus nodal-related gene expressed in the Spemann organizer. Dev Biol *184*, 367-72

Kageura, H. (1997). Activation of dorsal development by contact between the cortical dorsal determinant and the equatorial core cytoplasm in eggs of Xenopus laevis. Development *124*, 1543-51.

Kageura, H. (1990). Spatial distribution of the capacity to initiate a secondary embryo in the 32-cell embryo of Xenopus laevis. Dev Biol *142*, 432-8.

Kalionis, B., and O'Farrell, P. H. (1993). A universal target sequence is bound in vitro by diverse homeodomains. Mech Dev *43*, 57-70.

Kao, K. R., and Elinson, R. P. (1988). The entire mesodermal mantle behaves as Spemann's organizer in dorsoanterior enhanced Xenopus laevis embryos. Dev Biol *127*, 64-77.

Kaufmann, E., Paul, H., Friedle, H., Metz, A., Scheucher, M., Clement, J. H., and Knochel, W. (1996). Antagonistic actions of activin A and BMP-2/4 control dorsal lip- specific activation of the early response gene XFD-1' in Xenopus laevis embryos. Embo J *15*, 6739-49.

Kawabata, M., Imamura, T., and Miyazono, K. (1998). Signal transduction by bone morphogenetic proteins. Cytokine Growth Factor Rev *9*, 49-61.

Kelley, C., Yee, K., Harland, R., and Zon, L. I. (1994). Ventral expression of GATA-1 and GATA-2 in the Xenopus embryo defines induction of hematopoietic mesoderm. Dev Biol *165*, 193-205.

Kennedy, M. A., Gonzalez-Sarmiento, R., Kees, U. R., Lampert, F., Dear, N., Boehm, T., and Rabbitts, T. H. (1991). HOX11, a homeobox-containing T-cell oncogene on human chromosome 10q24. Proc Natl Acad Sci U S A *88*, 8900-4.

Kessler, D. S. (1997). Siamois is required for formation of Spemann's organizer. Proc Natl Acad Sci U S A *94*, 13017-22.

Kessler, D. S., and Melton, D. A. (1995). Induction of dorsal mesoderm by soluble, mature Vg1 protein. Development *121*, 2155-64.

Kessler, D. S., and Melton, D. A. (1994). Vertebrate embryonic induction: mesodermal and neural patterning. Science *266*, 596-604.

Kim, J., Johnson, K., Chen, H. J., Carroll, S., and Laughon, A. (1997). Drosophila Mad binds to DNA and directly mediates activation of vestigial by Decapentaplegic. Nature *388*, 304-8.

Kimelman, D., Abraham, J. A., Haaparanta, T., Palisi, T. M., and Kirschner, M. W. (1988). The presence of fibroblast growth factor in the frog egg: its role as a natural mesoderm inducer. Science *242*, 1053-6.

Kimelman, D., Christian, J. L., and Moon, R. T. (1992). Synergistic principles of development: Overlapping patterning system in Xenopus mesoderm induction. Development *116*, 1-9.

Kimelman, D., and Griffin, K. J. (1998). Mesoderm induction: a postmodern view [comment]. Cell *94*, 419-21.

Kimelman, D., and Kirschner, M. (1987). Synergistic induction of mesoderm by FGF and TGF-beta and the identification of an mRNA coding for FGF in the early Xenopus embryo. Cell *51*, 869-77.

Kingsley, D. M. (1994). The TGF-beta superfamily: new members, new receptors, and new genetic tests of function in different organisms. Genes Dev *8*, 133-46.

Kingston, R. E., Bunker, C. A., and Imbalzano, A. N. (1996). Repression and activation by multiprotein complexes that alter chromatin structure. Genes Dev *10*, 905-20.

Kintner, C. R., and Brockes, J. P. (1984). Monoclonal antibodies identify blastemal cells derived from dedifferentiating limb regeneration. Nature *308*, 67-9.

Kishimoto, Y., Lee, K. H., Zon, L., Hammerschmidt, M., and Schulte-Merker, S. (1997). The molecular nature of zebrafish swirl: BMP2 function is essential during early dorsoventral patterning. Development *124*, 4457-66.

Klein, P. S., and Melton, D. A. (1994). Hormonal regulation of embryogenesis: the

formation of mesoderm in Xenopus laevis. Endocr Rev *15*, 326-41.

Knochel, S., Lef, J., Clement, J., Klocke, B., Hille, S., Koster, M., and Knochel, W. (1992). Activin A induced expression of a fork head related gene in posterior chordamesoderm (notochord) of Xenopus laevis embryos. Mech Dev *38*, 157-65.

Kobel, H. R., and Du Pasquier, L. (1986). Genetics of polyploid Xenopus. Trends Genet. *3*, 310-315.

Kreig, P. A., and Melton, D. A. (1984). Functional RNAs are produced by SP6 in vitro transcripton of cloned DNAs. Nucl. Acids. Res. *12*, 7057-7070.

Kretzschmar, M., Doody, J., and Massague, J. (1997). Opposing BMP and EGF signalling pathways converge on the TGF-beta family mediator Smad1. Nature *389*, 618-22.

Kretzschmar, M., Liu, F., Hata, A., Doody, J., and Massague, J. (1997). The TGF-beta family mediator Smad1 is phosphorylated directly and activated functionally by the BMP receptor kinase. Genes Dev *11*, 984-95.

Kretzschmar, M., and Massague, J. (1998). SMADs: mediators and regulators of TGF-beta signaling. Curr Opin Genet Dev *8*, 103-11.

Krieg, P. A., Varnum, S. M., Wormington, W. M., and Melton, D. A. (1989). The mRNA encoding elongation factor 1-alpha (EF-1 alpha) is a major transcript at the midblastula transition in Xenopus. Dev Biol *133*, 93-100.

Kroll, K. L., and Amaya, E. (1996). Transgenic Xenopus embryos from sperm nuclear transplantations reveal FGF signaling requirements during gastrulation. Development *122*, 3173-83.

Ku, M., and Melton, D. A. (1993). Xwnt-11: a maternally expressed Xenopus wnt gene. Development *119*, 1161-73.

Labbe, E., Silvestri, C., Hoodless, P. A., Wrana, J. L., and Attisano, L. (1998). Smad2 and Smad3 positively and negatively regulate TGF beta-dependent transcription through the forkhead DNA-binding protein FAST2. Mol Cell *2*, 109-20.

LaBonne, C., Burke, B., and Whitman, M. (1995). Role of MAP kinase in mesoderm induction and axial patterning during Xenopus development. Development *121*, 1475-86.

LaBonne, C., and Whitman, M. (1997). Localization of MAP kinase activity in early Xenopus embryos: implications for endogenous FGF signaling. Dev Biol *183*, 9-20.

LaBonne, C., and Whitman, M. (1994). Mesoderm induction by activin requires FGF-mediated intracellular signals. Development *120*, 463-72.

Ladher, R., Mohun, T. J., Smith, J. C., and Snape, A. M. (1996). Xom: a Xenopus homeobox gene which mediates the early effects of BMP-4. Development *122*, 2385-2394.

Lagna, G., Hata, A., Hemmati-Brivanlou, A., and Massague, J. (1996). Partnership between DPC4 and SMAD proteins in TGF-beta signalling pathways. Nature *383*, 832-6.

Lamb, T. M., Knecht, A. K., Smith, W. C., Stachel, S. E., Economides, A. N., Stahl, N., Yancopolous, G. D., and Harland, R. M. (1993). Neural induction by the secreted polypeptide noggin [see comments]. Science *262*, 713-8.

Larabell, C. A., Torres, M., Rowning, B. A., Yost, C., Miller, J. R., Wu, M., Kimelman, D., and Moon, R. T. (1997). Establishment of the dorso-ventral axis in Xenopus embryos is presaged by early asymmetries in beta-catenin that are modulated by the Wnt signaling pathway. J Cell Biol *136*, 1123-36.

Latinkic, B. V., and Smith, J. C. (1999). Goosecoid and mix.1 repress Brachyury expression and are required for head formation in Xenopus. Development *126*, 1769-79.

Laughon, A. (1991). DNA binding specificity of homeodomains. Biochemistry *30*, 11357-67.

Laurent, M. N., Blitz, I. L., Hashimoto, C., Rothbacher, U., and Cho, K. W. (1997). The Xenopus homeobox gene twin mediates Wnt induction of goosecoid in establishment of Spemann's organizer. Development *124*, 4905-16.

Laurent, M. N., and Cho, K. W. (1999). Bone morphogenetic protein antagonism of Spemann's organizer is independent of wnt signaling [In Process Citation]. Dev Biol *206*, 157-62.

Le Roux, I., Joliot, A. H., Bloch-Gallego, E., Prochiantz, A., and Volovitch, M. (1993). Neurotrophic activity of the Antennapedia homeodomain depends on its specific DNA-binding properties. Proc Natl Acad Sci U S A *90*, 9120-4.

Lemaire, P. (1996). The coming of age of ventralising homeobox genes in amphibian development. Bioessays *18*, 701-4.

Lemaire, P., Darras, S., Caillol, D., and Kodjabachian, L. (1998). A role for the

vegetally expressed Xenopus gene Mix.1 in endoderm formation and in the restriction of mesoderm to the marginal zone. Development *125*, 2371-80.

Lemaire, P., Garrett, N., and Gurdon, J. B. (1995). Expression cloning of Siamois, a Xenopus homeobox gene expressed in dorsal vegetal cells of blastulae and able to induce a complete secondary axis. Cell *81*, 85-94.

Lemaire, P., and Gurdon, J. B. (1994). A role for cytoplasmic determinants in mesoderm patterning: cell- autonomous activation of the goosecoid and Xwnt-8 genes along the dorsoventral axis of early Xenopus embryos. Development *120*, 1191-9.

Liu, F., Hata, A., Baker, J. C., Doody, J., Carcamo, J., Harland, R. M., and Massague, J. (1996). A human Mad protein acting as a BMP-regulated transcriptional activator [see comments]. Nature *381*, 620-3.

Liu, F., Pouponnot, C., and Massague, J. (1997). Dual role of the Smad4/DPC4 tumor suppressor in TGFbeta-inducible transcriptional complexes. Genes Dev *11*, 3157-67.

Liu, F., Ventura, F., Doody, J., and Massague, J. (1995). Human type II receptor for bone morphogenic proteins (BMPs): extension of the two-kinase receptor model to the BMPs. Mol Cell Biol *15*, 3479-86.

Lo, R. S., Chen, Y. G., Shi, Y., Pavletich, N. P., and Massague, J. (1998). The L3 loop: a structural motif determining specific interactions between SMAD proteins and TGF-beta receptors. Embo J *17*, 996-1005.

Lustig, K. D., Kroll, K. L., Sun, E. E., and Kirschner, M. W. (1996). Expression cloning of a Xenopus T-related gene (Xombi) involved in mesodermal patterning and blastopore lip formation. Development *122*, 4001-12.

Macias-Silva, M., Abdollah, S., Hoodless, P. A., Pirone, R., Attisano, L., and Wrana, J. L. (1996). MADR2 is a substrate of the TGFbeta receptor and its phosphorylation is required for nuclear accumulation and signaling. Cell *87*, 1215-24.

Maeda, R., Kobayashi, A., Sekine, R., Lin, J. J., Kung, H., and Maeno, M. (1997). Xmsx-1 modifies mesodermal tissue pattern along dorsoventral axis in Xenopus laevis embryo. Development *124*, 2553-60.

Maeno, M., Mead, P. E., Kelley, C., Xu, R. H., Kung, H. F., Suzuki, A., Ueno, N., and Zon, L. I. (1996). The role of BMP-4 and GATA-2 in the induction and differentiation of

hematopoietic mesoderm in Xenopus laevis. Blood *88*, 1965-72.

Maeno, M., Ong, R. C., Suzuki, A., Ueno, N., and Kung, H. F. (1994). A truncated bone morphogenetic protein 4 receptor alters the fate of ventral mesoderm to dorsal mesoderm: roles of animal pole tissue in the development of ventral mesoderm [see comments]. Proc Natl Acad Sci U S A *91*, 10260-4.

Mahony, D., and Gurdon, J. B. (1995). A type 1 serine/threonine kinase receptor that can dorsalize mesoderm in Xenopus. Proc Natl Acad Sci U S A *92*, 6474-8.

Mailhos, C., Andre, S., Mollereau, B., Goriely, A., Hemmati-Brivanlou, A., and Desplan, C. (1998). Drosophila Goosecoid requires a conserved heptapeptide for repression of paired-class homeoprotein activators. Development *125*, 937-47.

Mann, R. S. (1995). The specificity of homeotic gene function. BioEssays *17*, 855-863.

Mann, R. S., and Affolter, M. (1998). Hox proteins meet more partners. Curr Opin Genet Dev *8*, 423-9.

Marques, G., Musacchio, M., Shimell, M. J., Wunnenberg-Stapleton, K., Cho, K. W., and O'Connor, M. B. (1997). Production of a DPP activity gradient in the early Drosophila embryo through the opposing actions of the SOG and TLD proteins. Cell *91*, 417-26.

Massague, J. (1998). TGF-beta signal transduction. Annu Rev Biochem *67*, 753-91.

Masuyama, N., Hanafusa, H., Kusakabe, M., Shibuya, H., and Nishida, E. (1999). Identification of two Smad4 proteins in Xenopus. Their common and distinct properties. J Biol Chem *274*, 12163-70.

McKendry, R., Hsu, S. C., Harland, R. M., and Grosschedl, R. (1997). LEF-1/TCF proteins mediate wnt-inducible transcription from the Xenopus nodal-related 3 promoter. Dev Biol *192*, 420-31.

Mead, P. E., Brivanlou, I. H., Kelley, C. M., and Zon, L. I. (1996). BMP-4-responsive regulation of dorsal-ventral patterning by the homeobox protein Mix.1. Nature *382*, 357-60.

Melby, A. E., Clements, W. K., and Kimelman, D. (1999). Regulation of dorsal gene expression in xenopus by the ventralizing homeodomain gene Vox [In Process Citation]. Dev Biol *211*, 293-305.

Mishina, Y., Suzuki, A., Ueno, N., and Behringer, R. R. (1995). Bmpr encodes a type I bone morphogenetic protein receptor that is essential for gastrulation during mouse

embryogenesis. Genes Dev *9*, 3027-37.

Mitchell, P. J., and Tjian, R. (1989). Transcriptional regulation in mammalian cells by sequence-specific DNA binding proteins. Science *245*, 371-8.

Molenaar, M., van de Wetering, M., Oosterwegel, M., Peterson-Maduro, J., Godsave, S., Korinek, V., Roose, J., Destree, O., and Clevers, H. (1996). XTcf-3 transcription factor mediates beta-catenin-induced axis formation in Xenopus embryos. Cell *86*, 391-9.

Moon, R. T., and Kimelman, D. (1998). From cortical rotation to organizer gene expression: toward a molecular explanation of axis specification in Xenopus. Bioessays *20*, 536-45.

Mowry, K. L., and Melton, D. A. (1992). Vegetal messenger RNA localization directed by a 340-nt RNA sequence element in Xenopus oocytes. Science *255*, 991-4.

Muller, C. W., and Herrmann, B. G. (1997). Crystallographic structure of the T domain-DNA complex of the Brachyury transcription factor. Nature *389*, 884-8.

Mullins, M. C., Hammerschmidt, M., Kane, D. A., Odenthal, J., Brand, M., van Eeden, F. J., Furutani-Seiki, M., Granato, M., Haffter, P., Heisenberg, C. P., Jiang, Y. J., Kelsh, R. N., and Nusslein-Volhard, C. (1996). Genes establishing dorsoventral pattern formation in the zebrafish embryo: the ventral specifying genes. Development *123*, 81-93.

Nakao, A., Afrakhte, M., Moren, A., Nakayama, T., Christian, J. L., Heuchel, R., Itoh, S., Kawabata, M., Heldin, N. E., Heldin, C. H., and ten Dijke, P. (1997). Identification of Smad7, a TGFbeta-inducible antagonist of TGF-beta signalling [see comments]. Nature *389*, 631-5.

Nakayama, T., Gardner, H., Berg, L. K., and Christian, J. L. (1998). Smad6 functions as an intracellular antagonist of some TGF-beta family members during Xenopus embryogenesis. Genes Cells *3*, 387-94.

Nakayama, T., Snyder, M. A., Grewal, S. S., Tsuneizumi, K., Tabata, T., and Christian, J. L. (1998). Xenopus Smad8 acts downstream of BMP-4 to modulate its activity during vertebrate embryonic patterning. Development *125*, 857-67.

Neave, B., Holder, N., and Patient, R. (1997). A graded response to BMP-4 spatially coordinates patterning of the mesoderm and ectoderm in the zebrafish. Mech Dev *62*, 183-95.

Nguyen, V. H., Schmid, B., Trout, J., Connors, S. A., Ekker, M., and Mullins, M. C.

(1998). Ventral and lateral regions of the zebrafish gastrula, including the neural crest progenitors, are established by a bmp2b/swirl pathway of genes. Dev Biol *199*, 93-110.

Niehrs, C., Keller, R., Cho, K. W., and De Robertis, E. M. (1993). The homeobox gene goosecoid controls cell migration in Xenopus embryos. Cell *72*, 491-503.

Niehrs, C., Steinbeisser, H., and De Robertis, E. M. (1994). Mesodermal patterning by a gradient of the vertebrate homeobox gene goosecoid. Science *263*, 817-20.

Nieuwkoop, P. D., and Faber, J. (1975). Normal Table of *Xenopus laevis* (Daudin) (Amsterdam: North Holland).

Nishimatsu, S., and Thomsen, G. H. (1998). Ventral mesoderm induction and patterning by bone morphogenetic protein heterodimers in Xenopus embryos. Mech Dev *74*, 75-88.

O'Reilly, M. A., Smith, J. C., and Cunliffe, V. (1995). Patterning of the mesoderm in Xenopus: dose-dependent and synergistic effects of Brachyury and Pintallavis. Development *121*, 1351-9.

Oda, S., Nishimatsu, S., Murakami, K., and Ueno, N. (1995). Molecular cloning and functional analysis of a new activin beta subunit: a dorsal mesoderm-inducing activity in Xenopus. Biochem Biophys Res Commun *210*, 581-8.

Ogbourne, S., and Antalis, T. M. (1998). Transcriptional control and the role of silencers in transcriptional regulation in eukaryotes. Biochem J *331*, 1-14.

Ohashi, Y., Brickman, J. M., Furman, E., Middleton, B., and Carey, M. (1994). Modulating the potency of a yeast in vitro transcription system. Molecular and Cellular Biology *14*, 2731-2739.

Onichtchouk, D., Gawantka, V., Dosch, R., Delius, H., Hirschfeld, K., Blumenstock, C., and Niehrs, C. (1996). The Xvent-2 homeobox gene is part of the BMP-4 signalling pathway controlling [correction of controling] dorsoventral patterning of Xenopus mesoderm. Development *122*, 3045-53.

Onichtchouk, D., Glinka, A., and Niehrs, C. (1998). Requirement for Xvent-1 and Xvent-2 gene function in dorsoventral patterning of Xenopus mesoderm. Development *125*, 1447-56.

Orphanides, G., Lagrange, T., and Reinberg, D. (1996). The general transcription factors of RNA polymerase II. Genes Dev *10*, 2657-83.

Padgett, R. W., St. Johnston, R. D., and Gelbart, W. M. (1987). A transcript from a Drosophila pattern gene predicts a protein homologous to the transforming growth factor-beta family. Nature *325*, 81-4.

Papalopulu, N., and Kintner, C. (1996). A Xenopus gene, Xbr-1, defines a novel class of homeobox genes and is expressed in the dorsal ciliary margin of the eye. Dev Biol *174*, 104-14.

Passner, J. M., Ryoo, H. D., Shen, L., Mann, R. S., and Aggarwal, A. K. (1999). Structure of a DNA-bound Ultrabithorax-Extradenticle homeodomain complex [see comments]. Nature *397*, 714-9.

Piccolo, S., Agius, E., Lu, B., Goodman, S., Dale, L., and De Robertis, E. M. (1997). Cleavage of Chordin by Xolloid metalloprotease suggests a role for proteolytic processing in the regulation of Spemann organizer activity. Cell *91*, 407-16.

Piccolo, S., Sasai, Y., Lu, B., and De Robertis, E. M. (1996). Dorsoventral patterning in Xenopus: inhibition of ventral signals by direct binding of chordin to BMP-4. Cell *86*, 589-98.

Pierce, S. B., and Kimelman, D. (1995). Regulation of Spemann organizer formation by the intracellular kinase Xgsk-3. Development *121*, 755-65.

Pillemer, G., Yelin, R., Epstein, M., Gont, L., Frumkin, Y., Yisraeli, J. K., Steinbeisser, H., and Fainsod, A. (1998). The Xcad-2 gene can provide a ventral signal independent of BMP-4. Mech Dev *74*, 133-43.

Pinsonneault, J., Florence, B., Vaessin, H., and McGinnis, W. (1997). A model for extradenticle function as a switch that changes HOX proteins from repressors to activators. Embo J *16*, 2032-42.

Piper, D. E., Batchelor, A. H., Chang, C. P., Cleary, M. L., and Wolberger, C. (1999). Structure of a HoxB1-Pbx1 heterodimer bound to DNA: role of the hexapeptide and a fourth homeodomain helix in complex formation. Cell *96*, 587-97.

Pollock, R., and Treisman, R. (1990). A sensitive method for the determination of protein-DNA binding specificities. Nucleic Acids Res *18*, 6197-204.

Pomerantz, J. L., and Sharp, P. A. (1994). Homeodomain determinants of major groove recognition. Biochemistry *33*, 10851-8.

Ptashne, M. (1988). How eukaryotic transcriptional activators work. Nature *335*, 683-9.

Rastegar, S., Friedle, H., Frommer, G., and Knochel, W. (1999). Transcriptional

regulation of xvent homeobox genes [In Process Citation]. Mech Dev *81*, 139-49.

Re'em-Kalma, Y., Lamb, T., and Frank, D. (1995). Competition between noggin and bone morphogenetic protein 4 activities may regulate dorsalization during Xenopus development. Proc Natl Acad Sci U S A *92*, 12141-5.

Rebagliati, M. R., Weeks, D. L., Harvey, R. P., and Melton, D. A. (1985). Identification and cloning of localized maternal RNAs from Xenopus eggs. Cell *42*, 769-77.

Roose, J., Molenaar, M., Peterson, J., Hurenkamp, J., Brantjes, H., Moerer, P., van de Wetering, M., Destree, O., and Clevers, H. (1998). The Xenopus Wnt effector XTcf-3 interacts with Groucho-related transcriptional repressors. Nature *395*, 608-12.

Rosa, F. M. (1989). Mix.1, a homeobox mRNA inducible by mesoderm inducers, is expressed mostly in the presumptive endodermal cells of Xenopus embryos. Cell *57*, 965-74.

Rowning, B. A., Wells, J., Wu, M., Gerhart, J. C., Moon, R. T., and Larabell, C. A. (1997). Microtubule-mediated transport of organelles and localization of beta- catenin to the future dorsal side of Xenopus eggs. Proc Natl Acad Sci U S A *94*, 1224-9.

Rubinfeld, B., Souza, B., Albert, I., Munemitsu, S., and Polakis, P. (1995). The APC protein and E-cadherin form similar but independent complexes with alpha-catenin, beta-catenin, and plakoglobin. J Biol Chem *270*, 5549-55.

Ruiz i Altaba, A., and Jessell, T. M. (1992). Pintallavis, a gene expressed in the organizer and midline cells of frog embryos: involvement in the development of the neural axis. Development *116*, 81-93.

Ruiz i Altaba, A., and Melton, D. A. (1989). Bimodal and graded expression of the Xenopus homeobox gene Xhox3 during embryonic development. Development *106*, 173-83.

Rupp, R. A., Snider, L., and Weintraub, H. (1994). Xenopus embryos regulate the nuclear localization of XMyoD. Genes Dev *8*, 1311-23.

Saha, M. S., and Grainger, R. M. (1993). Early opsin expression in Xenopus embryos precedes photoreceptor differentiation. Brain Res Mol Brain Res *17*, 307-18.

Saha, S., Brickman, J. M., Lehming, N., and Ptashne, M. (1993). New eukaryotic transcriptional repressors. Nature *363*, 648-52.

Sakai, M. (1996). The vegetal determinants required for the Spemann organizer move equatorially during the first cell cycle. Development *122*, 2207-14.

Sakanaka, C., Weiss, J. B., and Williams, L. T. (1998). Bridging of beta-catenin and glycogen synthase kinase-3beta by axin and inhibition of beta-catenin-mediated transcription. Proc Natl Acad Sci U S A *95*, 3020-3.

Sasai, Y., Lu, B., Steinbeisser, H., and De Robertis, E. M. (1995). Regulation of neural induction by the Chd and Bmp-4 antagonistic patterning signals in Xenopus [published errata appear in Nature 1995 Oct 26;377(6551):757 and 1995 Nov 23;378(6555):419]. Nature *376*, 333-6.

Sasai, Y., Lu, B., Steinbeisser, H., Geissert, D., Gont, L. K., and De Robertis, E. M. (1994). Xenopus chordin: a novel dorsalizing factor activated by organizer- specific homeobox genes. Cell *79*, 779-90.

Sato, S. M., and Sargent, T. D. (1991). Localized and inducible expression of Xenopus-posterior (Xpo), a novel gene active in early frog embryos, encoding a protein with a 'CCHC' finger domain. Development *112*, 747-53.

Savage, C., Das, P., Finelli, A. L., Townsend, S. R., Sun, C. Y., Baird, S. E., and Padgett, R. W. (1996). Caenorhabditis elegans genes sma-2, sma-3, and sma-4 define a conserved family of transforming growth factor beta pathway components. Proc Natl Acad Sci U S A *93*, 790-4.

Schmidt, J., Francois, V., Bier, E., and Kimelman, D. (1995). Drosophila short gastrulation induces an ectopic axis in Xenopus: evidence for conserved mechanisms of dorsal-ventral patterning. Development *121*, 4319-28.

Schmidt, J. E., Suzuki, A., Ueno, N., and Kimelman, D. (1995). Localized BMP-4 mediates dorsal/ventral patterning in the early Xenopus embryo. Dev Biol *169*, 37-50.

Schmidt, J. E., von Dassow, G., and Kimelman, D. (1996). Regulation of dorsal-ventral patterning: the ventralizing effects of the novel Xenopus homeobox gene Vox. Development *122*, 1711-21.

Schneider, S., Steinbeisser, H., Warga, R. M., and Hausen, P. (1996). Beta-catenin translocation into nuclei demarcates the dorsalizing centers in frog and fish embryos. Mech Dev *57*, 191-8.

Schulte-Merker, S., Hammerschmidt, M., Beuchle, D., Cho, K. W., De Robertis, E. M., and Nusslein-Volhard, C. (1994). Expression of zebrafish goosecoid and no tail gene products in wild- type and mutant no tail embryos. Development *120*, 843-52.

Schulte-Merker, S., Lee, K. J., McMahon, A. P., and Hammerschmidt, M. (1997). The zebrafish organizer requires chordino [letter]. Nature *387*, 862-3.

Schulte-Merker, S., and Smith, J. C. (1995). Mesoderm formation in response to Brachyury requires FGF signalling. Curr Biol *5*, 62-7.

Schulte-Merker, S., Smith, J. C., and Dale, L. (1994). Effects of truncated activin and FGF receptors and of follistatin on the inducing activities of BVg1 and activin: does activin play a role in mesoderm induction? Embo J *13*, 3533-41.

Scott, M. P. (1999). Hox proteins reach out round DNA [news; comment]. Nature *397*, 649, 651.

Sekelsky, J. J., Newfeld, S. J., Raftery, L. A., Chartoff, E. H., and Gelbart, W. M. (1995). Genetic characterization and cloning of mothers against dpp, a gene required for decapentaplegic function in Drosophila melanogaster. Genetics *139*, 1347-58.

Shapira, E., Marom, K., Yelin, R., Levy, A., and Fainsod, A. (1999). A role for the homeobox gene Xvex-1 as part of the BMP-4 ventral signaling pathway. Mech Dev *86*, 99-111.

Sharkey, M., Graba, Y., and Scott, M. P. (1997). Hox genes in evolution: protein surfaces and paralog groups. Trends Genet *13*, 145-51.

Shi, Y., Hata, A., Lo, R. S., Massague, J., and Pavletich, N. P. (1997). A structural basis for mutational inactivation of the tumour suppressor Smad4 [see comments]. Nature *388*, 87-93.

Shibuya, H., Iwata, H., Masuyama, N., Gotoh, Y., Yamaguchi, K., Irie, K., Matsumoto, K., Nishida, E., and Ueno, N. (1998). Role of TAK1 and TAB1 in BMP signaling in early Xenopus development. Embo J *17*, 1019-28.

Shibuya, H., Yamaguchi, K., Shirakabe, K., Tonegawa, A., Gotoh, Y., Ueno, N., Irie, K., Nishida, E., and Matsumoto, K. (1996). TAB1: an activator of the TAK1 MAPKKK in TGF-beta signal transduction. Science *272*, 1179-82.

Shimell, M. J., Ferguson, E. L., Childs, S. R., and O'Connor, M. B. (1991). The Drosophila dorsal-ventral patterning gene tolloid is related to human bone morphogenetic protein 1. Cell *67*, 469-81.

Siegfried, E., Chou, T. B., and Perrimon, N. (1992). wingless signaling acts through zeste-white 3, the Drosophila homolog of glycogen synthase kinase-3, to regulate engrailed and establish cell fate. Cell *71*, 1167-79.

Sirard, C., de la Pompa, J. L., Elia, A., Itie, A., Mirtsos, C., Cheung, A., Hahn, S., Wakeham, A., Schwartz, L., Kern, S. E., Rossant, J., and Mak, T. W. (1998). The tumor suppressor gene Smad4/Dpc4 is required for gastrulation and later for anterior development of the mouse embryo. Genes Dev *12*, 107-19.

Sive, H. L. (1993). The frog prince-ss: A molecular formula for dorsoventral patterning in Xenopus. Genes Dev. *7*, 1-12.

Slack, J. M. (1994). Inducing factors in Xenopus early embryos. Curr Biol *4*, 116-26.

Slack, J. M., Darlington, B. G., Heath, J. K., and Godsave, S. F. (1987). Mesoderm induction in early Xenopus embryos by heparin-binding growth factors. Nature *326*, 197-200.

Slack, J. M., Holland, P. W., and Graham, C. F. (1993). The zootype and the phylotypic stage [see comments]. Nature *361*, 490-2.

Slack, J. M. W. (1984). Regional biosynthetic markers in the early amphibian embryo. J. Embryol. exp. Morph *80*, 289-319.

Smith, J. (1999). T-box genes: what they do and how they do it. Trends Genet *15*, 154-8.

Smith, J. C. (1989). Induction and early amphibian development. Curr Opin Cell Biol *1*, 1061-70.

Smith, J. C. (1987). A mesoderm-inducing factor is produced by a Xenopus cell line. Development *99*, 3-14.

Smith, J. C. (1993). Purifying and assaying mesoderm-inducing factors from vertebrate embryos. In Cellular Interactions in Development - a Practical Approach, D. Hartley, ed. (Oxford: Oxford University Press), pp. 181-204.

Smith, J. C., Price, B. M. J., Green, J. B. A., Weigel, D., and Herrmann, B. G. (1991). Expression of a Xenopus homolog of *Brachyury* (*T*) is an immediate-early response to mesoderm induction. Cell *67*, 79-87.

Smith, J. C., Price, B. M. J., Van, N. K., and Huylebroeck, D. (1990). Identification of a potent *Xenopus* mesoderm-inducing factor as a homologue of activin A. Nature *345*, 732-4.

Smith, J. C., and Slack, J. M. (1983). Dorsalization and neural induction: properties of the organizer in Xenopus laevis. J Embryol Exp Morphol *78*, 299-317.

Smith, J. C., and Watt, F. M. (1985). Biochemical specificity of *Xenopus* notochord. Differentiation *29*, 109-115.

Smith, W. C., and Harland, R. M. (1992). Expression cloning of noggin, a new dorsalizing factor localized to the Spemann organizer in Xenopus embryos. Cell *70*, 829-40.

Smith, W. C., and Harland, R. M. (1991). Injected Xwnt-8 RNA acts early in Xenopus embryos to promote formation of a vegetal dorsalizing center. Cell *67*, 753-65.

Smith, W. C., McKendry, R., Ribisi, S., Jr., and Harland, R. M. (1995). A nodal-related gene defines a physical and functional domain within the Spemann organizer. Cell *82*, 37-46.

Sokol, S. Y. (1996). Analysis of Dishevelled signalling pathways during Xenopus development. Curr Biol *6*, 1456-67.

Sokol, S. Y. (1999). Wnt signaling and dorso-ventral axis specification in vertebrates [In Process Citation]. Curr Opin Genet Dev *9*, 405-10.

Sokol, S. Y., and Melton, D. A. (1992). Interaction of Wnt and activin in dorsal mesoderm induction in Xenopus. Dev Biol *154*, 348-55.

Solnica-Krezel, L. (1999). Pattern formation in zebrafish--fruitful liaisons between embryology and genetics. Curr Top Dev Biol *41*, 1-35.

Solnica-Krezel, L., Stemple, D. L., Mountcastle-Shah, E., Rangini, Z., Neuhauss, S. C., Malicki, J., Schier, A. F., Stainier, D. Y., Zwartkruis, F., Abdelilah, S., and Driever, W. (1996). Mutations affecting cell fates and cellular rearrangements during gastrulation in zebrafish. Development *123*, 67-80.

Stachel, S. E., Grunwald, D. J., and Myers, P. Z. (1993). Lithium perturbation and goosecoid expression identify a dorsal specification pathway in the pregastrula zebrafish. Development *117*, 1261-1274.

Steinbeisser, H., De Robertis, E. M., Ku, M., Kessler, D. S., and Melton, D. A. (1993). Xenopus axis formation: induction of goosecoid by injected Xwnt-8 and activin mRNAs. Development *118*, 499-507.

Steinbeisser, H., Fainsod, A., Niehrs, C., Sasai, Y., and De Robertis, E. M. (1995). The role of gsc and BMP-4 in dorsal-ventral patterning of the marginal zone in Xenopus: a loss-of-function study using antisense RNA. Embo J *14*, 5230-43.

Stennard, F., Carnac, G., and Gurdon, J. B. (1996). The Xenopus T-box gene, Antipodean, encodes a vegetally localised maternal mRNA and can trigger mesoderm formation. Development *122*, 4179-88.

Stewart, R. M., and Gerhart, J. C. (1990). The anterior extent of dorsal development of the Xenopus embryonic axis depends on the quantity of organizer in the late blastula. Development *109*, 363-72.

Su, M. W., Suzuki, H. R., Solursh, M., and Ramirez, F. (1991). Progressively restricted expression of a new homeobox-containing gene during Xenopus laevis embryogenesis. Development *111*, 1179-87.

Sun, B. I., Bush, S. M., Collins-Racie, L. A., LaVallie, E. R., DiBlasio-Smith, E. A., Wolfman, N. M., McCoy, J. M., and Sive, H. L. (1999). derriere: a TGF-beta family member required for posterior development in Xenopus. Development *126*, 1467-82.

Suzuki, A., Chang, C., Yingling, J. M., Wang, X. F., and Hemmati-Brivanlou, A. (1997). Smad5 induces ventral fates in Xenopus embryo. Dev Biol *184*, 402-5.

Suzuki, A., Kaneko, E., Maeda, J., and Ueno, N. (1997). Mesoderm induction by BMP-4 and -7 heterodimers. Biochem Biophys Res Commun *232*, 153-6.

Suzuki, A., Kaneko, E., Ueno, N., and Hemmati-Brivanlou, A. (1997). Regulation of epidermal induction by BMP2 and BMP7 signaling. Dev Biol *189*, 112-22.

Suzuki, A., Thies, R. S., Yamaji, N., Song, J. J., Wozney, J. M., Murakami, K., and Ueno, N. (1994). A truncated bone morphogenetic protein receptor affects dorsal-ventral patterning in the early Xenopus embryo [see comments]. Proc Natl Acad Sci U S A *91*, 10255-9.

Suzuki, A., Ueno, N., and Hemmati-Brivanlou, A. (1997). Xenopus msx1 mediates epidermal induction and neural inhibition by BMP4. Development *124*, 3037-44.

Sykes, T. G., Rodaway, A. R., Walmsley, M. E., and Patient, R. K. (1998). Suppression of GATA factor activity causes axis duplication in Xenopus. Development *125*, 4595-605.

Symes, K., and Smith, J. C. (1987). Gastrulation movements provide an early marker of mesoderm induction in *Xenopus*. Development *101*, 339-349.

Tada, M., O'Reilly, M. A., and Smith, J. C. (1997). Analysis of competence and of Brachyury autoinduction by use of hormone- inducible Xbra. Development *124*, 2225-34.

Tanda, S., and Corces, V. G. (1991). Retrotransposon-induced overexpression of a homeobox gene causes defects in eye morphogenesis in *Drosophila*. EMBO J. *10*, 407-417.

Tang, S. J., Hoodless, P. A., Lu, Z., Breitman, M. L., McInnes, R. R., Wrana, J. L., and Buchwald, M. (1998). The Tlx-2 homeobox gene is a downstream target of BMP signalling and

is required for mouse mesoderm development. Development *125*, 1877-87.

ten Dijke, P., Yamashita, H., Sampath, T. K., Reddi, A. H., Estevez, M., Riddle, D. L., Ichijo, H., Heldin, C. H., and Miyazono, K. (1994). Identification of type I receptors for osteogenic protein-1 and bone morphogenetic protein-4. J Biol Chem *269*, 16985-8.

Thomsen, G., Woolf, T., Whitman, M., Sokol, S., Vaughan, J., Vale, W., and Melton, D. A. (1990). Activins are expressed early in Xenopus embryogenesis and can induce axial mesoderm and anterior structures. Cell *63*, 485-93.

Thomsen, G. H., and Melton, D. A. (1993). Processed Vg1 protein is an axial mesoderm inducer in Xenopus. Cell *74*, 433-41.

Topper, J. N., Cai, J., Qiu, Y., Anderson, K. R., Xu, Y. Y., Deeds, J. D., Feeley, R., Gimeno, C. J., Woolf, E. A., Tayber, O., Mays, G. G., Sampson, B. A., Schoen, F. J., Gimbrone, M. A., Jr., and Falb, D. (1997). Vascular MADs: two novel MAD-related genes selectively inducible by flow in human vascular endothelium. Proc Natl Acad Sci U S A *94*, 9314-9.

Tsuneizumi, K., Nakayama, T., Kamoshida, Y., Kornberg, T. B., Christian, J. L., and Tabata, T. (1997). Daughters against dpp modulates dpp organizing activity in Drosophila wing development [see comments]. Nature *389*, 627-31.

Umbhauer, M., Marshall, C. J., Mason, C. S., Old, R. W., and Smith, J. C. (1995). Mesoderm induction in *Xenopus* caused by activation of MAP kinase. Nature *376*, 58-62.

Vincent, J. P., and Gerhart, J. C. (1987). Subcortical rotation in Xenopus eggs: an early step in embryonic axis specification. Dev Biol *123*, 526-39.

von Dassow, G., Schmidt, J. E., and Kimelman, D. (1993). Induction of the Xenopus organiser: expression and regulation of Xnot, a novel FGF and activin-regulated homeobox gene. Genes & Dev. *7*, 355-366.

Walmsley, M. E., Guille, M. J., Bertwistle, D., Smith, J. C., Pizzey, J. A., and Patient, R. K. (1994). Negative control of Xenopus GATA-2 by activin and noggin with eventual expression in precursors of the ventral blood islands. Development *120*, 2519-29.

Watabe, T., Kim, S., Candia, A., Rothbacher, U., Hashimoto, C., Inoue, K., and Cho, K. W. (1995). Molecular mechanisms of Spemann's organizer formation: conserved growth factor synergy between Xenopus and mouse. Genes Dev *9*, 3038-50.

Weinstein, D. C., Ruiz i Altaba, A., Chen, W. S., Hoodless, P., Prezioso, V. R., Jessell,

T. M., and Darnell, J. E., Jr. (1994). The winged-helix transcription factor HNF-3 beta is required for notochord development in the mouse embryo.. Cell *78*, 575-88.

Whitman, M. (1997). Signal transduction. Feedback from inhibitory SMADs [news; comment]. Nature *389*, 549-51.

Whitman, M., and Melton, D. A. (1992). Involvement of p21ras in Xenopus mesoderm induction. Nature *357*, 252-4.

Wieser, R., Wrana, J. L., and Massague, J. (1995). GS domain mutations that constitutively activate T beta R-I, the downstream signaling component in the TGF-beta receptor complex. Embo J *14*, 2199-208.

Wilson, D., Sheng, G., Lecuit, T., Dostatni, N., and Desplan, C. (1993). Cooperative dimerization of paired class homeo domains on DNA. Genes Dev *7*, 2120-34.

Wilson, D. S., Sheng, G., Jun, S., and Desplan, C. (1996). Conservation and diversification in homeodomain-DNA interactions: a comparative genetic analysis. Proc Natl Acad Sci U S A *93*, 6886-91.

Wilson, P. A., and Hemmati-Brivanlou, A. (1995). Induction of epidermis and inhibition of neural fate by Bmp-4. Nature *376*, 331-3.

Winnier, G., Blessing, M., Labosky, P. A., and Hogan, B. L. (1995). Bone morphogenetic protein-4 is required for mesoderm formation and patterning in the mouse. Genes Dev *9*, 2105-16.

Witta, S. E., and Sato, S. M. (1997). XIPOU 2 is a potential regulator of Spemann's Organizer. Development *124*, 1179-89.

Witzgall, R., O'Leary, E., Leaf, A., Onaldi, D., and Bonventre, J. V. (1994). The Kruppel-associated box-A (KRAB-A) domain of zinc finger proteins mediates transcriptional repression. Proc Natl Acad Sci U S A *91*, 4514-8.

Wolpert, L. B., R.; Brockes, J.; Jessell, T.; Lawrence, P. Meyerowitz, E. (1998). Principles of Development, first Edition (London: Current Biology Ltd).

Wrana, J. L., Attisano, L., Wieser, R., Ventura, F., and Massague, J. (1994). Mechanism of activation of the TGF-beta receptor. Nature *370*, 341-7.

Wu, R. Y., Zhang, Y., Feng, X. H., and Derynck, R. (1997). Heteromeric and homomeric interactions correlate with signaling activity and functional cooperativity of Smad3

and Smad4/DPC4. Mol Cell Biol *17*, 2521-8.

Wylie, C., Kofron, M., Payne, C., Anderson, R., Hosobuchi, M., Joseph, E., and Heasman, J. (1996). Maternal beta-catenin establishes a 'dorsal signal' in early Xenopus embryos. Development *122*, 2987-96.

Xu, R. H., Ault, K. T., Kim, J., Park, M. J., Hwang, Y. S., Peng, Y., Sredni, D., and Kung, H. (1999). Opposite effects of FGF and BMP-4 on embryonic blood formation: roles of PV.1 and GATA-2. Dev Biol *208*, 352-61.

Xu, R. H., Kim, J., Taira, M., Lin, J. J., Zhang, C. H., Sredni, D., Evans, T., and Kung, H. F. (1997). Differential regulation of neurogenesis by the two Xenopus GATA-1 genes. Mol Cell Biol *17*, 436-43.

Xu, R. H., Kim, J., Taira, M., Zhan, S., Sredni, D., and Kung, H. F. (1995). A dominant negative bone morphogenetic protein 4 receptor causes neuralization in Xenopus ectoderm. Biochem Biophys Res Commun *212*, 212-9.

Yamaguchi, K., Nagai, S., Ninomiya-Tsuji, J., Nishita, M., Tamai, K., Irie, K., Ueno, N., Nishida, E., Shibuya, H., and Matsumoto, K. (1999). XIAP, a cellular member of the inhibitor of apoptosis protein family, links the receptors to TAB1-TAK1 in the BMP signaling pathway. Embo J *18*, 179-87.

Yamaguchi, K., Shirakabe, K., Shibuya, H., Irie, K., Oishi, I., Ueno, N., Taniguchi, T., Nishida, E., and Matsumoto, K. (1995). Identification of a member of the MAPKKK family as a potential mediator of TGF-beta signal transduction. Science *270*, 2008-11.

Yamashita, H., ten Dijke, P., Franzen, P., Miyazono, K., and Heldin, C. H. (1994). Formation of hetero-oligomeric complexes of type I and type II receptors for transforming growth factor-beta. J Biol Chem *269*, 20172-8.

Yamashita, H., ten Dijke, P., Huylebroeck, D., Sampath, T. K., Andries, M., Smith, J. C., Heldin, C. H., and Miyazono, K. (1995). Osteogenic protein-1 binds to activin type II receptors and induces certain activin-like effects. J Cell Biol *130*, 217-26.

Yang, X., Li, C., Xu, X., and Deng, C. (1998). The tumor suppressor SMAD4/DPC4 is essential for epiblast proliferation and mesoderm induction in mice. Proc Natl Acad Sci U S A *95*, 3667-72.

Yang-Snyder, J., Miller, J. R., Brown, J. D., Lai, C. J., and Moon, R. T. (1996). A

frizzled homolog functions in a vertebrate Wnt signaling pathway. Curr Biol *6*, 1302-6.

Yasuda, G. K., and Schubiger, G. (1992). Temporal regulation in the early embryo: is MBT too good to be true? Trends Genet *8*, 124-7.

Yost, C., Farr, G. H., 3rd, Pierce, S. B., Ferkey, D. M., Chen, M. M., and Kimelman, D. (1998). GBP, an inhibitor of GSK-3, is implicated in Xenopus development and oncogenesis. Cell *93*, 1031-41.

Yost, C., Torres, M., Miller, J. R., Huang, E., Kimelman, D., and Moon, R. T. (1996). The axis-inducing activity, stability, and subcellular distribution of beta-catenin is regulated in Xenopus embryos by glycogen synthase kinase 3. Genes Dev *10*, 1443-54.

Yuge, M., Kobayakawa, Y., Fujisue, M., and Yamana, K. (1990). A cytoplasmic determinant for dorsal axis formation in an early embryo of Xenopus laevis. Development *110*, 1051-6.

Zeng, L., Fagotto, F., Zhang, T., Hsu, W., Vasicek, T. J., Perry, W. L., 3rd, Lee, J. J., Tilghman, S. M., Gumbiner, B. M., and Costantini, F. (1997). The mouse Fused locus encodes Axin, an inhibitor of the Wnt signaling pathway that regulates embryonic axis formation. Cell *90*, 181-92.

Zhang, C., and Evans, T. (1996). BMP-like signals are required after the midblastula transition for blood cell development. Dev Genet *18*, 267-78.

Zhang, C., and Evans, T. (1994). Differential regulation of the two xGATA-1 genes during Xenopus development. J Biol Chem *269*, 478-84.

Zhang, J., Houston, D. W., King, M. L., Payne, C., Wylie, C., and Heasman, J. (1998). The role of maternal VegT in establishing the primary germ layers in Xenopus embryos [see comments]. Cell *94*, 515-24.

Zhang, J., and King, M. L. (1996). Xenopus VegT RNA is localized to the vegetal cortex during oogenesis and encodes a novel T-box transcription factor involved in mesodermal patterning. Development *122*, 4119-29.

Zhang, Y., Feng, X., We, R., and Derynck, R. (1996). Receptor-associated Mad homologues synergize as effectors of the TGF- beta response. Nature *383*, 168-72.

Zimmerman, L. B., De Jesus Escobar, J. M., and Harland, R. M. (1996). The Spemann organizer signal noggin binds and inactivates bone morphogenetic protein 4. Cell *86*, 599-606.

Zoltewicz, J. S., and Gerhart, J. C. (1997). The Spemann organizer of Xenopus is patterned along its anteroposterior axis at the earliest gastrula stage. Dev Biol *192*, 482-91.

Zon, L. I., Mather, C., Burgess, S., Bolce, M. E., Harland, R. M., and Orkin, S. H. (1991). Expression of GATA-binding proteins during embryonic development in Xenopus laevis. Proc Natl Acad Sci U S A *88*, 10642-6.